Exploring the Potentials of FIKK Kinase(s) into Development of Antimalarial and Diagnostics

A Thesis
Submitted in Partial
Fulfillment of the Requirements for the degree of

DOCTOR OF PHILOSOPHY

by

Mr. ANIL KUMAR D

Department of Biosciences and Bioengineering
Indian Institute of Technology Guwahati
Guwahati 781039, Assam, India

September 2021

Dedicated to my beloved parents

Devakrishnan P and Meena N

Indian Institute of Technology Guwahati

Department of Biosciences and Bioengineering

Statement

I hereby declare that the matter embodied in the thesis entitled "**Exploring the Potentials of FIKK kinase(s) into Development of Antimalarial and Diagnostics"** is the result of investigations carried out by me in the Department of Biosciences and Bioengineering, Indian Institute of Technology Guwahati, India, under the supervision of **Prof. Vishal Trivedi.**

In keeping with the general practice of reporting scientific observations, due acknowledgements have been wherever the work of other investigators are referred.

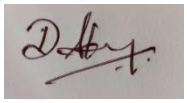

September, 2021

Anil Kumar D

Roll No: 156106005

Indian Institute of Technology Guwahati

Department of Biosciences and Bioengineering

Certificate

It is certified that the work described in this thesis entitled "**Exploring the Potentials of FIKK Kinase(s) into Development of Antimalarial and Diagnostics"** by **Anil Kumar D** (Roll no: 156106005), submitted to the Indian Institute of Technology Guwahati, India for the award of degree of Doctor of Philosophy, is an authentic record of results obtained from the research work carried out under the supervision at the Department of Biosciences and Bioengineering, Indian Institute of Technology Guwahati, India, and this work has not been submitted elsewhere for a degree.

Prof. Vishal Trivedi

(Supervisor)

Acknowledgements

First and foremost, I would like to thank my supervisor ***Prof. Vishal Trivedi*** *for providing me with great opportunity to undertake a PhD. I feel fortunate throughout my PhD duration for his constant support and guidance that helps to channelize my work. He provided me several opportunities including the chances to learn, publish and present my work in national and international conferences. I would like to thank him for his patience, understanding and wisdom of words which have contributed towards timely completion of my thesis work.*

I am equally thankful to all my Doctoral Committee members namely, Dr. Nitin Chaudhary, Dr. Sachin Kumar and Prof. Subhendu Sekhar Bag for their valuable advice and encouragement to make my work accomplished.

I extend my gratitude to the successive Heads of Department of Biosciences and Bioengineering, Indian Institute of Technology Guwahati, Prof. V.V Dasu, Prof. Kannan Pakshirajan and Prof. Latha Rangan for providing me the departmental facilities to carry out my research work. Further I would also like to thank non-teaching staffs for the valuable technical advice and helped me in handling the instruments. I would like to thank IIT Guwahati for giving this great opportunity and fellowship.

I am grateful to all faculties who taught me their invaluable knowledge at the time of course namely, Prof. Lingaraj Sahoo, Prof. Rakhi Chaturvedi, Prof. Vikash Kumar Dubey, Dr. Nitin Chaudhary, Dr. Shankar Prasad kanaujia and Prof. Pranab Goswami.

My special thanks to Scientists from CSIR-CDRI namely, Dr. Renu Tripathi, Dr. Saman Habib and Dr. Amogh Anant Sahasrabuddhe for their support by providing me the lab facilities for carry out some of the crucial part of my thesis work. I am also deeply appreciating the help and cooperation from their students namely, Mr. Prince, Ms. Deepti and Mr. Sadik.

I express heartiest gratitude to all my present and past Malaria Research Group members namely, Dr. S N Balaji, Dr. Suman Jyothi Deka, Dr. Sooram banesh, Mr. Ankur, Mr. Nitin, Ms. Pallavi, Ms. Vimee, Mr. Alok Kumar, Mr. Rafi, Mr. Siddharth, Mr. Rakesh, Ms. Shikha Mr. Umesh, Mr. M Rajendra Prasad and Mr. Shyam for being a part of the family and helping me in several ways throughout my research. I would specially thank Dr. S N Balaji for his valuable contribution and knowledge sharing during the initial phase of my PhD.

I would like to thank my neighboring labs and its lab members including Dr. B Anand lab, Dr. Gurwinder Saini lab, Prof. Rakhi Chaturvedi lab, Dr. Raj Kumar Thummer lab and Prof. Lingaraj Sahoo lab. I thank generous help from Dr. Yoganand and Dr. Himansu whenever I need.

I specially thank my friends Mr. Muthuvel, Dr. Padmavati, Dr. Vinoth Kumar, Dr. Sudhagar, Mr. Anbuthiruselvan, Mr. Krishna, Mr. Kamalesh, Ms. Chandrima, Ms. Nivedita, Mr. Dhanasingh and Mr. Sahaya for their support to keep myself motivated.

It's my privilege to express my thank to my Parents, Sister Anitha Shree and my wife K Pavani for their patience, belief, moral and emotional support throughout my research tenure. I would like to thank my in-law's family members for their patience and invaluable support.

Last but not the least, I would like to thank Dr. B R Ambedkar for his influence in my life to achieve the goals.

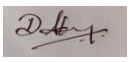

Anil Kumar D

September 2021

TABLE OF CONTENTS

LIST OF FIGURES

LIST OF TABLES

UNITS

Å	Angstrom
bp	Base pairs
Da	Dalton
°C	Degree Celsius
rpm	Revolution per minute
min	Minute
h	Hour
sec	Seconds
nm	Nanometer
µm	Micrometer
mAu	Milli absorbance units
kCal	Kilo calorie
Kbp	Kilo base pairs
kDa	Kilo Dalton
ns	Nanoseconds

mM	Millimolar
mg/ml	Milligram per milliliter
µM	Micromolar
µl	Microliter
ml	Milliliter
w/v	Weight/Volume
v/v	Volume/Volume
V	Volt
gm	Gram
gm/ml	Gram per milliliter
nM	Nanomolar
µM	Micromolar
nmol	Nanomoles
pmol	Picomoles
M	Molar

ABBREVIATIONS

ΔΨm	Mitochondrial membrane potential
ACE	Atomic Contact Energy
ALP	Alkaline Phosphatase
ACT	Artemisinin-based combination therapy
ATP	Adenosine Triphosphate
BSA	Bovine serum albumin
CelTOS	cell traversal protein for ookinetes and sporozoites
DNA	Deoxy-ribonucleic acid
DDT	Dichlorodiphenyl-trichloroethane
ELISA	Enzyme linked immuno sorbent assay
FPLC	Fast performance liquid chromatography
FHA	Forkhead associated
FIKK	Phe-Ile-Lys-Lys
FIKK9.1	FIKK9.1 kinase
GEST	Gamete egress and sporozoite traversal protein
HPLC	High performance liquid chromatography
IFA	Immuno-fluorescence antibody testing
IRBC	Infected Red blood cells
LB	Luria Bertani
MC	Maurer's cleft
MD	Molecular dynamics
NPP	New permeability pathway
NTE	N-terminal extensions
O.D	Optical Density
PV	parasitophorous vacuole
PCR	Polymerase Chain reaction
PDB	Protein Data bank
PCD	Programmed cell death
PBMC	Peripheral blood mononuclear cells
PEXEL	Parasite export element
PHF	Poly-herbal formulations
PSAC	Plasmodium surface antigen channel
PV	parasitophorous vacuole
QBC	Quantitative buffy coat
RBC	Red blood cells
RDT	Rapid detection test
RMSD	root mean square deviation
Rg	Radius of gyration
RMSF	root mean square fluctuation
ROS	Reactive oxygen species
SD	Standard Deviation
SDS-PAGE	Sodium dodecyl sulphate Polyacrylamide gel electrophoresis
SEM	Standard error mean
SPECT	sporozoite microneme protein essential for traversal
TUNEL	Terminal deoxynucleotidyl transferase (TdT) mediated dUTP nick and labeling
WHO	World health organisation

Chapter I

An Overview of Disease Biology, Drug Discovery and Diagnosis of Malaria

Summary

Malaria remains an important global public concern in both disease prevalent transmission regions and transmission controlled and/or eliminated regions. It is a complex disease that exhibits various clinical manifestations and epidemiology in different endemic regions. Children under the age of 5, pregnant women and people with weak immune are at higher risk transmission of severe to fatal illness of malaria. Though the control strategies are effective but it is not sufficient to achieve the goal of global eradication of malaria. This is mainly due to two reasons emergence of drug resistance and improper diagnosis of malaria. Antimalarial drug resistance is one of the primary challenges to control disease in recent times. The emergence of drug resistance increases the spread of disease to the regions which are not endemic to malaria and the regions where the it has been eradicated. For better surveillance and to eliminate malaria, affordable, rapid and easy to use diagnostic system is needed. Current methods of detections have pitfall on detecting parasites at species level with high sensitivity and specificity. In some instances, the rate of false negative and positive results increases due to mutations and deletions of markers used in the system. Therefore, there is a constant need of a target that leads to the development of new markers which can be used to develop new antimalarials and also in diagnostic systems. The purpose of this chapter is to widen our knowledge to identify a potential target that are highly diverged and crucial for survival of malaria parasite in human host.

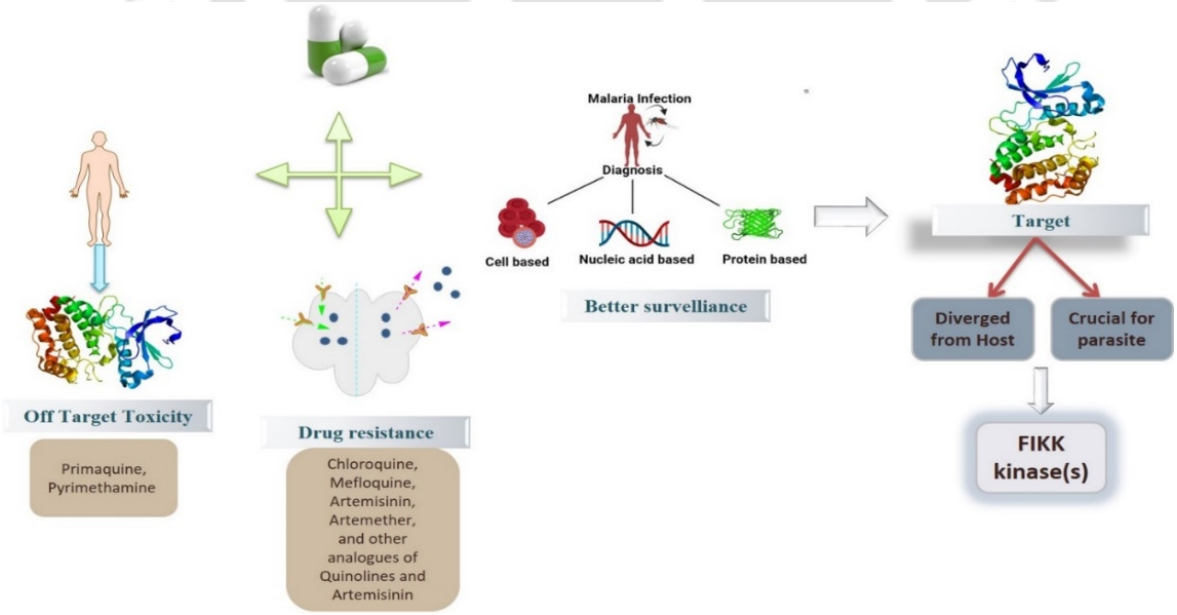

Scheme for Malaria Management through Drug Discovery and Diagnostics

1 Introduction

Malaria is a substantial infectious disease caused by *Plasmodium spp.* through the female anopheles' mosquito during a blood meal of human. *Plasmodium falciparum* is particularly a pernicious species among other malaria causative agents like *P.vivax*, *P.ovale*, *P.malariae,* and *P. knowlesi* in humans. The protists exhibits an apical complex that helps the parasite to penetrate the host cell, thus are known as Apicomplexa, and this apicomplexan parasite causing malaria is categorized in the *Plasmodium genus*. Malaria parasites are transmitted through more than 30 Anopheles species by the bite of infected female mosquitoes (WHO, 2020). Among all other vectors of malaria, *A. gambiae* leading disseminator in the African population and the Middle East and Indo-Pakistan subcontinent *A. stephensi* projects highly adaptable and potent vectors (Kamali et al., 2011; Subbarao et al., 2019).

Malarial infection is more prevalent in tropical and sub-tropical regions of the world. Precisely Saharan Africa, South-East Asia, and Latin America are highly endemic regions for lethal disease transmission. The prevalence is due to geographical conditions and sub-strand healthcare frameworks in those economically weaker countries (Figure 1.1).

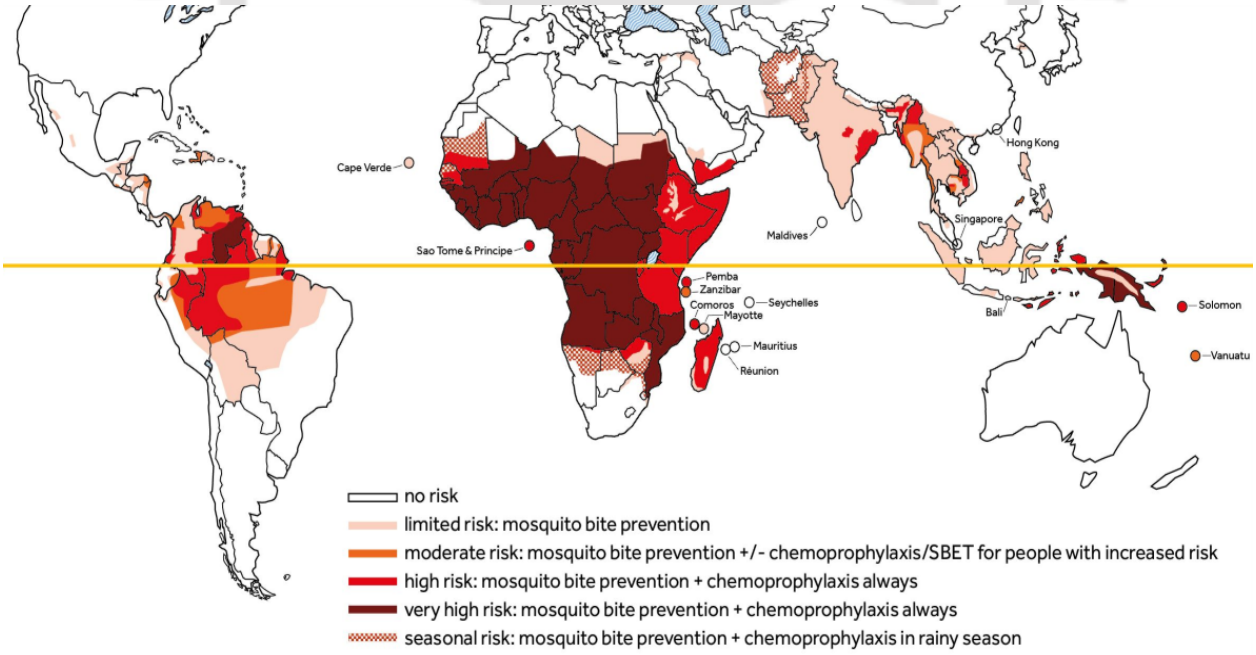

Figure 1.1: Geographic distribution of population living at risk of malaria infection and transmission. (Adopted from Source: https://www.itg.be/Files/docs/Reisgeneeskunde/MalariaWorld2019)

According to WHO (2020), 0.4 million mortalities and 229 million new cases of malaria were reported in 2019. Though substantial efforts were undertaken to eradicate malaria, the tropical disease remains as a major burden in developing countries where it accounts more than 90% of the deaths (WHO report 2020). WHO aims to eradicate malaria and decrease death caused by it to 90% by 2030 and thus the requirement of progressive strategies to eliminate malaria is the need of the hour. It has not only evolved as a threat to human life but also as a major burden for the socio-economic development of the developing nations.

1.1 Historical shreds of evidence on malaria

Malaria is one of the serious life threatening diseases since ancient times. Historically, Neolithic dwellers, Greeks, and Chinese were the major victims of the deadly malaria disease. Malaria accounted for 150 to 300 million deaths in the last century alone. This occupies 2 to 5 percent of the total deaths that occurred in the world. In recent times, people of South East Asia, Sub-Saharan Africa, and some tropical regions are the worst sufferers of malaria transmission. The history of malaria is a way long reign, Mesopotamian cuneiform scripts, the Indian Vedic writings (1500 to 800 BC), Chinese literature (270 BC), and the presence of malaria antigens in Egyptians (3200 and 1304 BC) suggests malaria could be believed as “King of Diseases”. Most of the ancient literatures elaborate systemic fever, chills, and headaches as common to represent malaria disease. The notable people like Hippocrates (450-370 BC), Plato (428-347 BC), and Aristotle (384-322 BC) have also mentioned malaria in different forms.

Malaria was discovered by Charles Louis Alphonse Laveran (1845-1922). He observed transparent crescent-shaped structures with dotted pigment in a crude microscopic blood sample. In his study, he recognized trophozoites, schizonts, male and female gametocytes stages of malaria in blood samples. The second puzzle of mosquito as an intermediate host for malaria transmission was discovered by Ronald Ross (1857-1932). He first discovered avian malaria developmental stages in mosquito and found identical developmental stages of human malaria in the mosquito. The third puzzle on the early developmental stages of sporozoites to infective form parasites in the liver of humans was discovered by P. C. C. Garnhamand H. E. Shorttin 1948. Subsequently, they identified all these plasmodium spp such as *P. vivax, P. malariae* and *P. falciparum* that follow similar developmental stages in the liver (Carter and Mendis, 2002; Cox, 2010). Starting from the pre-historic era till 21st century, this disease considered to be a huge burden to the world due to constant increase in disease transmissions (Figure 1.2). Still the

disease remains to be threatened, as elimination and eradication of malaria face serious technical, operative, and financial challenges. The poor access to health services in regions with vulnerable groups has decreased the global progress towards malaria control and elimination. In Addition to that, the success of antimalarial medications such as Chloroquine, Mefloquine, and Artemisinin is in the decline phase due to the evolution of drug-resistant parasites. The evolution of drug resistance even against newer frontline drugs in a short period, indeed an alarming to global health security. Additionally, the absence of a vaccine for the disease forced us to majorly depend on the source of chemotherapy which eventually leads to multi-drug resistance strains in parasites. To combat this vulnerable disease several public and private sector partners were collaboratively tasked to understand the biology of the parasite and coordinating implementation of malaria control (Ashley et al., 2018; Tanner et al., 2015)

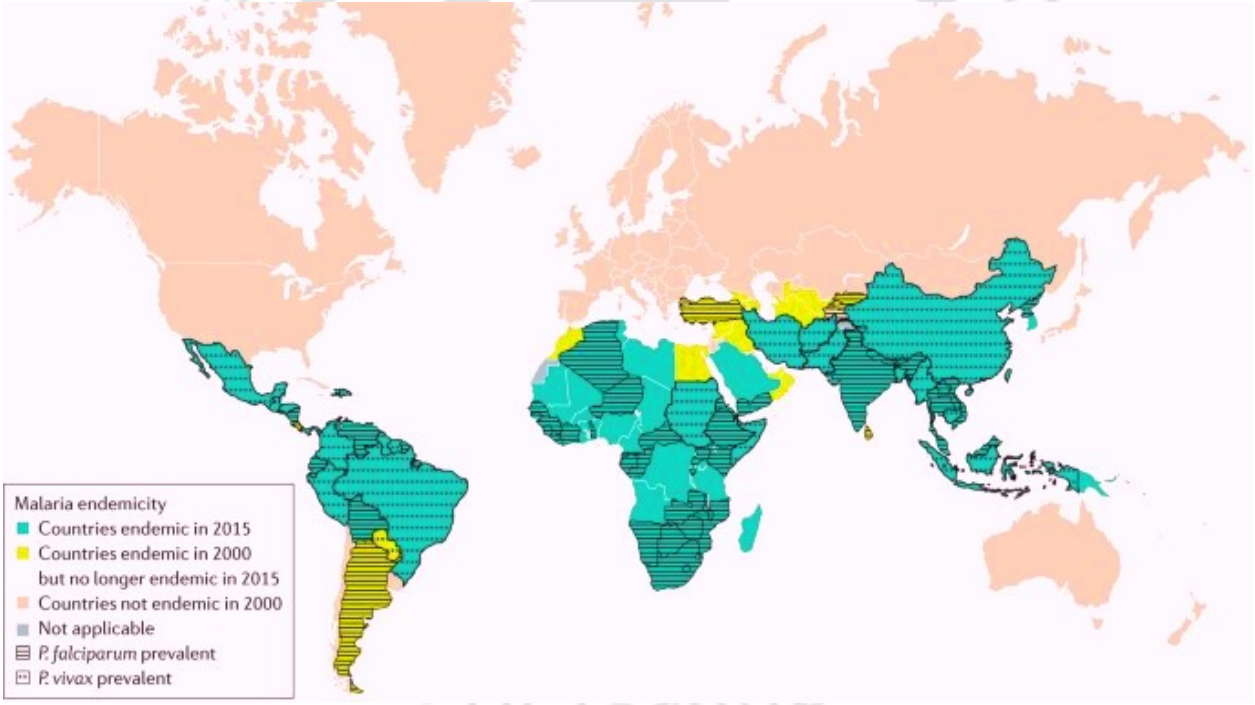

Figure 1.2: A map of malaria endemic regions around the globe [Adopted from source: (Phillips et al., 2017)].

1.2 Life Cycle of Malaria

The *Plasmodium falciparum* and other malarial causative parasites requires two hosts to complete their life cycle. The sexual cycle occurs inside the mosquito and the asexual cycle occurs inside human erythrocytes. The formation of sexual stages (gametocytes) is always in the

blood of the vertebrate host whereas gametogenesis and meiosis occur in the invertebrate host. Once the gametes are transmitted into a mosquito, they develop as male and female microgametes. These male and female gametes fuse together and form zygotes inside the mosquito. The zygote differentiates into motile mature ookinete which penetrates the mosquito midgut and further germinates into oocyst that contains sporogony. The sporogony in oocysts releases thousands of sporozoites upon bursting of the oocyst cell wall which invade the salivary glands of the mosquito (Figure 1.3). The sporozoites in salivary glands remain infective in the mosquito for 1-2 months and once it reaches a susceptible host, the life cycle of plasmodium begins (Beier, 1998; Venugopal et al., 2020).

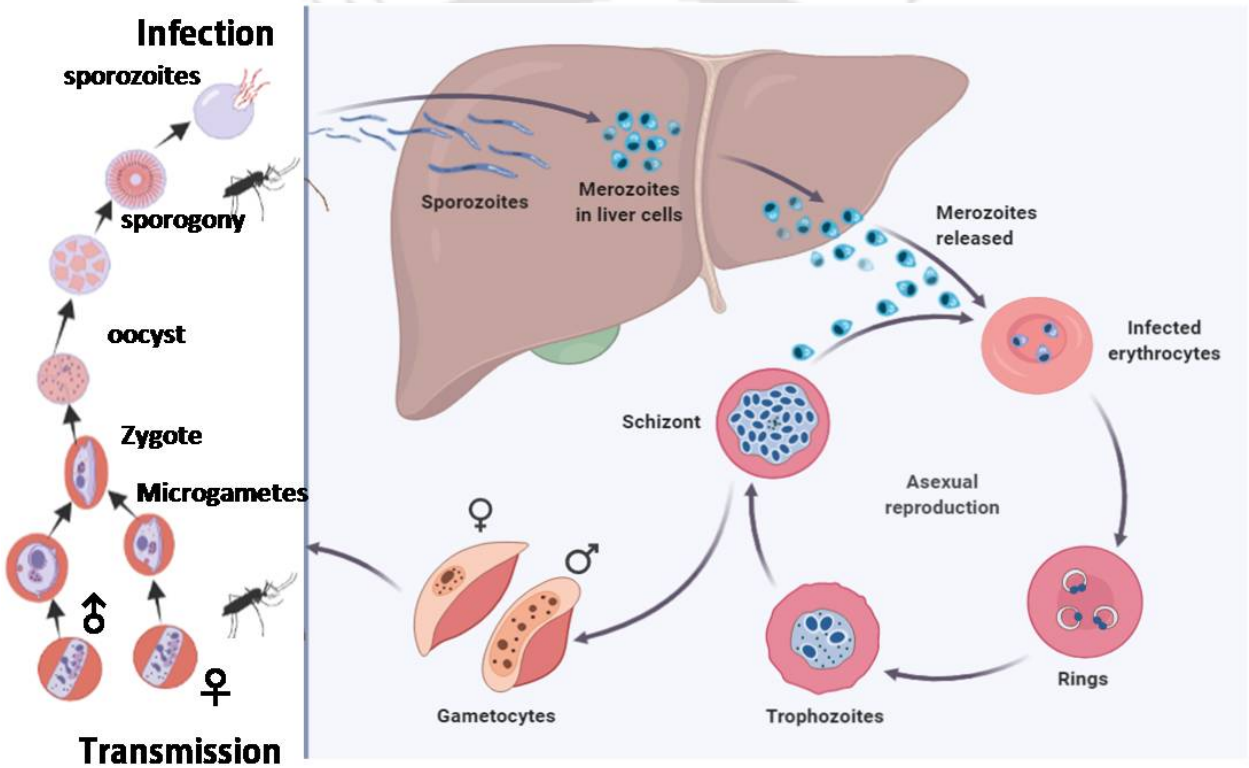

Figure 1.3: Life Cycle of Malaria in vertebrate and in the invertebrate host (Created using Biorender online server). Transmission of malaria starts during ingestion of gametocytes into mosquito while blood meal on an infected human. Both male and female gametes fuse together and undergo meiosis in the gut of the mosquito and then develop into oocyst. The oocyst will further develop into sporozoites and migrate to salivary glands through midgut wall of mosquito. The sporozoites are again transmitted to human while feeding. These ingested sporozoites are rapidly migrate to liver and infects specialized hepatocytes to starts it asexual replication. In the liver the sporozoites develop into schizonts and rupture the hepatocytes to release thousands of merozoites into blood stream. Once the merozoites released into blood stream, it immediately starts to invade erythrocytes. In the RBC, the parasite develops into ring, trophozoite and schizont stages over a 48 h period and releases merozoites into blood stream. The new asexual

cycle starts and repeats once the merozoites infect the new RBC's. During this process some of the schizonts will mature into gametocytes instead of producing merozoites. The gametocytes in blood are transmits to mosquito during blood meal and starts new transmission cycle.

The infection cycle of the parasite inside a human is initiated through the entry of sporozoites into the bloodstream of a healthy individual, via the saliva of an infected mosquito during a blood meal. Upon entry, the sporozoites invade specialized liver cells and undergo asexual division within the hepatocytes. After invasion into hepatocytes, sporozoites may either remains in hypnozoite state for several years or developed into schizonts and infective form merozoites. From a single hepatocyte cell, 16 to 32 merozoites are released into the bloodstream to invade RBC. Merozoites that invade RBC appeared to be as ring structures under a microscope. Once the parasite entered into erythrocytes, it continues to grow and develop in feeding phase This growing and feeding phase of a parasite is referred to as the trophozoite stage. During the trophozoite stage, the parasite occupies a large space and utilizes resources within infected erythrocytes to perform active cellular metabolism. At the end of the trophozoite stage nuclear division of the parasite occurs without any cytokinesis. The development of a multinucleate form parasite is known as Schizonts. During the development of schizonts, parasites alter RBCs to become more fragile which helps in releasing merozoites. *Plasmodium falciparum* takes approximately 48 hours to complete its asexual life cycle, initial ring stage development occurs for 24 h, trophozoite stage lasts for 18 h, schizont maturation occurs for 6 h and finally once the merozoite gets released it invade fresh RBC within a few minutes. The life cycle of malaria continues within RBC until host machinery suits for its growth (Figure 1.3). In the course of differentiation, some parasites differentiate into gametocytes and remain in the bloodstream. These gametocytes get ingested into mosquitoes while it encounters infected individuals and the sexual cycle of parasites begins (Aly et al., 2009; Bousema and Drakeley, 2011; Siciliano and Alano, 2015; Tuteja, 2007).

1.3 Hosts vulnerable to malaria disease

Malaria-causing parasites are predominantly found in mammals, birds, and reptiles. Studies on most of these hosts contributed to the understanding of the human malaria parasite. Laveran (1899) discovered parasites similar to malaria that belongs to *Hepatocystis* in non-human primates. Plasmodium spp. such as *P. inui, P. cynomolgi,* and *P. pitheci* in monkeys were discovered independently after 1907. In the 1930s *P. knowlesi* was discovered and in the 1960s including *P. knowlesi, P. inui* and, *P cynomolgi* are reported to be found in humans accidentally.

Such instances of *P. knowlesi* infection acquired in humans are very remote. The primary hosts of *P. knowlesi* in the vertebrate host is found to be leaf monkeys (*Presbytis* spp.) and macaque (*Macaca* spp.) monkeys with *Anopheles* mosquitoes belongs to *Leucosphyrus* group as invertebrate host. More than 24 species of avian malaria parasites were discovered and in the same period, human malaria causatives are also discovered. Notably, *P. relictum* of avian malaria parasites has been studied widely and it helps to improve our understanding of the transmission of malaria parasite in humans. *P. gallinaceum* infects chicken and provided the platform to observe exo-exrythrocytic stages of the malaria life cycle. Moreover, it also worked as a model for therapeutic studies until the development of rodent malaria models.

In 1948, the *P. berghei* was first isolated from rodents in Central Africa and subsequently, it was adapted to rats, hamsters, mice, and gerbils. Since then, three more species belonging to *P. yoelii, P. vinckei*, and *P. chabaudi* were identified and adopted to laboratory rodents. This acts as a mainstay for chemotherapies and serves as surrogate models for human malaria (2004; Cox, 2010).

1.4 Biology of malaria in the human host

Plasmodium is completely intracellular during its entire erythrocyte stage, which protects the parasite from the host immune response. Whereas, when the parasite is extracellular during transversal and before invasion into host cell, it becomes more vulnerable. Inside the human host, the parasite undergoes three major processes 1) Cell transversal, 2) Hepatocyte invasion and 3) Erythrocyte invasion. Cell transversal starts with the accumulation of sporozoites into the dermis of a host from the saliva of the infected mosquito during the blood meal and it remains in the dermis for 1-3hr. There after the parasite relies on gliding motion, the process by which parasites enters into the bloodstream. CelTOS (cell traversal protein for ookinetes and sporozoites), SPECT (sporozoite microneme protein essential for traversal), SPECT2 (also known as Perforin-like protein), Gamete egress and sporozoite traversal protein (GEST), and phospholipase (PL) are major protein involved in cell transversal process. During this process, some sporozoites remain in the dermis which is later cleared by lymphatics and generates host response. The Membrane Attack Complex/perforin-like (MAC/PF) domain in SPECT2, suggests that it may help in making holes in membranes. Except for SPECT2, the function of other proteins during cell transverse is not completely understood. The cell transversal through a

sinusoidal barrier is most crucial for sporozoites to priming into hepatocyte invasion (Amino et al., 2008; Steel et al., 2018; Yang and Boddey, 2017).

Sporozoites that cross the sinusoidal barrier migrates towards specialized hepatocytes, where they switch from migratory mode to infective mode. In detail, the migratory mode sporozoites reach the liver and recognize cells with higher sulfated heparin sulfate proteoglycans (HSPGs) that activates calcium-dependent protein kinase 6 (CDPK6). The interaction signals the sporozoites to develop as an invasive form of the parasite inside the hepatocyte upon entry. The scavenger receptor B1 (SR-B1) and CD81 are the most important surface proteins present in human hepatocytes required by *P. falciparum* sporozoites for invasion and formation of the parasitophorous vacuole. In contrast, the hepatocyte receptor EphA2 is not essential during hepatocyte invasion but for the establishment of parasitophorous vacuole and intra-hepatocytic development, the interaction of EphA2 with parasite proteins p52 and p36 are important (Dundas et al., 2019). Circumsporozoite protein (CSP) a key protein for invasion of sporozoite into hepatocyte and forms a dense coat around sporozoite's outer surface. It consists of a highly repetitive region and a type I thrombospondin repeat (TSR) domain (Cowman et al., 2016; Kumar and Tolia, 2019). A major event for hepatocyte invasion is the interaction of CSP with highly sulfated proteoglycans (HSPGs) and activating processing of CSP to remove N terminus for exposing of type I thrombospondin repeat TSR domain. Once sporozoite successfully establish hepatocyte infection, it transforms into liver stage (LS) or exo-erythrocytic form (EEF) over a span of 2–10 days, and hepatocyte development culminates after the release of ~40,000 merozoites from single hepatocyte into the bloodstream through budding of parasite-filled merosomes (Figure 1.4). Merosomes acts as a platform for several large complexes with different extrinsic proteins on the merozoite surface that binds erythrocytes.

Previously, it was believed that interaction of MSP1 of parasite and erythrocyte protein is a mandate for invasion but the studies report that merozoites lacking surface MSP1 also invade erythrocyte suggesting that MSP1 is not required for the invasion process. In the Pre-invasion process, the parasite causes actomyosin motor-driven deformation of the cell through interaction between merozoite and host erythrocyte. This process is mainly carried out by two protein families of type1 membrane protein in the malaria parasite, the *P. falciparum* reticulocyte-binding protein homologs (PfRhs) and erythrocyte binding-like proteins (EBLs).

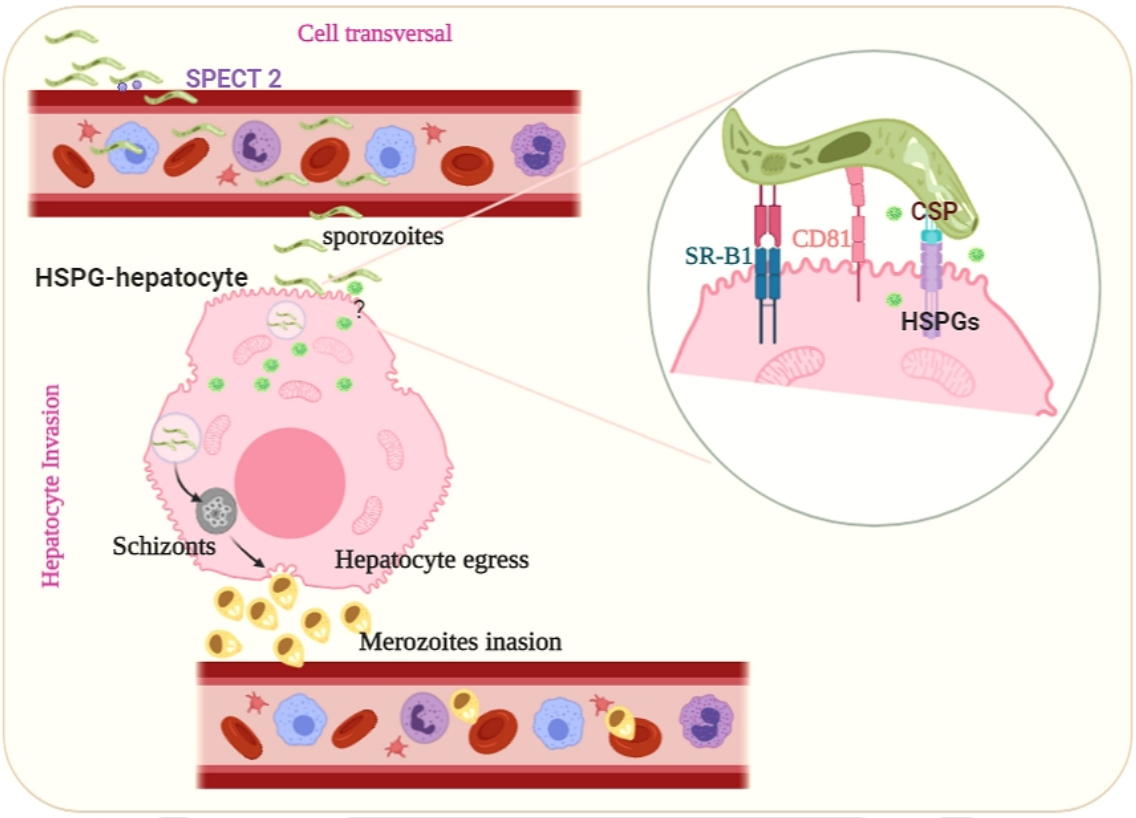

Figure 1.4: Process of cell transversal and hepatocyte invasion of sporozoites in the human host (Created using Biorender online server). During the process of cell transversal micronemes releases proteins that favor two types of events. First, protein such as TRAP has been released to promote gliding motion and then in second, SPECT and CeLTOS are released for breaching host hepatocyte membrane. It activates sporozoites and secretes 6 cys proteins to interact with host receptors (CD81 and SR-B1). This helps sporozoites to successfully establish invasion to hepatocytes.

These proteins specifically bind with erythrocyte receptors, including complement receptor 1 (CR1) and glycophorin A, B, C. These proteins are also involved in the activation of downstream signals for invasion. After egress, merozoites encounter low-potassium ion concentrations in blood plasma that leads to a steady increase in cytosolic calcium levels and triggers the release of EBL family, EBA-175 protein. The EBA-175 protein binds with glycophorinA receptor of erythrocytes and signals the release of proteins in rhoptries (Figure 1.5). Similarly, for PfRh4-CR1 parasite-host interaction mediated invasion requires the phosphorylation of cytoplasmic tail of PfRh4 by *P. falciparum* casein kinase 2 (PfCK2) (Tham et al., 2015) and PfRh1 leads Ca^{2+} signaling in the merozoite (Gao et al., 2013). The stabilization of interaction between EBL and PfRH proteins results in initiation of merozoite attachment to RBC through calcineurin.

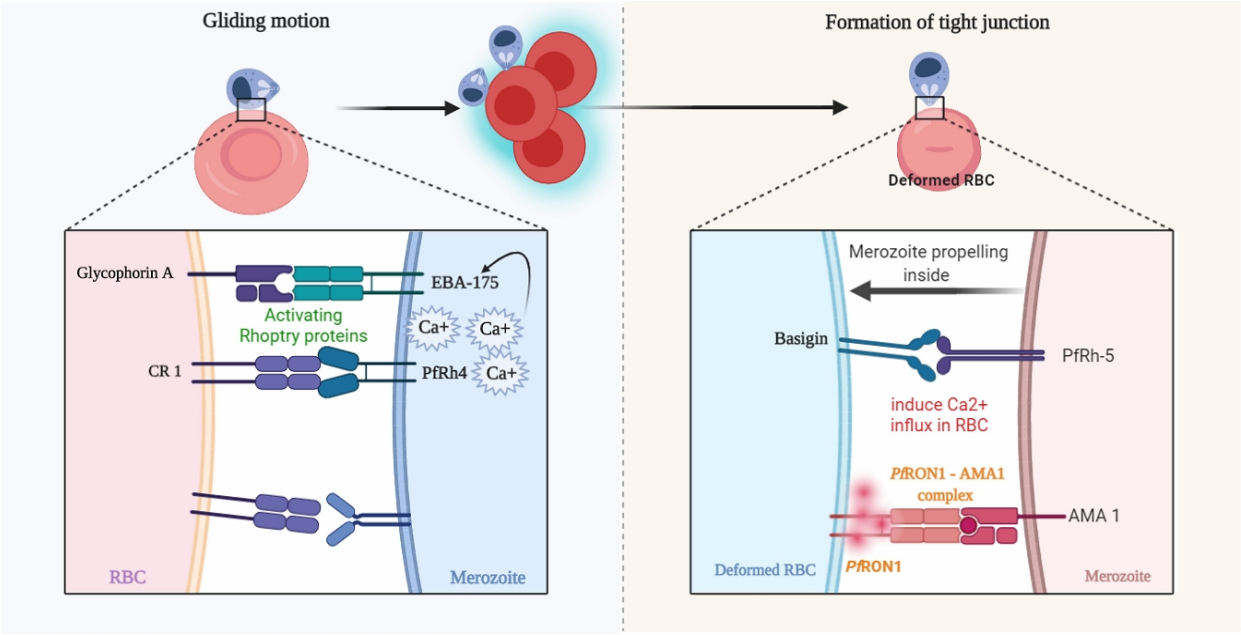

Figure 1.5: Important events of merozoites and RBC interaction for successful invasion of merozoites into host RBC (Created using Biorender online server). Invasion of merozoites into erythrocytes occurs from recognition of surface receptors in long distance. Initially, it follows gliding motion on the RBC surfaces with low affinity. Once the apical end of the parasite comes to contact with surface of erythrocytes, it forms a tight junction with host receptors.

The interaction between these proteins plays a crucial role in host-receptor ligation and signal transduction for further downstream invasion process (Paul et al., 2015). Once the erythrocyte is deformed, merozoites are reorientated so that the apical end leans onto the erythrocyte membrane. In this process, an atypical member of the PfRh family protein PfRh5 is found to play a major role by forming a complex with CyRPA (cysteine-rich protective antigen) (Reddy et al., 2015) and PfRipr (Rh5-interacting protein) (Chen et al., 2011). The binding of PfRh5 with host receptor basigin is the most important event for merozoite invasion (Crosnier et al., 2011) which is associated with Ca^{2+} influx into the host cell (Volz et al., 2016; Weiss et al., 2015). Likewise, the formation of a tight junction between erythrocytes and parasite-derived proteins, commonly of AMA1 and RON complexes leads to an irreversible attachment of erythrocytes and merozoites. The deposition of the RON complex in the erythrocyte, where RON2 spans the RBC membrane, binds to AMA1 on the merozoite surface (Besteiro et al., 2011). As soon as the merozoite is propelled inside the erythrocyte using force generated by the actomyosin motor of a parasite, the parasitophorous vacuole membrane is formed with the lipid-rich rhoptry contents (Riglar et al., 2011).

Once the active invasion phase is over, membranes at the posterior end of merozoite are fused to cover the parasite within the parasitophorous vacuole and erythrocyte. Echinocytosis causes the RBC to shrink and form spiky protrusions. After the successful establishment of infection, cell division starts to occur and release over 16-32 merozoites in the bloodstream within the subsequent 48 hours. The released merozoites without spending much time outside, invades new host cells. Several protein kinases include plant-like calcium-dependent protein kinase PfCDPK5 (Dvorin et al., 2010) and cGMP-dependent protein kinase (PfPKG) (Collins et al., 2013) plays an incumbent role to tightly regulate merozoite egress. MSP1 is also involved in merozoite egress by processing the subtilisin 1 on the merozoite surface to bind erythrocyte membrane protein spectrin (Das et al., 2015).

1.5 Clinical symptoms of malaria

Paroxysms, a systemic recurrent fever, is a major clinical symptom for malaria parasite infection which may develop in three distinct stages. The first stage is observed as severe shivering of the body due to chill and accompanied by muscle pain, fatigue, head ache, nausea, and diarrhea. The second stage is characterized as the infected individual display hot and dry skin and the final stage is found to have sweatiness due to extreme fatigue and limb weakening. The above-mentioned symptoms are classical manifestations of malaria and is caused due to host immune response against invading pathogens. Mostly, the symptoms are observed to occur 10 to 16 days after the infected mosquito bite normal individuals. The common symptom within the human may vary between populations to population which may be attributed to differences based on the strain of the plasmodium parasite that infects the host. An immune adult in an endemic region might not exhibit typical symptoms like fever or chill with increasing parasitemia while in contrast, a non-immune individual, an infectious bite may become a life threat. If the malaria is untreated, with increasing parasitemia the person encounters jaundice due to hemolysis of infected RBC which may also lead to liver dysfunction (Figure 1.6). The infected individual also suffers from anemia, an atypical feature that occurs during acute plasmodium infection. The heavy loss of hemoglobin due to the increase in parasite count results in rapid development of an anemic condition inside the human host. The increase of parasitemia also leads to renal dysfunction which is accountable for a sharp rise of creatinine levels and blood urea. During the erythrocytic stage of the *Plasmodium falciparum* life cycle, the levels of pro-inflammatory cytokines such as interleukin 1,6 and 12 are found to be increased (Lyke et al., 2004).

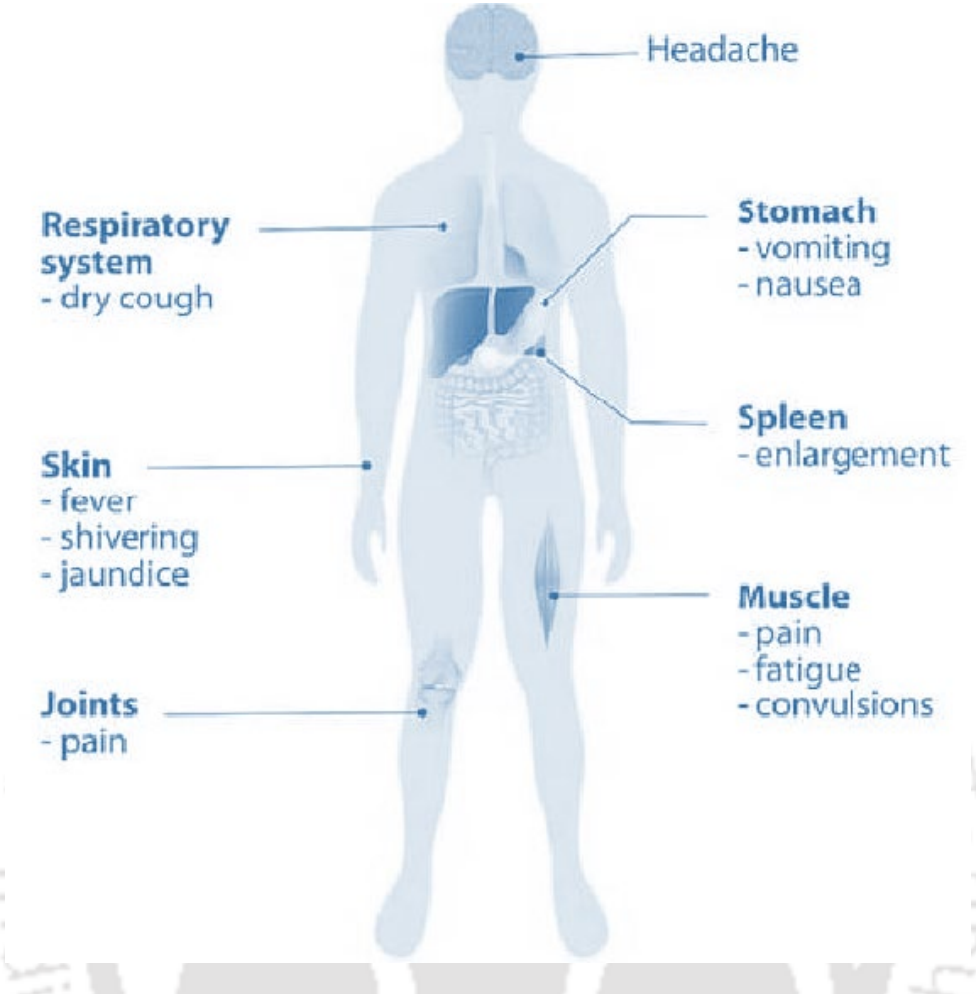

Figure 1.6: Common symptoms in humans during the course of malaria (Balaji et al., 2020).

Whereas, the levels of IL-10 and TGF-β tend to be decreased in the blood which results in classic manifestations of malaria such as fever and anemia. The abnormal levels of pro-inflammatory molecules are produced not only during anemic condition but also during the process of IRBC debris clearance by the spleen. Especially, IL-1 and TNF-α are found to be present in abnormal levels and plays a major role in the pathogenesis of malaria by damaging mitochondria and provokes expression of endothelial cell adhesion molecules (Viebig et al., 2005), (Arévalo-Herrera et al., 2015; Church et al., 1997; Crutcher and Hoffman, 1996; Dunst et al., 2017; Laishram et al., 2012).

1.6 Control and Elimination of malaria

In 1955, WHO started a malaria eradication program around the world. It mainly followed two different strategies to eradicate malaria, one is based on vector control by spraying insecticides like dichlorodiphenyl-trichloroethane (DDT) to kill mosquitoes (Bouwman et al., 2011) and

another most promising way is to control transmission through administering drugs like chloroquine to human. The initial phase of the DDT program produced successful results but later in 1969 it was abandoned due to large amount of accumulation of DDT in the environment (Sadasivaiah et al., 2007).

During the period of the 1970s and 1980s, Pyrethroids were developed and predominantly used as insecticides in Africa (Wat'senga et al., 2020). In the last decade, *Anopheles gambiae*an, an important vector for malaria acquired a high level of resistance to Pyrethroids and therefore it presses the need for alternative long-lasting insecticides to control the vector transmission of malaria (Awolola et al., 2018; Chandre et al., 1999). The other method such as non-insecticides genetic approach and bacterial symbionts used to kill mosquitoes are still in the developmental process (Ricci et al., 2012; Wang and Jacobs-Lorena, 2013). These approaches aim to reduce the life span, population size, and control vector transmission of malaria parasites. The administration of drugs to humans is the better approach to eliminate malaria in the present scenario. The current antimalarials principally act on erythrocytic stages that cause clinical complications in humans (Hussien et al., 2020). The two most prevalent malaria parasites *Plasmodium falciparum* and *Plasmodium vivax* are treated using different drug regimens (Figure 1.7). The usage of drugs completely depends on the complexity of malaria.

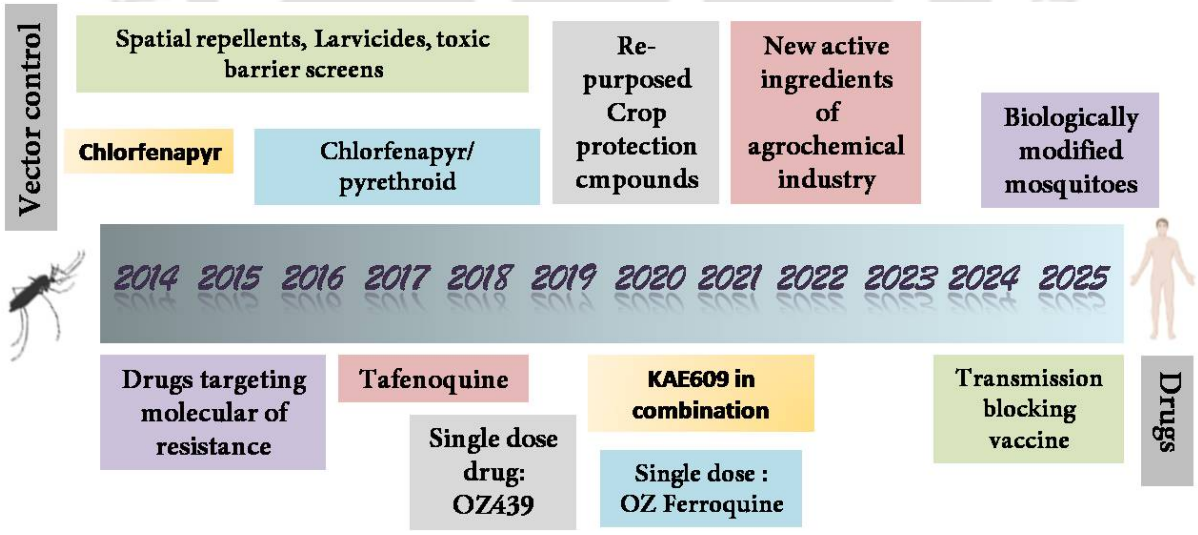

Figure 1.7: A timeline of measures undertake to control and eliminate malaria (Recreated from source: Wang & Jacobs-Lorena, 2013). Two major regimens are carried out and are in trials to control malaria. Vector control regimen consists of utilizing chemicals such as insecticides and new active ingredients, and biological modified mosquitoes to control the disease transmission. Drugs targeting important cellular pathway of parasites and vaccine discovery to

control Transmission in human is the other long standing regimen to achieve the goal of elimination of malaria.

4-aminoquinoline and chloroquine are used to treat uncomplicated malaria caused by *Plasmodium falciparum* (Menard and Dondorp, 2017). Chloroquine and primaquine are still considered as the first-line of drugs to the cure of *P.vivax* malaria. Quinine is the oldest drug, discovered from cinchona bark and is widely used in severe malaria conditions. Later the derivatives of quinine such as chloroquine, mefloquine, piperaquine and, primaquine were used to treat malaria. During acute malaria, artemisinin is considered to be the most effective drug but the poor bio-availability of the drug limits its usage as a single drug. The emergence of selected resistance for the important class of drugs and poor bio-availability of artemisinin encourages the use of artemisinin in combination therapy (2004; Tse et al., 2019). The ACT's mostly consists of the following combination such as artemether/ lumefantrine, dihydroartemisinin/ piperaquine, artesunate/ sulfadoxine-pyrimethamine, and artesunate/ mefloquine listed based on the recommendation of the world health organization (WHO). Moreover, the growing resistance against older drugs demands the use of artemisinin-based combination therapy (ACT) even for uncomplicated malaria (Wicht et al., 2020). This highlights the constant need for the development of new class of drugs (Cui et al., 2015; Rocamora and Winzeler, 2020; Subbarao et al., 2019; White, 2004).

1.7 Drugs and occurrence of drug resistance during malaria

Drugs to prevent malaria are much limited as compared to other life-threatening diseases. Quinine derivatives and antifolate combination drugs are the most prevalently used drugs to treat both complicated and uncomplicated malaria. Though the emergence of drug resistance against quinine derivatives, still it is preferred to be the drug of choice for the treatment of chemoprophylaxis and for uncomplicated malaria. Amodiaquine, a compound closely related to chloroquine is also widely used for similar conditions. Primaquine is one of the quinine derivatives specifically used to treat exoerythrocytic forms of *Plasmodium vivax* and *Plasmodium ovale.* Antifolate combination drugs consists of dihydrofolate inhibitors and sulfa drugs. Proguanil, pryimethamine, chlorproguanil and, trimetroprim belongs to the class of dihydrofolate inhibitors. The drugs sulfalene, sulfadoxine, sulfamethoxazole and, dapsone are group under sulfa drugs. Although parasites develop resistance rapidly to all these drugs when used alone, but still are found to be effective in combination therapies. For severe complications

of malaria, a class of sesquiterpine lactones, isolated from the plant *Artemisia annua* is widely used. This includes arteether, artesunate and artemether that are more effective in rapid clearance of malaria parasite.

Drug resistance to malaria emerged as a greater threat to the control and elimination of malaria. It is reported that the malaria parasite has developed resistance to all sorts of known antimalarials, even for artemisinin and some of its derivatives. The first report on antimalarial resistance against chloroquine was observed in the late 1950's near regions of the Thai-Cambodia border of Southeast Asia and Colombia of South America. Since then, resistance has spread across the globe and become a serious concern over malaria. The resistance spread all over Asia and the African subcontinent in 1978-1989. In India, the first instance of drug resistance of malaria occurred during the year of 1973 in Karbi, Anglong & Nowgong districts of Assam. Later parasite evolved resistant against chloroquine, Sulphadoxine, and pyrimethamine combination became a popular choice to treat malaria. Though the combination therapy worked well it didn't last long, as in mid of the 1960s parasites near the border of Thai-Combodia emerged to become resistant even for drugs used in combination therapies.

Mefloquine, a prominent drug, was used to treat malaria in endemic areas from the 1960s. But the reports of mefloquine resistance started to surface in the late 1980s near the Cambodia region and the drug resistance parasite strain continues to emerge around the world (Figure 1.8). Summary of reports on resistance for various drugs around the globe are depicted in Table (1.1).

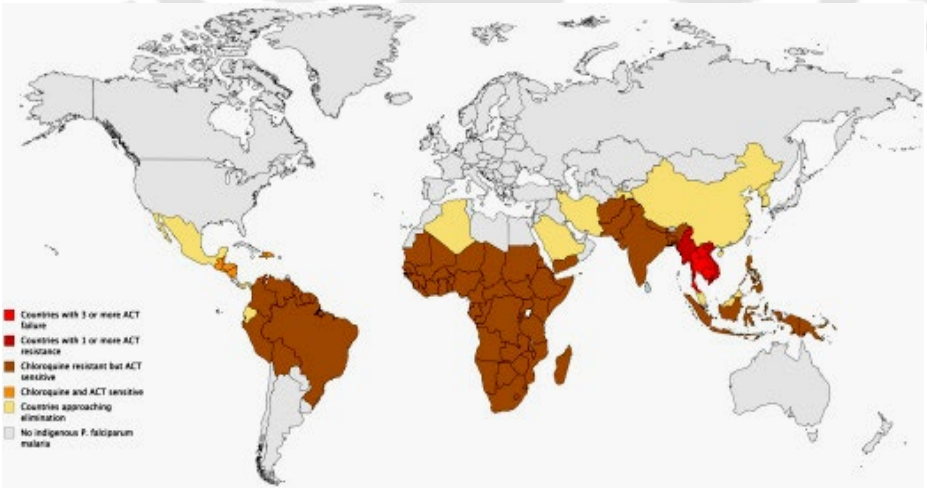

Figure 1.8: Distribution of drug resistance across the world. Adopted from source: (Plewes et al., 2019)**.**

Plasmodium falciparum follows a highly complex life cycle and its biology enables the parasite to adapt to various stringent conditions like metabolic stress, microenvironment changes in the host, and even high drug pressure. A general hypothesis is that drug resistance in parasites arose as a series of spontaneous mutations in the parasite genome upon continuous treatment of the drug. Once the resistant strain is evolved sensitive strain disappears through a natural selection process. Some of the molecular mechanisms behind the development of resistant parasites for different drugs has been reported in several reports. For example, the resistance against chloroquine follows an efflux pump strategy where the drugs are expelled out from the parasite once it gets in. It avoids accumulation of chloroquine inside the parasite to inhibit heme polymerization.

Table 1.1: Global analysis of occurrence of drug resistance

Region	Resistance reported		
	CQ	**S-P**	**MQ**
Indian Subcontinent	Y	N	N
Eastern Africa	Y	Y	N
Western Africa	Y	Y	Y
Southern Africa	Y	Y	N
South-East Asia & Oceania	Y	Y	Y
Caribbean (Dominican Republic & Haiti)	N	N	N
South America (Peru, SE Panama, Brazil, Ecuador, Columbia, Venezuela, Bolivia	Y	Y	Y
Central America (Nicaragua, El Salvador, Mexico, Honduras, Belize, Guatemala, NW Panama, Costa Rica)	N	N	N
East Asia (China)	Y	Y	Y

Note: CQ- Chloroquine, S-P- Sulphadoxine, and Pyrimethamine, MQ- Mefloquine

On a molecular basis, the mutations on *pfmdr*-1&2 and *pfcrt* genes play a major role in the development of resistance to quinolone derivatives such as quinine and chloroquine. Similarly, resistance was developed upon mutations against drugs like Sulphadoxine and pyrimethamine which inhibits the plasmodium dihydrofolate reductase (DHFR) and sulphone derivatives which act against parasite dihydropteroate synthase (Figure 1.9).

Drug resistance in malaria parasites increased the morbidity and made it difficult to eliminate this disease. As the parasite generates strategies to develop drug resistance rapidly, it is necessary to identify new classes of antimalarials against novel targets until a vaccine is developed to eradicate malaria.

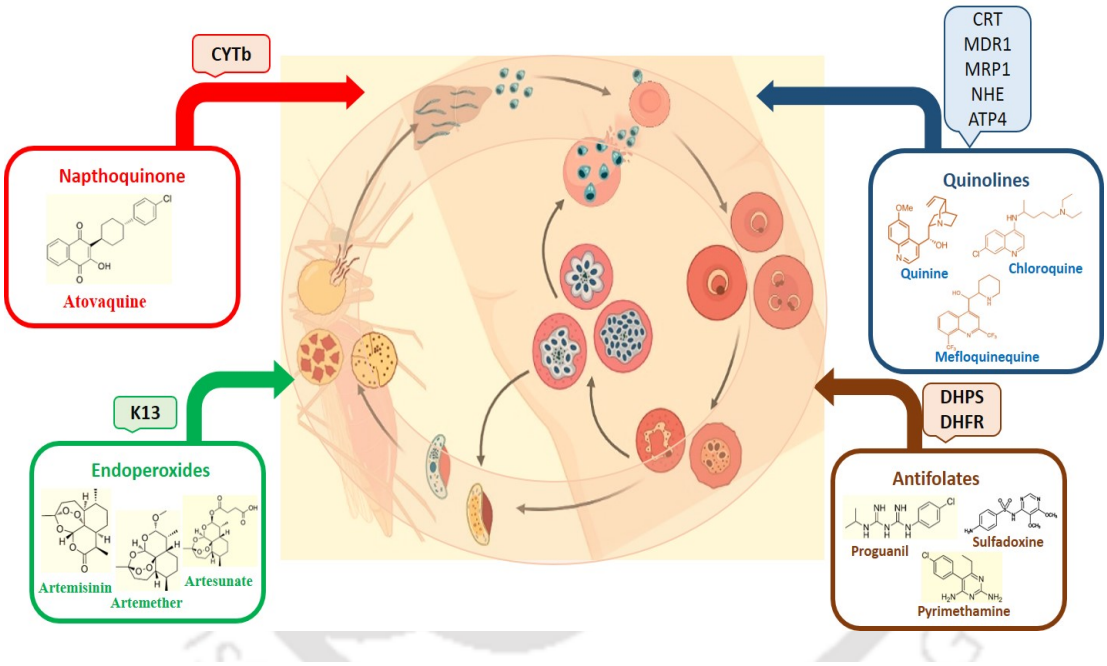

Figure 1.9: Chemical structure of popular antimalarial drugs and its reported mechanism of resistance (Created using Biorender online server)**.**

1.8 Potential Molecular targets of malaria parasite

The Sequencing of the entire *Plasmodium falciparum* genome in 2002 is a golden achievement in malarial research. Since then, identifying a major parasite target that involves crucial metabolic pathways becomes a research priority. Further development on identifying gene expression and proteomic profiles on different stages of parasite plays crucial roles in targeting specific life cycle stages (Gardiner et al., 2009; Hussien et al., 2020). The high-throughput proteomic analysis reveals that 43% of genes are expressed during the hepatocytic stage and more than 70 % of genes actively participate in the erythrocyte stages of the parasite. More

precisely it is identified that 43% of genes in sporozoite, 35% in merozoite, 42% in trophozoite and schizont whereas in gametocyte 47% of genes are being expressed (Gardiner et al., 2009). Research on disease model reveals many plausible targets present in parasite that serves as a better target to identify novel antimalarials. The proteins which could serve as excellent targets are proteases, dehydrogenases, and kinases from the plasmodium genome (Table 1.2).

Table 1.2: Drug targets in the malaria parasite based on oxidoreductase and hydrolase groups of enzyme classification.

S.no	Drug targets	Effective Drug
1	Dihydroorotate oxidase	Triazolo-pyrimidine
2	Dihydrofolate reductase	Triclosan, Phenylthiazolyl-triazine derivatives
3	NADH dehydrogenase	Antimycin A Atovaquone, and Dibenziodolium chloride
4	Glutathione reductase	Tertiary amides contain 4-aminoquinoline
5	Thioredoxin reductase.	6,7-dinitroquinoxaline and 4-nitrobenzothiadiazole
6	Cytochrome c reductase	4-aryloxy-*N*-arylanilines and Phthalimide Derivatives
7	HMB-PP reductase	-Nil-
8	Plasmepsins (aspartic acid Proteases)	Naphthoquinones
9	Dipeptidylaminopeptidase 1	DOPTACN compounds
10	S-adenosyl-l-homocysteine hydrolase	Nucleoside analogs and MDL 28842
11	Leucineaminopeptidase	ML392

1.9 Malarial Kinome

Plasmodium falciparum consists of 14 chromosomes that have a genome size of 22.8 Mbp, in which it encodes approximately 5,268 proteins. From total number of proteins present in the *Plasmodium falciparum,* 14% (733) are referred to as enzymes (Gardner et al., 2002). About 99 enzymes are considered to be protein kinases (PKs). The number of kinases present in plasmodium is found to be less compared to other eukaryotic organisms. A few number of kinases and divergence of proteins from other organisms elucidates that each kinase has a specific role in the parasite (Table 1.3) (Ward et al., 2004).

Table 1.3: Biochemical and functional characterization of *P. falciparum* kinome.

Group/Sub-group	Observation	Function	References
Casein Kinase (CK)			
CK1	Membrane association and found in culture media	Transcription process – "Spliceosome"	(Dorin-Semblat et al., 2015)
CK2		Modifying chromatin related proteins,	(Dastidar et al., 2012)
AGCgroup			
cAMP-dependent PfPKA	The plasma membrane of uninfected erythrocyte	Integrin dependent signaling pathway and Modulates Ca^{+} signal	(Merckx et al., 2008) (Beraldo et al., 2005)
cGMP-dependent PfPKG	------	Initiation of gametogenesis and involvement in gliding motility of ookinete,Inhibits mature schizonts egress	(Taylor et al., 2010), (Moon et al., 2009)& (Collins et al., 2013)
PKB	------	Phosphorylate PfGAP45 at S103 – protein associates with glideosome complex	(Thomas et al., 2012).
CMGC group			
Cyclin-dependent kinase (CDK's)	Pfcrk-3 – colocalized with histone proteins	Transcription regulation,	(Halbert et al., 2010)
MAPK (Mitogen-Activated protein kinase)	------	asexual cycle	(Dorin-Semblat et al., 2007)
GSK3	Maurer's cleft	Protein trafficking	(Droucheau et al., 2004)
CLK1	------	------	------
CamK			
CDPK's	Merozoites surface membrane	Crucial for the development of the parasite in the mosquito (sexual stage) and merozoite egress.	(Bansal et al., 2013; Dvorin et al., 2010; Green et al., 2008; Kumar et al., 2014)
TKL			
TLK	-----	------	--------
Orphan Kinases			
NIMA related kinases	-------	Phosphorylates pfmap-2 kinase	(Lye et al., 2006)
aTypical kinases			
PI3K kinase homolog	Rbc cytoplasm	Trafficking of hemoglobin	(Vaid et al., 2010)
pfRio kinases	----------	----------	--------

About 65 kinases were known to fall under the eukaryotic protein kinase (ePK's) group. Other remaining kinases have unique protein sequences with no homology and are highly diverged from auxiliary organisms.

1.9.1 Casein Kinase (CK's) group

In *Plasmodium falciparum*, two variants of casein kinase *pf*CK1 and *pf*CK2 are present and play a crucial role in various metabolic and signaling processes (Dastidar et al., 2012; Dorin-Semblat et al., 2015). Both enzymes are demonstrated to be essential for parasite survival during the asexual life cycle. *pf*CK1 is highly conserved to the eukaryotic organism and found to be an ectokinase due to its association with the host RBC membrane during the ring and early trophozoite stages of parasites. Though there is a lack of Plasmodium Export Element in *pf*CK1, it is found to be exported to host RBC cytoplasm and as well as outside IRBC. The feature has been observed in other genera as well, such as in leishmania (Dorin-Semblat et al., 2015). This suggests that the export of *pf*CK1 may follow a non-canonical pathway. Once the parasite developes into schizont stage, *pf*CK1 dissociates from the host RBC membrane and is found to be associated with the parasite nucleus (Dorin-Semblat et al., 2015). *pf*CK2 is a Ser/Thr kinase, localized in the cytoplasm and nucleus throughout the erythrocytic life cycle of parasites (Dastidar et al., 2012). Reports strongly suggest that *pf*CK2 may also be involved in mitotic cell division. It is a dual-specificity kinase and is involved in almost 17 metabolic processes in the plasmodium life cycle (Jones et al., 2012). Quinalizarin is found to be a profound inhibitor for *pf*CK2 (Graciotti et al., 2014). The crystal structure for one of the casein kinases (*pf*CK2) is shown in Figure (1.10).

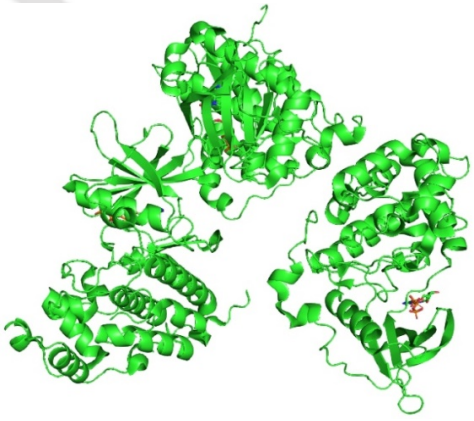

Figure 1.10: Crystal structure of *Plasmodium falciparum* Casein kinase family (Re-created using pymol from source: (Graciotti et al., 2014))

1.9.2 AGC group

The cAMP-dependent *pf*PKA, cGMP-dependent *pf*PKG, and *pf*PKB are clustered within this AGC protein kinase subfamily (Ward et al., 2004). These enzymes play a major role in many cellular processes that are elucidated through the lack of propagation of parasites upon inhibition of these kinases (Merckx et al., 2008; Ward et al., 2004). *pf*PKA interacts with integrin and induces the anionic channel conductance through associating with the plasma membrane of uninfected erythrocyte (Beraldo et al., 2005) but it is not clear that PKA is of parasite or erythrocyte origin (Merckx et al., 2008). The Ca^{+} signal modulates the cell cycle of the parasite and the ability of PKA to modulate Ca^{+} signal (Beraldo et al., 2005), postulates the potential role of PKA in the cell cycle process. Another protein of AGC kinase sub-family, PKG, is also known to play a key role in blood-stage schizonts (Taylor et al., 2010) and it also mediates the gametogenesis of parasites (McRobert et al., 2008).

1.9.3 CMGC group

The CMGC kinase group is derived from a) Cyclin-dependent kinase (CDK's) b) Mitogen-activated kinase c) Glycogen synthase kinase 3 (GSK3 family) and d) Cyclin-dependent kinase like kinases (CLK's). These families of proteins are crucial players in cell signaling, cell cycle progression, regulation of cellular RNA metabolism. It consists of 18 plasmodium kinases. An abundance of the CMGC group helps in successive proliferative and non-proliferative phases throughout the life cycle of the parasite (Ward et al., 2004).

1.9.3.1 Cyclin-Dependent kinases

A total 6 CDK-related kinases were present in *Plasmodium falciparum* (Ward et al., 2004). CDK-related proteins play a major role in chromatin modulation and transcription. The knockout analysis of CDK-related pfcrk-3 protein kinase results in the abolishment of the asexual proliferation of parasites. This illustrates the importance of CDK-related kinases for parasite survival. The association of *pfcrk-3* with histone protein suggests that it may have a possible role in chromatin assembly (Halbert et al., 2010). Moreover, two CDK's, *pf*PK5 and *pf*MRK, are found to be regulated by cyclin binding events.

1.9.3.2 Mitogen-activated kinases

Plasmodium falciparum consists of 2 MAPK kinase, *pf*map-1 does not possess any significant role in asexual growth, gametogenesis, or sexual development of parasite whereas *pfmap-2* is

essential for completion of the asexual cycle of parasites (Dorin-Semblat et al., 2007). Localization of GSK3 in Maurer's cleft proposed its involvement in protein trafficking (Droucheau et al., 2004). Still research is needed on GSK3 and CLK's proteins to elucidate its major function in parasite survival. On conclusion, CMGC group of kinases are potential targets for antimalarial development.

1.9.4 CamK (calcium/calmodulin-dependent kinases)

There are 13 CDPK's of *Plasmodium falciparum* that belongs to CamK group, orthologs to plant CDPK's but evolutionarily absent in human. Inhibition of *P. falciparum* CDPK1 and CDPK5 specifically inhibits the merozoite egress process by blocking the microneme discharge. This suggests kinases are also involving in egress process and plays an incumbent role in parasite invasion process. (Dvorin et al., 2010; Green et al., 2008). The deletion of CDPK7 does not affect the normal invasion process, except morphology aberrations of the parasite (Kumar et al., 2014). This suggests not all CDPKs are involved in the invasion but some are assigned for other specific roles. This elucidated the importance of CDPK for parasite survival.

1.9.5 Tyrosine Kinase like (TKL) group

Erythrocyte tyrosine kinase helps malaria parasite egress by phosphorylating Band 3 erythrocyte protein (Kesely et al., 2016), but there is no report/article regarding the role of five-member *pf*TKL kinase in plasmodium, which clusters with human TyrK's (Ward et al., 2004).

1.9.6 Orphan kinases and their role

The Kinome of *Plasmodium sp.* underwent unprecedented evolutionary divergence from other eukaryotic kinases. There are kinase(s) that doesn't come under any of the known kinase family due to their extreme divergence from ancestors. Such proteins are clustered under orphan kinases. About four members of the kinase family are classified under this group such as NIMA–related kinase (Nek's) family, *pf*PK7, *pf*PK9, and 21 FIKK family.

It is identified that these kinases were known to play central roles in gametogenesis, RBC remodeling and are involved in the oocyst formation process. Notably, Nek's are involved directly in the male gametogenesis process (Dorin-Semblat et al., 2011) and also involved indirectly in the gametogenesis process by phosphorylating MAPK like kinase, the protein that

plays important role in gametogenesis (Dorin-Semblat et al., 2007). *Plasmodium falciparum* FIKK's are the only kinase family among other eukaryotic

1.10 Kinases of plasmodium falciparum in drug discovery

The kinome of malaria has been widely characterized and reports suggests that protein kinases play essential roles in both the sexual and asexual life cycle of the parasite. Therefore, it provides target-based strategies to develop prophylactic, curative, and transmission-blocking drugs. The strategies of exploiting kinases as drug targets and their functional abnormalities in malaria parasite is detailed in Table (1.4).

1.11 Diagnosis of malaria

Accurate and effective treatment for malaria can only be achieved by specific detection of plasmodium species in the blood of infected person. Sensitive, rapid and cheap diagnostics systems are essential to successfully monitor the control, elimination and future global eradication of malaria programs. Currently, we rely on three basic tools such as cell-based detection, Nucleic acid based detection and Protein based detection of malaria (Figure 1.11). All these methods expanded our efforts to control malaria. Advantages and limitations of these methods have been briefly discussed in following sections.

1.11.1 Microscopic diagnosis using thick and thin blood smears

Microscopic examination of blood films using Wright's, Giemsa's, or Field's stains is the conventional method for diagnosis of malaria. For more than a century, microscopic techniques are widely adopted to screen the presence of malaria through thick blood smear and thin blood smear for differentiating malaria species. Both the techniques were advantageous because of their low cost on inspecting species level, ability to identify parasites presence, and assessing parasite density which eventually were useful for management and surveillance of malaria. Due to microscopic diagnosis in primary health care sectors, prescription of antimalarial drugs has been significantly reduced, and also improves the management of non-malarial fevers. However, low sensitivity, particularly at low parasitemia that requires considerable knowledge, and labor-intensive nature of the method is considered to be a disadvantage of microscopic diagnosis.

Table 1.4: Potentials of the kinase(s) as a drug target

Kinases	Inhibitors	Functional inhibition	References
***pf*CDPK1**	Imidazopyridazines derivatives, 2-Pyridyl derivatives	Microneme discharge	(Aher and Roy, 2017; Chapman et al., 2014)
***pf*CDPK4**	Pyrazolopyrimidine, 6-ethoxynaphthalen-2-yl, 5-Aminopyrazole-4-carboxamide analogs	Blocks microgametocyte Exflagellation and Malaria Transmission to Mosquitoes	(Ojo et al., 2014) (Huang et al., 2016)
***pf*CDPK5**	-	Inhibits Parasite egress	(Dvorin et al., 2010)
***pf*PI3K**	-	Trafficking of haemoglobin	(Vaid et al., 2010; Vaid et al., 2008) (2008)
PKA	H89, 3-methylisoquinoline-4-carbonitriles,	Inhibits parasite growth at Schizont stage	(Syin et al., 2001)&(Buskes et al., 2016)
PKB	A443654, U73122, PKC-specific inhibitors Go6976, and Go6983	Phosphorylate PfGAP45 at S103 – protein associates with glideosome complex	(Vaid et al., 2008) (2008)(Kumar et al., 2004)
***pf*PKG**	Compound 1 (4-[2-(4-fluorophenyl)-5-(1-methylpiperidine-4-yl)-1H pyrrol-3-yl]pyridine)	Inhibits mature schizonts egress	(Collins et al., 2013)
***pf*MAP-2**	pyridinylimidazole RWJ67657, pyrrolobenzimidazole RWJ68198	Gametogenesis development	(Brumlik et al., 2011; Dorin-Semblat et al., 2007)
***pf*PK6**	Olomoucine, roscovitine	-	(Bracchi-Ricard et al., 2000)
***pf*PK7**	Imidazopyridazines and Imidazopyridazines derivatives (34 Compounds)3-(1,2,3-triazol-1-yl)- and 3-(1,2,3-triazol-4-yl)pyrazolo[3,4-*d*]pyrimidin-4-amines	Impairment in oocyst development	(Klein et al., 2009)&(Dorin-Semblat et al., 2008)
***pf*PK5**	purvalanol B, olomoucine, flavopiridol, indirubin-3'-monoxime, xestoquinone.	malarial nuclear division cycles	(Holton et al., 2003),(Laurent et al., 2006)&(Graeser et al., 1996)
***pf*NEK-1**	Xestoquinonealisiaquinones A and B, alisiaquinol, homogentisic acid [methyl (2,4-dibromo- 3,6-dihydroxyphenyl)acetate]	Gametogenesis (male)	(Laurent et al., 2006) (Dorin-Semblat et al., 2011)
***pf*GSK3**	Kenpaullone, flavopiridol, alsterpaullone, indirubin-3'-monoxime, hymenialdisine, staurosporine, flavopiridol, lithium chloride, gwennpaullone, manzamine A, 8-hydroxymanzamine A	Inhibition of hemoglobin Trafficking	(Droucheau et al., 2004)
***pf*PI4K**	MMV390048	Effective in all stages of parasites	(Paquet et al., 2017)

Though the microscopic experts find 5 parasites/µl, the average microscopic analyst can able to detect only 50-100 parasites/µl that leads to underestimation of malaria cases (Mathison and Pritt, 2017; Moody, 2002).

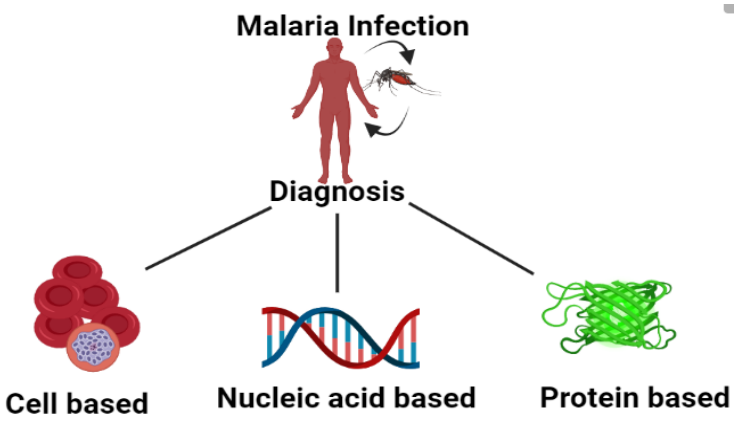

Figure 1.11: Common methods in diagnosis of malaria (Created using Biorender online server)

1.11.2 Diagnosis of malaria using fluorescence based techniques

The Quantitative buffy coat (QBC) is a malaria detection technique that involves staining parasite DNA using fluorescent dyes such as acridine orange, DAPI, or propidium iodide in micro-hematocrit tubes, and followed by visualizing through epi-fluorescence microscopy. Staining parasites using acridine orange leaves nuclei to fluorescent as bright green color while cytoplasm appears yellow-orange (Delacollette and Van der Stuyft, 1994). In most of the endemic areas, QBC based diagnostic method is preferred over light microscopy and RDT's due to sensitivity at low parasitemia and reagents for labeling are commercially available. The disadvantage of QBC is that it is little expensive compared to common light microscopy and is poor at differentiating species and determining parasites (Moody, 2002).

1.11.3 Immuno-fluorescence antibody-based testing

Immuno-fluorescence antibody testing (IFA) is a serological-based method for the detection of antibodies in the blood against malaria parasites. In the IFA test, either specific or crude antigens are used and determine both IgG and IgM antibodies in patient serum. Even though the IFA testing is time-consuming and subjective, it is more reliable because of its high specificity and sensitivity (Duo-Quan et al., 2009). It is useful for screening potential blood donors, during epidemiological surveys, and provides evidence on recent infection in non-immunes. Major

drawbacks of IFA are the necessity of trained professionals, high-end equipment's and impractical to use routinely in blood-transfusion centers (She et al., 2007).

1.11.4 PCR based detection methods

PCR based detection is a useful technique for diagnosis due to its ability to detect ≤5 parasites from 1 µl of blood, but it could not be considered as a rapid technique for primary diagnosis of malaria (Snounou et al., 1993). There are numerous methods for the detection of malaria using single and multiplex PCR methods from blood samples. Multiplex and nested PCR methods play a major role in differentiating malaria parasites at the species level during difficulty with morphological observation. Commonly circum-sporozoite genes and small subunits of 18S RNA are used to differentiate among Plasmodium species (Pieroni et al., 1998; Sethabutr et al., 1992; Wataya et al., 1993). In nested and reverse transcription PCR, a large subunit of RNA gene has been extensively used to distinguish plasmodium species and is suitable to identify target DNA region-specific to genus. Detecting low levels of parasitemia in patient samples and identification at species level pose a major advantage for PCR-based detection methods in malaria. The ability to detect parasites with 100% sensitivity in ≤5 parasites per µl makes it an ideal method during malarial therapy. Particularly PCR based methods are useful for analyzing variations in strains, mutations in the parasite, and to study genes involved in drug resistance of parasite. In the case of acute diagnosis, PCR-based methods are lagging behind and so microscopic examination remains the gold standard. Progress in developing new generation PCR like LAMP-based method and improvising of rapid DNA extraction methods might help in the field of acute diagnosis as well as in laboratories (Sirichaisinthop et al., 2011; Tambo et al., 2018).

1.11.5 Rapid Diagnostic Test's (RDT's)

In the early 1990s, immuno-chromatographic lateral-flow-strip based diagnostics were introduced to detect malaria and it remains common practice for detection till now. MRDTs are an evolving technology where new features are being included based upon the necessity for epidemiological settings, performance, and operational characteristics. A performance characteristic includes the ability to detect species level, sensitivity and specificity between species, detection of antigen in lower limits, and ability to detect during mixed infections. According to WHO, MRDT's should have 95% sensitivity for *P. falciparum* in 100 parasites/µl

of blood with more than 95% specificity. In case of operational characteristics, MRDT's should be simple, reproducible, less time-consuming, devoid of trained experts, and minimal storage requirements. Moreover, the cost of RDT's must be cheap for its use in the most endemic region around the world (Cunningham et al., 2019; Maltha et al., 2013).

Currently, RDT's are employed in a variety of diagnostic assays, the most common example is pregnancy strips. In lateral-flow immune-chromatographic assays, analytes move through the surface of the nitrocellulose membrane using capillary action. The strip usually contains two sets of antibodies, namely capture antibodies, and detection antibodies. Based on the requirement either monoclonal or polyclonal antibodies are incorporated. Monoclonal antibodies are highly specific and less sensitive whereas polyclonal antibodies are highly sensitive and less specific towards targeted antigen in a clinical sample. The antibodies are sprayed onto the membrane by a machine that remain bound to the membrane as an immobile phase. Other than antibodies, RDT consists of a sample pad for reagents to absorb and the absorption pad. The capture antibodies serve to extract parasite antigens from the clinical sample and the detection antibodies are conjugated with gold (indicator). If the target antigen is present in the sample, the gold conjugated antibodies bind to the parasite antigen and produce a visible line as a positive indication. It also contains a control line that validates assay by capturing one of the sample-specific proteins (Wilson, 2012). In malaria RDT's, antigens conserved across human causatives or specific to *Plasmodium sp.* are currently been using as diagnostic targets. For *P. falciparum* and *P. vivax* specific detection, monoclonal antibodies have been developed against lactate dehydrogenase and histidine-rich protein 2 (HRP-2). *Plasmodium* conserved lactate dehydrogenase (pLDH) and aldolase enzymes are used while detecting all human causatives (Maltha et al., 2013; Mouatcho and Goldring, 2013).

1.11.5.1 *pf*HRP-2

HRP-2 is a water-soluble protein, expressed throughout the asexual stages and early gametocyte stages of the malaria parasite. It is specific to *P. falciparum*, localized in the cytoplasm and surface membrane of infected RBC. Though HRP-2 is abundant in IRBC's, it was utilized as a first antigen to develop *P. falciparum* detection through RDT's. The detection limit of parasites using HRP-2 as the marker is evaluated as <250 parasites/µl with an 84% accuracy in Asia-Pacific regions. The level of detection in respect to parasite density is higher as compared to pan-malaria aldolase antigen. ParaSight F, ICT Pf, and PATH Falciparum Malaria IC are three

commercially available kits that utilize *pf*HRP-2 as a marker to detect *P. falciparum* specific malaria (Laurent et al., 2010; Ly et al., 2010).

1.11.5.2 *p*LDH

*p*LDH is an enzyme involved in the glycolytic pathway of all *Plasmodium* species and possess species specific isomers. the expression of *p*LDH have been observed in both sexual and asexual stages of malaria parasites. Initially, an Immuno-capture assay (IC assay) was carried out for detection of malaria using *p*LDH. The activity of the enzyme was compared with human LDH because the *p*LDH activity was determined to be high when it binds substrate 3-acetylpyridine adenine dinucleotide (APAD). The difference in activity is due to the presence of different isomer forms between host and parasite. Utilizing *p*LDH for detection is advantageous, as the activity can be detected in both sexual and asexual stages of the parasite. The second approach for malarial detection using *p*LDH is the development of RDT's. OptiMAL is the most extensively validated commercial RDT strip for the detection of *p*LDH antigen in a blood sample (Muhindo et al., 2012). Three monoclonal antibodies have been used in the OptiMAL dipstick for detecting *P. falciparum* and pan-malaria. Out of three, two are monoclonal antibodies (6C9 and 19G7) and are generated against pan-malaria *p*LDH antigen. The other monoclonal antibody (17E4) is specific to *P. falciparum* LDH (*pf*LDH). The sensitivity of OptiMAL is determined to be 97% with a detection limit of >100 parasites/µl (0.002% parasitemia). In detecting *P. falciparum* and *P. vivax*, sensitivity is obtained to be 94% and 88% respectively. The specificity is found to be 100% and 99% for *P. falciparum* and *P. vivax* respectively. Compared to other diagnostic methods OptiMAL based detection is found to be better in differentiating among parasite species. (Coldiron et al., 2019). A major drawback of RTDs is that it is not able to detect parasites below a level of 50 parasites/µl (0.001% parasitemia). Overall, OptiMAL is a valuable RDT for detecting malaria where a microscope may not readily available (Plucinski et al., 2019).

1.11.5.3 Aldolase

The human malaria parasite lacks the citric acid cycle for energy metabolism and so it completely depends on the glycolytic pathway for the production of ATP. A key enzyme in this pathway is aldolase. *Plasmodium* species contains two isozymes of aldolase, aldo-1 which is conserved and aldo-2 consists of 13% sequence divergence within *P. species*. The sequence divergence has been considered to be a target for developing RDT. Monoclonal antibodies

produced against it were used to detect pan-malaria. Therefore, the detection of plasmodium aldolase in RDT was used with the combination of *pf*HRP-2. The sensitivity was achieved to be 96% while RDT has the combination of pAldolase and *pf*HRP-2 with a detection limit of 500 parasites/µl (0.01% parasitemia). Many studies evaluated that RDT which combines both pAldolase and *pf*HRP-2 could be better diagnostic to detect *P.falciparum* and pan-malaria and those can be used during malarial treatment (Barber et al., 2013; Plucinski et al., 2019).

1.12 FIKK Kinase(s)

1.12.1 General Structure of FIKK kinases

In the genome of *Plasmodium falciparum*, the *fikk* gene family is dispersed in 11 out of 14 chromosomes (Gardner et al., 2002; Nunes et al., 2010). The presence of all *fikk* genes at the telomeric and sub telomeric regions (within~ 150kbp from telomere) suggests that it might perform some crucial roles in pathology of malaria.

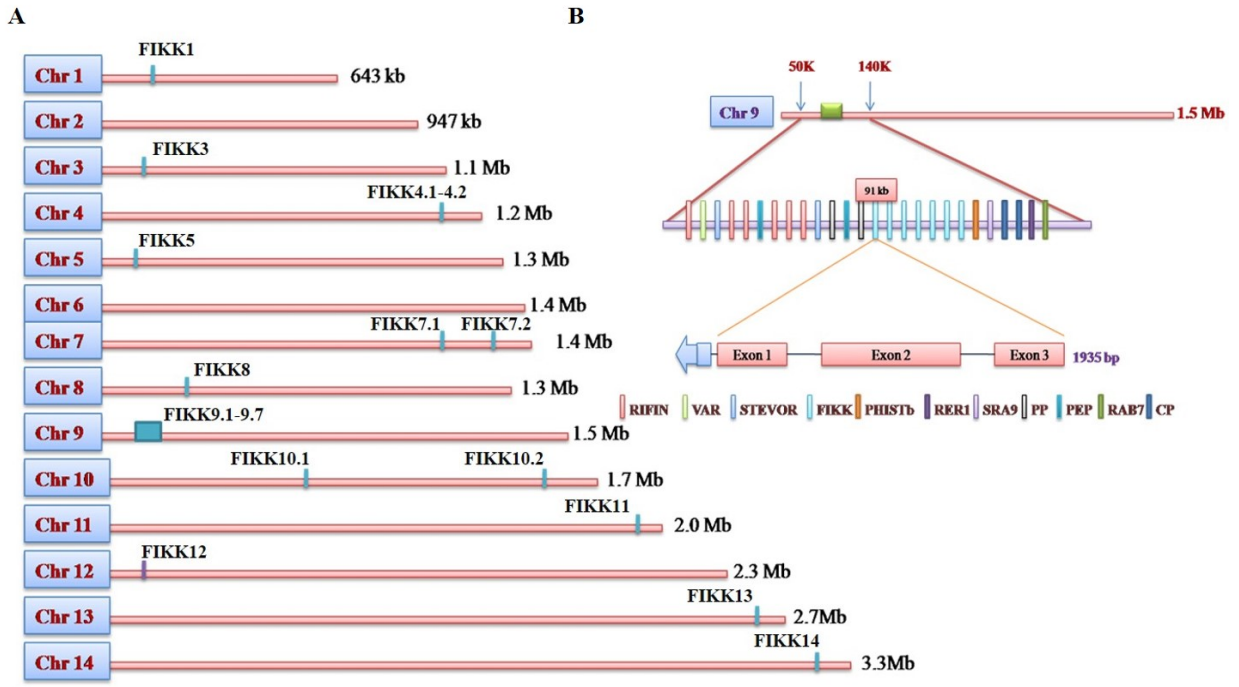

Figure 1.12: Genomic organization of different FIKK kinases in *Plasmodium falciparum*. A) Distribution of 20 *fikk* genes within 11 chromosomes out of 14, all were present (~150kb) near to telomere region and B) Single-gene organization of FIKK present in Chromosome 9, which have the highest cluster of 3 exon *fikk* genes (except *fikk* 8, which have 2 exons) respectively.

Initially, *fikk*'s were considered to be related to *var* genes, as it was present within the regions nearby to *rifin, stevor, var,* and *PfHISTb* (Figure 1.12 A). All these genes are found to be expressed as variable antigens in erythrocyte surface (Schneider and Mercereau-Puijalon, 2005). In certain chromosomes, *fikk* genes are present as clusters, identified from genomic data deduced from plasmoDB. Specially chromosome 9 has 7 *fikk* genes, the highest number of clusters in a single chromosome. All *fikk* genes of *Plasmodium falciparum* have three exons with high and repeated AT regions except *fikk*8 which doesn't have exon 1. The organization of one of the *fikk* gene is described in Figure 1.12 B, where it shows the presence of variance genes in and around it. Further orthologues of *fikk* sequences search with other organisms ended up with very little similarity, which propose FIKK's to have highly diverged sequences from other eukaryotic kinases.

1.12.2 Distribution of FIKK kinase(s) in different *Plasmodium species*

FIKK kinases remarkably expanded from its ancestor as a single gene to 21 in *P. falciparum* (human causative) *and P. reichenowi* (Apes). Interestingly it was expanded to 22 in *P. gaboni* (Chimpanzees causative), where all the genes of *P. gaboni* were synteny/orthologs to *P. falciparum* except *fikk*9.1 which is non-orthologue to other FIKK proteins. This might be because of the evolutionary transfer of the *fikk9.15* gene to *P. gaboni* before the last common ancestor *Laverania* (Sundararaman et al., 2016). *fikk*8, a gene considered to be important in *Plasmodium falciparum* (Nunes et al., 2010), and is the only gene syntenically transferred to most of the *Plasmodium spp.* as shown in (Table 1.6). It strongly suggests that *fikk*8 evolutionarily retains its important function in infected erythrocytes (Sundararaman et al., 2016). Unlike *fikk*8, *fikk* genes of certain *Plasmodium spp.* variably became pseudogenes. For example, *fikk* 7.2 & 14 are pseudogenes in *Plasmodium falciparum* (Schneider and Mercereau-Puijalon, 2005) (PlasmoDB 2017) but these genes appear to be functional in *P. gaboni, P. reichenowi* & *P. praefalciparum* orthologs (Sundararaman et al., 2016). Moreover, *fikk*9.5 was observed as a pseudogene in P. gaboni but intact in *P. falciparum and P .reichenowi* (Sundararaman et al., 2016).

Table 1.6: Distribution of FIKK Kinases in *Plasmodium species*

Plasmodium spp.	No.of FIKK*	Orthologs /synteny (*P.falciparum*)	Function	References
P. falciparum	21	-Nil-	Remodeling of host erythrocyte	(Brandt and Bailey, 2013; Kats et al., 2014; Nunes et al., 2010)
P. reichenowi	21	Duplicate	-Nil-	-Nil-
P. vivax	1	*fikk*8	-Nil-	-Nil-
P. malariae	1	*fikk*8	-Nil-	-Nil-
P. yoelii	1	*fikk*8	-Nil-	-Nil-
P. knowlesi	1	*fikk*8	--Nil-	-Nil-
P. berghei	1	*fikk*8	-Nil-	-Nil-
P. chabaudi	1	*fikk*8	-Nil-	-Nil-
P. coatneyi	0	-Nil-	-Nil-	-Nil-
P. cynomolgi	0	-Nil-	-Nil-	-Nil-
P. fragile	0	-Nil-	-Nil-	-Nil-
P. gaboni	22	All *fikk* and except *fikk* 9.15 has no homology with *Pf*	Possibly erythrocyte remodelling	(Sundararaman et al., 2016)
P. gallinaceum	1	*fikk*8	-Nil-	-Nil-
P. inui	0	-Nil-	-Nil-	-Nil-
P. ovale curtisi	1	*fikk*8	-Nil-	-Nil-
P. relictum	1	*fikk*8	-Nil-	-Nil-
P. vinckei	0	-Nil-	-Nil-	-Nil-

***Data deduced from PlasmoDB**

1.12.3 Localization of FIKK kinases in *Plasmodium falciparum* infected RBC

All the FIKK kinase(s) of *Plasmodium falciparum* were characterized to have parasitophorus export element (PEXEL) motif (Schneider and Mercereau-Puijalon, 2005) which signals parasite proteins to cross parasitophorous vacuole, except FIKK9.2 which doesn't have a PEXEL motif

which makes this protein to reside in the parasitophorous vacuole (Nunes et al., 2007). FIKK kinases were trafficked and distributed throughout parasite and infected erythrocyte; it recommends that FIKK may pursue important roles in Plasmodium. FIKK4.1 previously identified as R45 antigen was the only FIKK family protein detected by human immune sera (Bonnefoy et al., 1992) and possibly found to be localized in K-dots (responsible for knob formation in infected RBC), not with J-dots or Maurer's cleft (Kats et al., 2014). Colocalization of FIKK 9.3, 9.6 with PfSBP1 confirms the association of these FIKK's in Maurer's cleft with unknown function. Surprisingly 6/21 FIKK is predicted to be localized in the apicoplast (Ward et al., 2004), which plays a major role in the asexual lifecycle of the parasite (Figure 1.13).This was observed when the parasite died due to the loss of this essential organelle (Yeh and DeRisi, 2011).

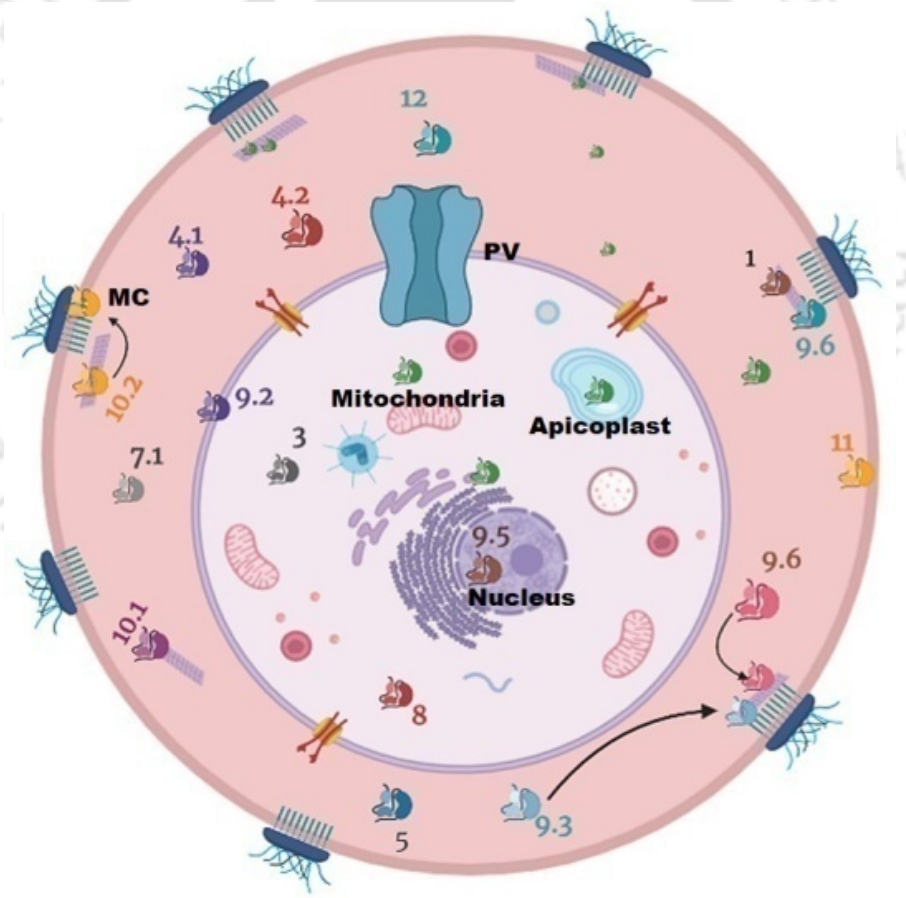

Figure 1.13: Distribution of FIKK kinases in infected erythrocyte. According to studies 9 out of 20 kinases were localized diversely over IE's and 2 FIKK (9.1&9.4) predicted to own the apicoplast target sequence. The localization of the remaining FIKK kinases (FIKK, 7.2, 8, 9.5, 10.1, 10.2, 11, 14) is yet to be known.

1.12.4 Transcription levels and Expression of FIKK Kinase(s)

Plasmodium falciparum follows a complex life cycle in erythrocytes. To complete the asexual cycle in humans, the parasite undergoes four distinct stages. After the successful invasion of merozoite into erythrocyte, it develops as early ring, trophozoite, schizont, and finally into merozoites. The process takes nearly 48-54 h to complete one life cycle from early ring to infective form merozoites (Gazzinelli et al., 2014). The *Pf* genes are expressed in a stage-specific manner, where the translated proteins perform specific roles associated with each stage. Similarly, genes of FIKK members are also transcribed stage specifically which is supported through mass spectrometry data of FIKK's in protein level. Transcripts levels suggest most of the FIKK genes are expressed equally as housekeeping gene like calmodulin. Only four FIKK's are found to have a very low level of transcripts in all stages. The higher levels of transcripts were observed to be present in the early ring and schizont stages. This serves as evidence for the observation of high levels of FIKK proteins in merozoites where almost all FIKK members are being expressed. FIKK may have a crucial role in the host defensive process as its transcript level varies upon interaction of IRBC with CD36 (Nunes et al., 2010).

1.12.5 Biochemical & Functional properties of FIKK kinase(s)

The kinase activity of all FIKK resides on the C-terminus of the proteins. Though in typical kinases, particular amino acid residues at the N-terminus are important, FIKKs were devoid of those residues in regions like the activation loop (RD) and Glycine rich region (GXGXXG) which are necessary for their catalytic activity (Ward et al., 2004). Out of 21 proteins, only 4 were experimentally proven to have kinase activity through biochemical analysis. Further, the importance of the diverged N-terminus from the typical kinases is also not yet revealed for any of the FIKK's. Hence the disparate N-terminal and conserved C-terminal of FIKK family proteins may provide new insights into a different mechanism of kinase activity as we know it.

FIKK 4.1

The presence of PEXEL motif guides FIKK4.1 into the maurer's cleft (MC) at early ring (Figure 1.13) which makes it to interact with dematin, where it resides throughout the life cycle of parasites (Nunes et al., 2007). Dematin, a protein that stabilizes the shape and rigidity of erythrocytes by anchoring the bundled actin with spectrin, β-adducin, and GLUT1 was identified as a substrate for FIKK4.1 of *Plasmodium falciparum*. Other kinases like cAMP kinase

phosphorylate the serine (S) 403 whereas FIKK4.1 phosphorylates the S110 (Brandt and Bailey, 2013) residues of dematin to disturb actin bundling and alter its protein-protein interactions. In conclusion, the interaction of FIKK4.1 and dematin may probably lead to alteration of RBC cell shape and rigidity, one of the hallmark events of malarial pathogenesis.

FIKK 4.2

FIKK 4.2 is also known as R2 antigen, as it is identified on the surface of IRBC, is the only FIKK family protein which could be detected in human sera (Bonnefoy et al., 1992). It consists of long six repeated amino acid regions that may help in the functional characteristics of the protein. The disruption of FIKK4.2 activity leads to drastic morphological changes in IE's. The noticeable difference is reduced rigidification of RBC membrane and decreased adherence of IRBC's to CD36. The morphology changes resemble erythrocytes of high knobs HbCC (hemoglobin CC-containing RBC) and low knobs HbAA (hemoglobin AA-containing RBC) structure in FIKK4.2 and FIKK4.2 KO clones respectively. The localization studies proposed that FIKK4.2 did not reside in MC as well as the J-dots, which were important for knob formation. Moreover, the appearance of too small and numerous fluorescence dots at cytoplasm of IRBC indicates that it may solely associates with k-dots. For better understanding on localization and as well as the substrates is certainly needed for suggesting the importance of FIKK4. 2 (Kats et al., 2014).

FIKK 7.1

Like other FIKK's, FIKK7.1 is also involved in modulating the membrane of the infected erythrocyte. The substrate was identified as 300 kDa protein of IE's but further analysis is required as the plasmodium protein (*Pf*EMP1) also has the same molecular weight. The involvement of FIKK7.1 in the invasion, replication, and as well as adhesion process of parasite infection was ruled out based on knockout analysis. FIKK7.1 KO clone elucidates the significant decrease of overall membrane rigidification in infected erythrocyte, recommending that it may have a role in splenic clearance (Nunes et al., 2010).

FIKK 8

FIKK 8 is one of the largest protein in FIKK family having amino acid residues of 1796 with some repeated residues. Upon 21 constructs of FIKK8, only 38 N-terminal extensions (NTE) protein were found to be stably expressed and auto-phosphorylated at serine1320

(phosphoserine) (Osman et al., 2015). This reveals the ability of auto-phosphorylation in FIKKs, which was previously not reported for any of its members. The ability of FIKK8 to phosphorylate bovine casein and MBP in presence of ATP affirmed that it could be a possible ATP-dependent kinase. Peptide array analysis strongly suggests that the activity of FIKK8 relies upon the presence of arginine at -3 and +3 positions in the substrate. Simultaneously, it was compared with homologs of *Cryptosporidium* FIKK proteins construct and their results were considered to be identical for NTE constructs of FIKK8 (Osman et al., 2015).

FIKK 12

The protein FIKK12 was observed to have a globalized occurrence in infected erythrocytes (IE's) stage specifically. During the early ring stage, it is exported from *Plasmodium* due to the presence of PEXEL motif and resides in Maurer's cleft (MC). Later in the trophozoite stage, it gets dissociated from MC and gets localized into the cytoplasm of IE's (Figure 1.13). It was confirmed through observing the co-localization of FIKK12 with *pf*SBP1 (marker for MC localization). Apart from localization of the protein, phosphorylation and its reversible action are important mechanisms in cellular events. Hence, the pursuit of FIKK12 affirmed through *in vitro* phosphorylating Myelin basic protein (MBP) assay. During the trophozoite stage, FIKK12 binds with Protein 4.1 in IE which makes partial membrane deformability of RBC. Knockout of FIKK12 neither affects the life cycle nor the growth of parasites which signifies that it has differential binding nature with other proteins (Nunes et al., 2010).

1.12 Significance of the work

Kinome of *Plasmodium spp.* underwent unprecedented evolutionary divergence from other eukaryotic kinases. Some of these kinases does not come under the known kinase family due to their extreme divergence from their ancestors. All these kinases are clustered as orphan kinases, FIKK kinases are one among them. *Plasmodium falciparum* FIKK's are the only kinase family among eukaryotic kinases which diverged extraordinarily and expanded from its ancestor. These proteins are trafficked throughout the parasite-infected erythrocytes and perform important tasks for the survival of plasmodium. FIKK kinases extensively modulate erythrocytes through direct or indirect interaction with the RBC cytoskeleton. In addition to that, some FIKK's are being localized in Maurer's cleft that speculates its involvement in PSAC and new permeability pathways (NPP) for nutrient uptake. Moreover, each FIKK has its unique N-terminal sequences with non-homologs to eukaryotic kinases as well as kinases present *Plasmodium sp*. These exclusive regions are highly potent to be antigenic which helps in producing specific antibodies against the FIKK kinase(s). Certainly, all those major factors such as its importance in parasite survival, stable expression in all stages, gene transfer, and regional specificity to *P. falciparum* paves a new insight in the field of antimalarial drug discovery and development of a new diagnostic marker for malaria. Based on the existing literature and our preliminary analysis, we would like to explore following research work:

- FIKK Kinase(s) are exclusive to the malaria parasite and we would like to find out whether they can be exploited as a potential drug target to develop antimalarials.
- The N-terminus region of FIKK kinases doesn't show any sequence similarity with the existing proteins present in host but they are very specifically matching with the plasmodium species. This suits to the criteria to exploit them for malaria diagnosis.

1.13 Aim of the study

On owing to our hypothesis the ability of FIKK kinase(s) has exploited to be a good candidate for drugs to target, leading to the discovery of new antimalarial and as well as to develop a diagnostic marker, we have framed the following objectives:

1) **Biochemical characterization of FIKK9.1 kinase**
   - 1a. Cloning, Over-expression and purification of FIKK9.1 kinase
   - 1b. Structure-function relationship of crucial active site residues of FIKK9.1 kinase
   - 1c. Identification of possible FIKK9.1 kinase substrate from *Plasmodium falciparum*
   - 1d. Study the interaction of FIKK9.1 kinase with ATP and other proteinous substrates
2) **Validation of FIKK9.1 kinase as a drug target for designing antimalarial agents**
   - 2a. Identification/Designing Suitable FIKK9.1 kinase inhibitor and study the inhibition mechanism of FIKK9.1 kinase
   - 2b. Mechanism of antimalarial action of selected FIKK9.1 kinase inhibitors
   - 2c. Immuno-localization of FIKK9.1 kinase in different stages of malaria parasite
3) **Validation of FIKK9.1 kinase as a diagnostic marker**
   - 3a. Polyclonal antibody generation against FIKK9.1 kinase in rabbit
   - 3b. Purification of polyclonal antibody using affinity purification from serum
   - 3c. Designing of suitable method to detect FIKK9.1 kinase present in malaria parasite grown under *in-vitro* culture conditions

Chapter II

Plasmodium falciparum FIKK9.1 is a monomeric serine-threonine protein kinase with features to exploit as a drug target

Summary

FIKK9.1 is essential for parasite growth and survival. Its structural and biochemical characterization will enable us to understand its role in the parasite life cycle. The recombinant FIKK9.1 kinase is monomeric with a native molecular weight of 60 ± 1.6 kDa. Structural characterization of FIKK9.1 kinase reveals that it consists of two domains; N-terminal FHA like domain and C-terminal kinase domain. The C-terminal domain has a well-defined pocket but it displayed RMSD deviation of 1.38 - 3.2 Å from host kinases. ITC analysis indicates that ATP binds to the protein with a K_d of 45.6 ± 2.4 µM. Mutational studies confirm the role of Val-244, Met-245, Lys-320, 324, Glu-366 for ATP binding. Co-localization studies revealed FIKK9.1 in the parasite cytosol with a component trafficked to the apicoplast and also to IRBC. FIKK9.1 has 23 pockets to serve as potential docking sites for substrates. Correlation analysis of peptides from the combinatorial library concluded that peptide P277 (MFDFHYTLGPMWGTL) was fitting nicely into the binding pocket. The peptide P277 picked up candidates from parasite and key players from RBC cytoskeleton. Interestingly, FIKK9.1 is phosphorylating spectrin, ankyrin, band-3 from RBC cytoskeleton. The study in this chapter highlights the structural and biochemical features of FIKK9.1 to exploit it as a drug target.

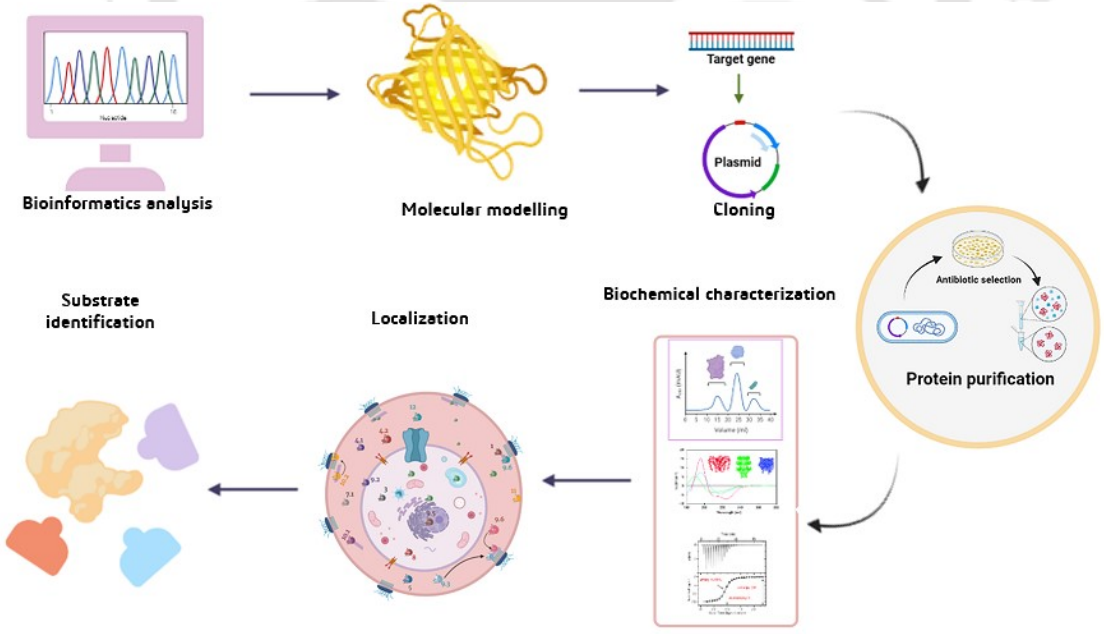

The content of this chapter is published as Anil Kumar D, Shrivastava D, Sahasrabuddhe AA, Habib S, Trivedi V. *Plasmodium falciparum FIKK9.1 is a monomeric serine-threonine protein kinase with features to exploit as a drug target*. Chem Biol Drug Des. 2021 Apr;97(4):962-977. doi: 10.1111/cbdd.13821.

2.1 Introduction

Malaria is one of the major burden for human health, responsible for high mortality and morbidity. Every year, half a million deaths are documented due to malaria. The 90 % mortality is associated with infection by two parasitic species, *Plasmodium falciparum* and *P. vivax* (Greenwood et al., 2005). The decline of anti-malarial efficacy on virulent strains is due to the emergence of drug resistance (Blasco et al., 2017), mass drug administration (Zuber and Takala-Harrison, 2018), incomplete course of medication, and improper administration of the drug to the patient (Nadjm and Behrens, 2012). Thus, finding new therapeutic molecules against novel targets to control the deadly parasitic disease is most important.

The nuclear genome of *P. falciparum* is comprised of ~5,300 genes which encode for ~5,268 predicted proteins, more than 50% of which are found to be hypothetical or with unknown functions (Gardner et al., 2002). The life cycle of the malaria parasite involves two hosts with several distinct developmental stages (Aly et al., 2009; Pease et al., 2013; Zuber and Takala-Harrison, 2018). During propagation in human RBC, the parasite needs to undergo a progression into different stages (ring, trophozoite, schizonts, and merozoites) as well as show active mechanistic processes such as invasion and egress (Cowman et al., 2016). Inside the RBC, the parasite relies heavily on host factors for nutrition and maintaining the pro-growth supportive environment. The breakdown of hemoglobin within the food vacuole of the parasite provokes the accumulation of free heme which in turn generates a large number of free radicals (Francis et al., 1997). The development of oxidative stress puts the parasite under heavy stress throughout the life cycle of the parasite (Percário et al., 2012). Moreover, proliferation within infected RBC reduces space for parasites, and that in turn induces rapid egress and invasion of new RBC (Glushakova et al., 2005). To combat the stress inside the erythrocyte, the parasites need to adapt and be equipped with efficient downstream signaling machinery (Vonlaufen et al., 2008). Parasite utilizes a network of protein kinases to sense different types of stresses (oxidative stress, space, osmotic and thermal stress) generated within infected RBCs and accordingly change the gene expression profiling within the parasite (Fennell et al., 2009). The *Plasmodium falciparum* consists of 85-100 ePK's (Ward et al., 2004) which controls several cellular processes such as central metabolic pathways, propagation, invasion, and egress (Gardner et al., 2002). It possesses only 35-65% identity with the human kinome and does not contain the tyrosine kinase family. It suggests the possibility of selective inhibition. Inhibition of protein kinases leads to disruption of

several cellular metabolic pathways, invasion, and egress to invade new RBC (Hallyburton et al., 2017; Ward et al., 2004). Indeed, out of 36 potential kinase targets, inhibiting 8 of these kinases leads to parasitic death on all the stages of malaria. Notably, a new class of antimalarials targeting PI(4)K, PKG, and *Pf*CDPK produce a promising effect on restricting parasite growth. Therefore, protein kinases represent an important class of enzymes that can be exploited to design better antimalarials. The differential expression level of proteome varies as per the need of the developmental stage, to undergo several cellular and metabolic processes and to adapt into a host for propagation and survival (Florens et al., 2002; Le Roch et al., 2004).

FIKK kinases are protein kinases exclusively present in the apicomplexan genre. *Plasmodium falciparum* contains 21 different FIKK kinase(s) whereas other species have a single FIKK protein. Sequence analysis of FIKK proteins indicates that the N-terminus of the enzyme is unique (non-homologous) to the parasite with low or no homology to hosts or other *Plasmodium sp.* (Schneider and Mercereau-Puijalon, 2005; Ward et al., 2004). Interestingly, the majority of FIKK kinases possess the PEXEL motif at the N-terminus, enabling them to cross the parasitophorous vacuole and localize to a different location(s) within the infected RBC (Schneider and Mercereau-Puijalon, 2005). Global protein expression analysis reveals that the FIKK kinases are being expressed in a stage-specific manner inside infected RBC (Pease et al., 2013). FIKK 4.1 is localized in Maurer's cleft (MC's) during ring and trophozoite stages (Nunes et al., 2007). It is found to phosphorylate dematin, an important RBC cytoskeleton protein (Brandt and Bailey, 2013). The phosphorylation at a specific site of dematin is involved in crucial interactions with parasite proteins inside the infected RBC (Lalle et al., 2011). Whereas, FIKK12 localizes in Maurer's cleft at the early stage and translocated to the erythrocyte membrane with the progression of parasite growth found to be involved in trafficking of parasite protein to RBC membrane. Similarly, FIKK 9.3 and 9.6 are localized in Maurer's cleft during ring and trophozoite stages (Nunes et al., 2007) with uncharacterized function. Disruption of FIKK7.1, FIKK12 and FIKK 4.2 in malaria parasite leads to the deformity of erythrocyte membrane involving cytoskeleton proteins but doesn't affect infection of uninfected RBCs and parasite life cycle (Kats et al., 2014; Nunes et al., 2010). A recent report enlightens five FIKK kinases namely FIKK3, FIKK9.1, FIKK9.5, FIKK10.1, and FIKK10.2 which are essential for growth during erythrocytic stages. Attempts to delete these genes from the parasite were ineffectual which shows the importance of those genes. Moreover, FIKK9.1 was found to be

localized in IRBC cytoplasm and as well as in MCs, a place where virulence protein trafficking occurs and also the place which is involved in critical uptake of nutrients for parasites. This suggests that targeting FIKK9.1 may block either of the pathways to inhibit parasite growth (Siddiqui et al., 2020). Interestingly, single FIKK protein which is present in rodent malaria is found to be crucial for parasite survival in both mosquito and liver stages and also involved in host immune modulations by regulating the level of anti-inflammatory cytokines IL-8 & IL-11 (Jaijyan et al., 2016). These studies highlight the importance of protein kinases belonging to the FIKK family and the need to characterize other members to explore their potential as drug targets. This will helpto design better anti-malarial for malaria treatment.

In this chapter, we have put an attempt to characterize FIKK9.1 (annotated as PF3D7_0902000) belonging to the FIKK kinase family in the *Plasmodium falciparum* 3D7 genome. Bioinformatics analysis reveals that FIKK9.1 is a unique protein as it harbors apicoplast targeting sequence and PEXEL motif. Structural studies suggest the presence of FHA-like domain which is a highly diverged N-terminus and a conserved Ser/Thr kinase domain in the C-terminus. It binds ATP with an affinity of (K_d) 45.6 ± 2.4 μM and efficiently catalyzing the phosphorylation of protein substrates. The protein-peptide docking study of 286 peptides finds MFDFHYTLGPMWGTL as a final peptide fitting nicely into the substrate-binding site. Interestingly, proteins such as Band 3, Spectrin α, and cell surface glycoprotein CD44 were aligned with screened final peptide and also found to be possible substrates through kinase assay. Overall, FIKK9.1 is a unique protein kinase from the FIKK family which can localize to apicoplast and phosphorylate proteinous factors to control the parasite life-cycle during RBC stages. In-depth study will eventually pave the way for drug development against malaria exploiting FIKK9.1 as a target.

2.2 Materials and Methods

2.2.1 Sequence analysis of FIKK9.1

The amino acid sequence of PF3D70902000 was retrieved from PlasmoDB (https://plasmodb.org/plasmo). It was blasted into the PDB database (https://blast.ncbi.nlm.nih.gov/Blast.cgi) using PSI-blast. The homologous sequences from the NCBI database were collected and multiple sequence alignment was done using MAFFT sequence alignment (https://www.ebi.ac.uk/Tools/msa/mafft/). Multiple sequence alignment was

used as an input to construct a phylogenetic tree. The improved interactive pedigree chart of the phylogenetic tree was made using the iTOL phylogenetic tree tool (https://itol.embl.de/).

2.2.2 Molecular Modelling of FIKK9.1

FIKK9.1 molecular model was prepared by *ab-inito* methods using I-TASSER an online server (https://zhanglab.ccmb.med.umich.edu/I-TASSER/). Models from the I-Tasser server were validated based on the comparison of RMSD value with template structure, lowest discrete optimized protein energy (DOPE) score, and Ramachandran plot analysis using the SAVES server (http://servicesn.mbi.ucla.edu/SAVES/). Out of five models, the model possesses a high C-score (-2.70) that was chosen for further study.

2.2.3 Determination of ATP biophore

To attain knowledge about crucial residues for ATP binding and kinase activity, we probed pharmacophore components from the different crystal structures of ATP-bound proteins deposited in the Protein Data bank (PDB). The ATP-bound co-crystallized protein structures (1ATP, 3A7H, 3DKC, 3DY7, 3TLX, 4FG8, 4GT3, 4XW5, 5DN3, 5XVU) were downloaded from PDB and analyzed with multiple parameters to extract the information about ATP biophore. The interacting amino acids present within 6Å of ATP bound region in proteins were characterized using the ContPro web server (http://procarb.org/contpro/). Based on interaction analysis, we have calculated the occurrence of 20 amino acids in the pharmacophore region. A Matrix of 110 X 31 atoms was decoded between those amino acids and ATP atoms to exploit hallmark residues that favor ATP binding in different protein kinases. Different color code has been assigned based on the distance and type of interaction between ATP and Protein atoms. The identified critical features of ATP biophore were validated by a docking study using Autodock 4.2 software (Morris et al., 2009). The FIKK9.1 model and ATP (from PDB ID ATP) were energy minimized using Swiss-PDB Viewer (SPDBV) and ChemBiodraw14 respectively. The grid for docking was placed where the high biophore interactions were observed. The docking was performed for 20 GA runs with the torsional degrees of freedom 6. The binding energy and scoring were calculated by performing a maximum of 2500000 energy evaluations. The interaction between ligands and receptors was analyzed through Ligplot+ and the results were visualized using Pymol (Educational user module).

2.2.4 Cloning of full-length FIKK9.1 and catalytic domain FIKK9.1CD2

The codon-optimized FIKK9.1(sequence deduced from PlasmoDB) gene (1626 bp) was procured in the pMK-T cloning vector backbone. Gene was PCR amplified from 82-1626 kbp using site-specific forward primer 5′-A**GGATCC**CTGAAT CTGGTGAATGTT-3′ with ***BamHI*** site (bold) and reverse primer 5′-TA**CTCGAG**ATTCTTGAACCA CCACGG-3′with ***XhoI*** site (bold) to eliminate predicted signal peptide motif for soluble expression. PCR amplification was performed for 20 cycles of denaturation and annealing for 30 sec at 95°C and 52°C respectively with an extension time of 1.5 min at 72°C. PCR amplified product was cloned into a pMD20 vector using a TA cloning kit (Takara Bio Inc, Japan). The clone was double digested with ***BamHI/XhoI*** to release the gene fragment and subsequently cloned in e. *coli* expression vector pET28a.This construct was termed as "FIKK9.1" throughout this study. Besides, the catalytic domain of FIKK9.1 (418 to1626 bps) was cloned into pET23a following the previously discussed procedure. This construct was termed as "FIKK9.1CD2" throughout this study. Both constructs were used in the bacterial expression system for heterologous protein production.

2.2.5 Over-expression and Purification

FIKK9.1 and FIKK9.1CD2 constructs were transformed into BL21(DE3) cells for over-expression. The transformed cells were grown in LB medium containing suitable antibiotics (ampicillin/kanamycin) at 37°C. When the absorbance reaches 0.6, culture was induced with 0.5 mM IPTG for 4 h at 37^0C. Cells were harvested by centrifugation at 8000 rpm for 30 min at 4°C and the resulting pellet was re-suspended in lysis buffer (20 mM Tris, pH7.5 containing 150 mM NaCl) containing 5% glycerol and stored in -80°C. On the day of purification, bacterial cells were disrupted by sonication (5 cycles "ON"/25cycles "OFF") for 1h with the amplitude of 33 A (Sonics vibra cell VC505). Protein expression was analyzed on 10% SDS-PAGE followed by western blotting using an anti-His antibody. The protein (FIKK9.1 or FIKK9.1CD2) was purified using Ni-NTA affinity chromatography (Qiagen, GmbH, Germany). In brief, cell lysate was loaded on the Ni-NTA affinity column pre-equilibrated with lysis buffer (20 mM Tris, pH7.5 containing 150 mM NaCl). The column was washed three times with lysis buffer and protein was eluted with a step gradient of imidazole (50, 100, 200, 300, 500 mM). The purity of each fraction was analyzed by resolving the fractions on a 10% SDS PAGE. The yield of purification was ~2.5

mg per liter of bacterial culture. Protein was desalted to remove imidazole and used for further study.

2.2.6 Determination of the oligomeric status of FIKK9.1

Purified protein was loaded on Superose12HR 10/30 column pre-equilibrated with degassed 20 mM Tris, pH 7.5 containing 150 mM NaCl. The column was calibrated with Gel filtration standard low molecular weight proteins (LMW gel filtration kit, GE healthcare) such as RnaseA (13.7 kDa), carbonic anhydrase (29 kDa), ovalbumin (43 kDa), and BSA (66 kDa). The partition coefficient K_{av} was calculated for each standard protein and the calibration curve was plotted between K_{av} vs Log. Mol.wt. FIKK9.1 was resolved under the identical buffer and instrument condition to calculate the partition coefficient $K_{av.}$ The partition coefficient K_{av} of FIKK9.1 was used to calculate the native molecular weight and oligomeric status of the protein.

2.2.7 Secondary structure determination of FIKK9.1

Purified FIKK9.1 (1 µM) was used for recording Far-UV (190–250 nm) CD spectrum at 100nm/second in 1mm path length cuvette in a JASCO J-1500 CD spectrophotometer (JASCO bio Inc, Japan) under constant nitrogen flow at 25°C. CD spectrum was analyzed by the K2D3 web server (http://cbdm-01.zdv.uni-mainz.de/~andrade/k2d3/) and DichroWeb web server (http://dichroweb.cryst.bbk.ac.uk) to estimate the secondary structural elements in FIKK9.1.

2.2.8 Interaction study of ATP with FIKK9.1

The interaction between ATP and FIKK9.1 was studied using isothermal titration calorimetry (PEAQ-ITC, Microcal). The binding analysis was carried out by loading the cell with purified FIKK9.1 (7 µM) and ATP (1 mM) was loaded into the syringe as the ligand. The reference power was set to 6 µcal s^{-1} and the experiment was conducted at 25°C. A total of 25 injections of ligand ATP (3 µl) were injected upon constant stirring at 500 rpm. The initial delay for the first injection was set 60 sec and for the rest of the ATP, injection is at an interval of 120 sec. The dilution effects of ligand were neglected by subtracting blank experiments for ligand and buffer with FIKK9.1 and ATP. The raw data obtained in titration were analyzed by origin 7 software (Origin Lab, USA) and the sigmoidal curve was well fitted with the one-site binding model to calculate dissociation constant K_D of ATP with FIKK9.1.

2.2.9 Generation and purification of polyclonal antibodies against FIKK9.1

For antibody generation, a large quantity of FIKK9.1 protein was purified using affinity chromatography. The highly concentrated purified FIKK9.1 was diluted in sterile water at a concentration of ~400 µg/0.5 ml. The first antigen injection was carried out by preparing an emulsion of FIKK9.1 protein with an equal amount of Freund's complete adjuvant using a syringe. Injection of antigen into the rabbit as an animal model for antibody production was carried out at CSIR-CDRI, Lucknow, in collaboration with Dr. Amogh A. Sahasrabuddhe. After the second booster of antigen, serum was collected from the rabbit for every subsequent booster and determined its titer using ELISA. To obtain a clear serum, the collected blood was centrifuged at 2000 rpm for 10 min at 4°C. The clear serum was carefully collected and stored at -20°C until use. The monospecific antibodies from serum were purified through antigen-antibody affinity chromatography.

2.2.10 Thermolysin protection assay

Thermolysin protection assay was performed as described by (van Dooren et al., 2009). Parasites were harvested by 0.05% saponin lysis of infected RBCs and washed with 1x PBS. The parasite was divided into three equal fractions and resuspended in 250 µl of assay buffer (50 mM HEPES-NaOH, pH 7.4, 0.5 mM $CaCl_2$, 300 mM sorbitol) containing detergents (either 0.05% digitonin, 1% Triton X-100 or 0.05% digitonin with 10 mM EDTA) and incubated on ice for 10 min. Thermolysin metalloprotease (25 µg/mg of protein) was added to three fractions with the thermolysin: protein molar ratio of 1:2 and incubated for 45 min on ice. Samples were made by boiling in 1X Laemmli buffer and electrophoresed on 10% SDS PAGE. Western blotting was done using anti-*Pf*FIKK9.1 Ab, anti-*Pf*Hsp70 Ab (kind gift from Dr.Niti Kumar, CSIR-CDRI, Lucknow) as a cytosolic marker and anti-*Pf*HUAb (Ram et al., 2008) as apicoplast marker.

2.2.11 Immunofluorescence assay and Confocal microscopy

Plasmodium falciparum-infected RBCs were fixed in PBS containing 4% (w/v) para-formaldehyde and 0.0075% (v/v) glutaraldehyde as described earlier (Ram et al., 2008). Fixed cells were washed with 1X chilled PBS and permeabilized with 0.1% (v/v) Triton X-100 in PBS. After extensive washing with chilled PBS, permeabilized cells were blocked in 3% BSA and then incubated overnight with primary antibodies (purified anti-*Pf*FIKK9.1 antibody (1:50) and mouse *Pf*HU anti-sera (1:200, used as a marker for apicoplast) in 3% BSA. After multiple

washes with chilled PBS, cells were probed with secondary antibodies i.e.; Alexa Fluor 568-tagged goat anti-rabbit Ab and Alexa Fluor 488-tagged goat anti-mouse Ab (dilution 1:1000, Invitrogen, USA) in 3% BSA. DAPI (20 µg/ml, Sigma-Aldrich) was added to the secondary Ab mix for nuclear staining. The cells were seeded on poly-L-Lysine (Sigma-Aldrich) coated coverslips. Coverslips were washed and mounted in anti-fade mounting media (Invitrogen). Imaging was performed on a Leica SP8 confocal microscope using 63X oil-immersion objective. For mitochondrial labeling, live cells were incubated with 50 nM Mitotracker Red CMXRos (Invitrogen) for 30 min at 37°C before fixation. Alexa Fluor 514-tagged goat anti-rabbit Ab (dilution 1:1000, Invitrogen) was used as a secondary Ab for detection of *Pf*FIKK9.1 signals in Mitotracker-stained cells.

2.2.12 Preparation of RBC ghost

The RBC ghost was prepared as described previously (Bryk and Wiśniewski, 2017). Blood was collected in citrate phosphate dextrose buffer from the healthy individuals by trained phlebotomists. The blood was washed 3 times with 25mM HEPES pH 7.4 buffer containing 150mM NaCl. The RBCs were separated from WBC by density gradient separation using Histopaque 1129 (Thermo Scientific, USA). The purified erythrocytes were lysed using hypotonic buffer (25 mM HEPES pH 7.4 containing 1 mM EGTA, 1 mM PMSF, and 0.5 mM DTT) and kept in an ice bath for 10 min. The lysed RBCs were centrifuged at 13,000 rpm for 30 min to remove hemoglobin content from RBC and the process was repeated several times until visible whitish ghosts formed an opaque pellet.

2.2.13 Protein Kinase assay

In a total volume of 250 µl, FIKK9.1CD2 (60 µg/ml) was incubated with BSA (100 µg/ml) in a reaction buffer 20 mM Tris pH7.4 containing 100 mM NaCl, 10 mM $MgCl_2$ at 37^0C. Kinase reaction was started by the addition of ATP (100µM) and a small aliquot of the reaction mixture was taken out at 30 or 60 min to measure the phosphorylation status of BSA by immunoblotting using anti-phosphoserine antibodies and the signal was quantified by Image lab (Bio-Rad laboratories, USA). To explore the proteinous substrates from human erythrocytes, RBC ghost lysate was prepared by treating with 0.01% Triton X-100. The lysate (150 µg/ml) was incubated with FIKK9.1 (80µg/ml) in 100 µl reaction buffer 20 mM Tris pH7.4 containing 100 mM NaCl, 10 mM $MgCl_2$ at 37^0C. The kinase reaction was started by the addition of ATP (100 µM) and

after 30 mins the reaction was stopped by keeping it at -20°C. The phosphorylated proteins in RBC ghosts were identified by immunoblotting using anti-phosphoserine antibodies.

2.2.14 Identification of Substrate Binding Pockets on FIKK9.1

To identify the potential substrate-binding regions within FIKK9.1, the available pockets present on the surface of the protein were analyzed using Fpocket (https://mobyle.rpbs.univ-paris-diderot.fr/cgi-bin/portal.py#forms::fpocket), PocketDepth (http://proline.physics.iisc.ernet.in/pocketdepth) and Pocket-Finder (http://www.bioinformatics.leeds.ac.uk/pocketfinder) server (Kalidas and Chandra, 2008). The best pockets were selected based on the volume of the pocket, surface chemistry, and closeness with bound ATP to accept terminal phosphate to facilitate kinase reaction.

2.2.15 Identification of substrate for FIKK9.1

In the interest to identify a suitable substrate for FIKK9.1, the identified pocket's surface was characterized. Pocket-10 has a surface area of 1344 $Å^2$ and it can be able to accommodate 15mer polyalanine peptides (http://proline.physics.iisc.ernet.in/pocketdepth/). The 15mer polyalanine model was prepared with the help of Modeller 9v15 through the EasyModeller interface using PDB ID 5LIJ as a template. Modeled peptide was docked into pocket-10 using PATCHDOCK webserver (https://bioinfo3d.cs.tau.ac.il/PatchDock/). FIKK9.1-polyalanine peptide complexes were analyzed considering Atomic Contact Energy (ACE) and binding score. Based on the molecular interaction of the bound peptide with FIKK9.1, combinatorial peptide libraries with 286 different peptides were generated with an intelligent guessing approach. Similar fitting of peptides into the pocket-10 was performed and results were sorted based on Atomic Contact Energy (ACE) and binding score. The interacting profile was examined using ContPro and docked conformations were visualized using Pymol version 1.7.4 (Educational user module).

2.3 Results

2.3.1 FIKK9.1 is a Ser-Thr kinase with unique features to exploit as a drug target

FIKK kinases are restricted only to *Plasmodium sp.* and their absence in other organisms makes them an excellent target to explore for drug development (Leroy and Doerig, 2008). The multiple Sequence Alignment (MSA) of FIKK9.1 with CHK2, CIPK3, HuAMPK, HuMARK3, and HuTITIN was performed using MAAFT MSA program (Katoh et al., 2002). The protein-protein

blast results indicate that the residues from 1-200 do not show any similarity (Figure 2.1 A) with other known proteins whereas the region from 201 to 542 residues gave high level of sequence similarity with diverged sequence (Figure 2.1 B). Specifically, the region from 284-382, 414-422, 457-477, and 507-542 is highly conserved (represented in yellow to red color code) whereas regions from 217-265, 385-397and 422-446 have diverged from other proteins (Violet-to-Blue color code). The c-terminal catalytic domain (230 to 542) of FIKK9.1 has eleven sub-domains with similarity to other protein kinases except for distinct features in two sub-domains. The glycine triad is absent in subdomain-I whereas arginine is replaced by leucine in the activation loop (HLD loop instead of HRD). The conserved motif SELYG (312-315), PENILI (365-370), and DFG (379-382) whereas diverged regions HLD (359-362) and PPE (418-420) are present in FIKK9.1 and these variations may play a vital role in catalysis (Figure 2.1 B). The conserved region 242-382 provides a suitable docking site for nucleotide (ATP) to catalyze the kinase reactions. The highly diverged sequences of FIKK9.1 makes it as excellent target to develop antimalarial and as well suitable biomarker for diagnostics (Figure 2.1 C).

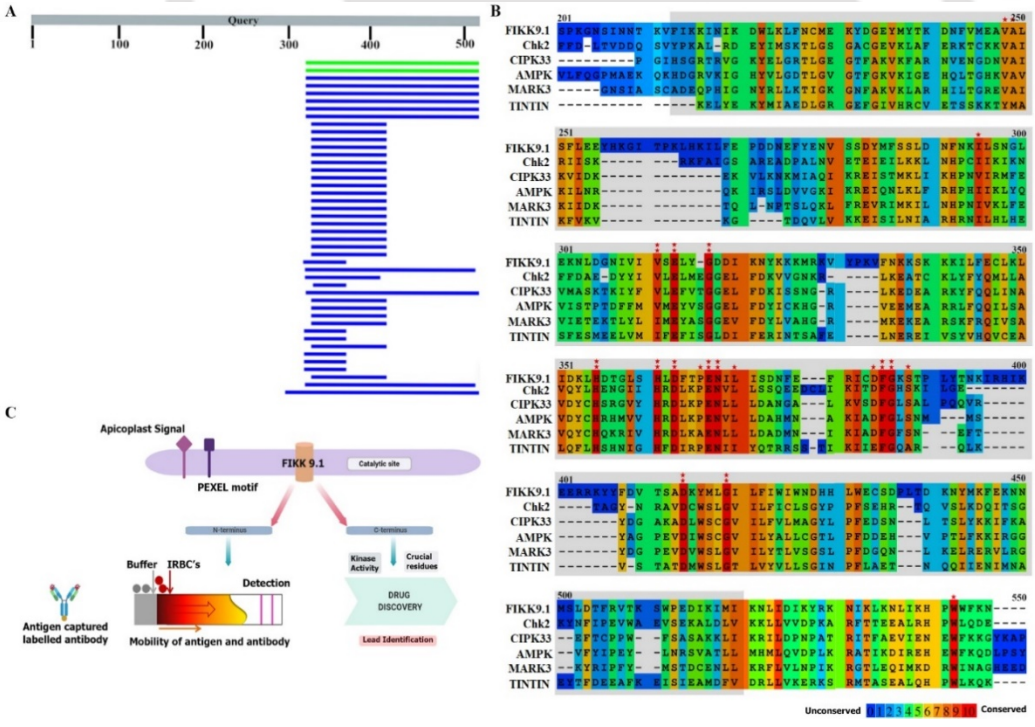

Figure 2.1 FIKK9.1 kinase has the potentials in drug discovery and diagnostics. (A) FIKK9.1 has a unique N-terminal region with no similarity to existed proteins in the database. The FIKK9.1 N-terminus region (1-213 residues) was blasted into the NCBI database and it didn't pick up any candidate protein from the database. (B) The C-terminus of the protein has a functional kinase domain with exclusive features to exploit the kinase as a drug target. The

multiple sequence alignment of the C-terminus region (214 to 512 residues) was performed using MAFFT with (Checkpoint Kinase 2) CHK2, (CBL-interacting ser/thr protein kinase 3) CIPK3, (Human AMP-activated protein kinase) HuAMPK, (Human Microtubule Affinity Regulating kinase 3) HuMARK3 and (Connectin) HuTITIN. The amino acids are shaded with different colors ranging from violet to red according to the similarity score. The most conserved residues in the nucleotide-binding domain of the C-terminus (243 to 443 residues) were denoted with asterisks. (C) The proposed role of FIKK9.1 in drug discovery and diagnostics. FIKK9.1 has two regions; the unique N-terminus region has no homology and can be exploited in the diagnosis of the disease whereas the c-terminal region is catalytically active with distinct features from host proteins to exploit as a drug target.

The first criterion of protein as a drug target is to have a distant relationship with the host proteins. The evolutionary relationship between FIKK9.1 and other proteins was done by the Neighbor-Joining method using EMBL Simple Phylogeny (https://www.ebi.ac.uk/Tools/phylogeny/simple_phylogeny/) and further improved by iTOL (https://itol.embl.de/tree/). The evolutionary analysis of FIKK9.1 depicts that it is present within the cluster representing apicomplexan orthologs (FIKK) kinases but it is distantly related from other eukaryotic proteins such as MAPK (Humans), KKQ8 (*C. cerevisiae*), AGC, CAMK kinases with a distance of 0.5 (Figure 2.2). Hence, bioinformatics and phylogenetic analysis indicate that FIKK9.1 has several biochemical features that can be used to design better antimalarials.

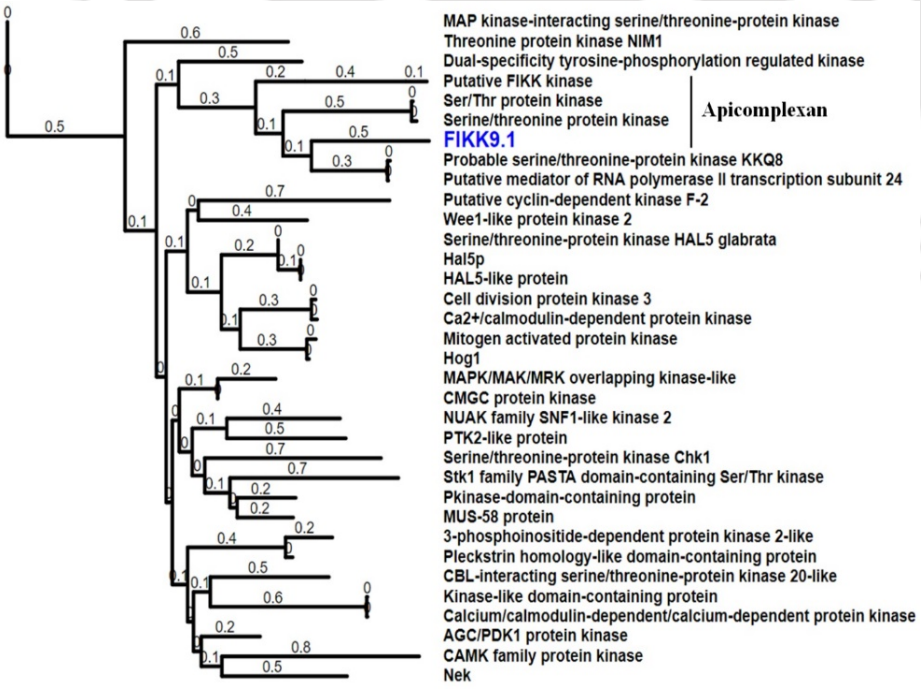

Figure 2.2: FIKK9.1 has a distant relationship with proteins present in the host. Phylogenetic Tree of FIKK9.1. The hierarchical clusters of homologs pairs were illustrated in a

0.1 scale tree distance. The dendrogram representation shows FIKK9.1 (Blue) is close to other proteins from apicomplexan but it is highly divergent from other eukaryotic kinases.

2.3.2 Overall Structure of FIKK9.1

The modeled structure obtained from I-TASSER is good with a significant confident score (C-Score) of -2.70. The 3-D molecular model of FIKK9.1 possesses two distinct domains; the unique N-terminal domain ranging from 1-212 and the C-terminal Catalytic domain present from 217 to 542 residues (Figure 2.3 A). The N-terminal and C- terminal domain are connected by the FIKK motif (213 to 216 residues) which is conserved throughout the FIKK kinase family. The secondary structure elements of the N-terminal domain comprised of seven β-sheets with three intermittent α-helices similar to the Forkhead associated (FHA) domain. The seven β-sheets of FHA like domain contains four strands β1 (56-62), β3 (75-71), β5 (141-146), and β7 (198-199) parallel to each other whereas the other four β2 (65-71), β4 (131-135), and β6 (175-177) are antiparallel to initial strands. The FHA-like domain shows a twisted β-strand structure which is a core architect of this kind to bury the hydrophobic regions (Durocher and Jackson, 2002). Whereas, the c-terminal catalytic domain contains two lobes (N-lobe and C-lobe) and the nucleotide substrate is present on the interface of both lobes.

The overall surface charge distribution shows FIKK9.1 consists of around 18% of amino acids which are basic in nature (figure 2.3 B). The formal charge of the N-terminus was calculated as +8.0 whereas, in C-terminus, it had a +11.0 charge, and surprisingly the active site which accommodates negatively charged ATP had a -1.0 charge. The pI of the protein was calculated as 8.79 using Prot Pi server (https://www.protpi.ch/Calculator/ProteinTool). Similar to other kinases, the N-lobe of the catalytic domain is folded into five stranded antiparallel β-sheet (β1 - 241 to 243, β2- 248-255, β3- 258-266, β4- 301-303, and β5- 306-311) and single α-C helix (276-287 residues) with the absence of glycine-rich loop region. The C-lobe is predominantly found to be helical in nature, consisting of highly conserved lysine residues (K 320 and324) and DFG (380 to 382 residues) motif (Figure 2.3 C). The two lobes are connected through a hinge region ranging from 223-245 residues. The hydrophobic residues forming β1 (P243) and loop (V244/M245) are present in the hinge region of the N-lobe to stabilize the adenine moiety of ATP whereas positively charged residues (K320, K324, and R431) of C-lobe interacts with the negatively charged phosphate group of the bound ATP. All the described features of the catalytic domain are mostly identical to well-characterized protein kinases such as CHK2, PKA, and MST

kinase. The surface charge distribution in and around the binding cavity formed between the lobes may provide a good binding site for ATP binding (Figure 2.4).

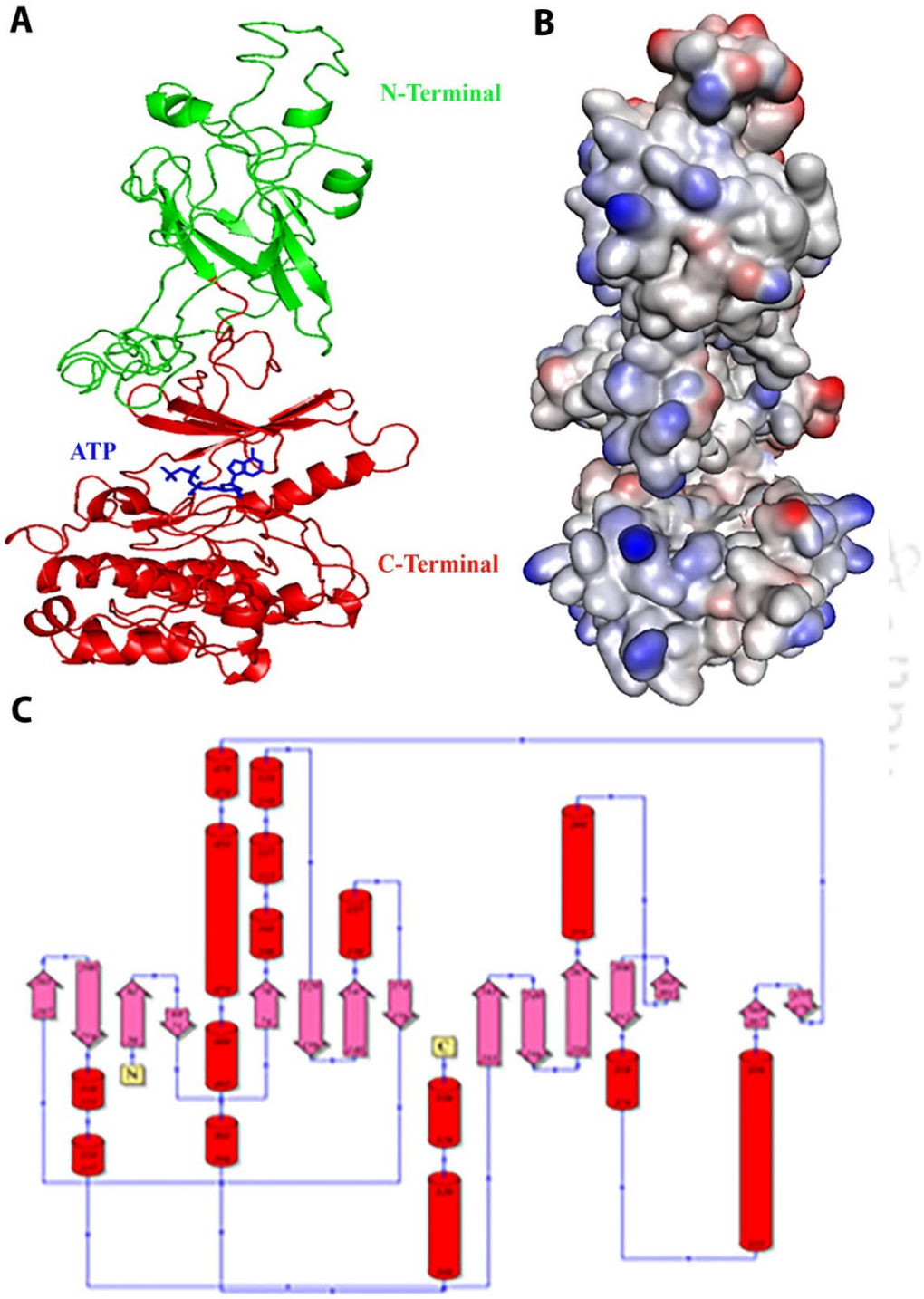

Figure 2.3: Structural Characterization of FIKK9.1 kinase from *Plasmodium falciparum*. (A)Molecular model of FIKK9.1. The 3-D structure of FIKK9.1 was represented in the ribbon model along with bound ATP in the ball and stick model. (B) The charge distribution on the

surface of the FIKK9.1model. The positive charge surface is depicted with red and negative charges with blue. (C) Topology diagram of FIKK9.1.

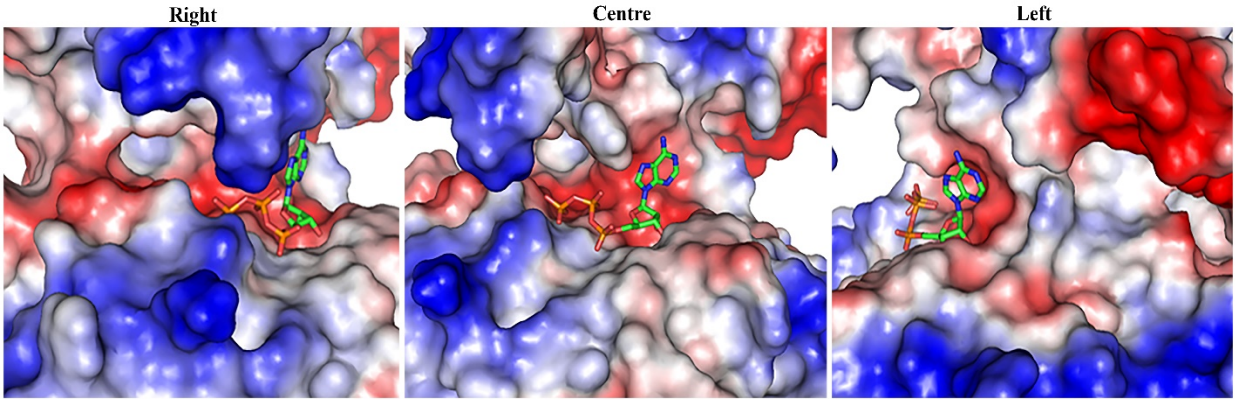

Figure 2.4: The view of the active site of FIKK9.1 with bound ATP. The active site cavity with the distribution of charge is represented in 3 modes; left, center, and right view of the protein model for more details.

In the model is validated using Ramachandran plot, Verify 3D and Errat plot. We observed more than 91% of residues were in the allowed region of Ramachandran plot (Figure 2.5).

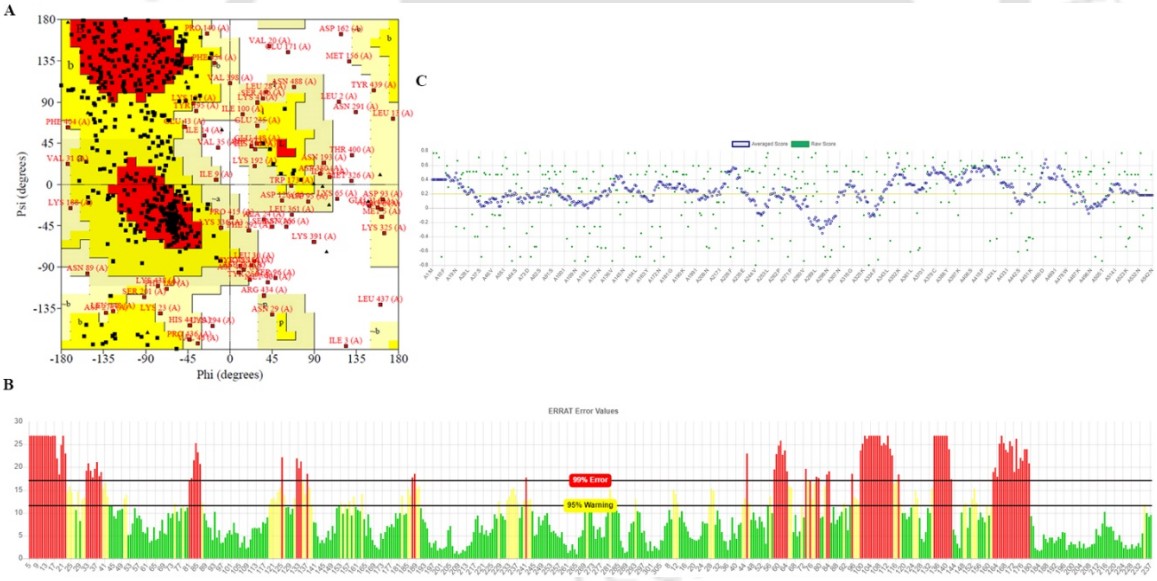

Figure 2.5: Validation of FIKK9.1 model structure. (A) Ramachandran plot analysis of FIKK9.1 structure. (B) Verify 3D analysis and (C) Errat plot**.**

2.3.3 FIKK9.1 has biophoric features for ATP

ATP biophore environment is well known in most of the kinases but the absence of crucial features in the FIKK family urges us to understand the novel pharmacophore environment to identify the specific inhibitor molecules for developing novel antimalarials. ATP fingerprinting

analysis on available kinase structures bound with ATP (1ATP, 3A7H, 3DKC, 3DY7, 3TLX, 4FG8, 4GT3, 4XW5, 5DN3 and 5XVU) reveal Alanine (A), Asparginine (N), Glycine (G), Valine(V) and Aspartic acid (D) as most recurring and crucial amino acids for interaction with ATP atoms (Figure 2.6 A). As seen in the most recurring amino acid of other template kinases, an ATP binding environment was observed in the FIKK9.1 model. It mainly constitutes hydrophobic residues that ensure ATP fits in the proper orientation as typical kinases (Figure 2.6 B). The alignment of negative and positive charged residues provides the overall charge of -1.0 within the binding pocket to facilitate ATP binding (Figure 2.6 C).

A

	LEU	ILE	GLY	THR	LYS	GLU	ARG	ALA	GLN	HIS	SER	ASN	PHE	VAL	TYR	ASP	CYS	MET	PRO	TRP
cAMP	1	0	1	1	1	1	1	1	0	0	1	1	1	1	1	1	0	1	0	0
MST	0	1	1	1	1	1	0	1	0	0	1	1	1	1	1	1	0	1	0	0
EKR2	0	1	1	1	1	1	1	1	1	0	1	1	0	1	0	1	1	1	0	0
METRT	0	1	1	0	1	0	1	1	0	1	0	1	1	1	1	1	0	1	1	0
CDPK	1	0	1	1	1	1	0	1	1	0	1	1	1	1	0	1	0	1	0	0
PKAc	1	1	1	1	1	1	1	1	0	0	1	1	1	1	1	1	0	1	0	0
Aurora	1	0	1	1	1	1	0	1	1	0	0	1	1	1	1	1	0	0	0	1
pfCK2	1	1	1	0	1	1	1	1	0	1	1	1	1	1	1	0	0	1	0	1
MEK1	1	0	1	0	1	1	0	1	1	1	1	1	0	1	0	1	1	1	0	0
Adenylate	1	1	1	1	0	0	1	1	1	1	1	1	0	0	0	1	0	0	1	0
	7	6	10	7	9	8	6	10	5	4	8	10	7	9	6	9	2	8	2	2

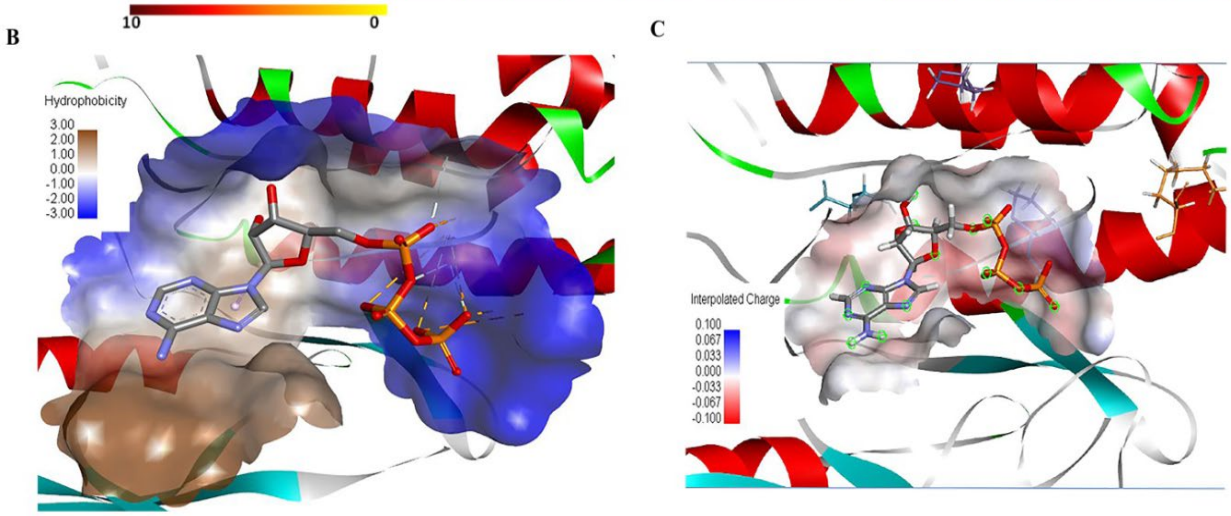

Figure 2.6 Mapping of ATP biophore. (A) The occurrence of different amino acid residues in ten ATP bound protein crystal structures present in Protein Data Bank (www.rcsb.org). The color code yellow to red details the increment propensity of amino acid represents with value (0 to10). (B) The colour density map represents hydrophobicity of ATP binding pocket in FIKK9.1 and (C) The charge distribution of FIKK9.1 in the ATP binding region.

The hydrogen bonding (Green, Yellow, and Orange) and hydrophobic interaction (Violet, Red, and Cyan) between ATP and amino acid residues were examined (Figure 2.7).

Figure 2.7. Fingerprint constituents of Protein-ATP complexes: The matrix of 101*31 atoms involved in protein-ATP complexes are extrapolated and represented as different color coding

depends on the nature of bonding concerning distance. The hydrogen bonding between atoms is represented in green, yellow, and orange whereas hydrophobic interaction is represented in purple, red, and cyan concerning distance.

Based on the distance matrix analysis we found the interaction between Ala (CB-N6, CB-N1, and CB-C6), Val (CG2-O4', CB-O4'), Met (CE-N7), and Glu (O-N6) with ATP atoms are recurring in eight out of ten proteins. The interaction of Ala (CB-N6), Met (CE-N7), and Glu (O-N6) stabilize the adenine and ribose moiety of ATP. The hydrogen bonding and salt bridge formation by Lys (CE-O2A) and Gly (CA - O1G, O2B, O3A and O4') with ATP atoms play a major role in transferring γ-phosphate to substrates. All the interactions are found to have the average bond length within a 4.0 Å region. The detailed atomic interaction analysis of the ATP co-crystal structure helps in understanding the possible microenvironment favoring binding of ATP in kinases. The cavity present between N and C lobes of the FIKK9.1 catalytic domain possesses biophoric elements to facilitate the efficient binding of ATP. The cavity comprised of a typical hydrophobic pocket lined by F243, V244, M245, I433, and I443, conserved lysine region (K320 and 324) and presence of DFG (379 to 382 residues) motif which decides the fate of kinases to be either active or inactive (Treiber and Shah, 2013). The uniqueness of FIKK kinases arose with the absence of a glycine triad which stabilizes the phosphate group of ATP for transferring γ-PO_4 to the substrate. In more than 95% of kinases, the loss of the conserved glycine triad leads the protein from the active state to inactive (McNamara et al., 2011). To find the FIKK9.1 interaction with ATP and to validate the ATP biophore in FIKK9.1, the molecular docking tool was used to generate FIKK9.1-ATP molecular model. The ATP was found to be binding and fitting into the catalytic pocket of FIKK9.1 with a binding energy of -6.13 kcal/mol. Surprisingly, most of the interacting features are matching well with other kinases, the adenine group of ATP surrounded by hydrophobic pocket possesses V244 and M245 residues (Figure 2.8 A).

The atomic interactions between Met 245 (CA/C – N1, C6, and C2 with an average distance of 3.55 Å) and Val 244 with ATP supports the adenine moiety, the ribose group is stabilized by Ile 443 and Asp 445 while Asn 321, Lys 320, and Lys 324 anchors the phosphate group. The residues K320 and K324 form hydrogen bonds and salt bridges with triphosphate groups in ATP atoms to provide stability through electrostatic interaction. The DFG motif present at the inner core of the binding pocket further supports ATP binding. The presence of positively charged

residues next to the phosphate group of ATP neutralizes the charge and stabilizes the triphosphate group.

2.3.4 FIKK9.1 has a distinct kinase domain to exploit as a drug target

The catalytic domain of FIKK9.1 (241 to 542) is structurally compared with the well characterized human protein kinase families such as cAMP-dependent kinase (1ATP), Calcium-dependent protein kinase (4FG8), Checkpoint kinase 2 (3I6U), and Dual specificity tyrosine phosphorylation regulated protein kinase 2 (3K2L). These proteins are frequently used to describe the structural difference and accessing active forms in novel kinase structure. Out of eleven conserved motifs, αC-helix and A-loop are important elements for protein kinases to be active (Vijayan et al., 2015), in FIKK9.1 both these motifs are structurally similar to other human kinase proteins. Superimpose of FIKK9.1 with other proteins displaying larger differences in N-lobe and substrate binding region on C-lobe with an RMSD ranges from 1.38 - 3.2 Å. cAMP-dependent kinase and Checkpoint kinase 2 are found to be most closely related structural kinases to FIKK9.1 with an RMSD of 1.38 Å and 1.52 Å respectively. The differential amino acid residues at ATP binding regions (under 4 Å) in human protein kinases (G50, G52, G55, M120, and K168) and FIKK9.1 (S312, K320, T364, and C379) leads to a subtle change in ATP binding pocket (Figure 2.8 B). The differences in ATP binding pockets and other locations of FIKK9.1 kinase might be relevant to exploit and design plasmodium-specific inhibitors.

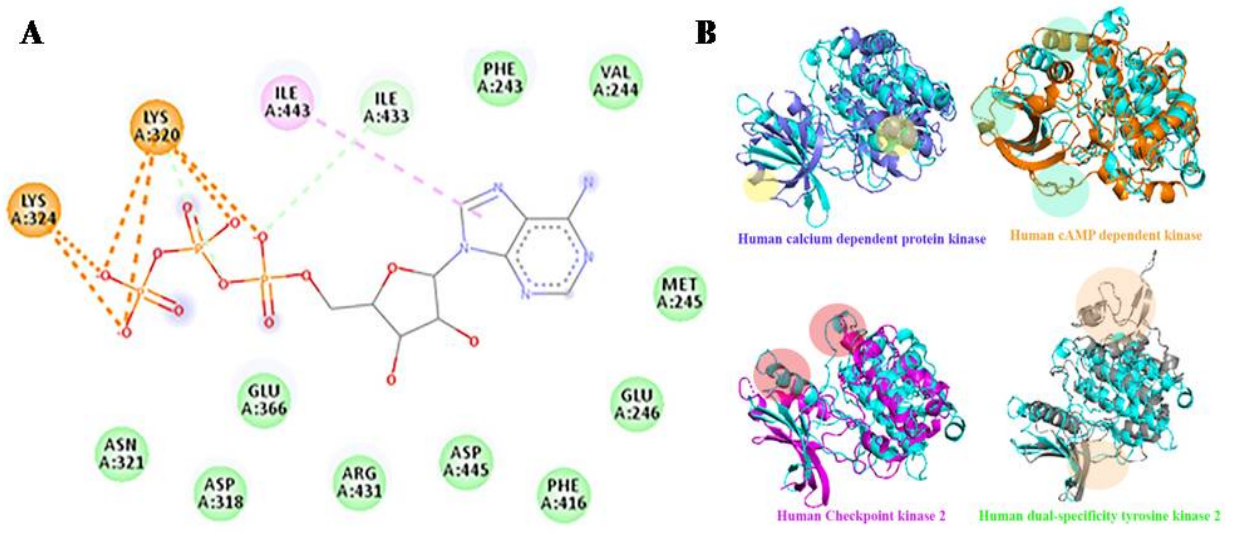

Figure 2.8: (A) Interaction of ATP docked within FIKK9.1 with amino acids crucial for ATP binding and catalysis. (B) FIKK9.1 has features of prospective drug target

2.3.5 Cloning, Over-expression, and Purification of FIKK9.1

To over-express FIKK9.1 in the *E. coli* expression system, a codon-optimized *fikk9.1* gene was synthesized for *E. coli* as a heterologous expression system. The cloned gene was failed to be expressed as a full length in BL21 (DE3) or in other *E. coli* expression strains and we could observe the degradation of protein with four bands in SDS-PAGE (data not shown). We assumed that it could be due to two possible reasons: firstly, the presence of apicoplast targeting sequence (1-27) and secondly, due to cryptic translational in *E. coli* (Jennings et al., 2016). We have amplified the *fikk9.1* gene excluding the apicoplast targeting sequence using site-specific primers. The PCR amplification yields a DNA fragment of ~1.6 Kbp on 0.8% agarose gel and it matches well with the expected DNA size 1544 bp (Figure 2.9 A, Lane 1). Double digestion of pET28a fikk9.1 clone with *BamHI /Xho-I* yield a fragment of ~1.6 Kbp (Figure 2.9 B, Lane 2) which was completely absent in digested pET28a vector (Figure 2.9 B, Lane 1) confirming the presence of *fikk9.1* (without Apicoplast targeting sequence) gene into the expression vector pET28a. The clone was further confirmed by DNA sequencing (data not shown) and it matches well with the nucleotide sequence of FIKK9.1 (https://plasmodb.org/plasmo/app/record/gene/PF3D7_0902000). The bacterial culture was induced with 0.5 mM IPTG under 37°C for optimal expression of FIKK9.1. After 3 hr of induction bacterial cells were harvested and expression was analyzed from un-induced and IPTG induced culture on 10% SDS-PAGE. A protein band with molecular weight ~66 kDa is observed in induced culture whereas the same band was completely absent in un-induced bacterial culture which denotes the expression of FIKK9.1 (Figure 2.9 C, Lane U & I). The induced bacterial pellet was lysed by mild sonication for 2 min (2 sec on/18 sec off) and the supernatant and pellet fractions were prepared. The cytosolic soluble (S) fraction and pellet (P) fraction were analyzed on a 10% SDS PAGE. The densitometric analysis of FIKK9.1 protein band in soluble or insoluble Pellet (Figure 2.9 C, Lane S & P) fractions indicates that the protein is mostly present in the soluble cytosolic fraction. The immune-reactive bands present in different fractions correspond to the molecular weight of ~66 kDa and indicate the presence of FIKK9.1 in the soluble fraction (Figure 2.9 C, lower panel). For purification of FIKK9.1, bacterial culture was allowed to grow in 500 ml LB medium up to 0.6 OD and then induced with 1mM IPTG for 3 hrs. Post induction, the resulting bacterial pellet was lysed by sonication for 45 min (5 sec on/20 sec off) at 4°C. Subsequently, the lysed bacterial cells were centrifuged at 13000 rpm for 30 min at 4°C to obtain clarified lysate. The clarified bacterial

lysate containing FIKK9.1 was loaded onto the Ni-NTA affinity column pre-equilibrated with re-suspension buffer. The column-bound protein was eluted by a step gradient of imidazole and protein starts eluting at 300 mM imidazole. No other proteins were found in 300 mM fractions and a single band of ~66 kDa was obtained in SDS PAGE as well as western blotting confirming the purification of FIKK9.1 to homogeneity (Figure 2.9 D). The immune-reactive bands present in different fractions correspond to the molecular weight of ~66 kDa and indicate the presence of FIKK9.1 in different fractions (Figure 2.9 D, lower panel). The yield of FIKK9.1 was found as ~2.5 mg purified protein from one liter of bacterial culture.

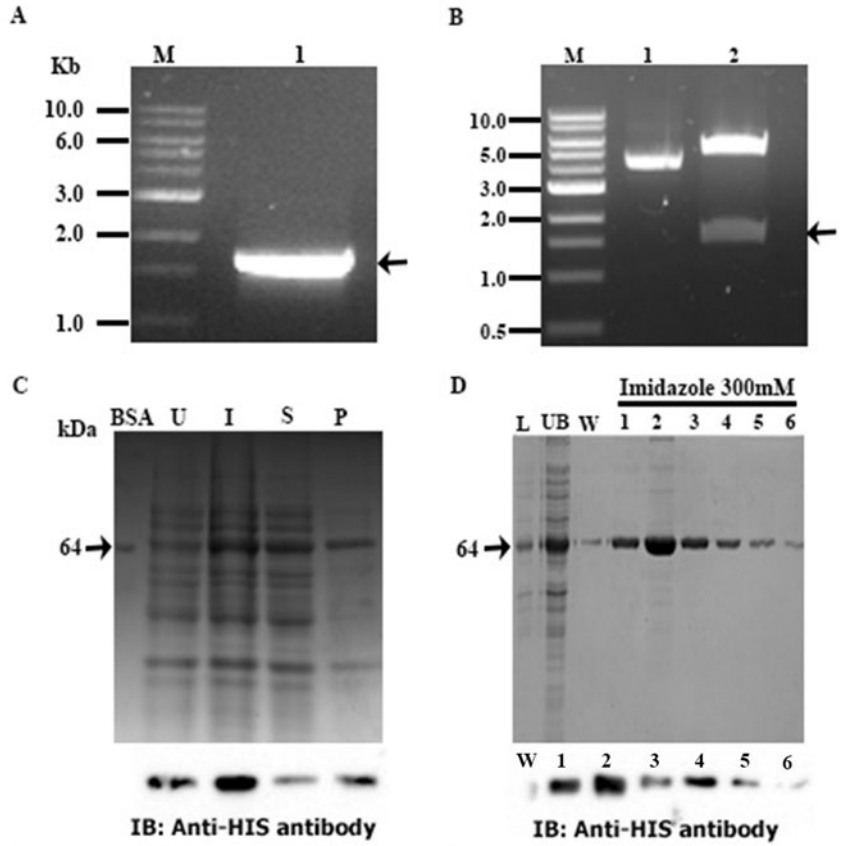

Figure 2.9: Cloning, overexpression, and purification of FIKK9.1. (A) The PCR amplification of the FIKK9.1 gene using site-specific primers. (B) Confirmation of FIKK9.1 clone into pET28a by restriction digestion by *BamHI and XhoI*. Double digestion of pET28a recombinant plasmid with BamHI/XhoI gives a 1.6 kb DNA band compared to the undigested pET28a. (C) Over-expression of FIKK9.1 in *E. coli* BL21 (DE3) by inducing with 0.5mM IPTG at 37°C. Un-uninduced, I-Induced, P-pellet fraction, S-Supernatant. (D) Purification of recombinant FIKK9.1 using Ni-NTA affinity chromatography. L-Load, UB- Unbound, W-wash, and eluted fractions 1-6. The cell lysate was analyzed on 10% SDS-PAGE followed by western blotting using an anti-poly histidine antibody.

2.3.6 FIKK9.1 is a monomeric protein and has distinct secondary structural elements

Earlier it was reported that FIKK4.1 and the catalytic domain of FIKK8 were monomeric to exhibit efficient phosphorylation of substrates (Kats et al., 2014; Osman et al., 2015). Therefore, it is crucial to explore the oligomeric nature of FIKK9.1 and the proper folding of protein over-expressed in a bacterial expression system. The purified FIKK9.1 was analyzed on Superose-12 HR10/30 size exclusion chromatography column as described in "material and methods". The chromatogram of FIKK9.1 after the gel filtration column gave two prominent protein peaks; first small peak at 8.2 ml, 2nd large and sharp peak at 10.2 ml, and few noise peaks at the end of the column, probably due to the presence of salt. The 1st peak was very close to the void volume (8.16 ml) and this peak might be due to high order protein contaminant or aggregated protein. The 2nd peak was corresponding to the molecular weight of 60.06 ± 1.6 kDa. It was collected and analyzed on SDS PAGE and it was giving a protein band corresponding to FIKK9.1 kinase (Figure 2.10 A). The results from gel filtration column chromatography indicate that FIKK9.1 is properly folded into the native conformation and is a monomeric protein kinase.

In the recent past, several attempts failed to crystallize *cp*FIKK (*Cryptrosprodium parvum*) orthologous and *Pf*FIKK8 kinase with good resolution (Osman et al., 2017) which limits the FIKK family to be explored as a drug target. Therefore, to understand the structural elements of FIKK9.1, CD spectroscopy was carried out. The analysis of the CD spectrum of FIKK9.1 indicates three major transitions: First, a negative band near 220 nm, which is due to the strong hydrogen-bonding environment and suggests the presence of helices. The 2nd transition was observed at 190 nm which is split into a positive band near 192 nm and a negative band near 208 nm. At last, due to β-sheets, there was a negative band near 215 nm and a positive band between 195 and 200 nm (Figure 2.10 B). The analysis of the CD spectrum with K2D3 indicates that FIKK9.1 possesses 27.24% α-helix, 20.32% β-sheet, and 52.44% random coils. The presence of a significant percentage of β-sheets in FIKK9.1 matches well with its similarity with the FHA domain.

2.3.7 FIKK9.1 interaction with ATP

The direct binding of ATP to the FIKK9.1 was done using isothermal titration calorimetry. The binding of ATP to the FIKK9.1 is associated with the release of heat (Figure 2.11 A). The curve fitting results indicate that the stoichiometry of interaction between FIKK9.1 and ATP is 1:1.

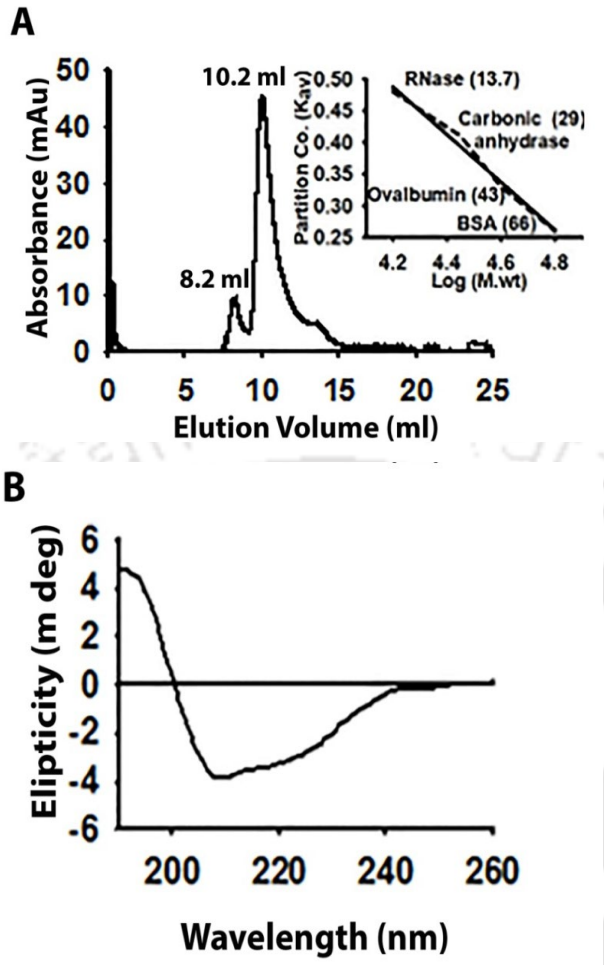

Figure 2.10: (A) FIKK kinase is a monomeric protein kinase. Purified FIKK9.1 was resolved on gel filtration column Sephacryl S12 and a sharp peak at 10.2 ml represents eluted protein with native molecular weight 60±1.6 kDa. The gel filtration column was calibrated with different standard proteins as described in "material and methods". **(B) FIKK9.1 kinase is a properly folded protein with defined secondary structures.** The far UV Circular dichroism (CD) Spectra of purified FIKK9.1 kinase was recorded in a spectral range of 180-250 nm.

The thermogram analysis showed the dissociation constant of ATP with FIKK9.1 as 45.6 ± 2.4 µM and observed favorable entropic contributing to binding (TΔS = -0.11 kcal/mol/deg). Similar dissociation constant values of FIKK9.1 kinase with ATP are also reported for other protein kinases with ATP. Even with K_d>100 µM, favorable condition for binding of the kinases with ATP was reported and is also proven through a crystal structure of ATP bound kinase (Hartmann et al., 2006; Rosado et al., 2013). The docking of ATP with FIKK9.1 shows that it fits nicely into the binding pocket with extensive interaction between FIKK9.1 and ATP (Figure 2.11 B).

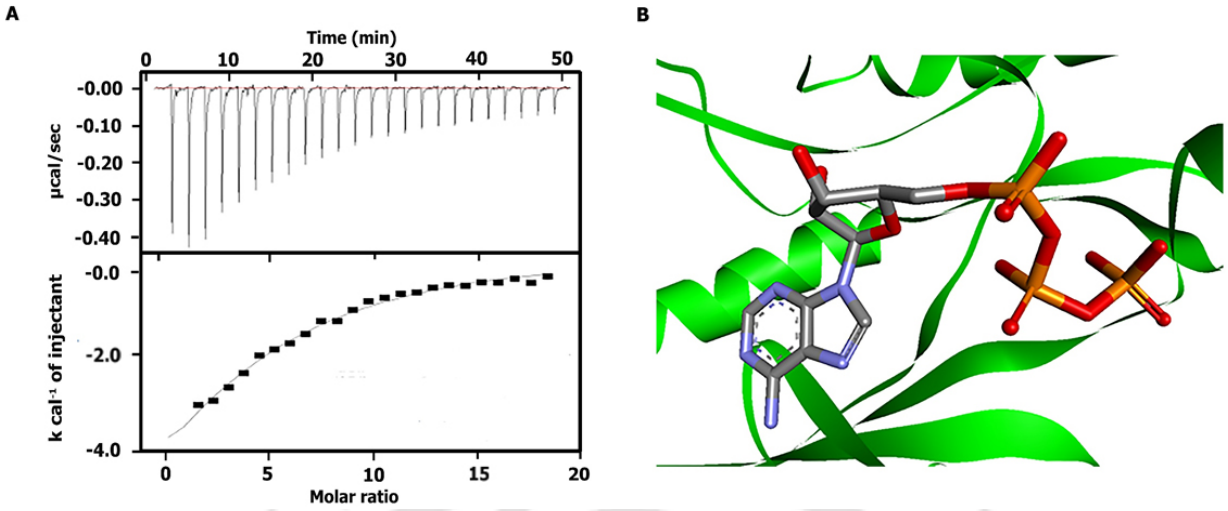

Figure 2.11: (A) ITC thermogram of FIKK9.1 with ATP. The interaction analysis of ATP with FIKK9.1 using isothermal calorimetry. Purified FIKK9.1 was titrated with different concentrations of ATP and heat exchange was measured until saturation was achieved. **(B) 3-D molecular model of the FIKK9.1-ATP complex.** ATP fits nicely into FIKK9.1 active cavity with extensive interactions.

2.3.8 FIKK9.1 is an active serine/threonine kinase

The apicoplast targeting sequence and PEXEL motif present in FIKK9.1 might help the protein in trafficking to different locations within the infected RBCs. The transportation of proteins to various compartments favors the establishment of several interaction networks within the infected RBCs (Brandt and Bailey, 2013; Lalle et al., 2011; Nunes et al., 2007). The cloned, overexpressed and purified FIKK9.1 kinase is monomeric, properly folded, and probably catalytically active. To explore the kinase activity of purified FIKK9.1, we have used BSA as a substrate. The kinase assay was carried out in reaction buffer 50 mM Tris pH 7.4 containing BSA (100 µg/ml), MgCl2 (1 mM), FIKK9.1 (native or denatured), and the reaction was initiated by the addition of ATP (100 µM). The reaction mixture was incubated at 37^0C for 30 or 60 min and was stopped by bringing down the temperature to -20°C. Further, the reaction mixture containing BSA was resolved on SDS-PAGE and phosphorylated BSA was detected using an anti-phosphoserine antibody. Initially, the reaction was carried out with a mixture containing BSA but not FIKK9.1CD2. The absence of a phosphorylated signal completely ruled out the possibility of phosphorylation of BSA by ATP directly (Figure 2.12, S1). While the reaction was allowed to continue in presence of active native FIKK9.1CD2, phosphorylated BSA signal appeared at 30 min (Figure 2.12, S2) and the relative intensity of the signal obtained was set to

1.0. Similarly, phosphorylation signal was completely absent in the reaction mixture containing heat-inactivated denatured FIKK9.1CD2 or no ATP. Therefore, the calculated relative intensity tends to be 0 (Figure 2.12, S3 & S4). Surprisingly almost one fold of the phosphorylation signal is significantly reduced when the kinase reaction extends to go further till 60 min (Figure 2.12, S5-S8). The kinase assay data indicate that the cloned FIKK kinase is catalytically active and it may show better kinase reaction with its natural substrates within infected RBCs.

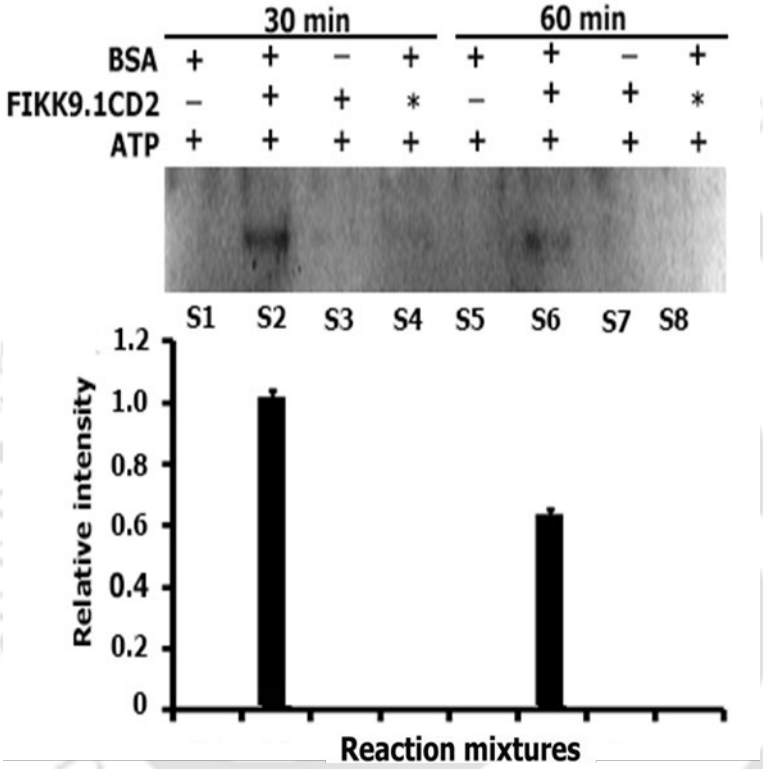

Figure 2.12: FIKK9.1 is a protein kinase. The purified FIKK9.1CD2 was incubated with BSA as substrate and BSA phosphorylation was measured by western blotting using anti-pSer antibodies. The immunoblot denotes a strong phosphorylation signal from phosphorylated BSA at 30min in presence of FIKK9.1CD2 (+) whereas there was no signal in the absence of FIKK9.1CD2 (-) or performing kinase reaction in presence of heat-denatured FIKK9.1 CD2 (*). The subsequent down panel shows the relative measurement of the signal obtained.

2.3.9 FIKK9.1 is localized to cytosol and Apicoplast within infected RBCs

To acquire precise knowledge on the cellular localization of FIKK9.1 in infected RBCs at different stages, we performed an immunolocalization assay on Pf3D7 using an anti-FIKK9.1 antibody. The fluorescence pattern is observed to change during various erythrocytic stages of the parasite.

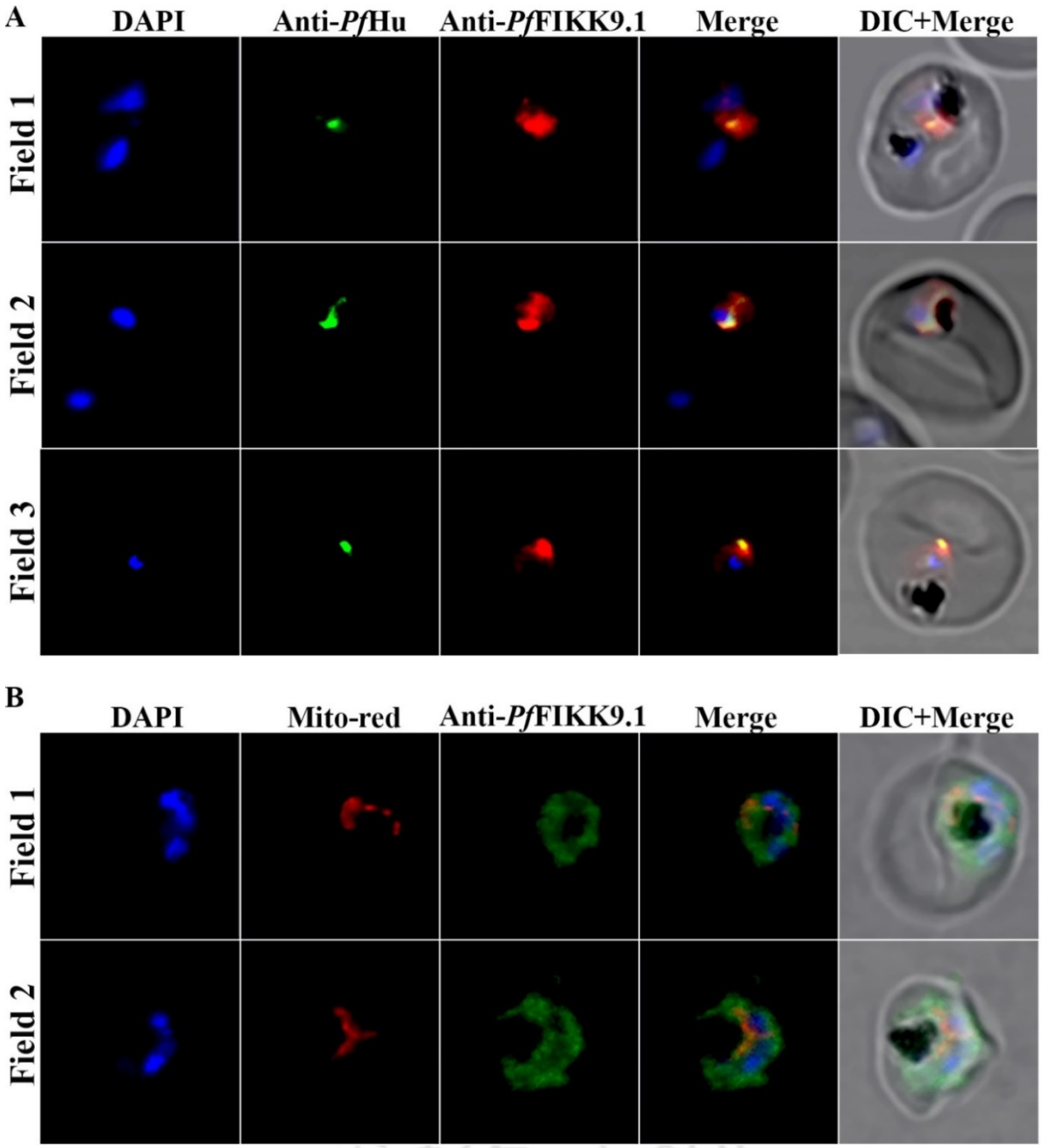

Figure 2.13: FIKK9.1 is an excellent drug target to develop antimalarials. (A) Colocalization of FIKK9.1 with apicoplast organelle marker protein. The cellular localization of FIKK9.1 in infected RBCs is identified by Immunofluorescence assay using an anti-FIKK9.1 antibody. The fluorescence signal obtained from FIKK9.1 is merged with anti-*pf*Hu protein (apicoplast marker) suggests FIKK9.1 association with apicoplast. In all the stages we observed that FIKK9.1 is localized in apicoplast and later in trophozoite and schizont stage FIKK9.1 spread throughout IRBC's cytoplasm. **(B)FIKK9.1 is not associated with mitochondria.** The punctuate dots (red) inside the parasite when stain with mito-tracker red is identified as mitochondria and the FIKK9.1

During ring and early trophozoite stages, FIKK9.1 pattern is similar to previously characterized apicoplast marker protein *Pf*Hup (Ram et al., 2008) whereas in late trophozoites a punctuate pattern spread throughout the cytoplasm of IRBC's. The punctuate pattern persists and is also observed in the periphery region of IRBC's till the schizont stage. This observation is found to be similar with the recent identification of FIKK9.1 association with murer's cleft (Siddiqui et al., 2020). To determine its association with apicoplast, colocalizing FIKK9.1 with Hup protein was carried out. In all the stages, we observed that FIKK9.1 is localized in apicoplast and also spreads to IRBC's cytoplasm in trophozoite and schizont stage FIKK9.1. Furthermore, the fluorescence signal is lost when parasites become matured into multinucleated schizonts (Figure 2.13 A). The signal (green) spread throughout IRBC but not merged with MR signal reveals FIKK9.1 is not trafficked to mitochondria. No overlap is seen with the mitochondrial marker Mitotracker Red (Figure 2.13 B).

Although previous identification of FIKK9.1 is associated with murer's cleft, our study reveals FIKK9.1 is explicitly targeted towards apicoplast. To ensure subcellular localization of FIKK9.1, a thermolysin protection assay was performed. In the presence of digitonin at low concentration the plasma membrane of parasites gets permeabilized but the organellar membranes remained intact, whereas the addition of triton X-100 leads to permeabilization of both organellar and plasma membranes. If permeabilized parasites using digitonin are treated with thermolysin, the protease digests all cytosolic protein fractions but it cannot cleave proteins present inside intact organellar membrane fractions. In the case of Triton X-100, permeabilized parasites are treated with thermolysin where digestion of both compartmentalized proteins has occurred. Moreover, the organellar and cytosolic membranes are intact when the parasites are treated with digitonin in presence of EDTA and thus both the protein fractions remain undigested (Figure 2.14). Hence this study proves that FIKK9.1 is a dual localized protein and exclusively targeted to the apicoplast. Besides the PEXEL motif, FIKK9.1 contains an APtargeting sequence to highlight the importance of FIKK9.1 for relaying downstream signaling within parasite apicoplast as well as throughout the infected RBC (outside parasite). Therefore, it is important to find the possible substrates present within the infected RBC. During ring and early trophozoite stages, FIKK9.1 pattern is similar to previously characterized apicoplast marker protein *Pf*Hup (Ram et al., 2008) whereas in late trophozoites a punctuate pattern spread throughout the cytoplasm of IRBC's.

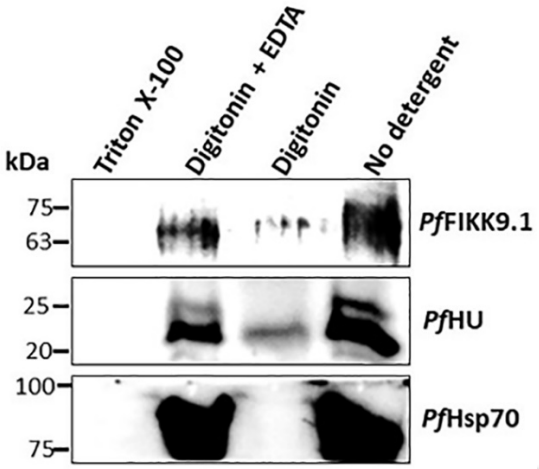

Figure 2.14: Confirmation of FIKK9.1 association with organelles. Thermolysin protection assay is performed to ensure FIKK9.1 is trafficked towards the organelle. At a low concentration of digitonin the plasma membrane of parasites permeabilized but the organellar membranes will be intact as a result FIKK9.1 organelle fraction is not degraded in presence of thermolysin. In addition of triton X-100 leads to permeabilization of both organellar and plasma membranes leads to complete digestion of FIKK9.1. The membrane is intact while the parasites are treated with digitonin in presence of EDTA which results in both cytosolic and organelle proteins to remain undigested. The assay was performed with control *Pf*Hsp70 as cytosolic fraction marker and *Pf*HU as apicoplast marker.

2.3.10 FIKK9.1 has several potential pockets for substrate binding

In the quest for identifying the substrate, the FIKK9.1 surface was analyzed to find the cavities using PocketDepth. A total of 23 pockets were found on the surface of FIKK9.1 with variable sizes. The pockets were screened based on the size, surface area and distribution of different physicochemical properties and proximity to the active site bound ATP. The surface area of the pockets varies from 514 to 1344 $Å^2$ (Figure 2.15). Based on the screening criterion, pocket 10 was found to be the most suitable as it is present near to the ATP binding site which can accommodate peptide of reasonable size and surface chemistry of the pocket can bind substrates with diversified amino acids. Pocket 10 has a surface area of 1344 $Å^2$ and theoretically, it canaz occupy 15mer polyalanine peptide. Protein-substrate interaction is influenced by the accessibility of surface area for interaction and charge distribution (Keskin et al., 2008). The pocket-10 has mixed charges (positive & negative) and hydrophobic patches throughout the cavity to provide a suitable micro-environment to facilitate the interaction with the substrate. The binding pocket is comprised of Gly 26 and Leu 29 present in the N-terminus of the protein, functionally important

residues in N-lobe from c-terminus such as Phe 243, Val 244, Met 245 and His 257 provides a strong hydrophobic environment. The amino acid residues Asp 318, Asn 321, Glu 364, and Ile 443 present deep inside the cavity in the c-lobe of C-terminus, provides a charged surface to make electrostatic contacts with the substrate.

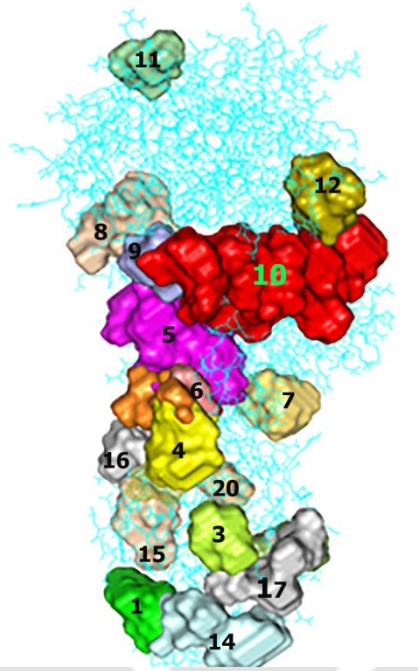

Figure 2.15 (A) FIKK9.1 possesses twenty-one possible pockets for substrate binding. Each pocket is denoted using different color codes with a specific number.

2.3.11 FIKK9.1 binding site prefers substrate with hydrophobic residues

The 3D topology of the binding pocket is used to design peptides to identify favorable interacting residues in the substrate. Initially, a 15-mer polyalanine model was built and docked into the binding pocket using the PatchDock server (Table 2.1). The polyalanine peptide fits into the binding site with an Atomic Contact Energy (ACE) of -223.02 kCal/mol. The analysis of FIKK9.1-peptide complex exhibits that the peptide is docking at the interface of two lobes (N and C) of catalytic domain with extensive interaction with N-lobe residues Phe 243, Val 244, Met 245 and His 257 and Asp 318, Asn 321, Glu 364 and Ile 443 from C-lobe (Figure 2.16, Violet peptide). Interaction analysis of polyalanine with FIKK9.1 depicts that the residues present in P1 at different positions (9, 10, 11, and 14) surrounded with negatively charged

residues from FIKK9.1 whereas residues at 1-5, 8, 12, 13, and 15 were involved in hydrophobic interactions with FIKK9.1.

Table 2.1: Molecular substitution of amino acid residues from the parent peptide to identify possible interacting residues in FIKK9.1 substrate.

PEPTIDE ID	Peptide Sequence															Score	Surface area Å²	ACE (kCal/mol)
P1	**A**	**A**	**A**	**A**	**A**	**A**	**A**	**A**	**A**	**A**	**A**	**A**	**A**	**A**	**A**	7688	1050.6	-189.08
P13	**M**	A	A	A	A	A	A	A	A	A	A	A	A	A	A	8686	1276.4	-572.34
P33	**M**	**F**	A	A	A	A	A	A	A	A	A	A	A	A	A	8890	1231	-475.27
P40	**M**	**F**	**D**	A	A	A	A	A	A	A	A	A	A	A	A	9656	1191.8	-313.78
P71	**M**	**F**	**D**	F	A	A	A	A	A	A	A	A	A	A	A	8876	1234.7	-453.62
P85	**M**	**F**	**D**	**F**	H	A	A	A	A	A	A	A	A	A	A	9960	1296.1	-277.48
P113	**M**	**F**	**D**	**F**	**H**	Y	A	A	A	A	A	A	A	A	A	8172	1050.5	-354.48
P131	**M**	**F**	**D**	**F**	**H**	**Y**	T	A	A	A	A	A	A	A	A	9372	1302	-337.74
P144	**M**	**F**	**D**	**F**	**H**	**Y**	**T**	L	A	A	A	A	A	A	A	8862	1249	-208.93
P159	**M**	**F**	**D**	**F**	**H**	**Y**	**T**	**L**	Q	A	A	A	A	A	A	8302	1237.8	-250.57
P184	**M**	**F**	**D**	**F**	**H**	**Y**	**T**	**L**	**G**	M	A	A	A	A	A	8776	1110.5	229.2
P203	**M**	**F**	**D**	**F**	**H**	**Y**	**T**	**L**	**G**	**P**	M	A	A	A	A	8490	1354	-341.98
P228	**M**	**F**	**D**	**F**	**H**	**Y**	**T**	**L**	**G**	**P**	**M**	W	A	A	A	8968	1588.5	-422.68
P236	**M**	**F**	**D**	**F**	**H**	**Y**	**T**	**L**	**G**	**P**	**M**	**W**	G	A	A	8468	1217.4	-431.11
P264	**M**	**F**	**D**	**F**	**H**	**Y**	**T**	**L**	**G**	**P**	**M**	**W**	**G**	T	A	8858	1474.1	-488.17
P277	**M**	**F**	**D**	**F**	**H**	**Y**	**T**	**L**	**G**	**P**	**M**	**W**	**G**	**T**	**L**	10420	1322.5	-241.06

Notably, the only two residues of polyalanine models A (6 & 7) were made contact with positive residues present within the binding pocket. A combinatorial peptide library of 286 peptides was generated to exploit peptide-FIKK9.1 interaction to identify possible peptides. The parent polyalanine peptide P1 was mutated with other amino acids at different positions as single, double, or triple substitutions. The substitution of amino acid residues was based on the intelligent guessing approach considering the microenvironment of FIKK9.1 binding pocket number 10.

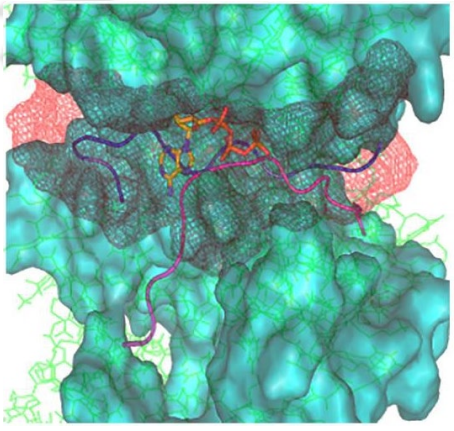

Figure 2.16: Screening of peptides from combinatorial peptide library against FIKK9.1 pocket 10. Pocket 10 was initially docked with polyalanine peptide (violet) to standardize the

combinatorial library of peptides from the initial polyalanine peptide (Violet) was generated and screened in the pocket-10 to identify the most suitable peptide fitting into FIKK9.1 substrate-binding pocket. Peptide 277 (magenta) was found to be a substrate for FIKK9.1.

Individual peptides present in the combinatorial peptide library were modeled and docked into binding pocket 10 as described in "material and methods". Alanine at position 1 was mutated to all other 19 amino acids and we found that substitution with methionine fits better than substitution with other residues. Iteratively, we have substituted alanine residues present at different positions in polyalanine peptide with other amino acids, and interaction profiling, as well as fitting into the binding sites, were analyzed. The side chain of threonine present at the seventh position of peptide P131 is located close to γ-phosphate of ATP bound to the active site and it may facilitate efficient phosphate transfer. Residues close to threonine such as H5, L8, G9 are involved in hydrophobic interaction whereas Y6 and L8 are involved in electrostatic interactions with charged residues (Lys 320 & 324) present within the binding pocket to stabilizes the peptide substrate for efficient phosphate transfer. Similar interactions were observed with serine present at seventh position in peptide P130 but the fitting of P131 is better than P130. Correlation analysis of peptides present in the combinatorial library concludes that peptide P277 with amino acid sequence MFDFHYTLGPMWGTL was fitting nicely into the binding pocket (Figure 2.16, Magenta peptide) with atomic contact energy of -241.06 kCal/mol. The peptide P277 is in extensive interaction with the residues present within the binding pocket (Table 2.2). The peptide residues M1, D3, P10, W12, and L15 were positioned in a hydrophobic rich region of FIKK9.1 due to the presence of Ile-186, Phe-243, Val-244, Ile-260, and Ile-443. The peptide residues Y6, F4 & F2 are surrounded with positive residues Arg 6, Lys 258, and 324 from FIKK9.1. The peptide residues H5 and L8 are surrounded by negatively charged Asp-317 and Glu-366 from FIKK9.1 in strong electrostatic interactions to anchor the peptide. The atomic interaction of Y6 with Asn-321, Glu-366, and Phe-243 might be responsible to stabilize the peptide within the binding pocket for efficient transfer of phosphate to T7 of the bound peptide. The residues present in C-terminus were involved in strong hydrophobic and Π-Π stacking interaction with the hydrophobic region of the peptide. The presence of bulky residues in substrate peptide P277 (M1&11, W12, P10, and F6) is due to a significant portion of the binding site with hydrophobic residues (Phe 243, Val-244, Leu 314, Gly 316, Leu 369, and Ile 443). The overall analysis shows that peptide rich in hydrophobic residues serves better substrate by interacting with hydrophobic pocket present in the FIKK9.1 active site.

Table 2.2: Atomic Interaction and their distance of Peptide P277 from combinatorial peptide library with FIKK9.1 residue which favors γ-phosphate of ATP.

Peptide P277	Peptide Atom	Protein residue	Protein atom	Distance Å	Location of Residue
M1	CE	GLY 26	CA	2.702	Hydrophobic region
M1	SD	LEU 30	CA	2.712	Hydrophobic region
M1	CA	ASN 29	OD1	2.773	Hydrophobic region
M1	N	HIS 257	HE1	3.142	Hydrophobic region
F2	CE1	LYS 258	HZ3	2.083	Hydrophobic region
F2	O	ILE 25	HD2	2.392	Hydrophobic region
F2	CE1	GLY 259	O	2.633	Hydrophobic region
D3	CA	ILE 25	HD3	3.685	Hydrophobic region
D3	O	GLY 316	HA2	3.751	Hydrophobic region
F4	CE1	TYR 315	O	2.144	Hydrophobic region
F4	CZ	LEU 314	3HD1	2.191	Hydrophobic region
F4	CE2	ASN 242	ND2	2.51	Hydrophobic region
H5	ND1	ASN 321	HB2	2.979	Hydrophobic region
H5	NE2	ASN 321	ND2	3.023	Hydrophobic region
H5	CB	ASP 317	HA	2.065	Charged surface
H5	CB	ASP 317	CG	2.156	Charged surface
H5	ND1	ASP 317	HB1	2.189	Charged surface
Y6	CZ	PHE 243	HB2	3.07	Hydrophobic region
Y6	CE1	ARG 6	1HH1	3.082	Hydrophobic region
Y6	CD1	ASN 242	O	3.107	Hydrophobic region
Y6	O	ASP 318	OD2	2.779	Hydrophobic region
T7	OG1	ASP 318	HB1	2.157	Charged surface
T7	CB	ASP 318	HB1	2.649	Charged surface
T7	CB	ASP 318	CB	3.617	Charged surface
L8	CD1	LYS 324	HE2	2.204	Charged surface
L8	O	GLU 366	HG1	2.972	Charged surface
L8	CD2	ASN 321	2HD2	3.102	Charged surface
L8	CG	LYS 320	HD1	3.807	Charged surface
G9	O	PHE 243	CZ	2.145	Hydrophobic region
G9	CA	PHE 243	HD2	2.177	Hydrophobic region
G9	CA	PHE 243	CE2	2.189	Hydrophobic region
G9	N	PHE 243	HE2	2.353	Hydrophobic region
P10	CA	PHE 243	HE2	2.499	Hydrophobic region

Peptide P277	Peptide Atom	Protein residue	Protein atom	Distance Å	Location of Residue
P10	O	VAL 244	HB	2.519	Hydrophobic region
P10	CG	MET 245	HA	2.759	Hydrophobic region
W12	CA	VAL 244	1HG2	3.364	Hydrophobic region
L15	CD1	ASN 137	HB2	2.626	Hydrophobic region
L15	CD2	ASN 138	1HD2	2.633	Hydrophobic region
L15	CD1	ASN 138	N	2.882	Hydrophobic region
L15	CD1	ASN 138	HB2	2.903	Hydrophobic region

2.3.12 FIKK9.1 phosphorylates proteins in RBC

FIKK kinases are highly expressed throughout the intra-erythrocytic stages of parasites. The differential localization of FIKK kinases during the asexual life cycle strongly suggests it may play an essential role in parasite survival. Besides its potential, till now none of the FIKKs functional role in the parasite is elucidated. FIKK 4.1 is the only protein found to be phosphorylated dematin in IRBC's (Brandt and Bailey, 2013). To identify substrate from erythrocytes, RBC ghost was isolated, and in-vitro kinase assay was performed. The SDS-PAGE shows the existence of hallmark proteins in RBC ghost and phosphorylated proteins were detected in immunoblot using an anti-phosphoserine antibody. The assay was carried out in the presence/absence of FIKK9.1with RBC ghost proteins. The phosphorylated protein signal from kinase assay was mimicked in mock blot considering their calculated molecular weights (Figure 2.17). From the comparison of phosphorylated signal with phospho-proteomic data (Wu et al., 2009), proteins with specific molecular weight were identified. A total of 39 proteins were observed which corresponds to twelve major phosphorylated bands in the mock blot. To the account of peptide library analysis, the final peptide was a pairwise sequence analyzed with identified proteins. The phosphorylated signals with a molecular weight of 280, 101.1, and 39.44 kDa in mock blot probably correspond to Spectrin α, Band 3, and CD44 respectively. These are identified as a plausible substrate for FIKK9.1 but more in-depth analysis is required to verify it.

2.4 Discussion

Protein kinases are essential for the malaria parasite to complete its complex life cycle in two different hosts (Meibalan and Marti, 2017). The PEXEL motif in malarial proteins allows them

to trafficked outside the parasitophorous vacuole and eventually involve in several crucial interactions.

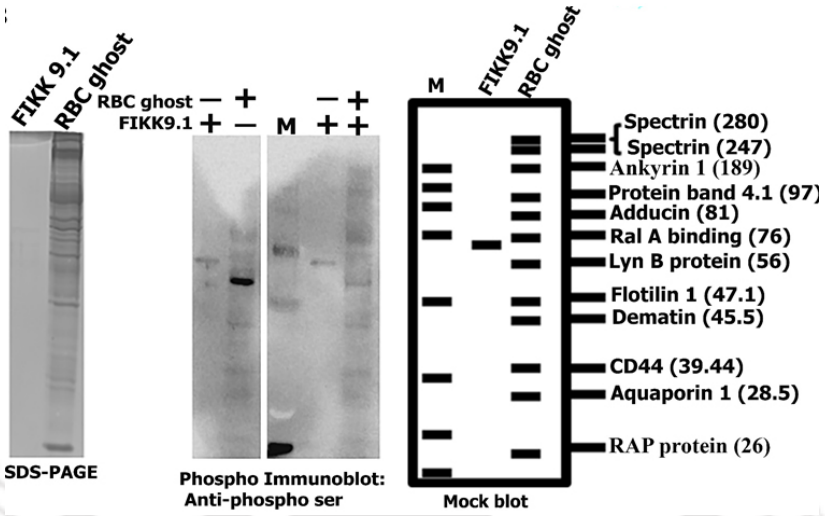

Figure 2.17: FIKK9.1 phosphorylates proteins present in RBC ghost. The RBC ghost lysate (150µg/Rnx) was used in kinase reaction and the phosphorylated proteins were analyzed through phospho immuno-blot. The differential signal was analyzed with phosphorylated RBC ghost in the presence (+) or absence (-) of FIKK9.1. The mock blot shown in the left panel depicts the signal obtained from immunoblot and possible phosphorylated proteins present in RBC ghosts.

The presence of *fikk* genes near the telomeric and sub-telomeric regions surrounds by *var*, *stevor*, *rifin,* and *phist* (Ward et al., 2004) which elucidates the functional importance of FIKK proteins in malaria pathology. The bioinformatics analysis indicates that FIKK9.1 belongs to the serine/threonine-protein kinase family. Its catalytic domain is similar to other known protein kinases but it has distinct features that can be exploited for utilizing FIKK9.1 as a drug target. Our study suggests that FIKK9.1 possesses two distinct domains, first an N-terminus FHA-like domain with uncharacterized function, and second, the conserved C-terminus catalytic domain which hosts for the substrate to bind. The C-terminus domain consists of two lobes N-lobe and C-lobe. Through the pharmacophore model generated for ATP, we identified the region present between two lobes N-lobe and C-lobe in the C-terminal domain that provides a suitable biophoric environment for ATP to bind in FIKK9.1. ATP docked perfectly into the predicted biophore region with a binding energy of -6.13 kcal/mol. The FIKK9.1- ATP interaction analysis shows conserved residues such as M245, K320, K324, D366, and R431 involved in anchoring ATP. Apart from the C-terminal kinase domain, FIKK9.1 contains a distinct N-terminal domain with no homology with the existing proteins present in the database. At the N-terminus, it has a PEXEL motif which will allow the protein to localize into cytoplasm of IRBC. The uniqueness

of the N-terminus domain and the ability of the protein to appear in host blood can be exploited to utilize this region of the protein as a diagnostic marker. Our study confirms that FIKK9.1 is a monomeric protein with a molecular weight of 60.06 ± 1.6kDa by successfully producing it in a bacterial expression system. The experimentally determined dissociation constant K_d of 45.6 ± 2.4 μM and ability to catalyze the phosphorylation of protein substrate defines FIKK9.1 as functionally active. FIKK9.1 is known to be trafficked to IRBC and maurer's cleft (Siddiqui et al., 2020). Our co-localization analysis reveals that it is not only localized in IRBC and maurer's cleft but it also associated with apicoplast in *Plasmodium falciparum* (3D7). This may pave way for FIKK9.1 to phosphorylate important proteins of the parasite as well as host. Therefore, in this study, we also detailed plausible proteins present in RBC ghost which could serve as a substrate for FIKK9.1. FIKK9.1 consists of 23 binding pockets, among which, the pocket10, present near to the ATP binding region is found to be a better site for substrate binding. Hence, the combinatorial peptide library of 286 peptides is created. Out of 286 peptides, the P277 peptide with an amino acid sequence MFDFHYTLGPMWGTL docked nicely with atomic contact energy of -241.06 kCal/mol. The interaction analysis showed hydrophobic residues in pocket10 such as Phe 243, Val-244, Leu 314, Gly 316, Leu 369, and Ile 443 prefer peptide with high hydrophobic residues. FIKK9.1 is following a bi-substrate kinetic mechanism due to its random or ordered nature of binding with substrate and ATP (Figure 2.18). The homologous kinase PKA follows a similar mechanism to catalyze the phosphate transfer (Wang and Cole, 2014). Moreover, the order of the reaction is decided based on the nature of the substrate in most of the kinases. Unlike other enzymes, catalysis of the phosphotransfer by kinases does not involve any intermediate state and causes direct transfer of phosphoryl group by nucleophilic attack from the substrate. The occurrence of a catalytic transfer of phosphate group from FIKK9.1 bound ATP to final Peptide-277 is demonstrated (Figure 2.18). Based on the current study, it is seen that phosphoryl transfers from FIKK9.1 bound ATP is majorly driven by conserved residues. ASP 318 interacts with Mg^{2+}(1) which chelates β and γ phosphate of ATP helps in masking the charge of γ phosphate and direct transfer of phosphoryl group to hydroxyl acceptor of final Peptide-277. The Lysine 320 & 324 residues make electrostatic contacts with β & γ phosphates and stably positioning the ATP for nucleophile attack. When P-site (phosphorylation site) of peptide-277 comes to contact hydroxyl group present in T7 attacks electrophile group of γ phosphate and phosphorylation occurs. The Asp 318 and Lys 324 of FIKK9.1 interaction with P-1 (Y6) and

P+1 (L8) sites of Peptide 277 stabilizes the complex for transfer of phosphate group. Therefore, the binding of ATP and phosphorylation of substrate follows a similar mechanism to other kinases but the lack of Glycine triad and replacement of HRD in activation loop shows FIKK9.1 is an attractive target to design a new class of antimalarials which leads to counteract off-target toxicity.

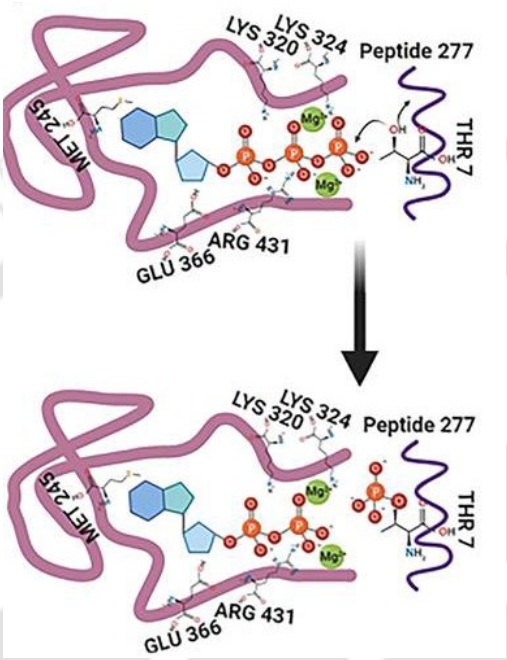

Figure 2.18: The possible catalytic mechanism of FIKK9.1.

Based on correlation analysis of peptide and immuno phosphorylation analysis on RBC ghost, proteins such as Spectrin α, Band 3, and CD44 may be possible substrates for FIKK9.1. Collectively, the study explored detailed structural characteristics of FIKK9.1 and recommends possible interacting partners present in host RBC. This is the first report on exploring structural details in the entire FIKK family around the species. Hence, in the current chapter we tried to highlight few crucial aspects of FIKK9.1 kinase: (i) detailed in-depth knowledge of structural and ATP binding environment of FIKK9.1, (ii) the biochemical characteristics of FIKK9.1 kinase and finally (iii) the identification of potential substrate and highlighting its role in parasitized RBCs. We are hopeful that these findings highlight the importance of FIKK9.1 as a druggable target and helps to design or identify better lead molecules against malaria.

Chapter III

Plasmodium falciparum FIKK9.1 kinase modeling to screen and identify potent antimalarial agents from chemical library

Summary

FIKK9.1 kinase is localized to cytosol as well as apicoplast and essential for parasite survival. Virtual screening of diverse organic structural scaffolds from chemical library has identified seven molecules, which could possibly arrest the growth of parasites by inhibiting FIKK9.1 kinase. The top hit compounds were fitting nicely into the ATP binding site through several molecular interactions. Evaluation of top hit compounds in anti-malarial activity assay indicate that the highly substituted 1,3-selenazolidin-2-imine 1 and thiophene 2 are inhibiting parasite growth with an IC_{50} of 9.293 ± 0.77 µM and 7.904 ± 0.42 µM, respectively. The functionalized heterocyclic compounds 1 and 2 are killing the malaria parasite with an IC_{50} of 7.734 ± 0.08 µM and 7.767 ± 0.35 µM, respectively. Isothermal titration calorimetry analysis indicate that ATP is binding to the FIKK9.1 kinase with dissociation constant (K_d) of 27.8 ± 2.07 µM with a stoichiometry of n=1. The heterocyclic scaffolds 1 and 2 were abolishing the binding of ATP into the binding pocket. They in-turn reduces the ability of FIKK9.1 kinase to phosphorylate its substrate and both compounds are potent inhibitor of FIKK9.1 kinase. Inhibition of FIKK9.1 kinase is disturbing the parasite life cycle and result into the death of the parasite. The study provides new insight to target FIKK9.1 kinase present in malaria parasite to develop potent anti-malarials.

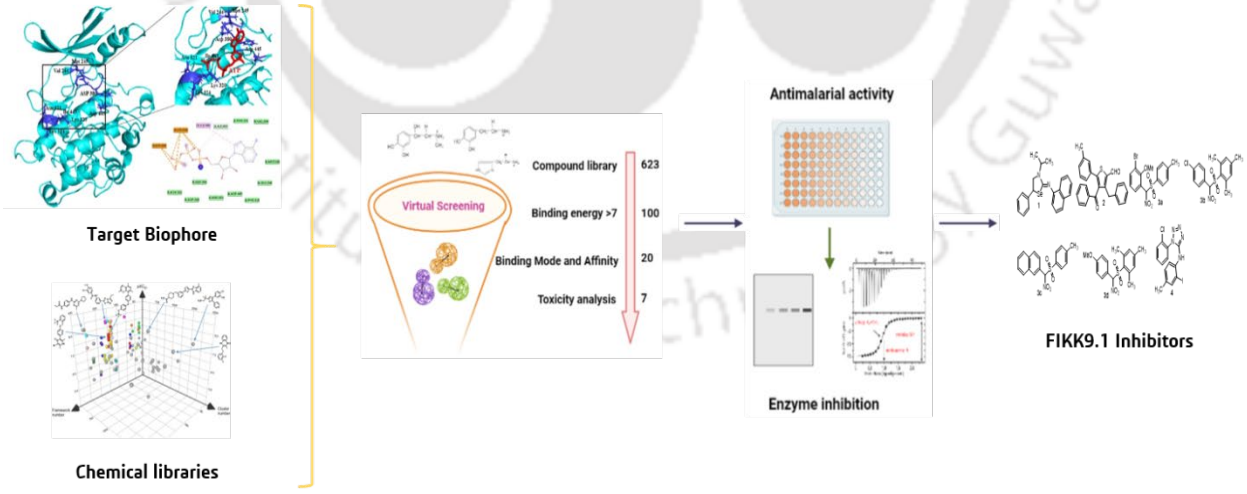

Identification of FIKK9.1 chemical inhibitor from chemical library

3.1 Introduction

Malaria is a pernicious disease causing nearly half million deaths each year (Organization, 2020). Although, malaria associated death is decreasing in last decade due to vector control (Mnzava et al., 2014) and stable artemisinin combination therapies (Pousibet-Puerto et al., 2016), steady increase in trajectory of malarial cases around the globe demands extensive effort to achieve the goal of eradication. In order to reach the state of eradication, we must ensure total cure of disease through safer and efficient development of new treatments. Earlier drugs such as chloroquine, mefloquine, sulfadoxine-pyrimethamine, lumefantrine and quinine are prevalently used in endemic regions as anti-malarials. Drug resistance and greater side effects of these drugs forced the introduction of artemisinin combination therapy ACT's in endemic areas (Haldar et al., 2018). However, the resistance and delayed death of parasites to artemisinin with some of its partner drugs are reported in Greater Mekong Sub-region (Menard and Dondorp, 2017) and Eastern India (Das et al., 2018). Although the current antimalarial drug pipeline is promising, there is no alternative therapy besides ACT to control malaria (Nsanzabana, 2019). Therefore, development of new anti-malarials against novel targets is important to control malaria.

During the parasite life cycle, early rings develop into trophozoites and schizonts before the merozoites rupture to invade other uninfected RBC's (Tuteja, 2007). The developmental process involves a cascade of signaling events to alter structural and functional changes of RBC's. The RBC's structural and functional aberrations include increased rigidity, decreased deformability and abnormal cyto-adherence of infected RBC's (Moxon et al., 2011). A number of proteins exported to infected RBC cytoplasm are characterized to understand the molecular mechanism behind RBC modulation and pathogenesis of parasites inside the host (Batinovic et al., 2017; Rug et al., 2014). Out of ~99 epk's, 27 families of kinase are exported outside parasites which includes FIKK kinases as well. These family of kinases plays major role in remodeling of RBCs. FIKK kinases are present exclusively in apicomplexan and don't have any orthologues to humans. In *Plasmodium falciparum* alone FIKK kinase extended to 21 proteins whereas other apicomplexan contains single FIKK kinase (Ward et al., 2004).

Among 21 FIKK kinases 17 FIKK's contains PEXEL (protein export element) motif in their sequence in order to export these proteins outside parasite. In contrast, even the presence of PEXEL motif in FIKK3 and FIKK9.5, has not found to be exported outside parasite. FIKK3

present in apical rhoptry organelle whereas FIKK9.5 is associated with parasite nucleus. It shows that FIKK3 may involve in invasion and FIKK9.5 may involve in controlling of nuclei division. All other FIKK's are targeted towards different location inside the IRBC's (infected RBC) and plays a crucial role in parasite survival. FIKKs (4.1, 9.3,9.4,9.6 and 9.7) are found to be non-essential proteins for parasite growth and are characterized to involve in pathogenicity of malaria (Davies et al., 2020). Based on in-effectual gene deletion of other FIKK kinases (9.1, 10.1 and 10.2) in *Plasmodium falciparum,* placed these as essential proteins for parasite survival during erythrocytic stages of parasite and may play an important role in novel pathways (Siddiqui et al., 2020). The complete phosphoproteomic analysis of FIKK's suggests each FIKK possess unique phosphorylation fingerprinting even it involves in same pathway (Davies et al., 2020). It shows each FIKK has its independent role in parasite to complete its life cycle in hosts. Previously killing parasite by inhibiting *Pv*FIKK and FIKK 8 using emodin suggests FIKK are potential target to develop anti-malarial (Lin et al., 2017a; Lin et al., 2017b). From earlier finding and reports, we found FIKK9.1 is localized in cytoplasm, Maurer's clefts (MC's) (Davies et al., 2020) and as well as in apicoplast (D et al., 2021) suggests it may involve in trafficking virulence proteins and/or drug related stresses linked to new permeability pathways (NPP). Therefore, FIKK kinase(s) could be used as potential target to develop new antimalarials.

In our study, we focused to identify FIKK9.1 kinase inhibitors using virtual screening approach. We have created library of more than 600 structural scaffolds with diversified chemical and biological features. The compounds are docked in previously identified ATP biophoric region in FIKK9.1 using Autodock (4.1) virtual screening tool. The compounds are shortlisted based on their high affinity and chemical complementarity with the surface of FIKK9.1. Top-ranked molecules are further screened through its drug-likeness and insilico toxicity predictions. Out of 623 compounds, seven compounds **1-4** are identified as possible inhibitors of FIKK9.1. Based on the schizont maturation assay anti-malarial activity of all compounds **1**-**4** is evaluated. Through *in-vitro* antimalarial assays, we found the Se and S-containing heterocycles, (Z)-3-isopropyl-N-(naphthalene-1-yl)-5-phenyl-1,3-selenazolidin- 2-imine **1** and 4-benzoyl-3-benzyl-5-(m-tolyl)thiophene-2-carbaldehyde **2,** significantly inhibit the growth of parasites with an IC_{50} 2.68 ± 0.02 µg/ml and 3.08 ± 0.14 µg/ml respectively. In order to find the killing of parasites using **1** and **2** are through inhibition of FIKK9.1, we studied effect of ATP binding with FIKK9.1 and kinase activity of FIKK9.1 under *in-vitro* conditions in presence and absence of compounds.

Both the heterocycles have deleterious effect on ATP binding with FIKK9.1 kinase and as well as significantly reduces the phosphorylation of Bovine serum albumin (BSA). Hence our data suggests FIKK9.1 kinase can be exploit as excellent drug target to develop new class of antimalarial.

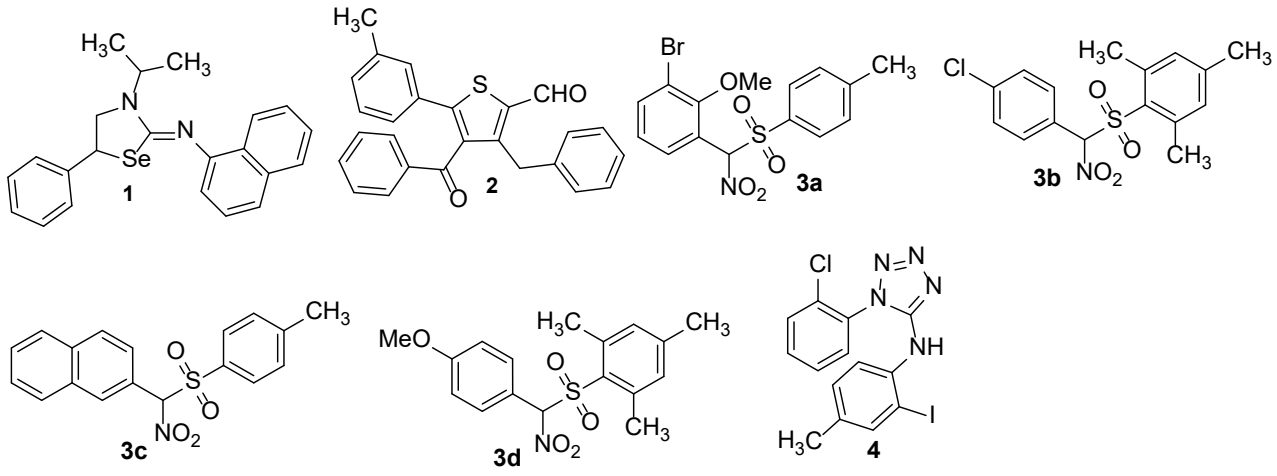

Figure 3.1: Structures of organic compounds. The heterocycle compounds are predicted to inhibit FIKK9.1 kinase and kills malaria parasite.

3.2 Experimental Procedure

3.2.1 Curation of heterocyclic compounds

The heterocyclic molecules synthesized and published for various benefits by our collaborating laboratories in the Department of Chemistry, Indian Institute of Technology Guwahati, India are curated for this study.

3.2.2 *In vitro* cultivation of *Plasmodium falciparum* 3D7

Plasmodium falciparum (3D7), a drug sensitive strain maintained in RPMI 1640 medium with 0.36 mM hypoxanthine, supplemented with 25 mM N-2-hydroxyethylpiperazine-N'-2-ethane-sulphonic acid (HEPES), 25mM NaHCO3, Gentamycin (40 µg/ml) and 5 g/l of AlbumaxR II (lipid-rich bovine serum albumin, GIBCO, Grand Island, NY, USA), together with 3-5% of human O^+ erythrocytes (blood is collected once in 21 days from healthy donor). Cultures are maintained at 37°C under an atmosphere of 4% CO2, 3% O2 and 93% N_2. Subcultures are done by diluting parasites to a parasitemia of between 0.5 and 1% and the medium was changed on every 24 h.

3.2.3 Virtual screening of chemically synthesized heterocyclic compounds

FIKK9.1 molecular model was used to identify pharmacophoric environment for ATP binding and it was used to dock heterocyclic compounds (D et al., 2021). The important ATP binding residues were marked and the grid was set with default spacing of 0.375 Å and covers the angle of 40° on each coordinate of X, Y & Z. AutoDOCK4.1 was used for virtual screening of compounds by setting the maximum number of evals and generation to 2500000 and 27000 respectively for 20 GA runs. Before proceeding with docking, the receptor and ligands were energy minimized through Swiss PDB viewer (SPDBV) and ChemBiodraw14 respectively. The interaction among ligands and receptors were analyzed through Ligplot+. Results of docking after analyzing are viewed using Pymol (Educational user module).

3.2.4 Generation of FIKK9.1 mutant and docking analysis

To validate the interaction of compound 1 and compound 2 with biophore residues of FIKK9.1, the most important residues were mutated with alanine and docking was carried out. To obtain mutated FIKK9.1, the structures of individual FIKK9.1 mutant were modeled using EasyModeller 4.0 GUI. The modelled FIKK9.1 mutant structures were energy minimized using swiss-PDBviewer v4.1 before performing docking analysis. The docking of ATP, Compound 1 and 2 in FIKK9.1 biophoric regions was carried out with similar coordinates used in virtual screening analysis. The binding energies of complexes were analyzed through AutoDOCK 4.1. For docking analysis of FIKK9.1 with heterocycles (1 and 2) in presence of ATP, the FIKK9.1-ATP complex structure was energy minimized and similar docking protocol was performed.

3.2.5 Molecular dynamic simulation analysis of FIKK9.1 and ligand complexes

The docked FIKK9.1-ligand (ATP, compound 1 and 2) complexes were used for molecular dynamics simulations. The CGenFF server is used to obtain topology file of ATP, compound 1 and 2. Charmm36_march2019 force field was used to perform simulations in GROMACS 4.6.5 package. The system is solvated by simple point charge (spc) water model and complexes were energy minimized in vacuum and water for 1ns. In order to neutralize the protein 19 chloride ions was included to the system. The production runs of 20 ns was performed for FIKK9.1-ligand (ATP, compound 1 and 2) complexes under NVT conditions. The MD trajectories of complexes after simulations were analyzed for Hydrogen bonding, radius of gyration (Rg), root mean square deviation (RMSD) and root mean square fluctuation (RMSF).

3.2.6 Isothermal Calorimetry Analysis of FIKK9.1 with ATP, Heterocycle 1 and 2

In order to precisely understand synthesized organic compounds that could disrupt FIKK9.1 interaction with ATP, ITC experiments were performed using ITC200 micro-calorimeter (MicroCal, Northampton, MA). ITC experiments were carried out at 30°C under constant stirring speed of 800 rpm with reference power of 6 µcal/s. During each calorimetry measurement, ATP (200 µM), compound 1(200 µM) or 2 (1 mM) in the syringe was titrated with FIKK9.1 (7 µM) present in the sample cell. In case of inhibition assays, FIKK9.1 protein was preincubated with **1** (100 µM) or **2** (100 µM) for 10 min at 30 °C in a water bath, then the ATP was titrated. The ITC data was analyzed using Origin software (Northampton, MA).

3.2.7 Protein Kinase assay

In a total volume of 250µl assay mixture, BSA (100 µg/ml) was incubated with FIKK9.1 (60 µg/ml) in a 20 mMTris pH7.4 reaction buffer contains 100mM NaCl, 10 mM $MgCl_2$ at 37^0C in the presence and absence of Heterocycle (1 and 2). ATP (100 µM) was added to start the kinase reaction and allowed it to proceed for 30 min at 37^0C. The phosphorylation of BSA was determined by immunoblotting using anti-phosphoserineantibodies. The acquired signal was quantified using Image lab (Bio-Rad laboratories, USA).

3.2.8 Antimalarial activity assay

Antimalarial activity assay was performed as described previously (Vimee et al., 2019). *Plasmodium falciparum* (3D7) was synchronised using 5% D-sorbitol to obtain ring stage parasites. For anti-malarial assay, 1% of ring stage parasites and 3% (final volume) of haematocrit was added to various compound concentrations (0-50µg/ml) and incubated for 38 h at 37°C in 5% CO_2 incubator. Blood smears were taken after 38h to examine the presence of schizont stage parasite and date was used to calculate schizonticidal activity of drugs. Parasitemia was calculated by observing the number of viable parasites/1000 RBC's for each concentration of drug.

3.2.9 Determination of the parasitostatic/parasitocidal nature

The compounds 1-4 were incubated with ring stage synchronized *P. falciparum* (3D7) parasitized cells at a range of drug concentrations from 0 µg/ml (Control) to 50 µg/ml. After 38 h compounds were removed by repeated washing with RPMI 1640 complete media and allowed the parasites to grow till 96 h in drug free medium. Blood smears were taken after 96 h to

examine the presence of viable parasites and minimum concentration of compounds 1-4 giving no viable parasite was used to calculate parasitocidal activity.

3.2.10 Microscopic imaging of parasite morphology

Giemsa stained thin smears of control as well as drug treated parasitized RBC were visualized under 100X objective in oil immersion and images were captured using a Nikon camera attached to the microscopy system.

3.2.11 Isolation of Peripheral blood mononuclear cells

The PBMC's were isolated from blood of healthy individual using HiSep 1077 (Himedia, India) density gradient method. The separation of the cells was based on manufacturer protocol. In brief, the blood was collected in anticoagulant solution and diluted with PBS in 1:1 ratio. The diluted blood was carefully overlay on top of the HiSep 1077. Then the blood was centrifuged at 1000 xg in room temperature for 30 min. The PBC's were resolved in between plasma and HiSep 1077 solution. The PBMC layer was carefully aspirated and performed cytotoxicity analysis.

3.2.12 Cytotoxicity analysis through MTT assay

The cytotoxic effect of heterocycles 1 and 2 were investigated using human embryonic kidney 293 cell line (HEK 293) at IC_{50} (3.5 µg/ml) and 2x IC_{50} (7 µg/ml) concentrations. In a 96 well plate, cell density of 10000 cells/well was incubated for 12 h to adhere. Compound stocks were made using incomplete media with 0.1 % of DMSO as final concentrations. Incomplete media containing DMSO (0.2%) was used as a control. The prepared media containing different concentrations of drugs was added to the cells and incubated for 24 h. The images were taken at 10X using Cytell cell imaging system and the effect of the drugs was evaluated by calculating the cell survival using 3-(4,5-dimethylthiazoyl-2-yl) 2,5-diphenyl tetrazolium bromide (MTT). After incubation, the media was removed, the cells were washed with PBS and media containing 20 µl of MTT (5 mg/ml) was added in the wells. The cells were incubated with MTT for 4 h at 37°C and media was removed after incubation period. DMSO (100 µl) was added in each well to dissolve tetrazolium crystals. Finally, the absorbance was measured at 550 nm and 690 nm for standard reference. Similarly, the compounds were also evaluated for its cytotoxicity on isolated PBMC's.

3.2 Results

3.2.1 FIKK9.1 has well defined ATP binding pocket within catalytic domain.

Structural features of FIKK9.1 catalytic domain is of typical kinase domain, which has similar structural arrangement to other protein kinases. The catalytic domain consists of two lobes where ATP and protein substrates tend to bind. N-lobe made with five β-strands and one α-helix whereas C-lobes consist of conserved α-helix structure. In comparison with structural elements of cAMP dependent kinases, calcium dependent kinases and protein kinase A (PKA) structures, FIKK9.1 possesses a number of conserved residues for ATP binding in between the lobes. Though it has conserved regions such as SELYG (312-315), PENILI (365-370) and DFG (379-382) motif, the absence of glycine triad and RD activation loop shows FIKK9.1 can be specifically targeted (Figure 3.2 A). To exploit the ATP binding region for virtual screening of potential inhibitors, ATP docked with FIKK9.1 interaction is analyzed. As like typical kinases, the region is lined with F243, V244, M245, I443, K320, K324, D379, F380 and G381 residues that makes a better region for ATP to bind with FIKK9.1. The ribose ring of ATP supported by hydrophobic residues such as V244, M245 and E246, and other residues notably F243, I443 and D445 covered adenine ring to stabilize ATP. Whereas the PO^4 group is anchored and correctly positioned for phosphor transfer by a positive-charged tunnel consists of R318, K320 and K324 residues (Figure 3.2 B). Besides the ATP binding pocket, there are residues which extensively interact with ATP and stabilize it for catalysis. The formation of salt bridge between I443 and adenine ring anchors ATP, whereas the hydrogen bonding of K320 with α-phosphate and K324 with leaving group γ-phosphate stabilizing and positioning the ATP for phospho transfer to substrate (Figure 3.2 C). These functionally important interacting residues of FIKK9.1with ATP have been exploited for further screening of inhibitors.

3.2.2 Compounds interact with important ATP binding residues in FIKK9.1.

In our collaborator's lab, who is extensively performing the organic synthesis of different types of compounds to explore its mechanistic details. The synthesized compounds are found to be structurally similar to the well-known bioactive compounds found in nature. So we created the library of the compounds to explore the possibility of identifying a potential antimalarial compound.

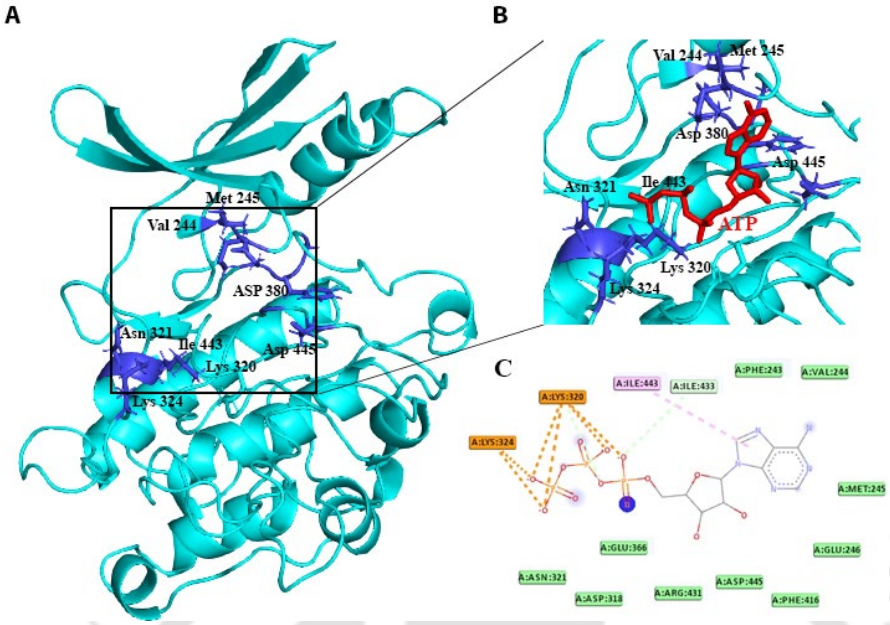

Figure 3.2: FIKK9.1 catalytic domain harbors ATP. (A) Structure of FIKK9.1 kinase catalytic domain with highlighted ATP binding pocket. (B) ATP (red) that rendered as ball and stick model, binds to FIKK9.1 catalytic site nicely. The important residues present around ATP binding is labelled. (C) Interaction of ATP with crucial residues of FIKK9.1catalytic domain.

Total 623 chemical inhibitors are extracted and virtual screened for identifying inhibitors of FIKK9.1 to develop antimalarials. All 623 compounds are docked into ATP pharmacophore environment. Docking pose of each compound is inspected and stored to identify potent inhibitors. Compounds are shortlisted based on binding affinity, binding geometry and interaction with most important residues of FIKK9.1. The binding energy of ATP (control for docking) is calculated to be -6.14 kcal/mol and energy required minimal than ATP for compounds to bind with FIKK9.1 are identified. From binding affinity and geometry inspection 20 compounds are identified as potential hit (Table 3.1). The binding affinity obtained for top compounds are ranged from -8.24 to -7.34 kcal/mol. Further all those molecules are analyzed for its toxicity profiling, most of the molecules follows Lipinski's rule of 5 and fewer molecules predicted to produce hepatotoxicity. Therefore, based on docking studies and toxicity profiling, seven compounds **1-4** are selected to perform *in-vitro* assays. All these molecules are binding exactly to the ATP pharamacophore environment and interact with FIKK9.1 (Figure 3.3). Bonding with most important residues for ATP binding suggests some of these molecules could be potential inhibitors of FIKK9.1.

Table 3.1: List of potential heterocyclic compounds to bind with FIKK9.1 better than ATP.

S. No	Compound	No. of conformation	Binding energy (kcal/mol)
1	3c	3	**-8.24**
2	472	3	**-8.06**
3	1	3	**-7.66**
4	264	2	**-8.36**
5	263	5	**-7.91**
6	258	3	**-7.79**
7	3a	2	**-7.74**
8	3d	1	**-7.6**
9	255	3	**-7.23**
10	277	2	**-7.62**
11	261	5	**-7.58**
12	2	3	**-7.4**
13	435	5	**-7.26**
14	3b	4	**-7.26**
15	275	2	**-7.69**
16	393	4	**-7.62**
17	260	2	**-7.56**
18	318	3	**-7.4**
19	4	3	**-7.34**
20	ATP	2	**-6.14**

Note: Autodock4.1 was used to calculate binding energy of heterocyclic compounds. ATP: Adenosine triphosphate.

Widely compounds form hydrophobic interaction to the biophore region, ligplot analysis reveals heterocycles **1** and **2** make extensive bonding and non-bonding interaction with active site residues (Figure 3.4 A&B). In comparable with ATP interaction, **1** and **2** making similar hydrophobic interaction and hydrogen bonding with L314, D318, E366 and I443 FIKK9.1 residue, which are responsible for anchoring and positioning of adenosine ring and phosphate residues in ATP (Table 3.2). The interactions are identified to be within 4 Å distance. Moreover, the interactions of heterocycles 1 and 2 with most important residues have been validated using *in-silico* mutation analysis. Amino acid residues involved in ATP binding are mutated and docked with heterocycles (1 and 2). The mutation of amino acids such as V244, M245 and E366

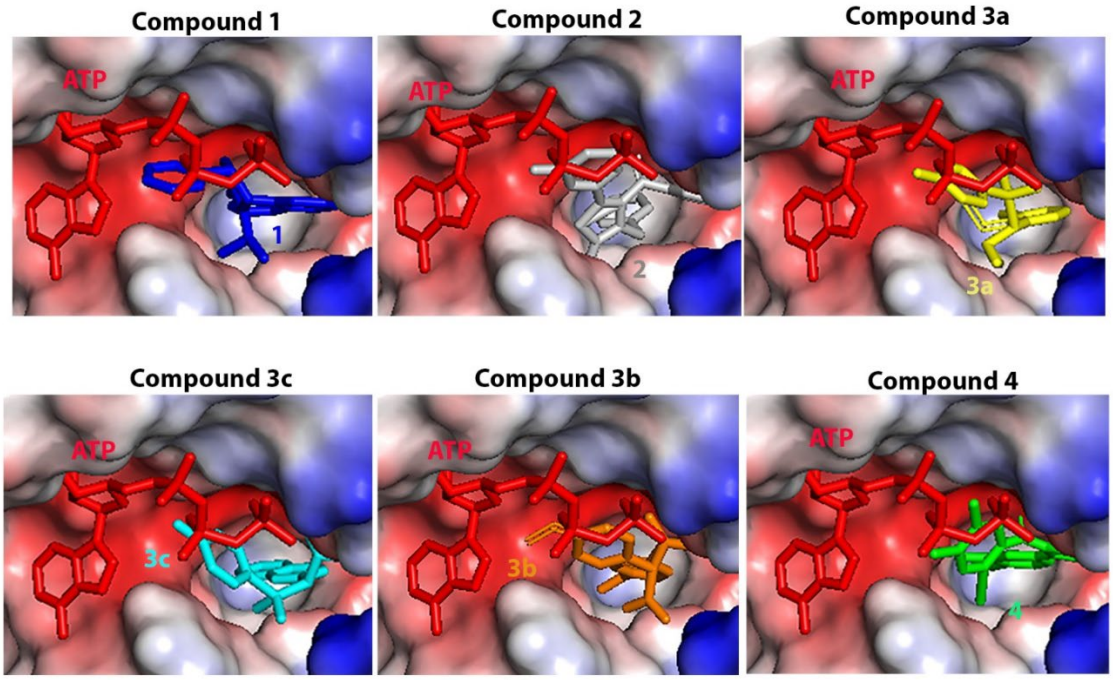

Figure 3.3: Screening of Scaffolds 1-4 in ATP pharmacophore region. The binding pose of top six molecules such as **4** (green), **1** (blue), **3a** (yellow), **3c** (cyan), **3b** (brown) and **2** (grey) within FIKK9.1 kinase binding pocket. ATP is shown in red.

are significantly decreasing the binding energies of FIKK9.1 with Compound (1 and 2). The difference of binding energies suggests that these heterocycles specifically binds and interact with ATP biophoric residues in FIKK9.1 (Table 3.3).

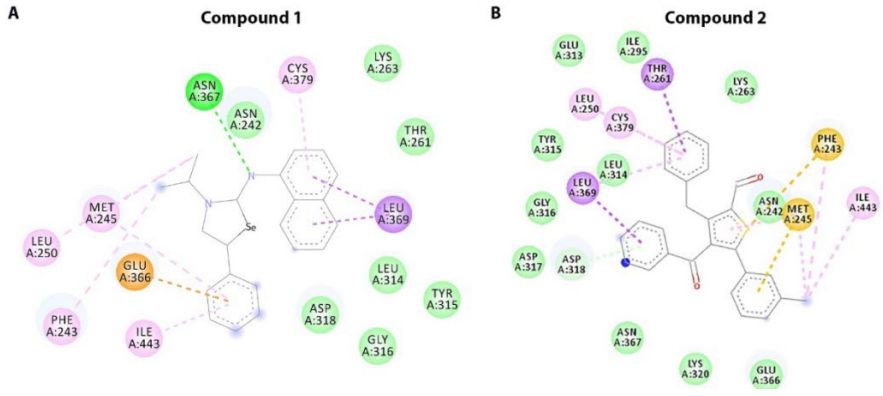

Figure 3.4: Heterocycles 1 and 2 make extensive interaction with residues present within FIKK9.1 kinase binding pocket. (A&B) The 2-D interaction profile shows **1** and **2** interact with residues which are important for ATP binding in FIKK9.1 kinase.

The stability of the interaction between FIKK9.1 with ATP and heterocycles (1 and 2) complexes were assessed through molecular dynamics simulations. The simulation of these complexes were performed under NVT conditions for 10 ns time scale. The FIKK9.1-complexes were analyzed for Hydrogen bonding, RMSD, RMSF and Radius of gyration.

Table 3.2: Interaction profiling of FIKK9.1 with its natural ligand (ATP) and inhibitors (Compound 1/2).

COMPOUND	RESIDUE NUMBER	AA	DISTANCE (Å)	LIGAND ATOM	PROTEIN ATOM	INTERACTION TYPE
1	243	PHE	3.55	5576	2444	Hydrophobic
	250	LEU	3.56	5570	2501	Hydrophobic
	314	LEU	3.02	5567	3129	Hydrophobic
	366	GLU	3.38	5579	3676	Hydrophobic
	369	LEU	3.32	5564	3707	Hydrophobic
	369	LEU	3.28	5565	3708	Hydrophobic
	443	ILE	3.34	5578	4467	Hydrophobic
	367	ASN	2.83	5560 [Npl]	3687 [O2]	Hydrogen bonding
	318	ASP	5.38	5558	-	Salt bridge
2	250	LEU	3.08	5574	2501	Hydrophobic
	261	THR	3.46	5574	2612	Hydrophobic
	295	ILE	3.25	5572	2959	Hydrophobic
	318	ASP	3.53	5581	3164	Hydrophobic
	366	GLU	3.08	5579	3676	Hydrophobic
	369	LEU	3.31	5571	3707	Hydrophobic
	369	LEU	3	5567	3708	Hydrophobic
ATP	242	ASN	1.71	2431 [Nam]	5561 [O3]	Hydrophobic
	263	LYS	3.09	2630 [N3+]	5572 [N2]	Hydrogen bonding
	315	TYR	2.67	3132 [Nam]	5575 [N2]	Hydrogen bonding
	318	ASP	2.91	3160 [Nam]	5565 [O3]	Hydrogen bonding
	318	ASP	1.91	5565 [O3]	3167 [O2]	Hydrogen bonding
	366	GLU	3.17	3679 [O3]	5585 [O2]	Hydrogen bonding
	366	GLU	2.84	5579 [O3]	3674 [O2]	Hydrogen bonding

Note: An AA indicates amino acid and a dash (-) indicates no interaction of specific atom.

Table 3.3: The binding energies of docked complexes of ATP and Heterocycles (1 and 2) with FIKK9.1 mutant.

Amino acid Mutation (FIKK9.1)	Binding Energy (kcal/mol)		
	ATP	Compound 1	Compound 2
Native	**-6.21**	**-7.84**	**-7.55**
V244A	-4.89	-5.67	-6.39
M245A	-5.38	-5.87	-5.76
E246A	-4.36	-6.02	-5.92
K320A	-4.33	-5.59	-5.94
N321A	-5.57	-5.86	-6.53
K324A	-3.27	-6.07	-6.1
E366A	-5.91	-4.97	-4.54

Through the hydrogen bonding analysis we observed that the interaction of FIKK9.1 and ATP is stabilized by hydrogen bond formation whereas the interaction of FIKK9.1 and heterocycles (1 and 2) anchored by hydrophobic interaction with formation of minimal hydrogen bond. The structural difference between coordinates and compactness of the protein structure in the docked state are analyzed using RMSD (Root Mean Square Deviation) and Radius of gyration for protein ligand complexes. For all the three complexes RMSD and Radius of gyration analysis suggests that the binding of ligands with protein does not create the unfolding of protein (Figure 3.5). However, we assessed the binding strength of the FIKK9.1 and ligand complexes using root mean square fluctuation (RMSF) analysis of FIKK9.1 residue. The average RMSF value of residues present in biophoric regions is found to be 0.3 nm for all complexes. This clearly suggests FIKK9.1 binding with ATP and heterocycles 1 and 2 are significantly stable in nature.

3.2.3 The Heterocycles 1 and 2 disrupts FIKK9.1 and ATP binding.

In order to identify the heterocycles **1** and **2** can disrupt FIKK9.1 and ATP binding, isothermal titration calorimetry experiment was performed. Upon titration of ATP with FIKK9.1 heat changes in the system is measured. Binding of ATP with FIKK9.1 found to be enthalpy driven as the interaction has lesser ΔH value, in terms it favors hydrogen bonding. The dissociation constant K_d is calculated to be 27.8±2.07 μM with a stoichiometry n=1 based on binding.

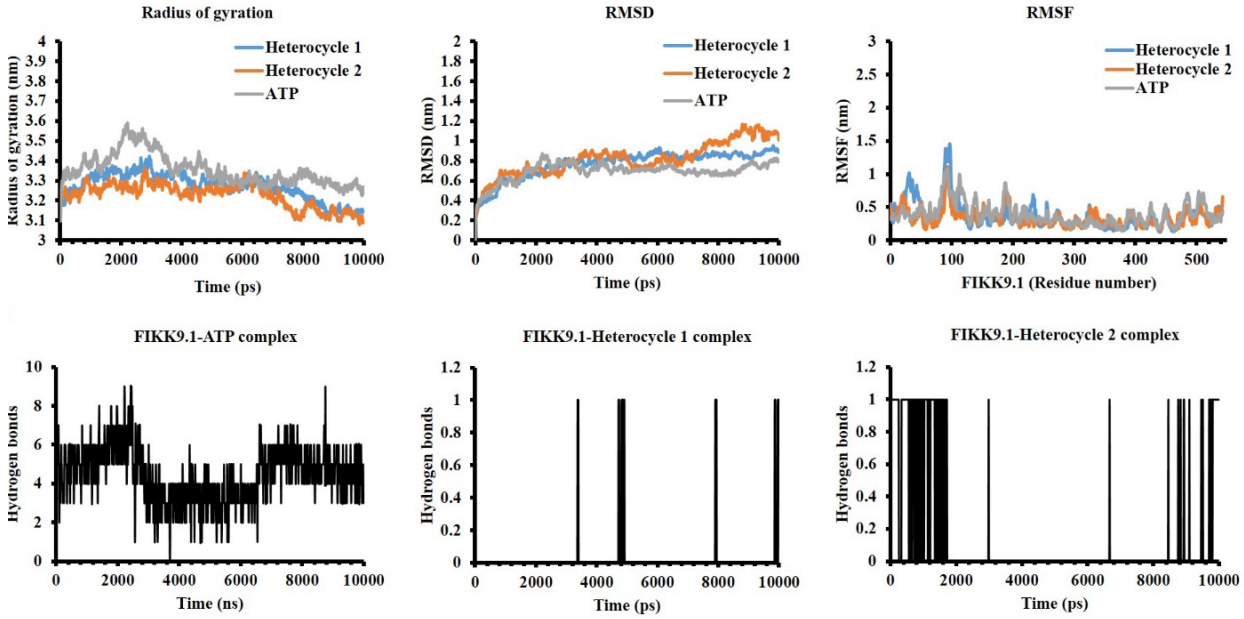

Figure 3.5: Molecular Dynamics Simulations analysis of FIKK9.1 with ATP and heterocycles (1 and 2). The stability of FIKK and ligand complexes was estimated using Radius of gyration and Root Mean Square Deviation (RMSD). The effect of binding of ligand in biophore region of FIKK9.1 have been analyzed through Root Mean Square Fluctuation (RMSF). The hydrogen bond formation between FIKK9.1 and ligands is analyzed for 10 ns using MD simulation.

The saturation of curve upon subsequent injection of titrant depicts ATP binding with FIKK9.1 (Figure 3.6 A). The ITC experiment was performed to calculate the binding affinities of heterocycles 1 and 2 with FIKK9.1. The heat of dilution was subtracted with the binding experiments. From the analysis we identified both the heterocycles binds to ATP with an K_d value of 9.6 ± 0.9 µM (compound **1**) and 1.21 ± 0.32 µM (compound **2**). The stoichiometry (n) of compound **1** and **2** is identified to be 0.977 and 0.956 respectively (Figure 3.6 B&C). To understand whether **1** and **2** are able to abolish ATP binding with FIKK9.1, ATP is titrated when FIKK9.1 pre-incubated with compound **1** or **2**. The interaction is observed to be affected as the dissociation constant tends to increase. The saturation curve shows that pre-incubation of heterocycle **1**/**2** produces unfavorable conditions for ATP to bind with FIKK9.1 (Figure 3.6 D&E). Additionally, the docking of heterocycles to FIKK9.1 in presence of ATP was performed, to show heterocycles share some of the most important residues invovlved ATP binding. The docking studies reveals that the compounds were binding deep inside into the ATP binding pocket in the absence of ATP whereas in the presence of ATP, binding of the molecules was

found to be disturbed and makes interaction on the surface of FIKK9.1 (Figure 3.6 F). Thus these heterocycles **1** and **2** are found to be potential inhibitors and utilized to test the *in-vitro* antimalarial activity.

3.3.4 Heterocycles 1 and 2 are potent antimalarials.

Based on results of virtual screening, top seven compounds **1-4** from library of 623 compounds are likely to be potent inhibitors of FIKK9.1 to give anti-malarial activity. Therefore, all seven

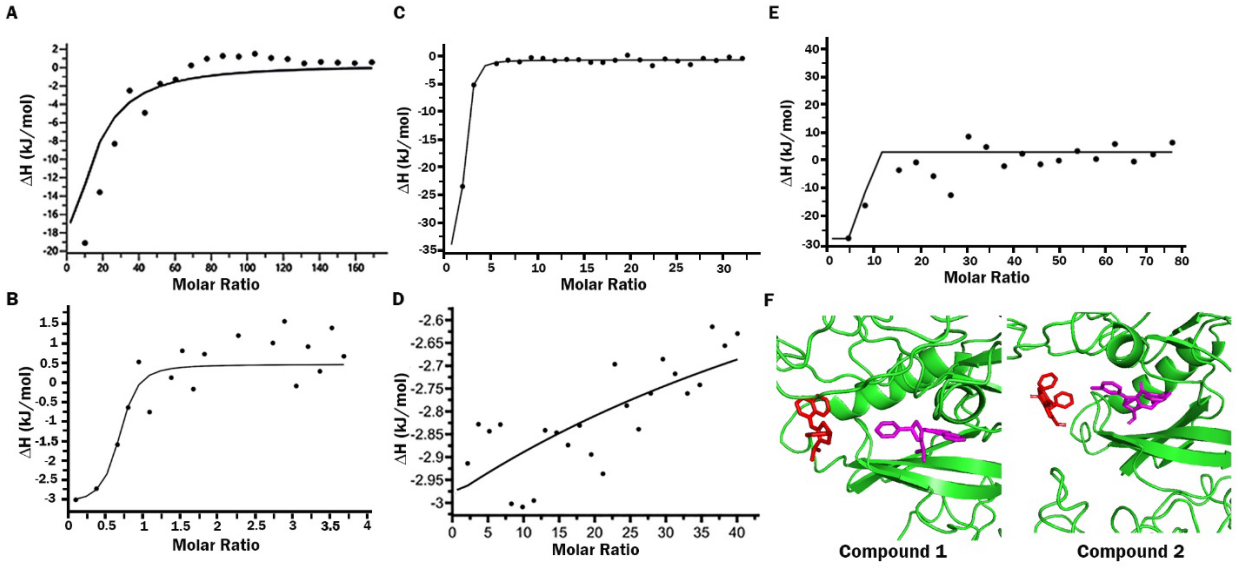

Figure 3.6: Heterocycles 1 and 2 abolishes ATP binding into the FIKK9.1 kinase binding pocket. The interaction of ATP with FIKK9.1 is analyzed in presence /absence of compound **1/2**. **(A)** Binding of FIKK9.1 with ATP. In the absence of **1/2** compounds, the saturation curve suggests ATP binding with FIKK9.1 Thermodynamic parameter of FIKK9.1 binding with heterocycles **(B)** 1 and **(C)** 2 were also measured using ITC. The graph shows binding of FIKK9.1 with heterocycle 1 and heterocycle 2. The effect of preincubation of compounds with FIKK9.1 on ATP binding was measured. In both the cases, the preincubation of **(D) compound 1** or **(E) compound 2** with FIKK9.1 disturbs the ATP binding with the protein. **(F)** The effect of ATP in hetrocycle 1 and 2 binding with FIKK9.1 was analysed through docking. The docked complexes in the presence (Red) and absence (Magenta) of ATP clearly shows that the binding of heterocycles 1 and 2 with FIKK9.1 was disturbed.

compounds were tested for its antimalarial activity using Pf3d7 parasite culture. Nitromethyl sulfone, 2-(((4-chlorophenyl)(nitro)methyl)sulfonyl)- 1,3,5-trimethylbenzene **3b** shows no activity, whereas 1-bromo-2-methoxy-3-(nitro(tosyl)- methyl)benzene **3a** and 1-(2-chlorophenyl)-*N*-(2-iodo-4-methylphenyl)-1H-tetrazole-5-amine **4** were giving very high IC_{50} in the range of 125 µM. Further, the sulfones, 2-(nitro(tosyl)methyl)- naphthalene **3c** and 2-(((4-methoxyphenyl)(nitro)methyl)sulfonyl)-1,3,5-trimethylbenzene **3d** showed moderate anti-

malarial activity. The heterocycles **1** and **2** are found to inhibit parasite growth with an IC_{50} of 7.734 ± 0.08 µM and 7.767 ± 0.35 µM respectively (Table 3.4). Among all, the heterocycles **1** and **2** are found to be potent anti-malarial. The compound treated parasite cultures are examined microscopically to understand structural abnormalities in RBCs and the ability of parasite to develop into schizont stage. The study uses chloroquine treated parasites as a positive control. In the beginning, infected RBCs were found to be healthy in both untreated and inhibitor treated cultures. But, after incubation with compounds for 38 h, parasites treated with chloroquine, heterocycle **1** or **2** showed dead ring, dead tropho and dead schizonts. In comparison, untreated parasites were showing all RBC stages and completion of erythrocytic life cycle.

Table 3.4: In vitro antimalarial activity of novel heterocyclic compounds.

S. No.	Compound ID	Schizonticidal Activity IC50 (µM ± SD)	Parasiticidal Activity IC50 (µM ± SD)
1	1	9.293 ± 0.77	7.734 ± 0.08
2	2	7.904 ± 0.42	7.767 ± 0.35
3	3a	>125	>125
4	3b	No Activity	No Activity
5	3c	>75	>75
6	3d	>75	>75
7	4	>125	>125

Note: IC_{50} values of heterocyclic compounds were calculated using regression analysis. Values were denoted in micromolar. SD: Standard Deviation

The microscopic examination reveals parasites are halting at one stage in treated samples and could not be able to complete its life cycle (Figure 3.7 A). It suggests that FIKK9.1 inhibitor block the erythrocyte developmental stages (from ring to schizont) of parasites. The FIKK9.1 inhibitors show good schizonticidal activity in *invitro* schizont maturation assay. The inhibitory concentration IC_{50} of **1** and **2** are observed to be 9.293 ± 0.77 µM and 7.904 ± 0.42 µM for schizonticidal activity and 7.734 ± 0.08 µM and 7.767 ± 0.35 µM for parasiticdal activity under *in-vitro* conditions (Figure 3.7 B). Although both the FIKK9.1 inhibitor are effective in blocking maturation of ring to schizont, we further asked if compounds were also causing parasite death and exhibiting parasiticidal activity. Compound treated parasite was washed 3 times with fresh

medium and then parasite was allowed to grow in fresh medium with compound for 96 h. After 96 h, thin smear is taken and viable parasites are counted through microscopy.

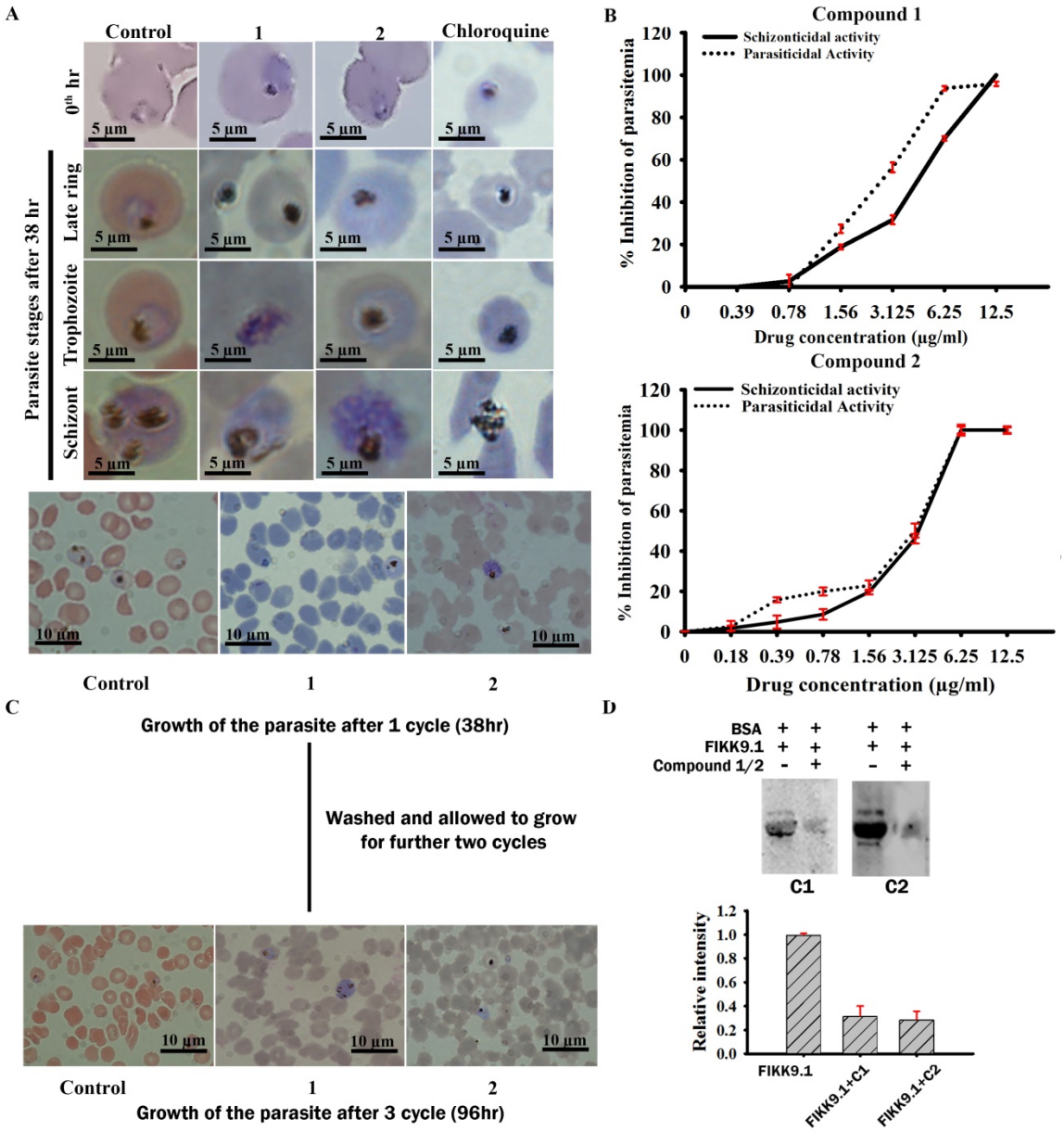

Figure 3.7: Heterocycles 1 and 2 are killing malaria parasite through inhibition of FIKK9.1 kinase. (A) Heterocycles 1 and 2 disturb parasite lifecycle. Parasite culture (ring stage parasite) was treated with the heterocycles for 38 h and thin smear of RBCs was observed under the microscope. Untreated parasite culture was exhibiting all RBC stages but compound treated parasites was showing only dead parasite (ring or trophozoite stage). **(B) Antimalarial activity of the heterocycles 1** and **2.** The growth of parasites (Pf3d7) was evaluated in presence of different concentration of compounds (0-12.5 µg/ml). **(C) Heterocycles 1 and 2 are killing malaria parasite.** Parasite culture was treated with the heterocyclic scaffolds for 38 h, culture

was washed with fresh medium and incubated for 96 h in fresh culture medium without the heterocycles. A thin smear of RBCs was observed under the microscope to monitor the growth of the parasite. Untreated parasite culture was exhibiting parasite and there was increase in parasitemia but compound treated parasites was showing only dead parasite. **(D) Heterocycles 1 and 2 are inhibiting FIKK9.1 kinase mediated BSA phosphorylation.** The BSA was incubated as a substrate with purified FIKK9.1 kinase in absence or presence of the heterocycles **1** and **2** the phosphorylation of BSA was measured using anti-pSer antibodies in western blot. The strong phosphorylation signal of phosphorylated BSA was obtained in the absence of the heterocycles **1** and **2** whereas the reduction of phosphosphorylated signal is observed in presence of the heterocycles **1** and **2**. The protein signal on blot was measured and used to calculate the inhibition of FIKK9.1 kinase activity. These values are represented in the graph to show the inhibition of FIKK9.1 kinase by the compounds.

3.3.5 The Heterocycles are killing malaria parasite through chemically knocking out FIKK9.1.

The untreated parasites were growing during this period to attain 2 fold parasitemia whereas no change in parasitemia was observed for treated parasite culture. In treated culture, most of the parasites were appeared to be dead and deformed states compared to control parasites (Figure 3.7 C). To confirm that parasite killing is mediated through chemical knockout of FIKK9.1, kinase inhibition assay has been performed. It is known that FIKK9.1 is a serine-threonine protein kinases and it efficiently phosphorylate BSA (D et al., 2021). We have analyzed *in-vitro* BSA phosphorylation status by FIKK9.1 in presence and absence of **1** and **2** inhibitors. In the absence of FIKK9.1 inhibitor, FIKK9.1 is extensively phosphorylating BSA by addition of ATP whereas in presence of inhibitors the phosphorylation of BSA is found to be decreased by several fold (Figure 3.7 D). It shows that FIKK9.1 is one of the primary targets for compound **1** and **2** for parasite death. This suggests FIKK9.1 is a drug target and possesses different unique salient features from host proteins which may provide deep insight to explore a new class of antimalarial.

3.3.6 The Heterocycles are nontoxic to cells.

The two promising antimalarial compounds is subjected to evaluate for its cytotoxicity on normal cell line (HEK 293) and PBMC's. Both these cells are treated with IC_{50} and 2x IC_{50} concentrations of heterocycles 1 and 2. The cells grown in incomplete media containing DMSO (0.2%) is used a no drug control for the experiment. In comparison to control, the morphology of HEK (Figure 3.8 A) and PBMC's (Figure 3.8 B) are found to be unaffected upon treatment of

heterocycles 1 and 2 at IC_{50} and 2x IC_{50} concentrations. The MTT assay is performed to find the percentage difference in the cell viability compared to control. The cell vaiblity percentage for compound 1 in HEK is determined to be 96.2 ± 3.56% and 92 ± 4.03% whereas compound 2 shows 97.75 ± 2.44% and 93.8 ± 0.43% for IC_{50} and 2x IC_{50} concentrations respectively. In case of PBMC's, the viable cells upon treatment with compound 1 are found to be 96.3 ± 4.1% and 94.1 ± 1.5% for IC_{50} and 2x IC_{50} conentrations whereas for compound 2 to 94 ± 7% and 84 ± 4% for IC_{50} and 2x IC_{50} conentrations. Thus the results suggest that both compounds are safe to use as an antimalarial.

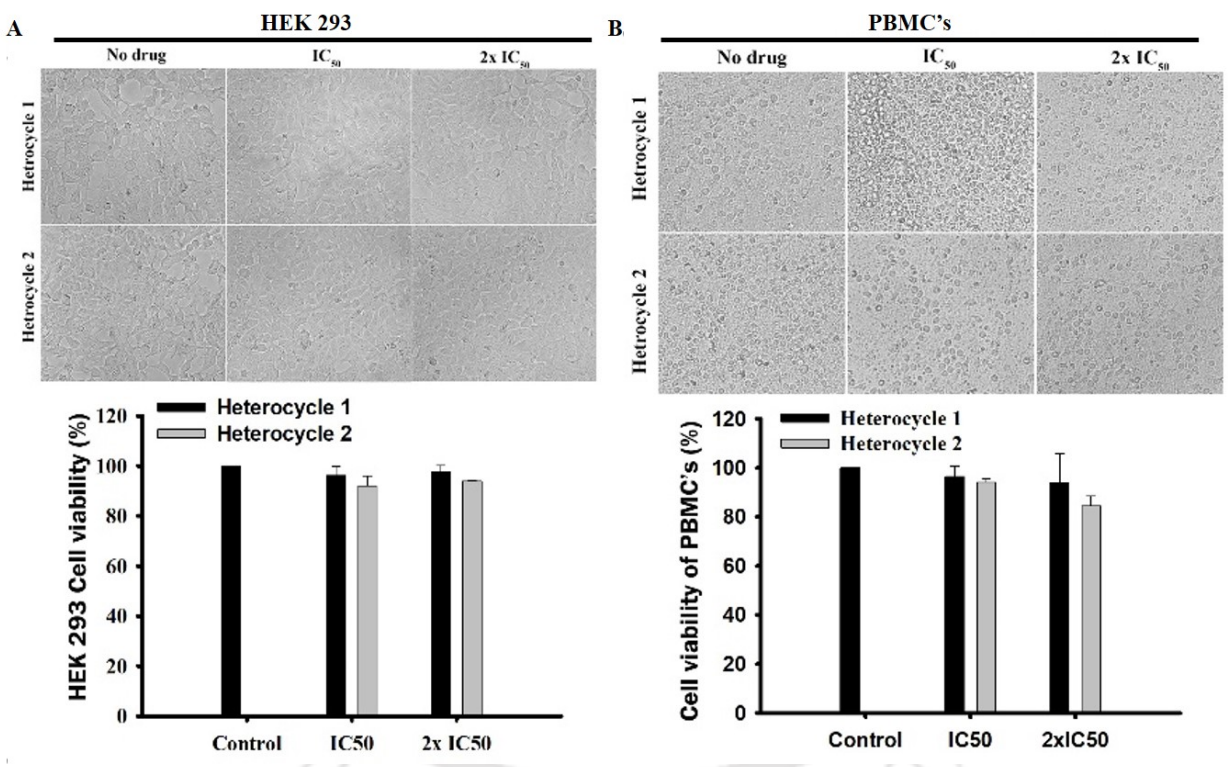

Figure 3.8: Heterocycles are not cytotoxic. The cytotoxicity of heterocycles 1 and 2 was evaluated in HEK 293 **(A)** and PBMC's **(B)** at IC_{50} and 2x IC_{50} concentrations. Percentage of cell viability was determined through MTT assay. The experiment performed in triplicates and the error bar represents the standard errors of mean (SEM).

3.4 Discussion

Kinases are the most important molecular targets in malaria, as we focus on deciphering new therapeutics against malaria (Arendse et al., 2021). The clusters of malarial kinases that fall with other eukaryotic kinases made it as underrated targets. However, FIKK kinase of *Plasmodium*

falciparum diverged from all other organisms and are exclusive to parasite only (Ward et al., 2004). Molecular function of most of FIKK's are uncharacterized but localization as well export of FIKK kinase outside infected RBCs suggests that they may perform important functions such as remodeling of host cells, cyto-adhesion and protein trafficking leads to parasite virulence (Davies et al., 2020; Lin et al., 2017b; Nunes et al., 2010; Siddiqui et al., 2020). FIKK9.1 is an exported FIKK family kinase, it spreads throughout IRBC's during erythrocyte stages of parasites. Notably, subcellular and MC's localization (D et al., 2021; Siddiqui et al., 2020) makes FIKK9.1 an exciting target. In this study we have exploited ATP pharmacophore environment in FIKK9.1 catalytic domain for identifying potential lead molecules (Figure 3.2 A). The ATP binding region in FIKK9.1 is versatile and possesses some of the unique features from host proteins. The identification of alignment of the hydrophobic region for adenine group to bind and pocket favors tri-phosphate group anchoring (Figure 3.2 B&C) makes it suitable to screen inhibitors. Total 623 compounds were screened and 20 molecules are predicted to inhibit parasite growth (Table 3.1). From 20 molecules, 7 compounds were found to interact with most important residues in FIKK9.1 for ATP binding (Figure 3.3). Mainly interaction of two compounds **1** and **2** with residues M245, E366 and I443 involved in ATP binding and as well interaction with C379 in CDFG motif, a motif act as ON or OFF switch for kinases (Vijayan et al., 2015) makes these compounds as probable inhibitor for FIKK9.1 (Figure 3.4 A&B). Additionally, the molecular dynamic simulation also suggests the interaction between heterocycles (1 and 2) and FIKK9.1 are stable in nature (Figure 3.5). Treating the parasites with all seven molecules suggests **1** and **2** are potential lead molecules to inhibit parasite under *in-vitro* condition (Table 3.4). Based on the ITC experiment the binding between heterocycles with FIKK9.1 was confirmed. Further, we found both these compounds were disrupting ATP binding with FIKK9.1 (Figure 3.6 A-E). Schizont maturation assay also suggests these compounds **1** and **2** is significantly decreasing parasite growth (Figure 3.7 A and B). Previously only emoidin has found as inhibitor for FIKK (*pf*FIKK8and *pv*FIKK) family of kinases (Lin et al., 2017a; Lin et al., 2017b) but here we showed compound that could inhibit parasite growth by targeting FIKK kinase. The inactivation of FIKK9.1 enzyme through factors such as specific spacio-constraints, strong ionic and hydrophobic interaction makes inhibitors to specific in nature. In addition, both the inhibitors are found to be killing parasite (Figure 3.7 C). The dual localization, sub-cellular and exported to IRBC cytoplasm makes FIKK9.1 an excellent target. In our study, by targeting

FIKK9.1 the parasite is killed irreversibly and which has been supported by kinase inhibition assay of FIKK9.1 on its substrate (Figure 3.7 D). The cytotoxicity analysis of the heterocycle compound 1 and 2 supports that these molecules are specifically kills the parasite but not the normal mammalian HEK293 cells or human PBMC's (Figure 3.8 A&B). These studies evident that FIKK9.1 could be potent drug target to develop new antimalarial of different chemical and biological sources.

Chapter IV

Exploring Ayurvedic Formulations as Potential Source to Develop Anti-malarials

Summary

The emergence of drug resistance in malaria parasite to all frontline antimalarial drugs urges continuous search of new antimalarials that would be beneficial for both chemotherapy and prophylaxis. In this chapter, we explored the potentials of Ayurvedic formulations as antimalarials and defined the mechanism and their mode of action. The water extract of 16 ayurvedic formulations were evaluated for their antimalarial activity. The extracted compounds were used to perform schizont maturation assays, among which five formulations showed IC_{50} values lower than 50 µg/ml. From the five formulations, Triphala churn and Shukrukramatrika bati showed promising antimalarial effects against *in-vitro* cultures of *Plasmodium falciparum* 3d7. The IC_{50} values of water extracts of Triphala churn and Shukrukramatrika bati were evaluated to be 5.75 ± 0.169 µg/ml and 28.875 ± 3.11 µg/ml for schizonticidal and IC_{50} of 2.1175 ± 0.058 µg/ml and 9.545 ± 0.084 µg/ml for parasiticidal activity. The antimalarial activity of both the water extracts revealed that the nature of inhibition of parasite is parasitiocidal. The characterization of these water extracts suggested that phytochemicals such as gallic acid, ellagic acid, chebulic and chebulinic acid were responsible for the antimalarial activity of Triphala and Shukramatrika. The cytotoxicity on HEK293 and hemolysis analysis suggested that both the formulations are safe to be used as antimalarials. The underlying mechanism of parasitic death was evaluated through the use of apoptotic biomarkers including ROS generation, mitochondrial dysfunction and, in-situ DNA fragmentation. Our results showed that Triphala and Shukramatrika induces oxidative stress by increasing ROS level and destabilizing the mitochondrial membrane which is followed by the increases in population parasites carrying fragmented DNA. Hence, the study concludes that Triphala and Shukramatrika kills the malaria parasites irreversibly through apoptotic pathway.

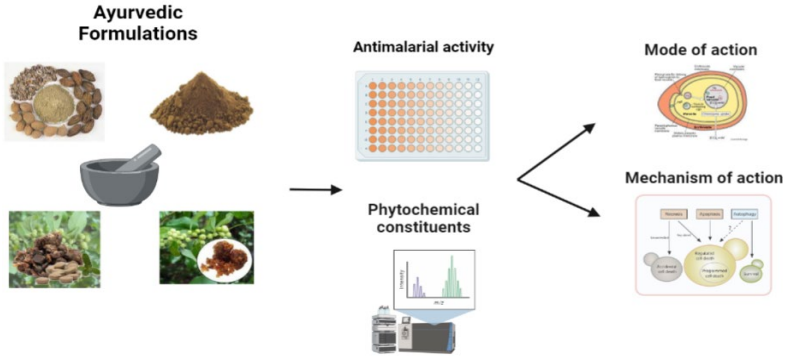

Schematic representation of Repurposing of Ayurvedic Formulation as antimalarial

4.1 Introduction

Traditional medicine practices are being used in different regions of the world over the centuries. According to reports more than 60 percent of the world's population still rely on traditional medicines to treat several diseases (Pinmai et al., 2010). These ancient practices are seen to be more prevalent in South-asian countries. In India, the primary traditional medicine practices are Siddha, Unnani, and Ayurveda. All these medicinal systems use combination of various sources such as herbal plants, minerals, and organic matter. Based on source of the material, Ayurvedic medicines are classified into three main classes, mineral, herbal and animal (Dhiman and Chawla, 2005). The herbal formulations of Ayurveda tend to have greater applicability and are used widely as compared to the others. This is related to the fact that the India subcontinent is recognized as one of the mega biodiversity centers in the world which accounts about 45,000 plant species. The abundancy of flora has made the country an important reservoir of herbal plants in the history of traditional medicine. It has been recorded that India has more than 15,000 medicinal plants and about 7,000-7,500 plants are commonly used in traditional medicine practices to cure several diseases (Bagavan, Rahuman, Kaushik, & Sahal, 2011). In Ayurveda, about 700 plant types have been documented for treatment of a wide range of diseases. These ancient records of herbal plants have time and again proven to be an indispensable source of active pharmacological ingredients which are found to have good efficacy in drug therapies. The phytochemicals present in the herbal plant preparations include tannins, alkenyl phenols, alkaloids, flavonoids, sesquiterpenes lactones, terpenoids, saponins and phorbol esters (Peterson, Denniston, & Chopra, 2017). It is also being seen that majority of these phytochemical constituents work synergistically to produce the desired pharmacological action.

Polyherbal formulations (PHF) are widely practiced to treat diseases like cancer, liver dysfunction, cardiovascular disorders, and others due to their synergistic effect between multiple components (Malik et al., 2017; Suryavanshi et al., 2019) (Dhiman and Chawla, 2005). Moreover, phytochemicals from several natural sources are already proven to have medicinal values to treat malaria. Quinine was the first antimalarial that was isolated from the bark of cinchona tree, an herbal plant used in traditional Chinese medicine, for the treatment of malaria. The frontline antimalarials such as atovaquone, artemisinin, and its derivatives artemether, artesunate, and artemether, in recent times, are also derived from herbal plants sources. All these compounds are proven to be highly effective against malaria (Tse et al., 2019). Although

Triphala, Nefang, SAABMAL, and other formulations are reported to have anti-plasmodial activity, the mode and mechanism of their action are poorly understood (Lawal et al., 2015; Obidike et al., 2015; Tarkang et al., 2014).

Triphala is one of the most widely characterized PHF used for the treatment of different diseases. It is a mixture of three herbs, *Phyllanthus emblica*, *Terminalia bellerica*, and *Terminalia chebula* and is commonly used to treat gingivitis, arthritis, constipation, and several other diseases. Triphala is also shown to have immunomodulatory, antimicrobial, and antioxidant properties due to the abundance of flavonoids, terpenoids, tannins, saponins and phenolic acids in it(Peterson et al., 2017). The herbs present in Triphala formulations are also widely characterized to have antiplasmodial activity (Bagavan et al., 2011; Joshi et al., 2016). One of the major constituent of Triphala, *Terminalia bellerica* is known to effectively inhibit parasite growth (Pinmai et al., 2010). Though the individual components are studied in detail, the synergistic effect of Triphala and the mechanism that leads to the death of malaria parasite is poorly understood. Gallic acid, chebulagic acid, chebulinic acid, and ellagic acid are major phytochemical constituents of Triphala (Sivasankar et al., 2015). Gallic acid and an uncharacterized anolignan present in *Terminalia chebula*, a constituent ofTriphala, are presumed to have significant antimalarial activity (Pinmai et al., 2010; Valsaraj et al., 1997). Other formulations used in our studies such as Shukramatrika Bati, Mahayograj Guggulu, Kaishor Guggulu, and Sariwadi Vati are used for various purposes like improving sexual debility, neurological disorders, urinary disorders and ear diseases. Except Triphala, none of the formulations used in this study were reported for any antimalarial activity. Therefore, it is necessary to understand the major constituents of these formulations including Triphala and their role in parasitic death.

In this study, we have extracted crude water-soluble phytochemicals from ayurvedic formulations and tested their potential to inhibit the growth of the malaria parasite. We have performed antimalarial activity of 16 ayurvedic formulations and identified Triphala and Shukramartika bati as potential antimalarials. The phytochemical constituents and mode of action for both the formulations was analyzed through HPLC and schizont maturation assay respectively. Further, we showed that treatment of the parasites with aqueous extracts of Triphala and Shukramartika bati induces oxidative stress in them, and subsequently leads to

depolarization of mitochondrial membrane potential ($\Delta\psi_m$) and fragmentation of DNA. Our results suggest that the blood-stage *P. falciparum* (3D7) undergo apoptotic-like cell death upon treatment with an aqueous extract of Triphala and Shukramatrika bati.

4.2 Experimental Procedures

4.2.1 Materials

RPMI1640, gallic acid, ellagic acid and gentamycin were purchased from Sigma, St. Louis, MO, USA. AlbumaxR II (lipid-rich bovine serum albumin) was purchased from GIBCO, Grand Island, NY, USA. Solvents, chemicals and other reagents used in this study are of analytical grade purity.

4.2.2 *Plasmodium falciparum* (3D7) culturing

Plasmodium falciparum (3D7) culture was maintained as mentioned already in the Chapter 3, Section 3.2.2, page no. 80.

4.2.3 Aqueous extraction of Ayurvedic formulation

A total of 16 different ayurvedic formulations were purchased from Baidyanath Asliayurved, India. The aqueous extraction of the Ayurvedic formulations was carried out by dissolving 5g of powder in 10ml of Milli-Q water and kept in 37ºC water bath for 2h. After the treatment, the supernatant was collected after centrifuging the samples at 8000 rpm in room temperature and an additional 10ml of Milli-Q water was added. The process was repeated twice to ensure that maximum extraction of the constituent phytochemicals from Ayurvedic formulations were extracted. The supernatant was lyophilized and the resultant powder was dissolved in phosphate buffer (pH 7.4). The extract was further filtered through 0.22 µm filter and stored in -20ºC until used to perform experiments.

4.2.4 Characterization of bioactive compounds from ayurvedic formulations

The phytochemical assessment of Triphala and Shukramartika bati aqueous extracts was carried out using high performance liquid chromatographic system (Shimadzu, Japan). The separation of Triphala and Shukramartika bati constituents was performed using C_{18} column (250×4.6 mm id) 5 micron. A gradient of 0-100% acetonitrile (ACN) with water in a mobile phase was used for separation process. To obtain a homogeneous solution, 0.5 ml of formic acid was added to water and degassed using bath sonicator. The peaks were detected at 254 nm, a standard wavelength

for phytochemicals.10 µl of 1 mg/ml Triphala and Shukramartika bati aqueous extract was injected to the column and the biomolecules were eluted using ACN gradient with a flow rate of 1 mg/ml. To identify the constituents, present in Triphala aqueous extract, standards such as Gallic acid, Ellagic acid and Chebulinic acid were separated in identical conditions. The retention time obtained on acetonitrile gradient based fractionation of Triphala and Shukramatrika extract was compared with standards such as gallic acid, ellagic acid, and chebulinic acid.

4.2.5 Antimalarial activity of Ayurvedic formulations

The aqueous extracts of the ayurvedic formulations were determined for antimalarial activity against *Plasmodium falciparum* (3D7). For initial screening of ayurvedic formulations, a fluorescence-based assay using SYBR green was performed. In detail, 2% hematocrit containing 1% parasitemia of synchronized ring-stage parasites were incubated in the absence or presence of different concentrations of ayurvedic formulation aqueous extract. The treatment was carried under normal parasite culturing conditions for 72 h. 0.2% DMSO and chloroquine were used as negative and positive controls respectively. After 72 h of treatment, lysis buffer {20 mM Tris (pH 7.5), 20 mM EDTA (5 mM), 0.008%; *w*/*v* saponin, and 0.08%; *v*/*v* Triton X-100} containing 2X SYBR Green I solution (Invitrogen, USA) was added to the parasites and incubated for 1 h at 37°C in dark condition. The fluorescence was recorded with Ex/Em of 485/530 nm, using a multi-well plate reader (Spico-biotech, India). The 50% inhibitory concentration (IC_{50}) was determined based on dose-response curve analysis. Sensitivity of *Plasmodium falciparum* (3D7) to Triphala and Shukramartika bati was determined through schizont maturation assay. The aqueous extract of Triphala and Shukramartika bati were made to a stock concentration of 100 µg/ml using complete media. Synchronized ring-stage parasites at 1% parasitaemia in 2% haematocrit were exposed to various concentration of the extracts and smear was taken for each concentration of both the formulations after 38 h to evaluate schizonticidal IC_{50} values. Additionally, to understand the nature of death of the parasite (parasiticidal/parastatic), they were allowed to grow for another 48 h after removal of extracts by repeated washing with complete media. The Parasiticidal or Parastatic death of parasites were determined through calculating parasitemia of various concentrations and compared to the respective controls. All smears were Giemsa stained and visualized under 100X objective in oil immersion.

4.2.6 Toxicity studies of Aqueous extract of Triphala and Shukramatrika bati on nucleated cells

In-vitro cyto-toxicity of Triphala and Shukramartika bati was carried out as described previously (Deshmukh and Trivedi, 2013). For cytotoxicity analysis of Triphala on nucleated cells, a thousand number of HEK 293 cells per 100 microliters of media were seeded into 96 well plates and allowed to adhere for 6 h at 37°C with a continuous supply of 5% CO_2. Once the adherence of cells was confirmed, media from the wells were removed and subsequently different concentration of Triphala and Shukramartika bati aqueous extract prepared in serum-free media was added on to cells and further incubated for 24 h. After the incubation, 0.5 µg/ml of MTT [3-(4,5-dimethylthiazol-2-yl)-2,5-diphenyltetrazolium bromide] was added in each well and kept for 4 h at 37°C with 5% CO_2. Finally, after the incubation period, media in the plate was completely removed and 50 µl of DMSO was added to the cells. To calculate the number of viable cells upon Triphala treatment, formazan product formation was measured at an absorbance of 570 nm.

4.2.7 Hemotoxicity of Aqueous extract of Triphala and Shukramatrika bati

In-vitro hemo-toxicity of Triphala and Shukramatrika bati was carried out as described previously (Balaji and Trivedi, 2012). To test the hemolysis effect of Triphala and Shukramartika bati, whole blood from humans was collected in a container containing CPD (citrate potassium dextrose) anticoagulant. RBCs were separated by centrifuging whole blood at 2000 rpm for 10 min at room temperature and the buffy coat settled on top of RBC pellet was aspirated along with liquid to remove white blood cells. The resultant pellet was repeatedly washed atleast 4 times with Phosphate buffer saline (PBS, pH 7.4). To analyze hemolysis, 3% of hematocrit was prepared in PBS (negative control), aqueous Triphala and Shukramatrika bati (250 µg/ml), and 0.1% TritonX-100 (positive control). Samples were incubated at 37°C for 1 h and liberated hemoglobin was measured at an absorbance of 540 nm using a spectrophotometer. The toxicity studies were carried out in triplicates and mean ± SE was calculated.

4.2.8 Measurement of ROS level in malaria parasite treated with Ayurvedic formulations

Intracellular reactive oxygen species (ROS) within the parasite was measured by flow-cytometry using 2,7 Dichloro-fluorescein diacetate (DCF-DA) as described previously (Gunjan et al., 2016; Vimee et al., 2019). In detail, RBC containing 8% parasitemia were treated with IC_{50} concentration of Triphala and Shukramartika bati for 24 h at 37 °C in a CO_2 incubator. After

incubation, parasite culture was washed two times with complete media and further incubated for 30 min with 10 µM DCF-DA at 37 °C in dark conditions. Further, the culture was washed and parasites were isolated by saponin lysis. The isolated parasites were suspended in PBS for Flow-cytometry analysis. The analysis was carried out in BD FACS Calibur (BD Biosciences) with a light source of 488 nm argon laser. Data analysis of Mean fluorescence intensity and DCF positive parasites was performed using FCS express Flow-cytometry software (De novo software., USA).

4.2.9 Measurement of mitochondrial membrane potential in malaria parasite treated with Ayurvedic formulations

Plasmodium falciparum (3D7) Infected RBCs were exposed with IC_{50} concentration of the extracts for 24 h. Once the culture was enriched with mature stage parasites, carbocynin dye JC-1 6 µM was added and incubated for 20 min at 37°C. The culture was washed twice with PBS and suspended in 0.5 ml of assay buffer. The differential fluorescence due to alteration in pRBC's mitochondria membrane was evaluated using BD FACS Calibur (BD Biosciences) and the FCS express Flow-cytometry software was used to perform data analysis.

4.2.10 Determination of *in-situ* DNA fragmentation through TUNNEL assay in malaria parasite treated with aqueous extract of Ayurvedic formulations.

DNA fragmentation is a hallmark characteristic of apoptotic cells, which can be detected using terminal deoxynucleotidyl transferase (TdT) mediated dUTP nick and labeling (TUNEL). To identify such events in parasites upon treatment of Triphala and Shukramartika bati, a TUNEL assay was performed using Cell Meter TUNEL Apoptosis assay kit (AAT Bioquest, USA) as per the manual instruction. In brief, parasites were grown till it reached 8% parasitemia and treated with aqueous extracts. After 24 h of incubation, the samples were fixed using 4% formaldehyde fixative buffer and permeabilized using 0.2% of TritonX-100. The fixed and permeabilized parasites were washed thrice with PBS. The samples were incubated with 1X Tunnelyte Red at 37°C for 60 min and the cells were washed 4 times with PBS. The DNA fragmented parasites were observed at the TRITC filter with Ex/Em 550/590-650 nm in BD FACS Calibur (BD Biosciences).

4.3 Results

4.3.1 Ayurvedic formulations have antimalarial activity

In this study, antimalarial potencies of 16 different ayurvedic formulations were evaluated through SYBR green method (Table 4.1). Except Triphala, all the other formulations were evaluated for the first time for their antimalarial activity in *P. falciparum* (3D7). The crude phytochemicals of ayurvedic formulations were extracted through the aqueous extraction process as described in section (4.2.2). The crude extracts of formulations were filtered using 0.2 µm filter and then used for treatment on *P. falciparum* (3D7) at different concentrations.

Table 4.1: Antimalarial activity of ayurvedic formulations against *Plasmodium falciparum* (3D7).

S.no	Formulations	Form	IC_{50} (µg/ml)
1	Triphala	Powder	2.55 ± 0.056
2	Mahayograj	Tablet	16.055 ± 2.11
3	Kaishor	Tablet	25.60 ± 0.289
4	Sariwadi	Tablet	30.54 ± 0.62
5	Shukramatrika	Tablet	30.61 ± 5.24
6	Nawayaslauh	Tablet	47.49 ± 7.77
7	Gokshuwardi	Powder	56.845 ± 1.13
8	Nityanand	Tablet	60.165 ± 1.43
9	Vridhivadhika	Tablet	76.075 ± 1.80
10	Kanchanar	Tablet	81.975 ± 7.3
11	Mahasudharsan	Powder	83.45 ± 46.03
12	Avipattikar	Tablet	92.585 ± 7.31
13	Agnitundi Bati	Tablet	125.18 ± 0.48
14	Ashokarist	Liquid	275 ± 7.07
15	Rohitkarist	Liquid	1945 ± 63.63961
16	Kumariasav	Liquid	1945 ± 261.6295
17	Chloroquine	Positive Control drug	15 ± 1.47 nM

Out of 16 Ayurvedic formulations, ten were in tablet form and others in powder (3) and liquid (3) forms. Most of these ayurvedic formulations showed promising antimalarial activity on *Plasmodium falciparum* (3D7). The nature of formulation availability and the calculated IC_{50} of formulations were shown in (Table 4.1). Notably, five formulations such as Triphala, Mahayograj, Kaishor, Sariwadi and Shukramatrika were found to inhibit parasite growth significantly under <50 µg/ml of IC_{50} value. Aqueous extract of Triphala showed promising effect on parasite growth with an IC_{50} of 2.55 ± 0.056 µg/ml whereas other formulations such as Mahayograj (16.055 ± 2.11 µg/ml), Kaishor (25.60 ± 0.289 µg/ml), Sariwadi (30.54 ± 0.62 µg/ml), and Shukramartika (30.61 ± 5.24 µg/ml) also showed significant growth inhibitory effect on *P. falciparum* (3D7). Other formulations were evaluated to have >50 µg/ml of IC_{50} value. From the assay, it was observed that none of the liquid formulations possessed antimalarial activity even at very high concentrations. Therefore, Triphala, Mahayograj, Kaishor, Sariwadi, and Shukramatrika extracts were used to analyze their mode of action as antimalarials.

4.3.2 Aqueous extracts of Ayurvedic formulations has active biomolecules with antimalarial activity

To investigate the inhibitory action of the aqueous extracts of the top five formulations, they were tested on *P. falciparum* 3D7 cultures. Initially, the parasites were treated with different concentrations of extracts and incubated for 38 h. The thin blood smears were taken at 0h, 38h, and after 96 h of culture and the parasitemia was calculated via microscopic examination. In comparison, parasites of the untreated sample were found to grow normally from 0^{th} h whereas parasites treated for 38 h and 96 h with different concentrations of Triphala, Mahayograj, Kaishor, Sariwadi and Shukramatrika bati were found to have reduced level of parasitemia. In the treated samples, retarded growth was observed along with dead and shrunken parasites clearly visible in both 38 h and 96 h treatment conditions (Figure 4.1). For schizonticidal activity, the percentage of schizont parasites were calculated for untreated/treated samples and then the IC_{50} for each formulation was calculated by comparing with untreated samples. Based on the observation of 38h treatment, the schizonticidal IC_{50} of Triphala, Mahayograj, Kaishor, Sariwadi and Shukramatrika bati was determined to be 5.75 ± 0.169 µg/ml, 44.874 ± 2.177 µg/ml, 69.126 ± 2.5 µg/ml, 15.645 ± 0.49 µg/ml, and 28.875 ± 3.11 µg/ml respectively. To understand whether these ayurvedic formulations acts through parasitic or parastatic mechanism of killing, parasites were allowed to grow for another cycle (96 h) after removing ayurvedic

formulation extracts. After 96 h, smears were taken and the parasitemia was calculated for each concentration. Even after the removal of drugs the parasitemia continued to decrease. This suggests that the ayurvedic formulations (except Sarwardi) caused an irreversible effect on parasite growth (Figure 4.1).

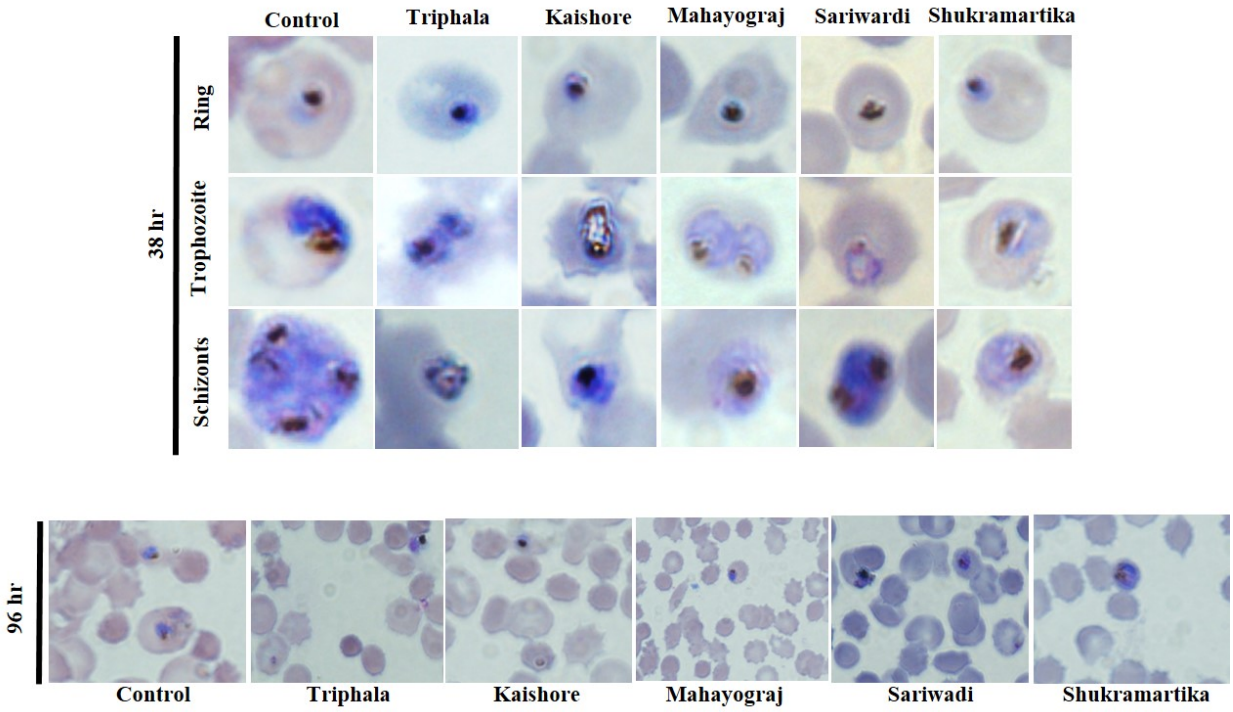

Figure 4.1: Ayurvedic formulations inhibit parasites growth irreversibly. Effect of formulations at different stages of parasites in first and second life cycle. The microscopic images showed observable changes in morphology in PHF treated parasites compared to the control parasites at different stages after 38h and 96h. The microscopic images also showed that parasites were able to grow for 96h after removal of the aqueous extracts. All these formulations were exhibiting parasiticidal activity (except sariwadi).

Finally, the inhibition growth curve was plotted and the parasiticidal activity IC_{50} value of Triphala Mahayograj, Kaishor, Sariwadi and and Shukramatrika were calculated to be 2.1175 ± 0.058 µg/ml, 16.851 ± 0.184 µg/ml, 14.122 ± 0.549 µg/ml, 32.334 ± 0.417 µg/ml, and 9.545 ± 0.084 µg/ml respectively. The death of the parasites was observed to be in a dose-dependent manner. The increase in concentration resulted in the decrease of the maturation of rings to schizonts This confirmed that Triphala Mahayograj, Kaishor and Shukramartikabati were parasitocidal in nature (Figure 4.2 A&B). Through the results obtained from SYBR green method and schizont maturation assays we choosed Triphala and Shukramatrika bati for further studies.

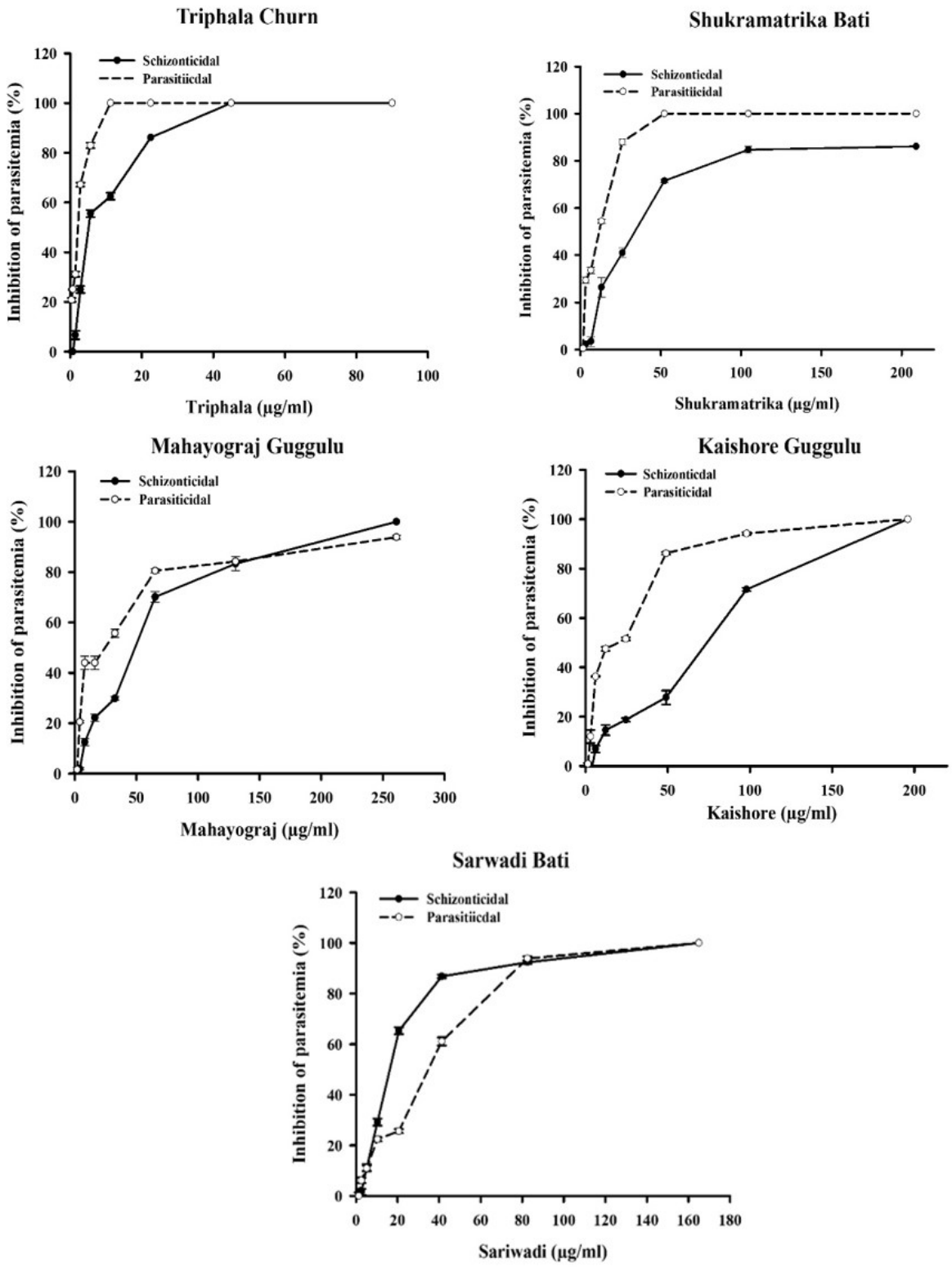

Figure 4.2: Ayurvedic formulations inhibits parasite growth in a dose-dependent manner. The inhibition of *Plasmodium falciparum* 3d7 is determined in presence of various concentrations of Ayurvedic formulation.

4.3.3 Triphala and Shukramatrika has promising antimalarial constitutent

To identify the phytochemical constituents behind the antimalarial activity of Triphala and Shukramartika bati, the aqueous extract was fractionated using HPLC. Firstly, Triphala aqueous extract was fractionated based on polarity of the components. In HPLC fractionation we obtained four major peaks from the Triphala extract. A major Peak 1 was obtained at retention time of 11.48 min with solvent (water: acetonitrile) ratio of 62:38. The subsequent peaks 2, 3 & 4 were obtained at 15.5 min, 16.38 min and 16.78 min respectively (Figure 4.3).

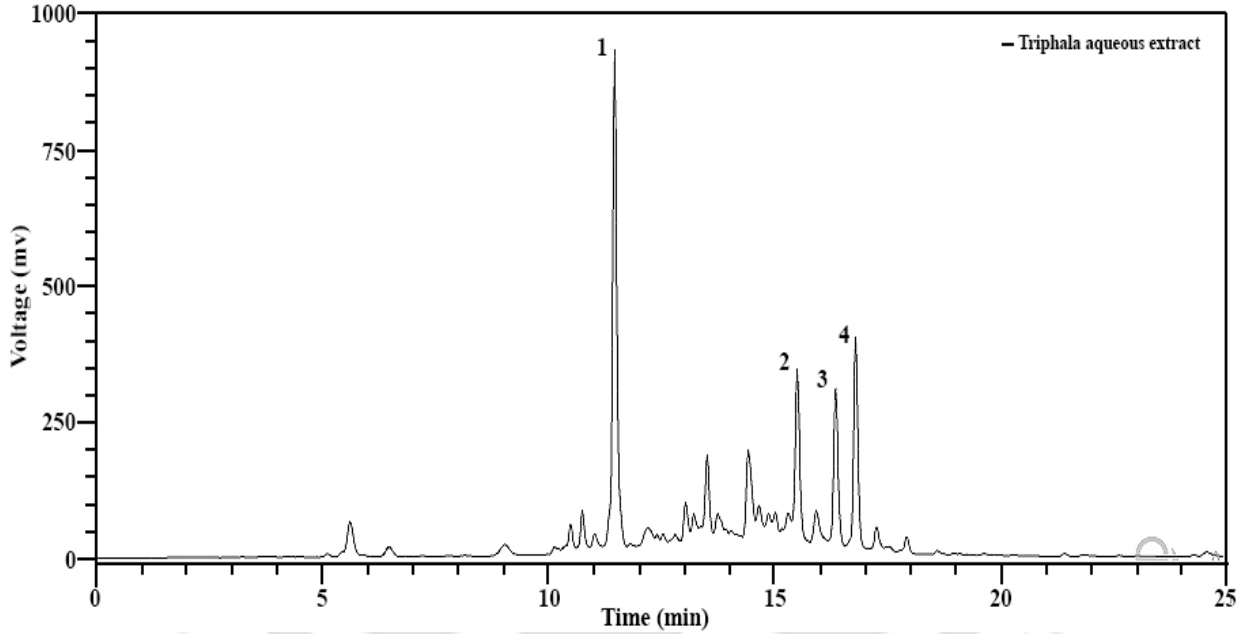

Figure 4.3: HPLC chromatogram of crude aqueous extract of Triphala.

The retention time of each peak were compared with standards. Through comparison of the standards with the peaks obtained from aqueous extract of Triphala we identified Peak 1, 3 and 4 to be of gallic acid, ellagic and chebulinic acid respectively. Similarly, in HPLC fractionation of Shukramartika bati, we obtained three major peaks. Peak 1 at 5.5 min, peak 2 at 11.37 min, and peak 3 at 17.32 min (Figure 4.4). The comparison of those peaks with standards revealed the presence of chebulic acid, gallic acid and ellagic acid.

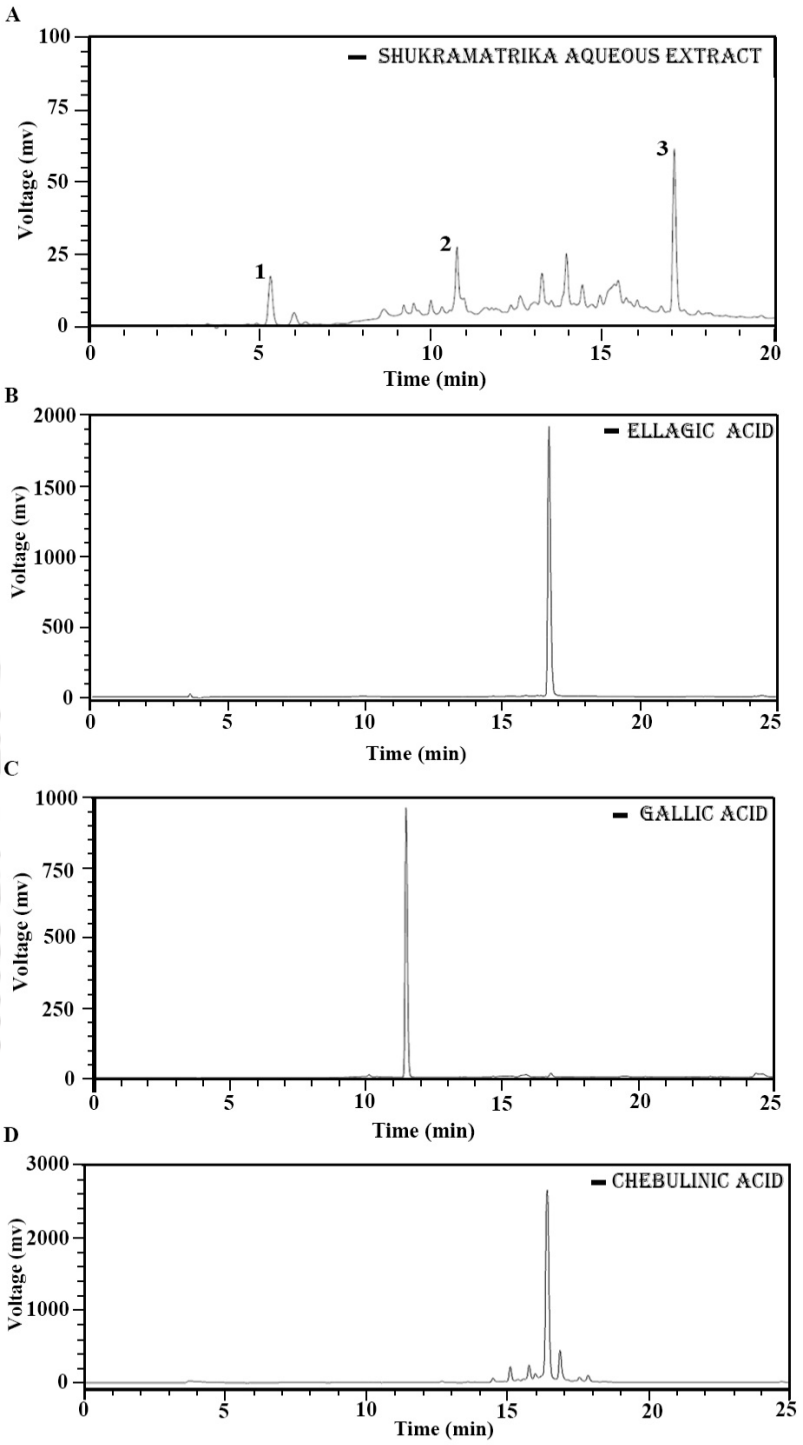

Figure 4.4: Characterization of phytochemical constituents of aqueous extract of Shukramatrika bati. (A) The chromatogram of crude aqueous extract of Sukramatrika was compared with the chromatogram of standards such as (B) Ellagic acid, (C) Gallic acid and (D) Chebulinic acid.

4.3.4 Triphala and Shukramatrika aqueous extracts are safe for developing potent anti-malarials

The water extract of Triphala and Shukramartika bati were treated on HEK-293 cells using various concentrations and the morphology of HEK-293 cells treated with and without Triphala/Shukramartika bati water extract was observed through phase-contrast microscopy. The cells treated with high concentrations of extract (250 and 500 µg/ml) were found to be shrunken and detach from wells whereas in lower concentrations (1 and 100 µg/ml), the cells appeared mostly viable and adherent, similar to the untreated controls (Figure 4.5 A).

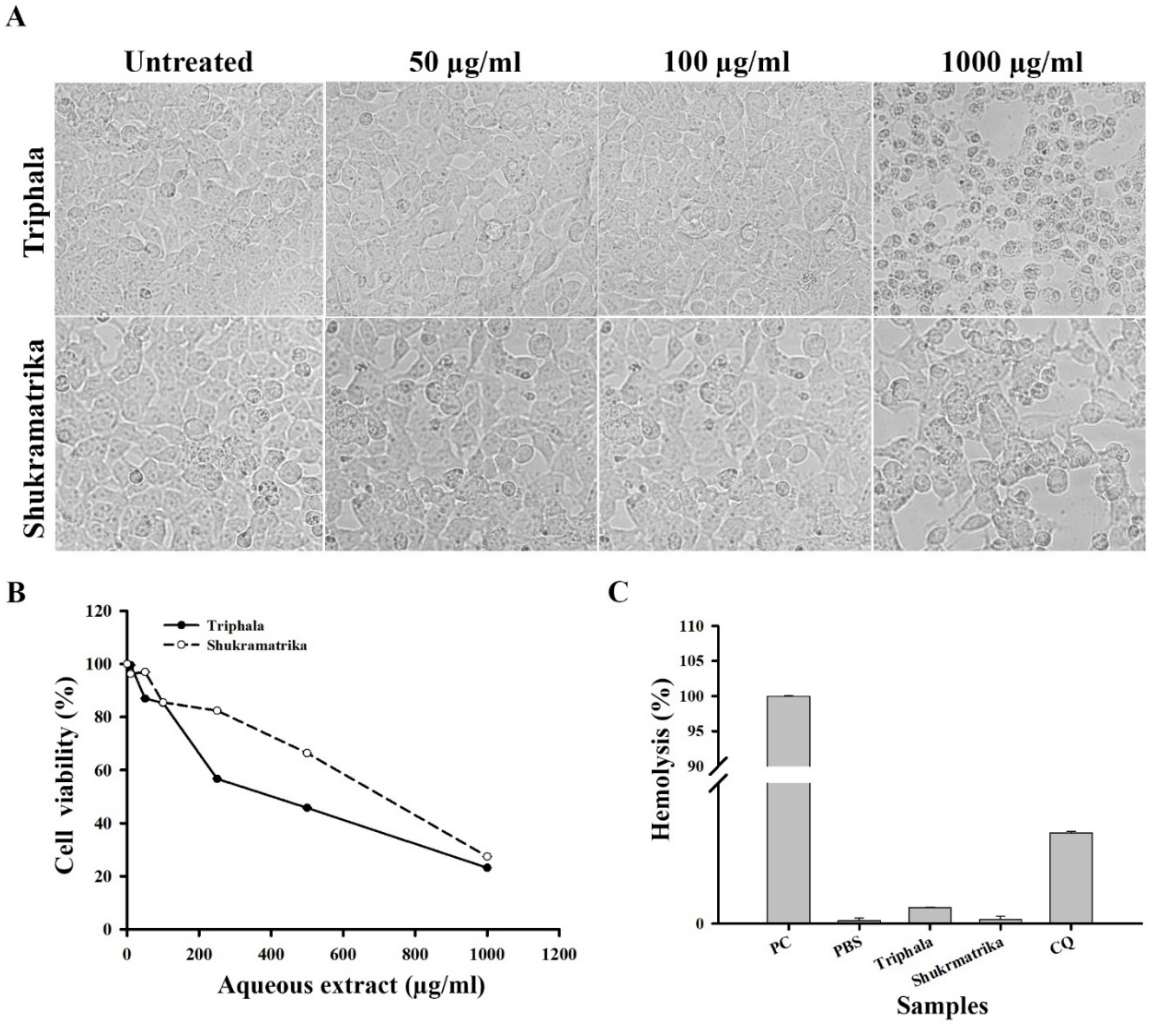

Figure 4.5: Formulations are safe to use. (A) Cytotoxic effect of Triphala and Shukramatrika on HEK293 cell. Microscopic images of Triphala and Shukramatrikabati treated on HEK-293 cells compared with untreated cells. **(B) Both Triphala and Shukramatrika is not toxic to cells**. Various concentrations (1-1000 µg/ml) of Triphala and Shukramatrika treated on HEK293 cells and found concentrations below 200 µg/ml for Triphala and 500 µg/ml for shuikramatrika have possessed no cytotoxic effect. **(C) Effect of Triphala**

and Shukramatrika on RBC. The hemolysis upon incubation Triphala and shuikramatrika with the highest concentration (500 µg/ml) was measured and compared with controls such as PBS, Chloroquine, and 1% Triton X-100.

The growth of HEK-293 cells was observed to be inhibited in a dose-dependent manner. In higher concentrations of Triphala and Shukramartika bati (250 to 1000 µg/ml), the growth of the cells was markedly decreased compared to control at 48 h incubation. In lower concentrations (1 to 100 µg/ml), Triphala/Shukramartika bati does not show any effect on cell growth (Figure 4.5 B). Meanwhile, hemolysis was evaluated using a higher concentration of Triphala and Shukramartika bati aqueous extract and compared with controls. The values obtained from hemolysis are compared to the RBCs lysed in 1% triton X-100 (positive control), in presence of Chloroquine and, in Phosphate buffer saline (pH7.4). The results suggest that Triphala and Shukramartika bati has no significant effect on RBCs even at 500 µg/ml concentration (Figure 4.5 C).

4.3.5 An increased level of ROS is generated in *Plasmodium falciparum* upon treatment with Triphala/Shukramatrika bati

The high metabolic rate due to rapid multiplication and host immune responses normally generates reactive oxygen species (ROS) inside malaria parasites (Kavishe et al., 2017). Drugs like chloroquine and mefloquine elevate the ROS level abnormally inside parasites and lead to the death of the parasite by inducing programmed cell death (PCD) (Ch'ng et al., 2010; Gunjan et al., 2016). Therefore, to understand if treating parasites with Triphala and Shukramartika bati triggers PCD mechanism by increasing level of ROS, DCFDA as a ROS probe was used. The ROS generation within the treated parasites with IC_{50} value of Triphala/Shukramartika bati for 24h was determined and compared with untreated parasites. In flowcytometry analysis, parasites treated with Triphala and Shukramartika bati showed an increased DCF positive parasites of about 21.54% and 22.08% compared to untreated parasites after 24 h exposure (Figure 4.6). The percent increase in ROS levels are comparable to the chloroquine control with 23.42% ROS increase from untreated parasites. This suggests that Triphala and Shukramartika bati causes oxidative outburst which results in a significant increase of intracellular ROS generation inside parasites.

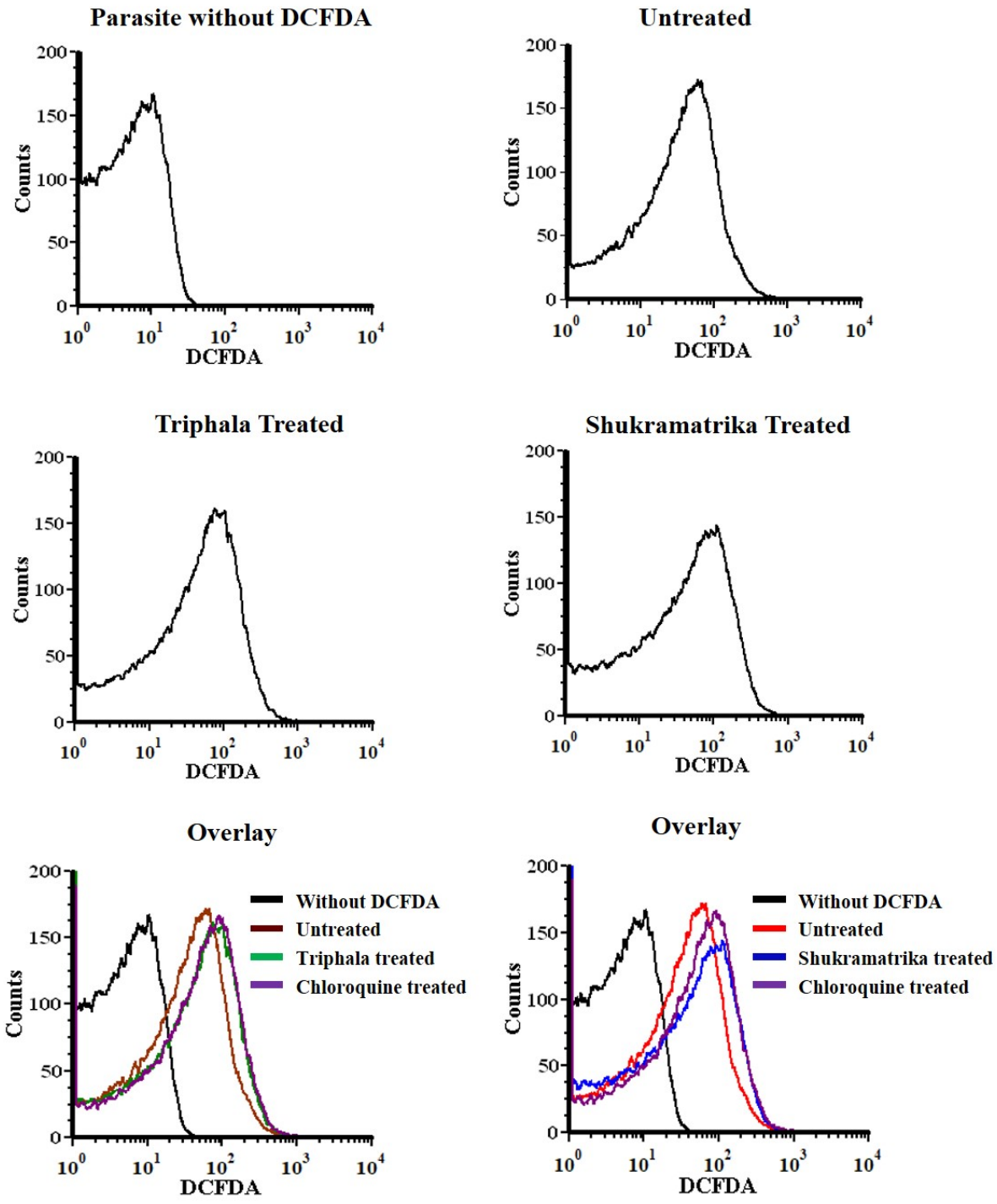

Figure 4.6: Ayurvedic formulations induces ROS generation in malaria parasites. The generation of ROS inside the parasites was evaluated using a DCFDA probe. The histogram obtained from flowcytometric analysis showing an increased level of ROS-positive cells upon Triphala and Shukramatrika treatment. Overlay histograms showing a difference of DCFDA positive cells between treated and control samples.

4.3.6 Triphala and Shukramatrika bati destabilizes mitochondrial membrane potential ($\Delta\psi_m$) of *Plasmodium falciparum*

Mitochondrial membrane potential (ΔΨm), an index of mitochondrial function, was examined to evaluate the effect of Triphala/Shukramartika bati on mitochondria of asexual blood stages of Plasmodium. The detection of mitochondrial membrane potential in drug-treated/untreated parasites was performed using JC-1, a cationic probe that aggregates in the mitochondria due to the electronegative environment inside and exhibits red color fluorescence. However, at depolarization state of mitochondrial membrane (low mitochondrial membrane potential) JC-I remains in monomeric form and exhibits green color fluorescence.

To evaluate the destabilization of mitochondrial membrane potential in untreated and formulation treated samples, the uptake of JC1 in parasites was measured using FACS. The green and red signal were observed in FL1 and FL2 channel. Dot plot analysis of the aqueous extracts treated parasites suggests significant changes in green fluorescence intensity in comparison to untreated parasites after 24 h treatment. JC-1 fluorescence was recorded in both green fluorescence channel (apoptotic cell population) and red fluorescence (non-apoptotic cell population) channel. In untreated parasites, the non-apoptotic cell population was calculated to be 26.3% cells whereas apoptotic cell population was found to be 38.1% cells. In Triphala/Shukramatrika bati treated cells, red signal population decreased to 17.4%/18.6% and percentage of green signal population increased to 51.3%/49.2% after 24h. The similar level of increase in red/green signal population was observed for chloroquine treated parasites. The Percentage increment of JC-1 monomer confirms that membrane potential in mitochondria was decreased significantly (Figure 4.7).

4.3.7 Triphala causes *in-situ* DNA fragmentation in parasites

DNA fragmentation upon Triphala/Shukramartika bati treatment in the parasite was detected using TUNEL assay. The dUTP-fluorescein incorporated into DNA nicks formed in Triphala treated parasites was measured using rTDT (recombinant terminal deoxynucleotidyl transferase) to quantify the proportion of DNA nicks. The fluorescence value produced from dUTP-fluorescein was observed to be directly proportional to the DNA nicks formation in the treated parasite population. The DNA nicks formed was compared with untreated parasite sample.

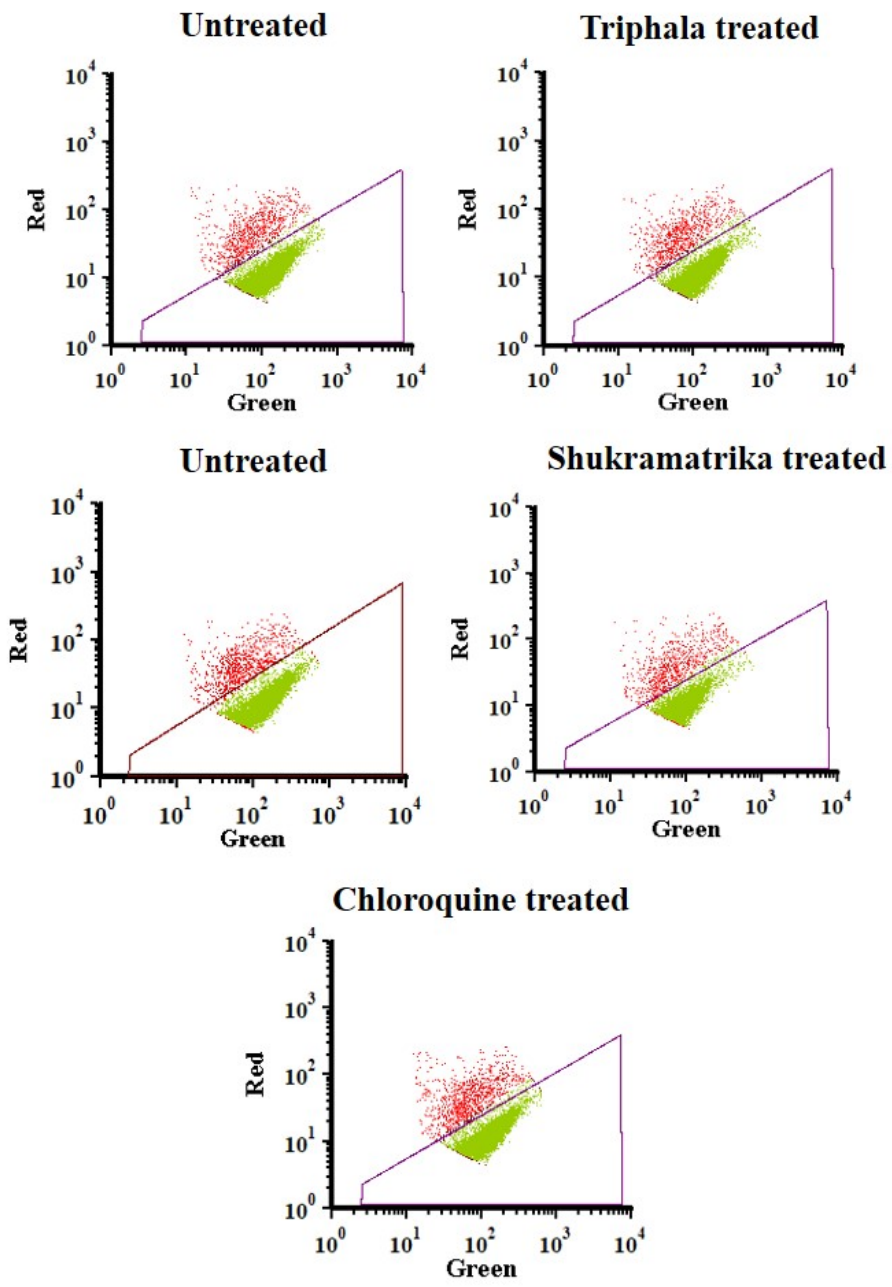

Figure 4.7: Triphala and Shukramatrika destablizes mitochondria membrane potential. Alteration of mitochondrial membrane potential (ΔΨm) in treated and control parasites were evaluated using JC-1 staining. Dot plot showing the difference of aggregated (Red) and non-aggregated monomer (Green) JC-1 dye in treated and control parasites. Both Triphala and Shukramatrika treated parasites showed an increase in JC-1 monomer compared to control parasites.

The percentage difference of 0.06% between unstained and untreated stained (control) parasite samples in TUNEL positive population indicates the absence of formation of DNA nicks. In the Triphala treated parasite sample, the enhanced dUTP-flurescien signal of TUNEL positive

population was about 14.49%, suggesting that a significant population of parasites contained nuclear DNA that was fragmented. In comparison with Triphala, Shukramatrikabati and chloroquine (positive control) samples were found to have limited percent (1.49% and 1.69%) of parasites that had undergone DNA fragmentation (Figure 4.8). From the study based on ROS generation, mitochondria membrane potential and, *in situ* DNA fragmentation, it was concluded that Triphala and Shukramartika bati induces programmed cell death pathway in parasites.

4.4 Discussion

The ayurvedic formulations were prevalently used to treat several diseases from ages. The abundance of phytochemicals present in ayurvedic formulations helps to cure many zoonotic infections, especially as elucidated in case of Triphala (Peterson et al., 2017). Extensive studies on phytochemical constituents of Triphala and their role is explored in several reports. Chebulinic acid, one of the major phytochemicals present in Triphala is previously found to be a potent antimalarial (Thu et al., 2017). Though Triphala is known for its antimalarial activity, but its use as an antimalarial is limited, due to lack of knowledge on their mechanism and mode of action. A similar trend is also observed with almost all other formulations. Therefore, we examined the mode of action behind the parasitic death, and additionally considering the importance of programmed cell death in the parasite upon treatment with different ayurvedic formulations. This is the first inference to show that ayurvedic formulations causes death in parasites via the PCD pathway. Chloroquine, a known antimalarial that induces PCD pathway in parasites is used a control for assessing the cell death by PHFs. Since, extraction using solvents like methanol, acetone, and DMSO has its limitations (Ameer et al., 2017), we focused on water extraction of 16 ayurvedic formulations and evaluated its antimalarial activity on *Plasmodium falciparum* (3D7). From the 16 formulations, five formulations potentially kill the parasites at <50µg/ml concentrations. Primarily, we investigated the effects of Triphala and Shukramatrika bati on *Plasmodium falciparum* (3D7) culture and then elucidated the induction of type 1 PCD apoptotic pathway related to parasite death. In our analysis, the water extract of Triphala/Shukramartika significantly kills the parasites, and the IC_{50} of schizonticidal and parasiticidal activity were determined to be 5.75 ± 0.169 µg/ml/ 28.875 ± 3.11 µg/ml and 2.1175 ± 0.058 µg/ml/ 9.545 ± 0.084 µg/ml respectively. The IC_{50} values of schizonticidal and parasiticidal activity shows Triphala/Shukramatrika affects the parasites growth irreversibly.

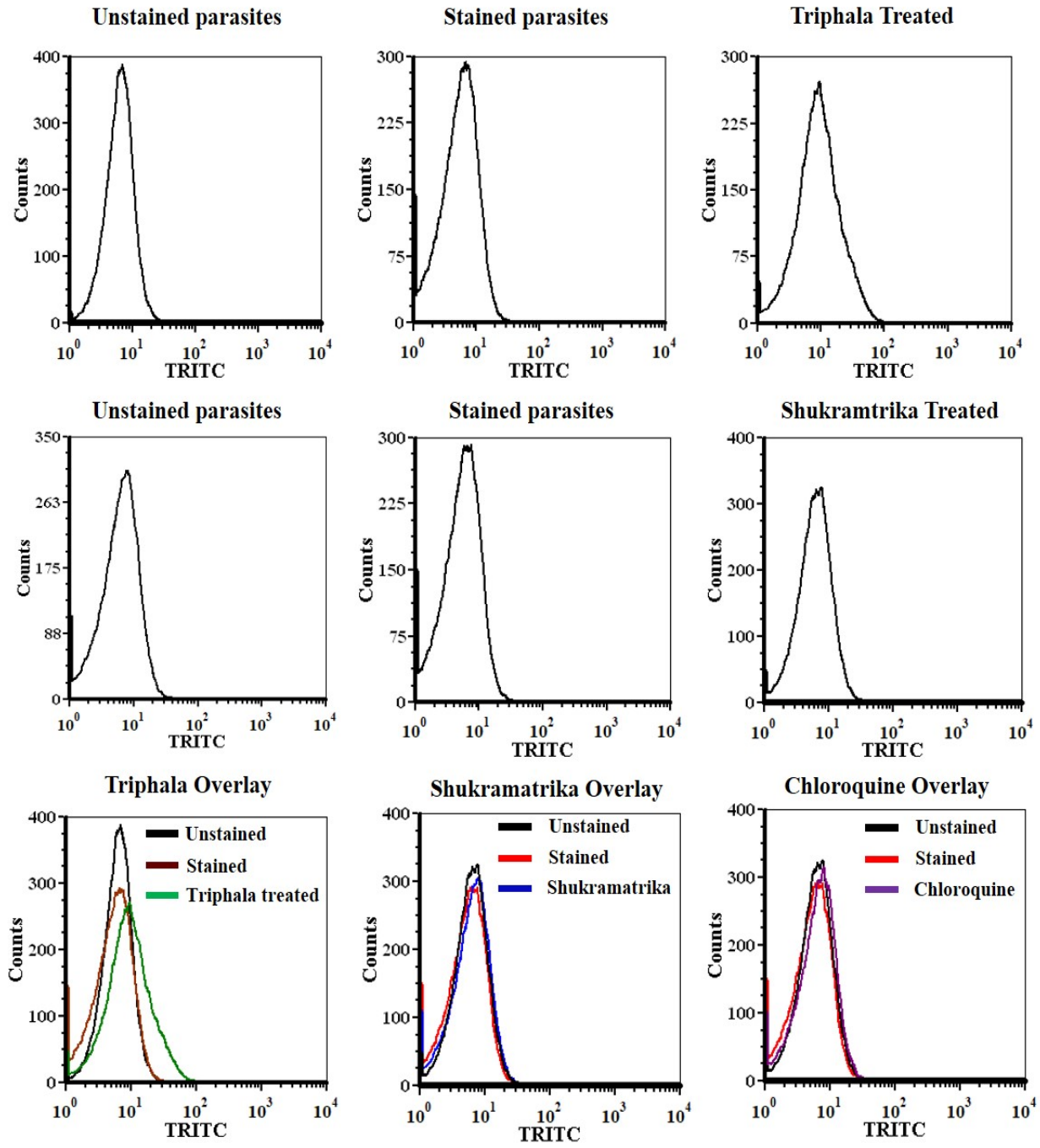

Figure 4.8: Triphala and Shukramatrika induces apoptosis in *Plasmodium falciparum*. Triphala and Shukramatrika leads to DNA fragmentation in *Plasmodium falciparum*. DNA nicks formed in control/treated parasites were analyzed using TUNEL staining. Histograms shows that parasites treated with Triphala, Shukramatrika and chloroquine have a shift towards TRITC channel whereas unstained and untreated samples have no significant changes in flow-cytometry analysis.

Additionally, the mode of death is observed to be parasiticidal in nature. The fractionation of aqueous extract of Triphala suggested the presence of gallic acid, ellagic acid and chebulinic acid. Whereas, fractionation of Shukramartika reveals presence of chebulic acid, gallic acid and ellagic acid. Therefore, our analysis suggests these are the phytochemical constituents may synergistically be responsible for the inhibition of malaria parasites growth. Subsequently, we assessed the biological parameters of parasite death to determine the involvement of the apoptotic pathway. In this, we evaluated ROS production, in-situ DNA fragmentation and, the mitochondrial membrane potential in treated/untreated parasites of Triphala/Shukramatrika bati and compared with chloroquine (positive control).

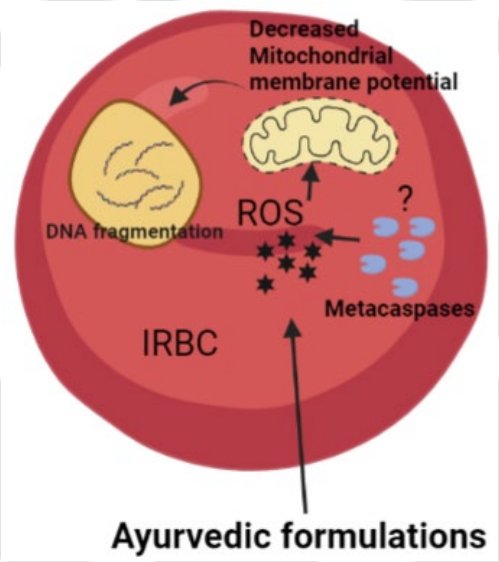

Figure 4.9: Proposed mechanism of action of Ayurvedic formulation induced cell death in P*lasmodium falciparum*

Several reports suggest that drugs like mefloquine and, chloroquine elevates intracellular ROS and induces apoptosis in parasites. Thus, the ROS generation in parasites, treated with Triphala/Shukramartika was quantified by probing with DCF-DA. The ROS generated inside the parasites shows a 21.54%/22.03% increases compared to control. The similar population of parasites (23.42%) were also observed in chloroquine treated parasites. This increased ROS modulates permeability of the mitochondrial membrane and was is detected using JC1. The lipophilic dye has the capacity to permeate into the cell and emit red fluorescence while it gets aggregated inside the mitochondria. During apoptosis, the mitochondrial membrane permeability decreases ($\Delta\Psi m$) which results in restriction of the dye to enter the mitochondria. This causes

JC1 to be localized in the cytosol as a monomer and emit green fluorescence. Therefore, the differential ratio of red and green fluorescence caused due to ΔΨm in treated parasites was measured. In untreated parasite the ratio of red:green signal was found to be 1.44 whereas in the treated parasites the ratio was measured to be 2.94 for Triphala and 1.89 for Shukaramartikai. Further, to conclude that Triphala/Shukramatrika follow apoptotic pathway to cause death in parasites, DNA fragmentation inside the parasites was visualized. The formation of nicks in parasites nuclear DNA was identified through TUNEL assay. A population of 14.44% in Triphala and 1.49% in Shukramatrika produced enhanced dUTP-fluorescein signal and thus are found to be TUNEL positive cells. From our study we propose that Triphala/Shukaramartika bati induces apoptotic cell death in parasites by generating significant level of ROS. The generation of reactive oxygen species leads to depolarization of mitochondrial membrane and causes permeabilization of mitochondrial membrane which consecutively triggers DNA fragmentation inside the parasites (Figure 4.9). In conclusion, all these cascade of events indicates that Triphala/Shukaramartika ayurvedic formulations may cause the parasitic death irreversibly through an apoptotic pathway.

Chapter V

FIKK9.1 kinase has potential as diagnostic marker for malaria detection

Summary

Since the past two decades, the world has seen an increasing emergence of drug resistance across the plasmodium species (Ippolito et al., 2021). The major cause of ineffectual elimination is due to the lack of health care resources in tropical and sub-tropical regions (Tanner et al., 2015). To strengthen the ongoing effort for malaria elimination, a sensitive point of care detection system is required. The improved detection system would help in the prevention of severe complications associated with malaria (Mousa et al., 2020). WHO guidelines recommend that the malaria diagnostic targets should be used to address the issues such as lack of sensitive, inability to quantify the density of parasites, and incompetence in differentiating parasites at species level (WHO 2020). Based on our preliminary analysis, we have found FIKK9.1 as a useful target to develop the specific and sensitive diagnostic system for malaria. Our analysis shows that FIKK9.1 has potential immunogenic regions that are exclusive to *Plasmodium falciparum* and are extremely diverged from human sequences. Therefore, anti-FIKK9.1 was generated, purified and characterized for its potential use as a diagnostic target for malaria detection. The purified antibody was found to be highly sensitive to FIKK9.1 with a limit of detection at 3 nmole concentration of the protein. The selectivity of purified anti-FIKK9.1 was evaluated using various biological samples. The results suggest that the antibody produced is highly specific to FIKK9.1 and does not react with host blood components and proteins from other organisms. Validation of the purified antibody was done using mock patient samples, which elucidated that the antibody may semi-quantitatively detect the parasite load in the samples with an average accuracy of 95.45%. Our overall study suggests that FIKK9.1 can be exploited to develop new diagnostic system for malaria.

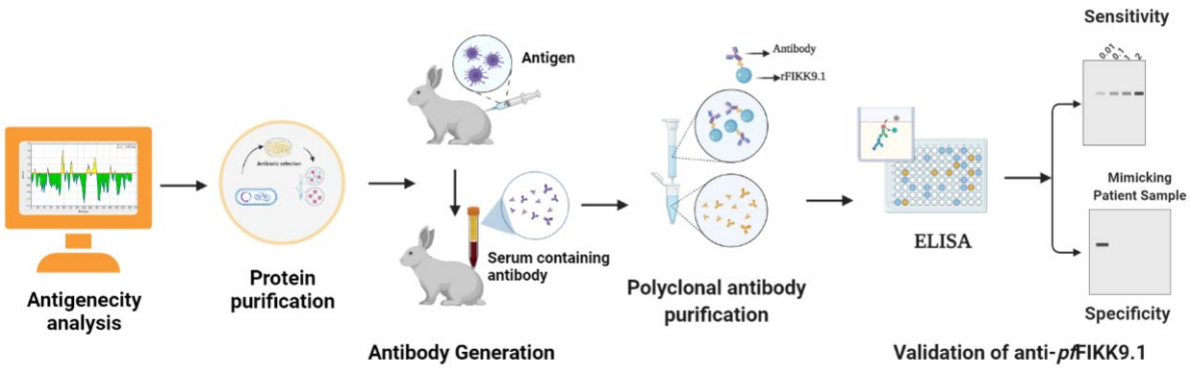

Schematic presentation to explore the potentials of FIKK9.1 kinase in malaria diagnosis

5.1 Introduction

Effective management and surveillance are the only solution for the eradication of malaria (Hatherell et al., 2021; Lourenço et al., 2019). To achieve this goal, rapid and specific diagnosis of malaria is a prerequisite. WHO recommends early diagnosis of malaria using microscopy or rapid diagnostic test (RDT's) for all patients with symptoms before treatment to reduce morbidity and mortality (WHO 2020). Improved and high-quality diagnostics will aid in proper disease management and effectively minimize the emergence of drug resistance in the parasites (Ippolito et al., 2021; Mousa et al., 2020). Currently, diagnostic tools available for the detection of malaria include microscopy, immuno-chromatographic assays (known as rapid diagnostic tests, RDTs), fluorescence microscopy, and nucleic acid amplification techniques (NATs) (Zimmerman and Howes, 2015). The microscopic method for detecting malaria is currently considered to be the "gold standard". Diagnostic of malaria in laboratories often face problems such as unavailability of appropriate microscopy expertise, strain variations, morphological changes of malaria due to drug pressure and blood collection approaches (Moody, 2002; Tangpukdee et al., 2009). It stipulates the need for Rapid Diagnostic Tests (RDT), which could be capable of detecting .001% of parasites in patient's blood, and the ability to perform semi-quantitative measurements for monitoring high-throughput drug screening results (Cunningham et al., 2019). In the guidelines of WHO, the diagnostic device should be specific, highly sensitive, cheap, and should rapidly detect malaria. The diagnostic device must have the ability to detect a minimum of 100 parasites per micro liter of blood. For this purpose, several valuable immuno-chromatographic methods exist. These rapid diagnostics are constructive even in the most challenging areas as they are convenient and straight forward to use. The ability to differentiate among the malarial species through immunogenic differences in the proteins is considered to be a significant advantage over other methods (Tangpukdee et al., 2009). Although the RDTs can reliably detect malaria at 100 parasites/µl, still the threshold for detection is significantly higher than the microscopic method. Since these methods utilize proteins as analytes, it is not suitable for analysis or tracking rapid responses during chemotherapies.

Immuno-chromatographic and ELISA-dipstick tests are the alternative diagnostic method for malaria (Murray et al., 2008). The commercially available RDT kits are primarily based on detecting malarial antigens such as plasmodial lactate dehydrogenase (pLDH), histidine-rich protein II (pfHRP-II) and malarial aldolase. Generally, dipstick assays detect host antibodies

produced against malaria proteins. Although, we can discriminate between malaria at the species level, the detection method seems to fail in cases of co-infection. Nevertheless, the dipstick assays are pretty expensive and possesses no significant advantages over microscopic methods (Poti et al., 2020). Therefore, a constant search for other alternatives and improvement in strategies is required in the field of malaria detection. In this regard, proper knowledge about biomarkers is prerequisite, to identify a specific bio-recognition element and utilize it to develop reliable detection system for malaria. Among the various biomarkers, plasmodial lactate dehydrogenase and histidine-rich protein II (HRP II) have received increasing attention for developing rapid and reliable RTDs (Jain et al., 2014). However, species level detection is limited while using these biomarkers. This provides the need to search for novel targets that could show more sensitivity as well as species exclusiveness in the parasites.

In this chapter, we describe the characterization of polyclonal antibody generated against FIKK9.1 for the development of malaria detection. Our preliminary bioinformatics analysis of FIKK9.1 sequence elucidates that it has features to be potential diagnostic target for malaria. Therefore, the antibodies have been generated in rabbit against FIKK9.1. The generated antibodies were purified from serum through an affinity column, which was made of CNBR activated beads coupled with purified FIKK9.1 protein. The sensitivity and selectivity of the FIKK9.1 antibody towards the parasite was examined to determine its suitability in a malaria detection system. After preliminary characterization of antibody, the performance of the anti-FIKK9.1 was evaluated using mock patient samples. The semi-quantitative detection possesses an average of 95.45% accuracy while comparing with microscopic studies. Altogether, our analysis suggests that FIKK9.1 can be a better diagnostic target for malaria.

5.2 Experimental procedures

5.2.1 Materials

CNBR activated Sepharose beads were purchased from Sigma Chemical Co., St. Louis, MO, USA. Blotting sheets (Nitrocellulose) was purchased from Bio-rad laboratories, Hercules, California, USA. Other reagents used in this study are of analytical purity.

5.2.2 Parasite culture

Plasmodium falciparum (3D7), a drug-sensitive strain is cultured as we have already described in Chapter 3, section 3.2.2, page no. 80.

5.2.3 Identification of antigenicity of FIKK9.1

Bioinformatics tools were utilized to identify the regions in FIKK9.1 that are highly antigenic and diverged both from the host and other plasmodium species. The protein sequence was retrieved from plasmoDB and BLAST was performed using NCBI and PlasmoDB database. The PlasmoDB server was used to study the sequence homology with other species in the *Plasmodium* genus and the NCBI server was utilized for sequence homology studies with other organisms. The proteins sequence was then uploaded in the IDEB analysis resource with default parameters to predict the antigenicity of the protein. Based on the threshold value obtained in Kolaskar and Tongaonkar antigenicity scale (Kolaskar and Tongaonkar, 1990) the antigenic regions are considered to be as high antigenic, low and no antigenic regions.

5.2.4 Generation of polyclonal antibody in rabbit

For antibody generation, a large quantity of FIKK9.1 protein was purified using affinity chromatography. The highly concentrated purified FIKK9.1 was diluted in sterile water at a concentration of ~400 µg/0.5 ml. The first antigen injection was carried out by preparing an emulsion of FIKK9.1 protein with an equal amount of Freund's complete adjuvant using a syringe. Injection of antigen into the rabbit as an animal model for antibody production was performed at CSIR-CDRI, Lucknow, in collaboration with Dr. Amogh A. Sahasrabuddhe. After the second booster of antigen, serum was collected from the rabbit every subsequent booster and its titer was determined using ELISA. To obtain a clear serum, the collected blood was centrifuged at 2000 rpm for 10 min at 4°C. The clear serum was carefully collected and stored at -20°C until use.

5.2.5 Generation of CNBr – FIKK9.1 affinity column

To generate CNBr-FIKK9.1 affinity column, purified FIKK9.1 was coupled to CNBr-activated sepharose 4B beads (Sigma Chemical Co., St. Louis, MO, USA) as per the manufacturer protocol. In detail, FIKK9.1 kinase was purified through gel filtration chromatography as described in Section 2.6 and dialyzed against coupling buffer (0.1 M $NaHCO_3$, pH 8.3 containing 0.5 M NaCl) overnight at 4°C. Sepharose beads were then incubated with 1 mM HCl for at least 30 min and washed with 10 to 15 ml of coupling buffer. The purified FIKK9.1 protein was then added to CNBr activated Sepharose resin and incubated overnight at 4ºC.The unreacted proteins were washed away using coupling buffer and the column was blocked with a blocking buffer

containing 0.2 M Glycine (pH 8.0). Finally, FIKK9.1 coupled sepharose beads were transferred to the column and washed with PBS at least three times. A similar process was carried out to generate CNBr-BSA affinity column.

5.2.6 Purification of Polyclonal antibody using FIKK9.1 based affinity column

To obtain FIKK9.1-specific antibodies, we incorporated a subtraction step in the protocol to washout antibodies from serum that may non-specifically bind to the protein. The crude rabbit antiserum was passed sequentially into two columns (prepared as mentioned in section 5.2.4). The first column contained CNBr beads coupled with BSA that would bind to non-specific antibodies and subtract them away from the fractions. In contrast, the antibodies specific to FIKK9.1 will not react to the column and be swept away in the flow-through fraction. The second column consisted of beads coupled with FIKK9.1 and it is utilized for affinity purification of anti-FIKK9.1. The flow-through fraction collected from the first column was incubated overnight at 4ºC with column two. After incubation, a stringent washing step was performed by sequential addition of alkaline buffer (0.1 M Tris, pH 9.5 contains 0.5 M NaCl) and acid buffer (0.1 M acetic acid, pH 4.0 contains 0.5 M NaCl). The alkaline and acidic washes were repeated at least five times to remove nonspecific antibodies that bind to FIKK9.1 with low affinity. At last, the antibodies that bind at a high affinity with FIKK9.1 were eluted through a strong acidic buffer (0.15 M NaCl, pH 2.5) condition, and it is immediately neutralized.

5.2.7 Evaluation of purified anti-FIKK9.1 polyclonal antibodies titer

ELISA (Enzyme linked immune sorbent assay) was performed, as described previously, to evaluate the titration of purified anti-FIKK9.1 polyclonal antibodies (Singh et al. 2018). Elaborately, 200 µL of coating buffer containing 10 µg/ml of purified FIKK9.1 was added on a 96 well plate and incubated at 4°C overnight. After the protein was coated, the wells were washed with PBS at least three times and incubated with blocking solution for 2 h. Once the blocking step was completed, the solution was removed, and the protein was probed with different dilutions of rabbit serum. After incubation for 2 h at room temperature, the serum was washed with PBST and PBS three times each and incubated with goat anti-rabbit HRP conjugated secondary antibody (1:5000 dil) for 1 h at room temperature. Then the final washing step was performed and TMB substrate solution was added in each well. The reaction was terminated by adding 50 µl of 0.1 N H_2SO_4 and the absorbance recorded at 450 nm.

5.2.8 Sensitivity of anti-FIKK9.1 polyclonal antibodies

To test the sensitivity of purified anti-FIKK9.1, dot blot of FIKK9.1 probed with anti-FIKK9.1 antibody was performed. In detail, a varying concentration of purified FIKK9.1 kinase (prepared as described in section 2.6) is dotted on the nitrocellulose membrane. The blot is air-dried and incubated with blocking solution (PBS, pH7.4 contains 3% BSA) for 1 h at room temperature and then washed with 1X PBST and 1X PBS thrice. After washing, the blot was incubated with the antibody (1:5000 dil) at 4ºC overnight. Once the blot was probed, it was washed with PBST and PBS 3 times for 5 minutes each and incubated with goat anti-rabbit HRP conjugated secondary antibody (1:6000 dil) for 45 min at room temperature. Finally, the chemiluminescent substrate was added to the blot and the signal captured using gel-doc system (Bio-rad, USA).

5.2.9 The purified anti-FIKK9.1 polyclonal antibody specifically detects parasite protein

The specificity of the anti-FIKK9.1 antibody was evaluated through probing it in different samples such as complete media, human serum, parasite culture media and parasite culture. The Samples were dotted on blotting membrane and blocked with 3% BSA solution. After blocking, the blots were sequentially probed with primary anti-FIKK9.1 antibody (1:5000 dil) and secondary antibody (1:6000 dil) with washing steps in between. The results were evaluated by comparing it with purified FIKK9.1 chemiluminescence intensities.

5.2.10 Selectivity of anti-FIKK9.1 during other infectious diseases by mocking coinfection

To determine the anti-FIKK9.1 specificity during the time of co-infection, parasites were detected in human blood, contaminated with laboratory strains of various infectious agents such as *E. coli*, *M. smegmatis*, Yeast, Newcastle disease virus (NDV), Japanese encephalitis virus (JV), Duck plaque virus (DPV) and Herpes simplex virus (HERPES). In detail, the human blood containing 2% parasitemia was contaminated with various concentration of infectious agents to mimic co-infection conditions. Human blood, devoid of the malaria parasite and containing only the infectious agents were used as a negative control for this study. The human blood contaminated with malaria parasites were taken as positive control. All these mock co-infection samples and their respective controls were processed and blotted into nitrocellulose membrane. The blotting technique and subsequent steps were performed as described in the section 5.2.9.

5.2.11 Validating anti-FIKK9.1 in whole blood sample containing parasites (Blind approach)

Human blood was collected with the help of phlebotomist from 20 healthy individuals having different blood groups. To mimic the patient samples and to validate the detection through blind approach, some of the collected blood samples were anonymously contaminated with *in-vitro* cultured parasites. All the twenty mock samples were lysed by continuous freeze thawing cycle for 2 times. The lysed blood was diluted to 50 µg/ml concentration with lysis buffer containing 2% SDS. Later, the samples were blotted in the form of dots on nitrocellulose membrane and is air dried completely. The dried membrane was blocked with 3% BSA in PBS for 1 h at room temperature. After incubation, excess BSA was washed out using PBS pH7.4, containing 0.05% of tween-20. Once the blocking step was completed, anti-*pf*FIKK9.1 antibody was added to the blot and incubated for 2 h at room temperature. The blot was washed with PBST and PBS for 4-5 times each to remove excess primary antibody. Secondary antibody (ALP-conjugated anti-rabbit) was added on the blot and incubated at room temperature for 1 h. The membrane was washed extensively with PBST and PBS for 4-5 times each in shaking condition for 5 min to eliminate any non-specific signal. The NBT-BCIP dissolved in DMF (Dimethylformamide) substrate was then added onto the membrane and the signal was acquired using gel doc (Bio-rad) system. The parasitemia of the positive and negative samples were quantified by comparing their signal intensities with a standard curve plot, prepared from known parasitemia controls. The percentage accuracy based on the results were calculated using the following formula:

$$\text{Percentage error} = (I(V_o - V_a)I/V_a) * 100) \quad \ldots\ldots\ldots\ldots\ldots\ldots\ldots\ldots\ldots\ldots\ldots\ldots (1)$$

Whereas, V_0 is Calculated parasitemia value, V_1 is Microscopic examination value and the $I(V_o - V_a)I$ is a non-negative value

$$\text{Percentage accuracy} = 100 - \text{percentage error} \quad \ldots\ldots\ldots\ldots\ldots\ldots\ldots\ldots\ldots\ldots\ldots\ldots (2)$$

5.3 Results

5.3.1 FIKK9.1 has antigenic regions that are exclusive to *Plasmodium falciparum*

Bioinformatics analysis was carried out using PlasmoDB and NCBI database. From the sequence homology analysis, we categorized FIKK9.1 into four different regions. The first category contains the regions that are exclusive to *Plasmodium falciparum*, followed by the second and

third category comprising residues that show homology with either *Plasmodium spp.* or human. The fourth category represents the regions conserved in both *Plasmodium spp.* and human (Figure 5.1A, B & C). Our analysis suggests that most of the N-terminal regions are exclusive to *Plasmodium falciparum* whereas C-terminal domain is well conserved with *Plasmodium spp*. and very few regions are conserved with humans (Figure 5.1 A). Further, to evaluate regions that can be exploited for detection of malaria, the antigenicity score was given for different regions of FIKK9.1 using Kolaskar & Tangaonkar server. To predict the antigenic score, the server follows a semi empirical method which utilizes physicochemical properties of amino acid residues and their frequencies to be antigenic with help of known structural segmented epitopes.

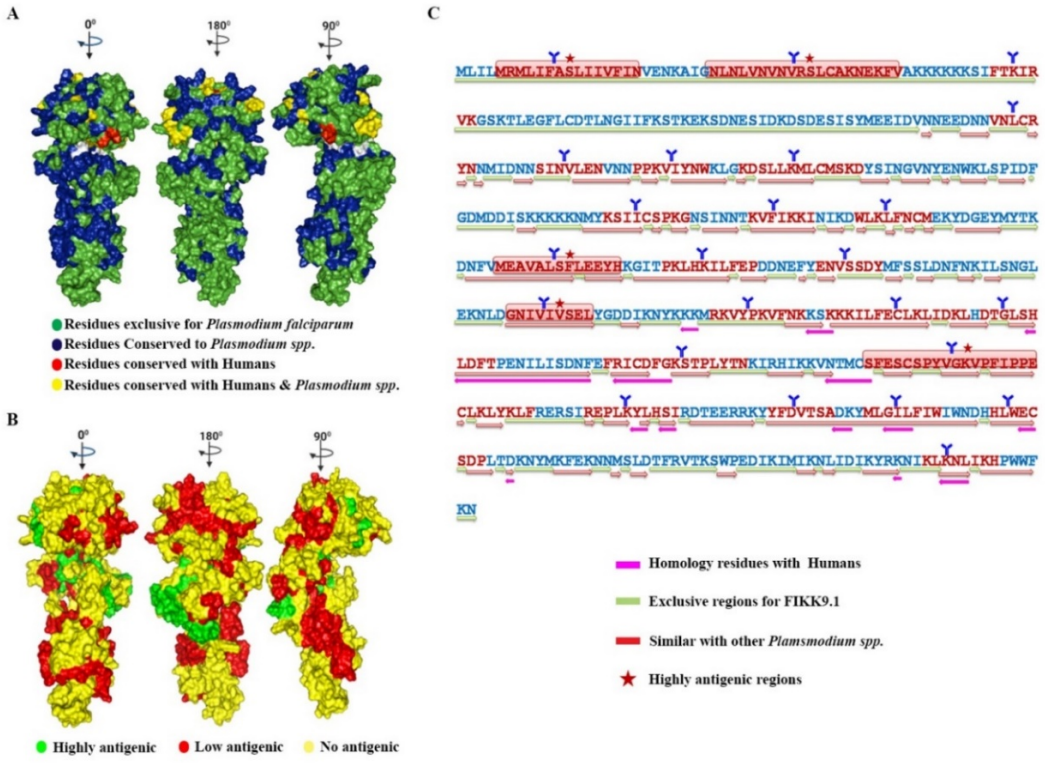

Figure 5.1: FIKK9.1 has exclusive regions with potential features for detection of malaria. **(A)** Surface model shows FIKK9.1 region that are exclusive to *Plasmodium falciparum* (Green), conserved in the Plasmodium species (Blue), similar with Humans (Red), and conserved in both Plasmodium and humans (yellow) at different angular views. **(B)** Epitope prediction by Kolaskar&Tongankar. The surface model shows predicted antigenic propensity of FIKK9.1 in different views. The region with antigenic values greater than 1.12 were predicted as highly antigenic (Green), antigenic value of 0.9 to 1.1 are low antigenic (Red) and values lesser than thre threshold, i.e., 0.9 are considered as no antigenic regions (Yellow). **(C)** FIKK9.1 has highly antigenic regions that are exclusively conserved to *Plasmodium falciparum*.

Based on antigenicity score, we predicted 25 regions that may induce the immune response in hosts. Moreover, using the predicted antigenic score, we segregated the regions into highly antigenic, low antigenic and no antigenic regions (Figure 5.1 B). The regions which has >1.12 antigenic score were considered as high antigenic regions whereas the regions below that threshold value were considered as low antigenic (0.9 to 1.1). The regions with antigenic score of 0.9 or lesser were considered as no antigenic regions. Based on the antigenicity score, 5 out of 25 regions of FIKK9.1 were found to be highly antigenic in nature. Further, these regions are exclusive for *Plasmodium spp.* and has high divergence from humans. The sequence homology and antigenicity data suggest that FIKK9.1 can be used for generating antibodies to explore its potential in malaria diagnosis (Figure 5.1 C).

5.3.2 Anti-FIKK9.1 serum specifically detects FIKK9.1

ELISA was performed to define the titre of anti-FIKK9.1 against 50 µg/ml of rFIKK9.1. The serum of different dilutions (1: 10 to 1:10000) was used to calculate the titre. As a positive control the rFIKK9.1 was probed with anti-His antibody. The absorbance value of the titers was subtracted from the control sets devoid of the antigen. In ELISA, we observed the decrease of absorbance with respect to increase in dilution. The dilution 1:100 to 1:2000 gives slightly higher signal and dilution 1: 4000 to 1:7000 gives low signal compared to positive control. Therefore, 1:3000 dilution titer of serum was found to be optimal for further analysis (Figure 5.2 A). The western blotting analysis of purified rFIKK9.1 and parasite lysate were performed to confirm the detection of FIKK9.1 with anti-FIKK9.1 antibody in the serum. The specific signal was obtained near 65 kDa in both SEC (size exclusion chromatography) purified FIKK9.1 (Figure 5.2 B) and parasite lysate. No signal was observed in RBC lysate which rules out the possibility of cross-reactivity (Figure 5.3 C) and thus it suggests that anti-FIKK9.1 in serum may specifically detect FIKK9.1 in parasite lysate.

5.3.3 Affinity purification of polyclonal anti-FIKK9.1

Antisera collected from rabbit immunized with FIKK9.1 was clarified and pooled. The antisera were found to have high titer of specific antibodies against FIKK9.1. Affinity purification of antiFIKK9.1 antibody involves two different CNBR coupled column, one coupled with BSA and the other coupled with FIKK9.1. The coupling of CNBR with BSA helps in preventing non-specific antibodies, such as the linear epitopes of *E. coli* proteins and other antibodies from

serum onto the column. The coupling of FIKK9.1 with CNBR activated beads was confirmed by loading an aliquot of sample into SDS-PAGE. A visible band obtained at nearly the molecular weight of FIKK9.1 confirms the coupling of FIKK9.1 with CNBR activated beads (Figure 5.3 A). Once the coupling was confirmed, the antisera depleted of nonspecific antibodies was passed onto to FIKK9.1-CNBR beads. Purified polyclonal anti-FIKK9.1 antibody was collected from the column and evaluated through ELISA by comparing it with antisera. ELISA was performed using antisera, flow through and elution fractions at different end point dilutions. The ELISA results shows that the absorbance of the elution fractions is almost equal to the antisera and was 2.5-fold more than the flow through collected during purification. The absorbance of BSA control suggests that purified FIKK9.1 antibody is specific to FIKK9.1 protein (Figure 5.3 B).

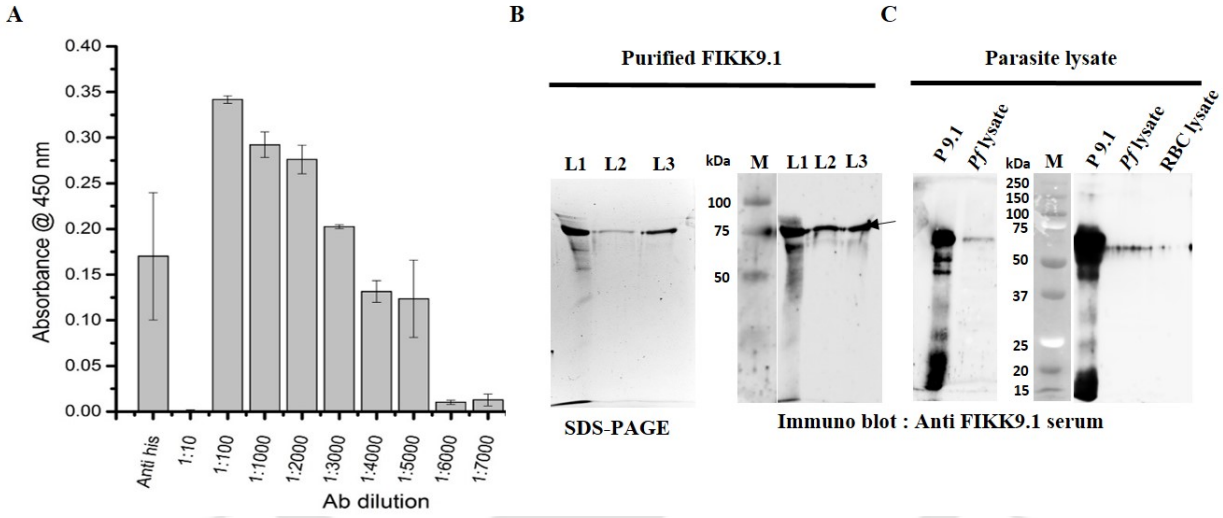

Figure 5.2: Antisera collected from rabbit detects recombinant and parasite FIKK9.1 protein. (A) The determination of anti-FIKK9.1 serum titer against purified FIKK9.1. ELISA shows linear decrease of absorbance value with increase of antisera dilution. The titre of 1:3000 dilution of antisera was found to be optimal for further studies. **(B)** Detection of purified FIKK9.1 using antisera through western blotting. The affinity purified (L1) and SEC purified protein (L2 & L3) was loaded on SDS PAGE gel and transferred to nitrocellulose membrane for western blotting analysis. The Immunoblot of purified protein suggests antisera detects rFIKK9.1. **(C)** Detection of FIKK9.1 from parasite (*pf*3D7) culture grown under *in-vitro* conditions. Proteins extracted from the parasites were probed using antisera. The Immuno blot shows specific signal at 65kDa from parasite lysate whereas no signal or cross reactivity was observed in RBC lysate.

Western blotting and dot blot analysis were performed to confirm that the purified FIKK9.1 antibody detects the FIKK9.1 protein. The BL21(DE3) lysate and purified proteins samples were used to perform western blotting analysis. A single band obtained in both the samples shows that

the antibody was purified (Figure 5.3 C). Further, the protein was diluted to different concentrations (100 µg/ml to 2.5 µg/ml) and probed using affinity purified anti-FIKK9.1antibody. The signal was obtained with the FIKK9.1 protein at different concentrations and there was no reactivity of the antibody with BSA controls suggesting that the FIKK9.1 antibody could be binding specifically to our targeted protein (Figure 5.3 D). These observations confirm the purification of polyclonal anti-FIKK9.1 antibody.

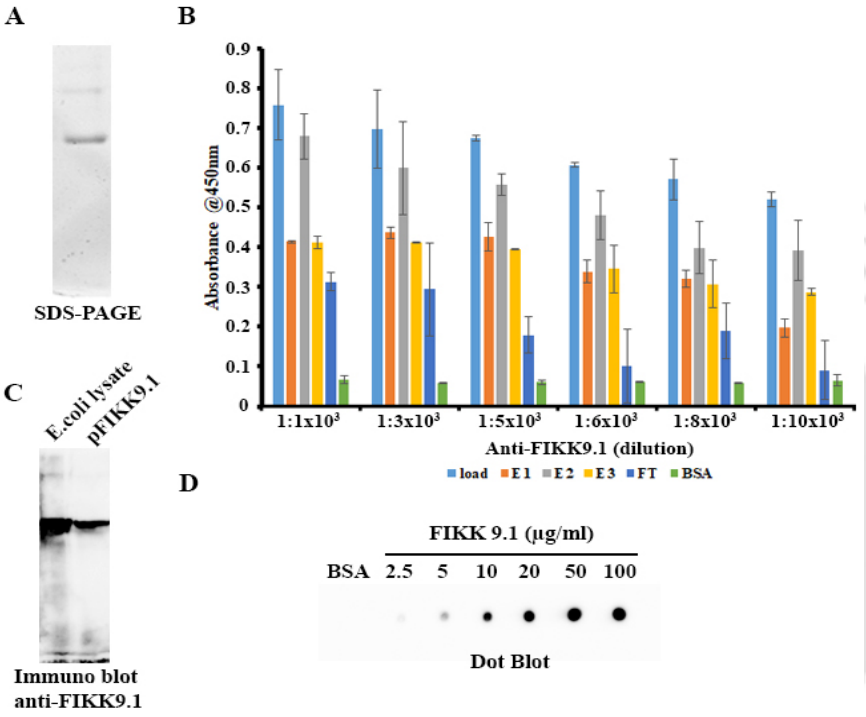

Figure 5.3: Purification of polyclonal anti-FIKK9.1 from serum. (A) Preparation of CNBR activated column coupled with rFIKK9.1. An aliquot of coupled beads is separated in SDSPAGE to confirm the coupling of FIKK9.1 with CNBR activated beads. A protein band appears nearly at 65 kDa upon coomassie staining. Purification of anti-FIKK9.1 from serum using affinity column is evaluated through (B) ELISA and (C) Dot blot analysis

5.3.4 Anti-FIKK9.1 antibody is highly sensitive and non-reactive with body fluids

The sensitivity of polyclonal antibody was evaluated using purified protein. To determine its appropriate sensitivity, the purified protein at different concentrations (90 µmol to 30 pmol) was applied on the membrane slowly and probed with anti-FIKK9.1 antibody. The signal was acquired using gel doc system (Biorad) and its relative intensity measured by Image lab (Biorad). The sensitivity of antibody decreases linearly with decreasing concentration of protein. The dot blot analysis suggests that the limit of detection of anti-FIKK9.1 is about 3 nmol of protein. The

limit of detection at 3 nmol is stable in multiple detections. BSA is used as control for cross reactivity. The absence of signal in BSA indicates that the signal obtained from the reaction is specific (Figure 5.4 A). Human serum collected from whole blood and the complete media in which *in-vitro* parasite culture was maintained, were used for assessing the cross-reactivity of the purified antibody as well. This would help to rule out any possible cross-reactivity of the polyclonal antibody to a myriad host blood proteins and media components. Therefore, the serum and complete media were blotted on nitrocellulose membrane at different dilutions (1:1 to 1:20) along with BSA. The plain blot shows that the samples have been evenly applied on the membrane. Further, the blot was probed and developed for analyzing the specificity of the antibody. The developed chemiblot showed no signal in both samples and its subsequent dilutions (Figure 5.4 B). This clearly proposed that antiFIKK9.1 does not react with human serum and parasite culture media components.

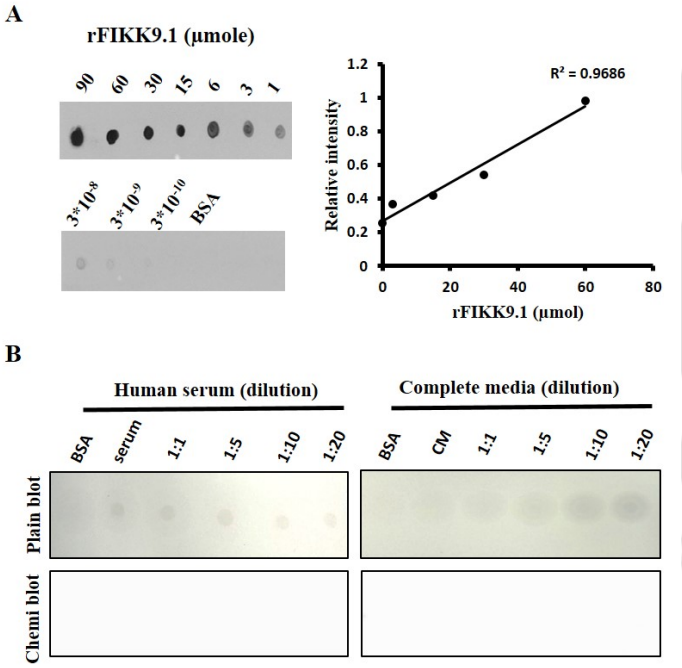

Figure 5.4: Characterization of purified anti-FIKK9.1 antibody. (A) The sensitivity of purified antibody assessed by probing rFIKK9.1 at different concentrations. The Dot blot shows that the polyclonal antibody detects rFIKK9.1 up to 3 nmol concentration. The standard curve based on relative intensity depicts the linearity of FIKK9.1 detection by purified polyclonal antibody. **(B) Cross-reactivity of anti-FIKK9.1 was evaluated using human serum and culture media (CM)**. The samples of various dilution (1:1 to 1:20 dilution) was analyzed through dot blotting technique. BSA has been used as a control. The blot is developed using chemiluminescence substrate (Chemi blot) and as a control before applying substrate the image of blot spotted with is acquired (Plain blot).

5.3.5 The polyclonal anti-FIKK9.1 antibody selectively detects FIKK9.1 during co-infection.

The improper diagnosis in presence of co-infecting pathogen may affect the outcomes of disease, treatment, or drug resistance. Therefore, it is necessity to evaluate the performance of detection system in presence of other infectious agents. In this study we analyzed any possible interference of the detection system in presence of other organisms such as *E. coli*, *M. smegmatis*, Yeast, New castle disease virus (NDV), Japanese encephalitis virus (JV), Duck plaque virus (DPV) and Herpes simplex virus (HERPES). Initially we performed dot blot analysis with infections agents alone to understand that the anti-FIKK9.1 shows no non-specific interactions with them. An absence of signal from any of the organisms would suggest that there is no cross-reactivity of the antibody with these infectious agents. In identical conditions, we also checked the ability of the antibody to detect the protein by mixing parasites with high titers of the organisms and the preparing the lyste for probing and detection. The chemiluminescent signals obtained from the chemi blot shows that the presence of the organisms did not interfere with the ability of anti-FIKK9.1 antibody in detecting FIKK9.1 protein from parasite lysate (Figure 5.5).

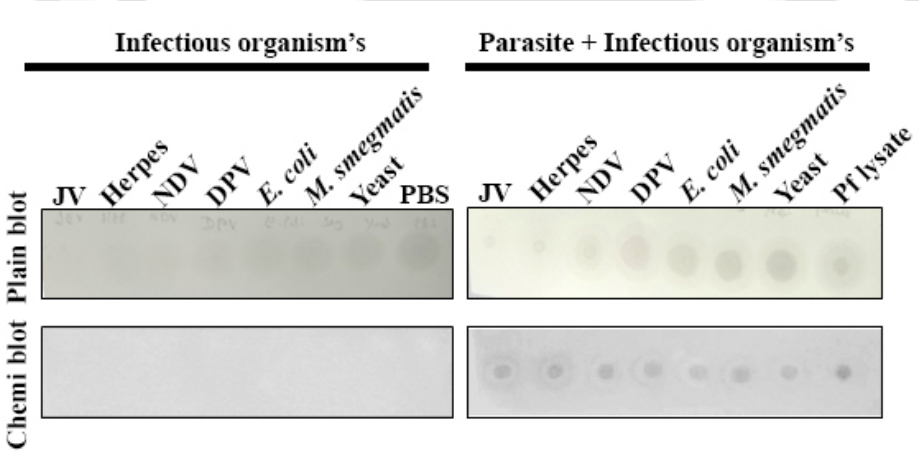

Figure 5.5: Selectivity of FIKK9.1. Lysates of organisms such as JV, Herpes, NDV, DPV, *E. coli*, *M. smegmatis* and yeast were applied on to the nitrocellulose membrane (Plain blot). The blot was probed and developed for signal acquisition (Chemi blot). No signal was obtained for the sample contains only infectious agents whereas in the sample contains parasites shows significant level of FIKK9.1 signal. The parasite lysate is used as a positive control for the study.

Although, there is no interference of other organism at specific concentration, we were interested to analyze the same in a range of infectious agent concentrations with the parasites in presence of RBC lysate. The microbial cell count ranged from $60x10^3$ to $480x10^3$cells/µl and the titre of the

virus particles ranged from $0.5x10^3$ to $5x10^3$ particles/µl were analyzed. The highest titre of prokaryotes and viruses was used as the infectious agent control. The parasitized RBC and uninfected RBC were used as positive and negative controls. The samples were probed using anti-FIKK9.1 antibody followed by ALP-conjugated secondary antibodies. The blot was developed using NBT/BCIP substrate which showed signals in all the samples containing the parasites while any signal was not detected in the samples that contained only infectious agents. No interference has been observed in any of the sample. The presence of a strong signal in positive controls and absence of signal in negative control suggests that the antibody specifically recognize the parasite FIKK9.1. To confirm there is no interference of organism, we analyzed the signal intensity of each sample and compared with positive control. The graph proves that there is no significant difference in the signal obtained from any of the samples (Figure 5.6 A&B).

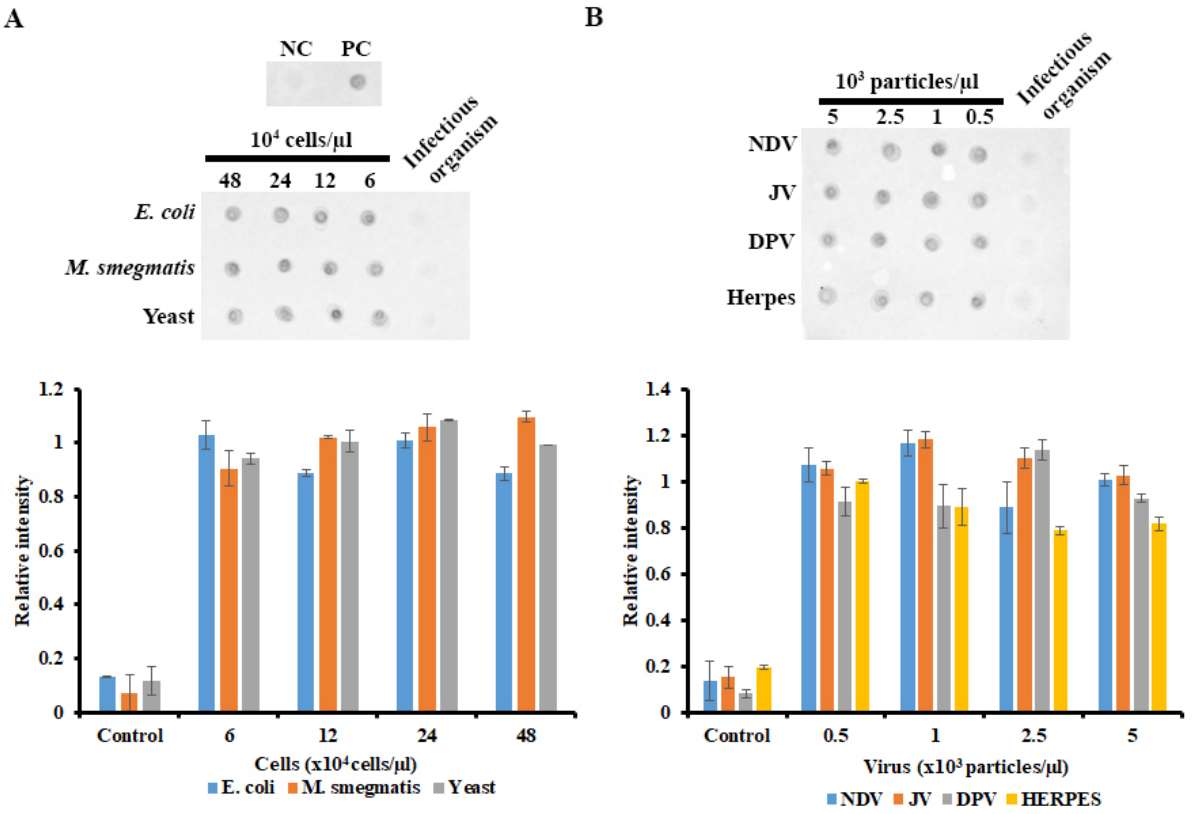

Figure 5.6: Parasitized RBC contaminated with different concentrations of bacteria ($60x10^3$ to $480x10^3$cells/µl), yeast ($60x10^3$ to $480x10^3$cells/µl) and virus ($0.5\ x10^3$ to $5x10^3$ particles/µl) are studied for its interference in the detection of FIKK9.1. The RBC lysate and parasitized RBC

lysate are used as Negative control (NC) and Positive control (PC). The signal intensities are measured and compared to positive control.

5.3.6 Anti-FIKK kinase antibodies detects parasite in Mock patient samples

To understand the performance of purified antibody in real scenario, blood of 20 volunteers was collected and mimicked as blood of malaria patients by blindly contaminating with *in-vitro* parasites culture in few of the samples. The smears of the samples were taken and examined microscopically as a reference standard. The standard curve of different percentage of parasitemia was evaluated to find the parasitemia percentage in the sample. The IRBC of 8% to 0.5% is lysed, diluted to 50 µg/ml and dot blot analysis was performed. Uninfected RBC lysate has been used as a control. The blot was probed with purified anti-FIKK9.1 and developed using ALP conjugated secondary antibody substrates. The signal obtained from the blot was measured and its standard curve plotted using relative intensity. The standard curve shows linear signal on different parasite percentage. No signal in RBC lysate indicated that the signals obtained were specifically from the parasites (Figure 5.7 A).

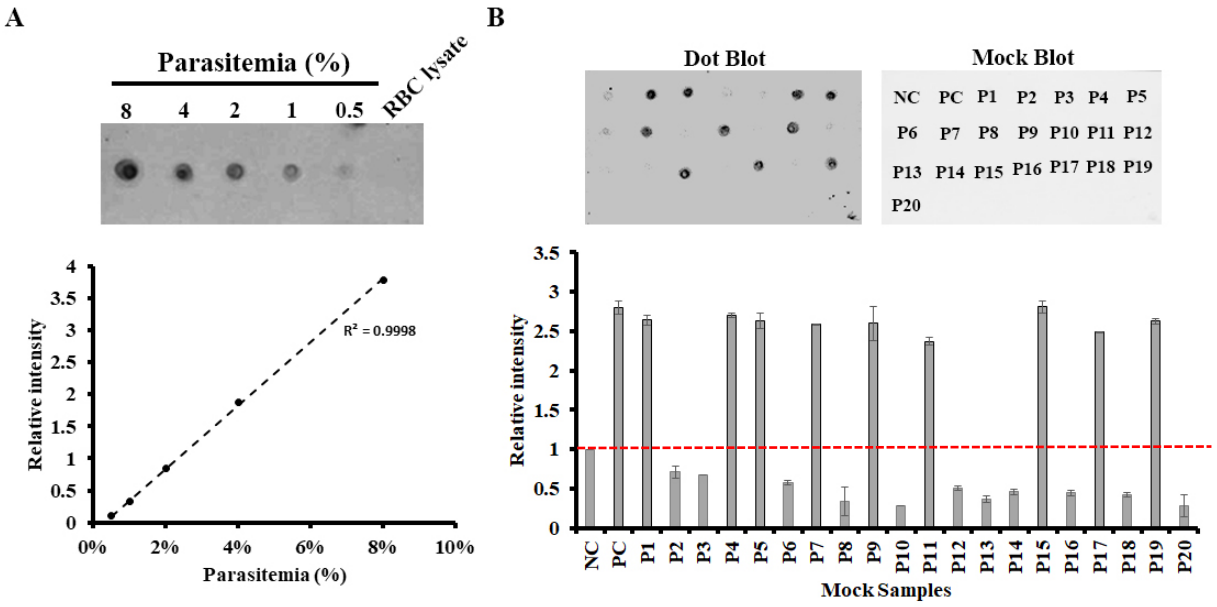

Figure 5.7 Validation of anti-FIKK9.1 using mock malaria patient sample. (A) Dot blot analysis was performed using different levels of parasitemia (0.5 % to 8%) with uninfected RBC lysate as control. The standard curve was plotted based on the relative intensities of the samples. **(B)** Whole blood collected from 20 individuals was blindly contaminated with *in-vitro* parasite culture. The samples are subjected to dot blot analysis to predict the samples containing parasites. The blot is developed using ALP-substrates and the relative intensities are measured from the samples (Dot blot). The Infected RBC lysate and the uninfected RBC lysate are used as

a negative (NC) and positive control (PC). The dotted line (Red) in the graph represents the threshold of the intensities to find the presence of parasites in the sample.

Out of the 20 mock samples, bright signals were obtained from 9 samples and 11 samples showed no signals. Relative intensity was calculated from the signal obtained in each sample. Uninfected RBC lysate and infected RBC lysates were used as negative and positive controls respectively. The relative intensity of all the samples were plotted to find the negative and positive in the mock test samples (Figure 5.7 B). The intensity of the negative control is set to 1.0 and it is used as a threshold. Based on threshold values, it was identified that 9 out of 16 was positive and the remaining 11 samples were negative. The results were also validated through microscopic examination. To measure the parasitemia present in the sample, the signal intensity of mock samples was compared with standard parasitemia curve. The parasitemia of each sample was calculated through the signal intensity obtained and microscopic examination. The study predicted that the samples were contaminated with approximately 2% parasitemia (Table 5.1). The percentage accuracy was evaluated by comparing the parasitemia calculated using signal intensity and microscopic examination. The microscopic examination of the samples reveals that the results are coinciding with an average accuracy of 95.45% in the samples found to contain parasites. The overall accuracy within the study population is found to be 100%. Our preliminary analysis suggests FIKK9.1 could be used as a novel molecular target for detection of malaria.

5.4 Discussion

Although microscopy remains to be a gold standard method for malaria diagnosis, RDTs (Rapid diagnostics tests) are prominently used in numerous regions because of its easy accessibility and user-friendly nature (Murray et al., 2008). Currently, all available commercial antibody based RDT's are detecting three major plasmodium proteins such as *pf*HRP2, pLDH and Aldolase. The combination of *pf*HRP2 with pLDH/Aldolase is used to differentiate among malarial species (Jain et al., 2014). All these antigens have certain limitations to achieve 98-100% accuracy detection of malaria in real-time. Therefore, there is a constant need to develop new system to detect malarial antigens that paves way to detecting malaria with >98% accuracy and potential to differentiate among species (Adu-Gyasi et al., 2018; Park et al., 2020). From our bioinformatics analysis, we identified FIKK9.1 as a potential diagnostic target. The FIKK9.1 N-terminal domain

Table 5.1: Validation of anti-FIKK9.1 for detecting malaria in comparison with standard microscopy method.

Mock samples	Calculated parasitemia (%)	Microscopic examination (%)	Percentage accuracy (%)
P1	1.918 ± 0.02	1.96 ± 0.02	97.89462 ± 0.52
P2	0	0	100
P3	0	0	100
P4	2.011 ± 0.07	2.034 ± 0.024	98.86553 ± 0.76
P5	1.931 ± 0.007	2.03 ± 0.17	95.16009 ± 0.19
P6	0	0	100
P7	1.864 ± 0.02	1.91 ± 0.01	97.62795 ± 0.64
P8	0	0	100
P9	1.827 ± 0.07	1.985 ± 0.025	92.0819 ± 1.7
P10	0	0	100
P11	1.904 ± 0.05	2.08 ± 0.01	93.95917 ± 0.14
P12	0	0	100
P13	0	0	100
P14	0	0	100
P15	1.9 ± 0.07	2.01 ± 0.01	94.55972 ± 1.4
P16	0	0	100
P17	1.921 ± 0.09	1.935 ± 0.045	99.29716 ± 1.29
P18	0	0	100
P19	1.854 ± 0.103	2.015 ± 0.035	92.05298 ± 2.36
P20	0	0	100

Note: S.D for calculated parasitemia and microscopic examination

shares no sequence similarity with other existing eukaryotic proteins. Most of these regions are predicted to be highly antigenic in nature. These regions can be used to develop specific detection of malaria. Additionally, certain regions in FIKK kinases are found to be conserved within plasmodium species that may help to develop species-specific detection of malaria. This preliminary analysis strongly suggests that FIKK9.1 can be used for diagnosis of malaria. We started with purification of rFIKK9.1 using affinity and gel filtration chromatography. Further the purified protein was mixed with adjuvant and used to immunize rabbit and generate antibodies. After second booster we started to collect the serum contains anti-FIKK9.1 antibody from rabbit till the fourth booster. The presence of anti-FIKK9.1 in serum was evaluated by detecting purified FIKK9.1. In our preliminary studies through western blotting, we identified the anti-FIKK9.1 antibody present in serum specifically detects purified FIKK9.1 and as well as

pfFIKK9.1 present in parasite lysate but does not give any cross reactivity to proteins present in RBC lysate. The anti-FIKK9.1 was purified through affinity chromatography using FIKK9.1 coupled CNBR active sepharose column. The titration and sensitivity of purified anti-FIKK9.1 antibody was determined through ELISA. The dilution of 1:3000 was found to be optimum for the detection of FIKK9.1 by purified polyclonal anti-FIKK9.1 antibody. The sensitivity and selectivity of the antibodies were assessed by performing dot blot analysis using various biological samples. The sensitivity of purified anti-FIKK9.1 polyclonal antibody was validated by estimating its limit of detection using rFIKK9.1 protein. We found that the purified anti-FIKK9.1 detects antigens upto 3 nmoles. Further the cross reactivity was analyzed using human serum and complete media devoid of parasites. Both the samples show no cross reactivity with anti-FIKK9.1. The anti-FIKK9.1 antibody detects FIKK9.1 antigen at least to 0.5% parasitemia grown under *in-vitro* conditions. Further, the purified antibody is found to be highly selective towards FIKK9.1 in parasites over other infectious organism's proteins. The development of detection system along with semi-quantitative measurement of samples is more useful in analyzing drug screening process. Therefore, the performance of anti-FIKK9.1 antibody was analyzed for semi-quantitative measurement. The anti-FIKK9.1 antibody was validated by mimicking the patient sample. The results suggest that using anti-FIKK9.1 we would semi-quantitatively detects the parasite with an accuracy of 95.45%. In conclusion, our study suggests FIKK9. 1 could be a used as a platform to develop immuno-chromatographic strips for the detection of malaria.

FUTURE PROSPECTS

1) To identify exclusive interaction partner of FIKK9.1 in *Plasmodium falciparum.*
2) To study the effect of compounds on FIKK kinases expression and interaction in *Plasmodium falciparum.*
3) To study the individual molecules from ayurvedic formulations responsible for antimalarial activity.
4) To detect the presence of FIKK9.1 in real-time patient sample to develop malaria diagnostic kit.

Bibliography

1) (2004). In Saving Lives, Buying Time: Economics of Malaria Drugs in an Age of Resistance, K.J. Arrow, C. Panosian, and H. Gelband, eds. (Washington DC: 2004 by the National Academy of Sciences).
2) Adu-Gyasi, D., Asante, K.P., Amoako, S., Amoako, N., Ankrah, L., Dosoo, D., Tchum, S.K., Adjei, G., Agyei, O., Amenga-Etego, S., *et al.* (2018). Assessing the performance of only HRP2 and HRP2 with pLDH based rapid diagnostic tests for the diagnosis of malaria in middle Ghana, Africa. PloS one *13*, e0203524.
3) Aher, R.B., and Roy, K. (2017). Exploring the structural requirements in multiple chemical scaffolds for the selective inhibition of Plasmodium falciparum calcium-dependent protein kinase-1 (PfCDPK-1) by 3D-pharmacophore modelling, and docking studies. SAR and QSAR in environmental research *28*, 390-414.
4) Aly, A.S., Vaughan, A.M., and Kappe, S.H. (2009). Malaria parasite development in the mosquito and infection of the mammalian host. Annual review of microbiology *63*, 195-221.
5) Ameer, K., Shahbaz, H.M., and Kwon, J.H. (2017). Green Extraction Methods for Polyphenols from Plant Matrices and Their Byproducts: A Review. Comprehensive reviews in food science and food safety *16*, 295-315.
6) Amino, R., Giovannini, D., Thiberge, S., Gueirard, P., Boisson, B., Dubremetz, J.F., Prévost, M.C., Ishino, T., Yuda, M., and Ménard, R. (2008). Host cell traversal is important for progression of the malaria parasite through the dermis to the liver. Cell host & microbe *3*, 88-96.
7) Arendse, L.B., Wyllie, S., Chibale, K., and Gilbert, I.H. (2021). Plasmodium Kinases as Potential Drug Targets for Malaria: Challenges and Opportunities. ACS infectious diseases.
8) Arévalo-Herrera, M., Lopez-Perez, M., Medina, L., Moreno, A., Gutierrez, J.B., and Herrera, S. (2015). Clinical profile of Plasmodium falciparum and Plasmodium vivax infections in low and unstable malaria transmission settings of Colombia. Malaria journal *14*, 154.
9) Ashley, E.A., Pyae Phyo, A., and Woodrow, C.J. (2018). Malaria. Lancet (London, England) *391*, 1608-1621.
10) Awolola, T.S., Adeogun, A., Olakiigbe, A.K., Oyeniyi, T., Olukosi, Y.A., Okoh, H., Arowolo, T., Akila, J., Oduola, A., and Amajoh, C.N. (2018). Pyrethroids resistance intensity and resistance mechanisms in Anopheles gambiae from malaria vector surveillance sites in Nigeria. PloS one *13*, e0205230.
11) Bagavan, A., Rahuman, A.A., Kaushik, N.K., and Sahal, D. (2011). In vitro antimalarial activity of medicinal plant extracts against Plasmodium falciparum. Parasitology research *108*, 15-22.

12) Balaji, S., Deshmukh, R., and Trivedi, V. (2020). Severe malaria: Biology, clinical manifestation, pathogenesis and consequences. Journal of Vector Borne Diseases *57*, 1-13.
13) Balaji, S.N., and Trivedi, V. (2012). Extracellular Methemoglobin Mediated Early ROS Spike Triggers Osmotic Fragility and RBC Destruction: An Insight into the Enhanced Hemolysis During Malaria. Indian journal of clinical biochemistry : IJCB *27*, 178-185.
14) Bansal, A., Singh, S., More, K.R., Hans, D., Nangalia, K., Yogavel, M., Sharma, A., and Chitnis, C.E. (2013). Characterization of Plasmodium falciparum calcium-dependent protein kinase 1 (PfCDPK1) and its role in microneme secretion during erythrocyte invasion. The Journal of biological chemistry *288*, 1590-1602.
15) Barber, B.E., William, T., Grigg, M.J., Piera, K., Yeo, T.W., and Anstey, N.M. (2013). Evaluation of the sensitivity of a pLDH-based and an aldolase-based rapid diagnostic test for diagnosis of uncomplicated and severe malaria caused by PCR-confirmed Plasmodium knowlesi, Plasmodium falciparum, and Plasmodium vivax. Journal of clinical microbiology *51*, 1118-1123.
16) Batinovic, S., McHugh, E., Chisholm, S.A., Matthews, K., Liu, B., Dumont, L., Charnaud, S.C., Schneider, M.P., Gilson, P.R., de Koning-Ward, T.F., *et al.* (2017). An exported protein-interacting complex involved in the trafficking of virulence determinants in Plasmodium-infected erythrocytes. Nature communications *8*, 16044.
17) Beier, J.C. (1998). Malaria parasite development in mosquitoes. Annu Rev Entomol *43*, 519-543.
18) Beraldo, F.H., Almeida, F.M., da Silva, A.M., and Garcia, C.R. (2005). Cyclic AMP and calcium interplay as second messengers in melatonin-dependent regulation of Plasmodium falciparum cell cycle. J Cell Biol *170*, 551-557.
19) Besteiro, S., Dubremetz, J.F., and Lebrun, M. (2011). The moving junction of apicomplexan parasites: a key structure for invasion. Cellular microbiology *13*, 797-805.
20) Blasco, B., Leroy, D., and Fidock, D.A. (2017). Antimalarial drug resistance: linking Plasmodium falciparum parasite biology to the clinic. Nature medicine *23*, 917-928.
21) Bonnefoy, S., Guillotte, M., Langsley, G., and Mercereau-Puijalon, O. (1992). Plasmodium falciparum: characterization of gene R45 encoding a trophozoite antigen containing a central block of six amino acid repeats. Experimental parasitology *74*, 441-451.
22) Bousema, T., and Drakeley, C. (2011). Epidemiology and infectivity of Plasmodium falciparum and Plasmodium vivax gametocytes in relation to malaria control and elimination. Clinical microbiology reviews *24*, 377-410.
23) Bouwman, H., van den Berg, H., and Kylin, H. (2011). DDT and malaria prevention: addressing the paradox. Environmental health perspectives *119*, 744-747.
24) Bracchi-Ricard, V., Barik, S., Delvecchio, C., Doerig, C., Chakrabarti, R., and Chakrabarti, D. (2000). PfPK6, a novel cyclin-dependent kinase/mitogen-activated

protein kinase-related protein kinase from Plasmodium falciparum. The Biochemical journal *347 Pt 1*, 255-263.

25) Brandt, G.S., and Bailey, S. (2013). Dematin, a human erythrocyte cytoskeletal protein, is a substrate for a recombinant FIKK kinase from Plasmodium falciparum. Molecular and biochemical parasitology *191*, 20-23.
26) Brumlik, M.J., Nkhoma, S., Kious, M.J., Thompson, G.R., 3rd, Patterson, T.F., Siekierka, J.J., Anderson, T.J., and Curiel, T.J. (2011). Human p38 mitogen-activated protein kinase inhibitor drugs inhibit Plasmodium falciparum replication. Experimental parasitology *128*, 170-175.
27) Bryk, A.H., and Wiśniewski, J.R. (2017). Quantitative Analysis of Human Red Blood Cell Proteome. Journal of proteome research *16*, 2752-2761.
28) Buskes, M.J., Harvey, K.L., Prinz, B., Crabb, B.S., Gilson, P.R., Wilson, D.J., and Abbott, B.M. (2016). Exploration of 3-methylisoquinoline-4-carbonitriles as protein kinase A inhibitors of Plasmodium falciparum. Bioorg Med Chem *24*, 2389-2396.
29) Carter, R., and Mendis, K.N. (2002). Evolutionary and historical aspects of the burden of malaria. Clinical microbiology reviews *15*, 564-594.
30) Ch'ng, J.H., Kotturi, S.R., Chong, A.G., Lear, M.J., and Tan, K.S. (2010). A programmed cell death pathway in the malaria parasite Plasmodium falciparum has general features of mammalian apoptosis but is mediated by clan CA cysteine proteases. Cell death & disease *1*, e26.
31) Chandre, F., Darrier, F., Manga, L., Akogbeto, M., Faye, O., Mouchet, J., and Guillet, P. (1999). Status of pyrethroid resistance in Anopheles gambiae sensu lato. Bulletin of the World Health Organization *77*, 230-234.
32) Chapman, T.M., Osborne, S.A., Wallace, C., Birchall, K., Bouloc, N., Jones, H.M., Ansell, K.H., Taylor, D.L., Clough, B., Green, J.L., *et al.* (2014). Optimization of an imidazopyridazine series of inhibitors of Plasmodium falciparum calcium-dependent protein kinase 1 (PfCDPK1). Journal of medicinal chemistry *57*, 3570-3587.
33) Chen, L., Lopaticki, S., Riglar, D.T., Dekiwadia, C., Uboldi, A.D., Tham, W.H., O'Neill, M.T., Richard, D., Baum, J., Ralph, S.A., *et al.* (2011). An EGF-like protein forms a complex with PfRh5 and is required for invasion of human erythrocytes by Plasmodium falciparum. PLoS pathogens *7*, e1002199.
34) Church, L.W., Le, T.P., Bryan, J.P., Gordon, D.M., Edelman, R., Fries, L., Davis, J.R., Herrington, D.A., Clyde, D.F., Shmuklarsky, M.J., *et al.* (1997). Clinical manifestations of Plasmodium falciparum malaria experimentally induced by mosquito challenge. The Journal of infectious diseases *175*, 915-920.
35) Coldiron, M.E., Assao, B., Langendorf, C., Sayinzoga-Makombe, N., Ciglenecki, I., de la Tour, R., Piriou, E., Yarima Bako, M., Mumina, A., Guindo, O., *et al.* (2019). Clinical diagnostic evaluation of HRP2 and pLDH-based rapid diagnostic tests for malaria in an area receiving seasonal malaria chemoprevention in Niger. Malaria journal *18*, 443.

36) Collins, C.R., Hackett, F., Strath, M., Penzo, M., Withers-Martinez, C., Baker, D.A., and Blackman, M.J. (2013). Malaria parasite cGMP-dependent protein kinase regulates blood stage merozoite secretory organelle discharge and egress. PLoS Pathog *9*, e1003344.
37) Cowman, A.F., Healer, J., Marapana, D., and Marsh, K. (2016). Malaria: Biology and Disease. Cell *167*, 610-624.
38) Cox, F.E. (2010). History of the discovery of the malaria parasites and their vectors. Parasit Vectors *3*, 5.
39) Crosnier, C., Bustamante, L.Y., Bartholdson, S.J., Bei, A.K., Theron, M., Uchikawa, M., Mboup, S., Ndir, O., Kwiatkowski, D.P., Duraisingh, M.T., *et al.* (2011). Basigin is a receptor essential for erythrocyte invasion by Plasmodium falciparum. Nature *480*, 534-537.
40) Crutcher, J.M., and Hoffman, S.L. (1996). Malaria. In Medical Microbiology, S. Baron, ed. (Galveston (TX): University of Texas Medical Branch at GalvestonCopyright © 1996, The University of Texas Medical Branch at Galveston.).
41) Cui, L., Mharakurwa, S., Ndiaye, D., Rathod, P.K., and Rosenthal, P.J. (2015). Antimalarial Drug Resistance: Literature Review and Activities and Findings of the ICEMR Network. The American journal of tropical medicine and hygiene *93*, 57-68.
42) Cunningham, J., Jones, S., Gatton, M.L., Barnwell, J.W., Cheng, Q., Chiodini, P.L., Glenn, J., Incardona, S., Kosack, C., Luchavez, J., *et al.* (2019). A review of the WHO malaria rapid diagnostic test product testing programme (2008-2018): performance, procurement and policy. Malaria journal *18*, 387.
43) D, A.K., Shrivastava, D., Sahasrabuddhe, A.A., Habib, S., and Trivedi, V. (2021). Plasmodium falciparum FIKK9.1 is a monomeric serine-threonine protein kinase with features to exploit as a drug target. Chemical biology & drug design.
44) Das, S., Hertrich, N., Perrin, A.J., Withers-Martinez, C., Collins, C.R., Jones, M.L., Watermeyer, J.M., Fobes, E.T., Martin, S.R., Saibil, H.R., *et al.* (2015). Processing of Plasmodium falciparum Merozoite Surface Protein MSP1 Activates a Spectrin-Binding Function Enabling Parasite Egress from RBCs. Cell host & microbe *18*, 433-444.
45) Das, S., Saha, B., Hati, A.K., and Roy, S. (2018). Evidence of Artemisinin-Resistant Plasmodium falciparum Malaria in Eastern India. The New England journal of medicine *379*, 1962-1964.
46) Dastidar, E.G., Dayer, G., Holland, Z.M., Dorin-Semblat, D., Claes, A., Chêne, A., Sharma, A., Hamelin, R., Moniatte, M., Lopez-Rubio, J.J., *et al.* (2012). Involvement of Plasmodium falciparum protein kinase CK2 in the chromatin assembly pathway. BMC biology *10*, 5.
47) Davies, H., Belda, H., Broncel, M., Ye, X., Bisson, C., Introini, V., Dorin-Semblat, D., Semblat, J.P., Tibúrcio, M., Gamain, B., *et al.* (2020). An exported kinase family mediates species-specific erythrocyte remodelling and virulence in human malaria. Nature microbiology *5*, 848-863.

48) Delacollette, C., and Van der Stuyft, P. (1994). Direct acridine orange staining is not a 'miracle' solution to the problem of malaria diagnosis in the field. Transactions of the Royal Society of Tropical Medicine and Hygiene *88*, 187-188.
49) Deshmukh, R., and Trivedi, V. (2013). Methemoglobin exposure produces toxicological effects in macrophages due to multiple ROS spike induced apoptosis. Toxicology in vitro : an international journal published in association with BIBRA *27*, 16-23.
50) Dhiman, R.K., and Chawla, Y.K. (2005). Herbal medicines for liver diseases. Digestive diseases and sciences *50*, 1807-1812.
51) Dorin-Semblat, D., Demarta-Gatsi, C., Hamelin, R., Armand, F., Carvalho, T.G., Moniatte, M., and Doerig, C. (2015). Malaria Parasite-Infected Erythrocytes Secrete PfCK1, the Plasmodium Homologue of the Pleiotropic Protein Kinase Casein Kinase 1. PLoS One *10*, e0139591.
52) Dorin-Semblat, D., Quashie, N., Halbert, J., Sicard, A., Doerig, C., Peat, E., Ranford-Cartwright, L., and Doerig, C. (2007). Functional characterization of both MAP kinases of the human malaria parasite Plasmodium falciparum by reverse genetics. Molecular microbiology *65*, 1170-1180.
53) Dorin-Semblat, D., Schmitt, S., Semblat, J.P., Sicard, A., Reininger, L., Goldring, D., Patterson, S., Quashie, N., Chakrabarti, D., Meijer, L., *et al.* (2011). Plasmodium falciparum NIMA-related kinase Pfnek-1: sex specificity and assessment of essentiality for the erythrocytic asexual cycle. Microbiology (Reading, England) *157*, 2785-2794.
54) Dorin-Semblat, D., Sicard, A., Doerig, C., Ranford-Cartwright, L., and Doerig, C. (2008). Disruption of the PfPK7 gene impairs schizogony and sporogony in the human malaria parasite Plasmodium falciparum. Eukaryotic cell *7*, 279-285.
55) Droucheau, E., Primot, A., Thomas, V., Mattei, D., Knockaert, M., Richardson, C., Sallicandro, P., Alano, P., Jafarshad, A., Baratte, B., *et al.* (2004). Plasmodium falciparum glycogen synthase kinase-3: molecular model, expression, intracellular localisation and selective inhibitors. Biochimica et biophysica acta *1697*, 181-196.
56) Dundas, K., Shears, M.J., Sinnis, P., and Wright, G.J. (2019). Important Extracellular Interactions between Plasmodium Sporozoites and Host Cells Required for Infection. Trends in parasitology *35*, 129-139.
57) Dunst, J., Kamena, F., and Matuschewski, K. (2017). Cytokines and Chemokines in Cerebral Malaria Pathogenesis. Frontiers in cellular and infection microbiology *7*, 324.
58) Duo-Quan, W., Lin-Hua, T., Zhen-Cheng, G., Xiang, Z., and Man-Ni, Y. (2009). Application of the indirect fluorescent antibody assay in the study of malaria infection in the Yangtze River Three Gorges Reservoir, China. Malaria journal *8*, 199.
59) Durocher, D., and Jackson, S.P. (2002). The FHA domain. FEBS letters *513*, 58-66.
60) Dvorin, J.D., Martyn, D.C., Patel, S.D., Grimley, J.S., Collins, C.R., Hopp, C.S., Bright, A.T., Westenberger, S., Winzeler, E., Blackman, M.J., *et al.* (2010). A plant-like kinase in Plasmodium falciparum regulates parasite egress from erythrocytes. Science *328*, 910-912.

61) Fennell, C., Babbitt, S., Russo, I., Wilkes, J., Ranford-Cartwright, L., Goldberg, D.E., and Doerig, C. (2009). PfeIK1, a eukaryotic initiation factor 2alpha kinase of the human malaria parasite Plasmodium falciparum, regulates stress-response to amino-acid starvation. Malaria journal *8*, 99.
62) Florens, L., Washburn, M.P., Raine, J.D., Anthony, R.M., Grainger, M., Haynes, J.D., Moch, J.K., Muster, N., Sacci, J.B., Tabb, D.L., *et al.* (2002). A proteomic view of the Plasmodium falciparum life cycle. Nature *419*, 520-526.
63) Francis, S.E., Sullivan, D.J., Jr., and Goldberg, D.E. (1997). Hemoglobin metabolism in the malaria parasite Plasmodium falciparum. Annual review of microbiology *51*, 97-123.
64) Gao, X., Gunalan, K., Yap, S.S., and Preiser, P.R. (2013). Triggers of key calcium signals during erythrocyte invasion by Plasmodium falciparum. Nature communications *4*, 2862.
65) Gardiner, D.L., Skinner-Adams, T.S., Brown, C.L., Andrews, K.T., Stack, C.M., McCarthy, J.S., Dalton, J.P., and Trenholme, K.R. (2009). Plasmodium falciparum: new molecular targets with potential for antimalarial drug development. Expert review of anti-infective therapy *7*, 1087-1098.
66) Gardner, M.J., Hall, N., Fung, E., White, O., Berriman, M., Hyman, R.W., Carlton, J.M., Pain, A., Nelson, K.E., Bowman, S., *et al.* (2002). Genome sequence of the human malaria parasite Plasmodium falciparum. Nature *419*, 498-511.
67) Gazzinelli, R.T., Kalantari, P., Fitzgerald, K.A., and Golenbock, D.T. (2014). Innate sensing of malaria parasites. Nat Rev Immunol *14*, 744-757.
68) Glushakova, S., Yin, D., Li, T., and Zimmerberg, J. (2005). Membrane transformation during malaria parasite release from human red blood cells. Current biology : CB *15*, 1645-1650.
69) Graciotti, M., Alam, M., Solyakov, L., Schmid, R., Burley, G., Bottrill, A.R., Doerig, C., Cullis, P., and Tobin, A.B. (2014). Malaria protein kinase CK2 (PfCK2) shows novel mechanisms of regulation. PloS one *9*, e85391.
70) Graeser, R., Wernli, B., Franklin, R.M., and Kappes, B. (1996). Plasmodium falciparum protein kinase 5 and the malarial nuclear division cycles. Molecular and biochemical parasitology *82*, 37-49.
71) Green, J.L., Rees-Channer, R.R., Howell, S.A., Martin, S.R., Knuepfer, E., Taylor, H.M., Grainger, M., and Holder, A.A. (2008). The motor complex of Plasmodium falciparum: phosphorylation by a calcium-dependent protein kinase. The Journal of biological chemistry *283*, 30980-30989.
72) Greenwood, B.M., Bojang, K., Whitty, C.J., and Targett, G.A. (2005). Malaria. Lancet (London, England) *365*, 1487-1498.
73) Gunjan, S., Singh, S.K., Sharma, T., Dwivedi, H., Chauhan, B.S., Imran Siddiqi, M., and Tripathi, R. (2016). Mefloquine induces ROS mediated programmed cell death in malaria parasite: Plasmodium. Apoptosis : an international journal on programmed cell death *21*, 955-964.

74) Halbert, J., Ayong, L., Equinet, L., Le Roch, K., Hardy, M., Goldring, D., Reininger, L., Waters, N., Chakrabarti, D., and Doerig, C. (2010). A Plasmodium falciparum transcriptional cyclin-dependent kinase-related kinase with a crucial role in parasite proliferation associates with histone deacetylase activity. Eukaryot Cell *9*, 952-959.
75) Haldar, K., Bhattacharjee, S., and Safeukui, I. (2018). Drug resistance in Plasmodium. Nature reviews Microbiology *16*, 156-170.
76) Hallyburton, I., Grimaldi, R., Woodland, A., Baragaña, B., Luksch, T., Spinks, D., James, D., Leroy, D., Waterson, D., Fairlamb, A.H., *et al.* (2017). Screening a protein kinase inhibitor library against Plasmodium falciparum. Malaria journal *16*, 446.
77) Hartmann, M.D., Bourenkov, G.P., Oberschall, A., Strizhov, N., and Bartunik, H.D. (2006). Mechanism of phosphoryl transfer catalyzed by shikimate kinase from Mycobacterium tuberculosis. Journal of molecular biology *364*, 411-423.
78) Hatherell, H.A., Simpson, H., Baggaley, R.F., Hollingsworth, T.D., and Pullan, R.L. (2021). Sustainable Surveillance of Neglected Tropical Diseases for the Post-Elimination Era. Clinical infectious diseases : an official publication of the Infectious Diseases Society of America *72*, S210-S216.
79) Holton, S., Merckx, A., Burgess, D., Doerig, C., Noble, M., and Endicott, J. (2003). Structures of P. falciparum PfPK5 test the CDK regulation paradigm and suggest mechanisms of small molecule inhibition. Structure (London, England : 1993) *11*, 1329-1337.
80) Huang, W., Hulverson, M.A., Zhang, Z., Choi, R., Hart, K.J., Kennedy, M., Vidadala, R.S.R., Maly, D.J., Van Voorhis, W.C., Lindner, S.E., *et al.* (2016). 5-Aminopyrazole-4-carboxamide analogues are selective inhibitors of Plasmodium falciparum microgametocyte exflagellation and potential malaria transmission blocking agents. Bioorg Med Chem Lett *26*, 5487-5491.
81) Hussien, M., Abdel Hamid, M.M., Elamin, E.A., Hassan, A.O., Elaagip, A.H., Salama, A.H.A., Abdelraheem, M.H., and Mohamed, A.O. (2020). Antimalarial drug resistance molecular makers of Plasmodium falciparum isolates from Sudan during 2015-2017. PloS one *15*, e0235401.
82) Ippolito, M.M., Moser, K.A., Kabuya, J.B., Cunningham, C., and Juliano, J.J. (2021). Antimalarial Drug Resistance and Implications for the WHO Global Technical Strategy. Current epidemiology reports, 1-17.
83) Jaijyan, D.K., Verma, P.K., and Singh, A.P. (2016). A novel FIKK kinase regulates the development of mosquito and liver stages of the malaria. Scientific reports *6*, 39285.
84) Jain, P., Chakma, B., Patra, S., and Goswami, P. (2014). Potential biomarkers and their applications for rapid and reliable detection of malaria. BioMed research international *2014*, 852645.
85) Jennings, M.J., Barrios, A.F., and Tan, S. (2016). Elimination of truncated recombinant protein expressed in Escherichia coli by removing cryptic translation initiation site. Protein expression and purification *121*, 17-21.

86) Jones, M.L., Collins, M.O., Goulding, D., Choudhary, J.S., and Rayner, J.C. (2012). Analysis of protein palmitoylation reveals a pervasive role in Plasmodium development and pathogenesis. Cell host & microbe *12*, 246-258.
87) Joshi, B., Hendrickx, S., Magar, L.B., Parajuli, N., Dorny, P., and Maes, L. (2016). In vitro antileishmanial and antimalarial activity of selected plants of Nepal. Journal of intercultural ethnopharmacology *5*, 383-389.
88) Kalidas, Y., and Chandra, N. (2008). PocketDepth: a new depth based algorithm for identification of ligand binding sites in proteins. Journal of structural biology *161*, 31-42.
89) Kamali, M., Sharakhova, M.V., Baricheva, E., Karagodin, D., Tu, Z., and Sharakhov, I.V. (2011). An integrated chromosome map of microsatellite markers and inversion breakpoints for an Asian malaria mosquito, Anopheles stephensi. The Journal of heredity *102*, 719-726.
90) Katoh, K., Misawa, K., Kuma, K., and Miyata, T. (2002). MAFFT: a novel method for rapid multiple sequence alignment based on fast Fourier transform. Nucleic acids research *30*, 3059-3066.
91) Kats, L.M., Fernandez, K.M., Glenister, F.K., Herrmann, S., Buckingham, D.W., Siddiqui, G., Sharma, L., Bamert, R., Lucet, I., Guillotte, M.*, et al.* (2014). An exported kinase (FIKK4.2) that mediates virulence-associated changes in Plasmodium falciparum-infected red blood cells. Int J Parasitol *44*, 319-328.
92) Kavishe, R.A., Koenderink, J.B., and Alifrangis, M. (2017). Oxidative stress in malaria and artemisinin combination therapy: Pros and Cons. The FEBS journal *284*, 2579-2591.
93) Kesely, K.R., Pantaleo, A., Turrini, F.M., Olupot-Olupot, P., and Low, P.S. (2016). Inhibition of an Erythrocyte Tyrosine Kinase with Imatinib Prevents Plasmodium falciparum Egress and Terminates Parasitemia. PloS one *11*, e0164895.
94) Keskin, O., Gursoy, A., Ma, B., and Nussinov, R. (2008). Principles of protein-protein interactions: what are the preferred ways for proteins to interact? Chemical reviews *108*, 1225-1244.
95) Klein, M., Dinér, P., Dorin-Semblat, D., Doerig, C., and Grøtli, M. (2009). Synthesis of 3-(1,2,3-triazol-1-yl)- and 3-(1,2,3-triazol-4-yl)-substituted pyrazolo[3,4-d]pyrimidin-4-amines via click chemistry: potential inhibitors of the Plasmodium falciparum PfPK7 protein kinase. Organic & biomolecular chemistry *7*, 3421-3429.
96) Kolaskar, A.S., and Tongaonkar, P.C. (1990). A semi-empirical method for prediction of antigenic determinants on protein antigens. FEBS letters *276*, 172-174.
97) Kumar, A., Vaid, A., Syin, C., and Sharma, P. (2004). PfPKB, a novel protein kinase B-like enzyme from Plasmodium falciparum: I. Identification, characterization, and possible role in parasite development. The Journal of biological chemistry *279*, 24255-24264.
98) Kumar, H., and Tolia, N.H. (2019). Getting in: The structural biology of malaria invasion. PLoS pathogens *15*, e1007943.

99) Kumar, P., Tripathi, A., Ranjan, R., Halbert, J., Gilberger, T., Doerig, C., and Sharma, P. (2014). Regulation of Plasmodium falciparum development by calcium-dependent protein kinase 7 (PfCDPK7). The Journal of biological chemistry *289*, 20386-20395.

100) Laishram, D.D., Sutton, P.L., Nanda, N., Sharma, V.L., Sobti, R.C., Carlton, J.M., and Joshi, H. (2012). The complexities of malaria disease manifestations with a focus on asymptomatic malaria. Malaria journal *11*, 29.

101) Lalle, M., Currà, C., Ciccarone, F., Pace, T., Cecchetti, S., Fantozzi, L., Ay, B., Breton, C.B., and Ponzi, M. (2011). Dematin, a component of the erythrocyte membrane skeleton, is internalized by the malaria parasite and associates with Plasmodium 14-3-3. The Journal of biological chemistry *286*, 1227-1236.

102) Laurent, A., Schellenberg, J., Shirima, K., Ketende, S.C., Alonso, P.L., Mshinda, H., Tanner, M., and Schellenberg, D. (2010). Performance of HRP-2 based rapid diagnostic test for malaria and its variation with age in an area of intense malaria transmission in southern Tanzania. Malaria journal *9*, 294.

103) Laurent, D., Jullian, V., Parenty, A., Knibiehler, M., Dorin, D., Schmitt, S., Lozach, O., Lebouvier, N., Frostin, M., Alby, F., *et al.* (2006). Antimalarial potential of xestoquinone, a protein kinase inhibitor isolated from a Vanuatu marine sponge Xestospongia sp. Bioorganic & medicinal chemistry *14*, 4477-4482.

104) Lawal, B., Shittu, O.K., Kabiru, A.Y., Jigam, A.A., Umar, M.B., Berinyuy, E.B., and Alozieuwa, B.U. (2015). Potential antimalarials from African natural products: A reviw. Journal of intercultural ethnopharmacology *4*, 318-343.

105) Le Roch, K.G., Johnson, J.R., Florens, L., Zhou, Y., Santrosyan, A., Grainger, M., Yan, S.F., Williamson, K.C., Holder, A.A., Carucci, D.J., *et al.* (2004). Global analysis of transcript and protein levels across the Plasmodium falciparum life cycle. Genome research *14*, 2308-2318.

106) Leroy, D., and Doerig, C. (2008). Drugging the Plasmodium kinome: the benefits of academia-industry synergy. Trends in pharmacological sciences *29*, 241-249.

107) Lin, B.C., Harris, D.R., Kirkman, L.M.D., Perez, A.M., Qian, Y., Schermerhorn, J.T., Hong, M.Y., Winston, D.S., Xu, L., and Brandt, G.S. (2017a). FIKK Kinase, a Ser/Thr Kinase Important to Malaria Parasites, Is Inhibited by Tyrosine Kinase Inhibitors. ACS omega *2*, 6605-6612.

108) Lin, B.C., Harris, D.R., Kirkman, L.M.D., Perez, A.M., Qian, Y., Schermerhorn, J.T., Hong, M.Y., Winston, D.S., Xu, L., Lieber, A.M., *et al.* (2017b). The anthraquinone emodin inhibits the non-exported FIKK kinase from Plasmodium falciparum. Bioorganic chemistry *75*, 217-223.

109) Lourenço, C., Tatem, A.J., Atkinson, P.M., Cohen, J.M., Pindolia, D., Bhavnani, D., and Le Menach, A. (2019). Strengthening surveillance systems for malaria elimination: a global landscaping of system performance, 2015-2017. Malaria journal *18*, 315.

110) Ly, A.B., Tall, A., Perry, R., Baril, L., Badiane, A., Faye, J., Rogier, C., Touré, A., Sokhna, C., Trape, J.F., *et al.* (2010). Use of HRP-2-based rapid diagnostic test for Plasmodium falciparum malaria: assessing accuracy and cost-effectiveness in the villages of Dielmo and Ndiop, Senegal. Malaria journal *9*, 153.

111) Lye, Y.M., Chan, M., and Sim, T.S. (2006). Pfnek3: an atypical activator of a MAP kinase in Plasmodium falciparum. FEBS letters *580*, 6083-6092.

112) Lyke, K.E., Burges, R., Cissoko, Y., Sangare, L., Dao, M., Diarra, I., Kone, A., Harley, R., Plowe, C.V., Doumbo, O.K., *et al.* (2004). Serum levels of the proinflammatory cytokines interleukin-1 beta (IL-1beta), IL-6, IL-8, IL-10, tumor necrosis factor alpha, and IL-12(p70) in Malian children with severe Plasmodium falciparum malaria and matched uncomplicated malaria or healthy controls. Infection and immunity *72*, 5630-5637.

113) Malik, A., Mehmood, M.H., Channa, H., Akhtar, M.S., and Gilani, A.H. (2017). Pharmacological basis for the medicinal use of polyherbal formulation and its ingredients in cardiovascular disorders using rodents. BMC complementary and alternative medicine *17*, 142.

114) Maltha, J., Gillet, P., and Jacobs, J. (2013). Malaria rapid diagnostic tests in travel medicine. Clin Microbiol Infect *19*, 408-415.

115) Mathison, B.A., and Pritt, B.S. (2017). Update on Malaria Diagnostics and Test Utilization. Journal of clinical microbiology *55*, 2009-2017.

116) McNamara, L.K., Brunzelle, J.S., Schavocky, J.P., Watterson, D.M., and Grum-Tokars, V. (2011). Site-directed mutagenesis of the glycine-rich loop of death associated protein kinase (DAPK) identifies it as a key structure for catalytic activity. Biochimica et biophysica acta *1813*, 1068-1073.

117) McRobert, L., Taylor, C.J., Deng, W., Fivelman, Q.L., Cummings, R.M., Polley, S.D., Billker, O., and Baker, D.A. (2008). Gametogenesis in malaria parasites is mediated by the cGMP-dependent protein kinase. PLoS biology *6*, e139.

118) Meibalan, E., and Marti, M. (2017). Biology of Malaria Transmission. Cold Spring Harbor perspectives in medicine *7*.

119) Menard, D., and Dondorp, A. (2017). Antimalarial Drug Resistance: A Threat to Malaria Elimination. Cold Spring Harbor perspectives in medicine *7*.

120) Merckx, A., Nivez, M.P., Bouyer, G., Alano, P., Langsley, G., Deitsch, K., Thomas, S., Doerig, C., and Egée, S. (2008). Plasmodium falciparum regulatory subunit of cAMP-dependent PKA and anion channel conductance. PLoS pathogens *4*, e19.

121) Mnzava, A.P., Macdonald, M.B., Knox, T.B., Temu, E.A., and Shiff, C.J. (2014). Malaria vector control at a crossroads: public health entomology and the drive to elimination. Transactions of The Royal Society of Tropical Medicine and Hygiene *108*, 550-554.

122) Moody, A. (2002). Rapid diagnostic tests for malaria parasites. Clinical microbiology reviews *15*, 66-78.

123) Moon, R.W., Taylor, C.J., Bex, C., Schepers, R., Goulding, D., Janse, C.J., Waters, A.P., Baker, D.A., and Billker, O. (2009). A cyclic GMP signalling module that regulates gliding motility in a malaria parasite. PLoS pathogens *5*, e1000599.

124) Morris, G.M., Huey, R., Lindstrom, W., Sanner, M.F., Belew, R.K., Goodsell, D.S., and Olson, A.J. (2009). AutoDock4 and AutoDockTools4: Automated docking with selective receptor flexibility. Journal of computational chemistry *30*, 2785-2791.

125) Mouatcho, J.C., and Goldring, J.P.D. (2013). Malaria rapid diagnostic tests: challenges and prospects. Journal of medical microbiology *62*, 1491-1505.

126) Mousa, A., Al-Taiar, A., Anstey, N.M., Badaut, C., Barber, B.E., Bassat, Q., Challenger, J.D., Cunnington, A.J., Datta, D., Drakeley, C.*, et al.* (2020). The impact of delayed treatment of uncomplicated P. falciparum malaria on progression to severe malaria: A systematic review and a pooled multicentre individual-patient meta-analysis. PLoS medicine *17*, e1003359.

127) Moxon, C.A., Grau, G.E., and Craig, A.G. (2011). Malaria: modification of the red blood cell and consequences in the human host. British journal of haematology *154*, 670-679.

128) Muhindo, H.M., Ilombe, G., Meya, R., Mitashi, P.M., Kutekemeni, A., Gasigwa, D., Lutumba, P., and Van Geertruyden, J.P. (2012). Accuracy of malaria rapid diagnosis test Optimal-IT(®) in Kinshasa, the Democratic Republic of Congo. Malar J *11*, 224.

129) Murray, C.K., Gasser, R.A., Jr., Magill, A.J., and Miller, R.S. (2008). Update on rapid diagnostic testing for malaria. Clinical microbiology reviews *21*, 97-110.

130) Nadjm, B., and Behrens, R.H. (2012). Malaria: an update for physicians. Infectious disease clinics of North America *26*, 243-259.

131) Nsanzabana, C. (2019). Resistance to Artemisinin Combination Therapies (ACTs): Do Not Forget the Partner Drug! Tropical medicine and infectious disease *4*.

132) Nunes, M.C., Goldring, J.P., Doerig, C., and Scherf, A. (2007). A novel protein kinase family in Plasmodium falciparum is differentially transcribed and secreted to various cellular compartments of the host cell. Mol Microbiol *63*, 391-403.

133) Nunes, M.C., Okada, M., Scheidig-Benatar, C., Cooke, B.M., and Scherf, A. (2010). Plasmodium falciparum FIKK kinase members target distinct components of the erythrocyte membrane. PLoS One *5*, e11747.

134) Obidike, I.C., Amodu, B., and Emeje, M.O. (2015). Antimalarial properties of SAABMAL (®): an ethnomedicinal polyherbal formulation for the treatment of uncomplicated malaria infection in the tropics. The Indian journal of medical research *141*, 221-227.

135) Ojo, K.K., Eastman, R.T., Vidadala, R., Zhang, Z., Rivas, K.L., Choi, R., Lutz, J.D., Reid, M.C., Fox, A.M., Hulverson, M.A.*, et al.* (2014). A specific inhibitor of PfCDPK4 blocks malaria transmission: chemical-genetic validation. The Journal of infectious diseases *209*, 275-284.

136) Organization, W.H. (2020). World malaria report 2020: 20 years of global progress and challenges.

137) Osman, K.T., Lou, H.J., Qiu, W., Brand, V., Edwards, A.M., Turk, B.E., and Hui, R. (2015). Biochemical characterization of FIKK8--A unique protein kinase from the malaria parasite Plasmodium falciparum and other apicomplexans. Molecular and biochemical parasitology *201*, 85-89.

138) Osman, K.T., Ye, J., Shi, Z., Toker, C., Lovato, D., Jumani, R.S., Zuercher, W., Huston, C.D., Edwards, A.M., Lautens, M., *et al.* (2017). Discovery and structure activity relationship of the first potent cryptosporidium FIKK kinase inhibitor. Bioorganic & medicinal chemistry *25*, 1672-1680.

139) Paquet, T., Le Manach, C., Cabrera, D.G., Younis, Y., Henrich, P.P., Abraham, T.S., Lee, M.C.S., Basak, R., Ghidelli-Disse, S., Lafuente-Monasterio, M.J., *et al.* (2017). Antimalarial efficacy of MMV390048, an inhibitor of Plasmodium phosphatidylinositol 4-kinase. Science translational medicine *9*.

140) Park, S.H., Jegal, S., Ahn, S.K., Jung, H., Lee, J., Na, B.K., Hong, S.J., Bahk, Y.Y., and Kim, T.S. (2020). Diagnostic Performance of Three Rapid Diagnostic Test Kits for Malaria Parasite Plasmodium falciparum. The Korean journal of parasitology *58*, 147-152.

141) Paul, A.S., Saha, S., Engelberg, K., Jiang, R.H., Coleman, B.I., Kosber, A.L., Chen, C.T., Ganter, M., Espy, N., Gilberger, T.W., *et al.* (2015). Parasite Calcineurin Regulates Host Cell Recognition and Attachment by Apicomplexans. Cell host & microbe *18*, 49-60.

142) Pease, B.N., Huttlin, E.L., Jedrychowski, M.P., Talevich, E., Harmon, J., Dillman, T., Kannan, N., Doerig, C., Chakrabarti, R., Gygi, S.P., *et al.* (2013). Global analysis of protein expression and phosphorylation of three stages of Plasmodium falciparum intraerythrocytic development. Journal of proteome research *12*, 4028-4045.

143) Percário, S., Moreira, D.R., Gomes, B.A., Ferreira, M.E., Gonçalves, A.C., Laurindo, P.S., Vilhena, T.C., Dolabela, M.F., and Green, M.D. (2012). Oxidative stress in malaria. International journal of molecular sciences *13*, 16346-16372.

144) Peterson, C.T., Denniston, K., and Chopra, D. (2017). Therapeutic Uses of Triphala in Ayurvedic Medicine. Journal of alternative and complementary medicine (New York, NY) *23*, 607-614.

145) Phillips, M.A., Burrows, J.N., Manyando, C., van Huijsduijnen, R.H., Van Voorhis, W.C., and Wells, T.N.C. (2017). Malaria. Nature reviews Disease primers *3*, 17050.

146) Pieroni, P., Mills, C.D., Ohrt, C., Harrington, M.A., and Kain, K.C. (1998). Comparison of the ParaSight-F test and the ICT Malaria Pf test with the polymerase chain reaction for the diagnosis of Plasmodium falciparum malaria in travellers. Transactions of the Royal Society of Tropical Medicine and Hygiene *92*, 166-169.

147) Pinmai, K., Hiriote, W., Soonthornchareonnon, N., Jongsakul, K., Sireeratawong, S., and Tor-Udom, S. (2010). In vitro and in vivo antiplasmodial activity and cytotoxicity of water extracts of Phyllanthus emblica, Terminalia chebula, and Terminalia bellerica. Journal of the Medical Association of Thailand = Chotmaihet thangphaet *93 Suppl 7*, S120-126.

148) Plewes, K., Leopold, S.J., Kingston, H.W.F., and Dondorp, A.M. (2019). Malaria: What's New in the Management of Malaria? Infect Dis Clin North Am *33*, 39-60.

149) Plucinski, M.M., McElroy, P.D., Dimbu, P.R., Fortes, F., Nace, D., Halsey, E.S., and Rogier, E. (2019). Clearance dynamics of lactate dehydrogenase and aldolase following antimalarial treatment for Plasmodium falciparum infection. Parasites & vectors *12*, 293.

150) Poti, K.E., Sullivan, D.J., Dondorp, A.M., and Woodrow, C.J. (2020). HRP2: Transforming Malaria Diagnosis, but with Caveats. Trends in parasitology *36*, 112-126.

151) Pousibet-Puerto, J., Salas-Coronas, J., Sánchez-Crespo, A., Molina-Arrebola, M.A., Soriano-Pérez, M.J., Giménez-López, M.J., Vázquez-Villegas, J., and Cabezas-Fernández, M.T. (2016). Impact of using artemisinin-based combination therapy (ACT) in the treatment of uncomplicated malaria from Plasmodium falciparum in a non-endemic zone. Malaria Journal *15*, 339.

152) Ram, E.V., Naik, R., Ganguli, M., and Habib, S. (2008). DNA organization by the apicoplast-targeted bacterial histone-like protein of Plasmodium falciparum. Nucleic acids research *36*, 5061-5073.

153) Reddy, K.S., Amlabu, E., Pandey, A.K., Mitra, P., Chauhan, V.S., and Gaur, D. (2015). Multiprotein complex between the GPI-anchored CyRPA with PfRH5 and PfRipr is crucial for Plasmodium falciparum erythrocyte invasion. Proceedings of the National Academy of Sciences of the United States of America *112*, 1179-1184.

154) Ricci, I., Valzano, M., Ulissi, U., Epis, S., Cappelli, A., and Favia, G. (2012). Symbiotic control of mosquito borne disease. Pathogens and global health *106*, 380-385.

155) Riglar, D.T., Richard, D., Wilson, D.W., Boyle, M.J., Dekiwadia, C., Turnbull, L., Angrisano, F., Marapana, D.S., Rogers, K.L., Whitchurch, C.B., *et al.* (2011). Super-resolution dissection of coordinated events during malaria parasite invasion of the human erythrocyte. Cell host & microbe *9*, 9-20.

156) Rocamora, F., and Winzeler, E.A. (2020). Genomic Approaches to Drug Resistance in Malaria. Annual review of microbiology *74*, 761-786.

157) Rosado, L.A., Vasconcelos, I.B., Palma, M.S., Frappier, V., Najmanovich, R.J., Santos, D.S., and Basso, L.A. (2013). The mode of action of recombinant Mycobacterium tuberculosis shikimate kinase: kinetics and thermodynamics analyses. PloS one *8*, e61918.

158) Rug, M., Cyrklaff, M., Mikkonen, A., Lemgruber, L., Kuelzer, S., Sanchez, C.P., Thompson, J., Hanssen, E., O'Neill, M., Langer, C., *et al.* (2014). Export of virulence

proteins by malaria-infected erythrocytes involves remodeling of host actin cytoskeleton. Blood *124*, 3459-3468.

159) Sadasivaiah, S., Tozan, Y., and Breman, J.G. (2007). Dichlorodiphenyltrichloroethane (DDT) for indoor residual spraying in Africa: how can it be used for malaria control? The American journal of tropical medicine and hygiene *77*, 249-263.

160) Schneider, A.G., and Mercereau-Puijalon, O. (2005). A new Apicomplexa-specific protein kinase family: multiple members in Plasmodium falciparum, all with an export signature. BMC Genomics *6*, 30.

161) Sethabutr, O., Brown, A.E., Panyim, S., Kain, K.C., Webster, H.K., and Echeverria, P. (1992). Detection of Plasmodium falciparum by polymerase chain reaction in a field study. The Journal of infectious diseases *166*, 145-148.

162) She, R.C., Rawlins, M.L., Mohl, R., Perkins, S.L., Hill, H.R., and Litwin, C.M. (2007). Comparison of immunofluorescence antibody testing and two enzyme immunoassays in the serologic diagnosis of malaria. Journal of travel medicine *14*, 105-111.

163) Siciliano, G., and Alano, P. (2015). Enlightening the malaria parasite life cycle: bioluminescent Plasmodium in fundamental and applied research. Frontiers in microbiology *6*, 391.

164) Siddiqui, G., Proellochs, N.I., and Cooke, B.M. (2020). Identification of essential exported Plasmodium falciparum protein kinases in malaria-infected red blood cells. British Journal of Haematology *188*, 774-783.

165) Sirichaisinthop, J., Buates, S., Watanabe, R., Han, E.T., Suktawonjaroenpon, W., Krasaesub, S., Takeo, S., Tsuboi, T., and Sattabongkot, J. (2011). Evaluation of loop-mediated isothermal amplification (LAMP) for malaria diagnosis in a field setting. The American journal of tropical medicine and hygiene *85*, 594-596.

166) Sivasankar, S., Lavanya, R., Brindha, P., and Angayarkanni, N. (2015). Aqueous and alcoholic extracts of Triphala and their active compounds chebulagic acid and chebulinic acid prevented epithelial to mesenchymal transition in retinal pigment epithelial cells, by inhibiting SMAD-3 phosphorylation. PloS one *10*, e0120512.

167) Snounou, G., Viriyakosol, S., Jarra, W., Thaithong, S., and Brown, K.N. (1993). Identification of the four human malaria parasite species in field samples by the polymerase chain reaction and detection of a high prevalence of mixed infections. Molecular and biochemical parasitology *58*, 283-292.

168) Steel, R.W.J., Pei, Y., Camargo, N., Kaushansky, A., Dankwa, D.A., Martinson, T., Nguyen, T., Betz, W., Cardamone, H., Vigdorovich, V., *et al.* (2018). Plasmodium yoelii S4/CelTOS is important for sporozoite gliding motility and cell traversal. Cell Microbiol *20*.

169) Subbarao, S.K., Nanda, N., Rahi, M., and Raghavendra, K. (2019). Biology and bionomics of malaria vectors in India: existing information and what more needs to be known for strategizing elimination of malaria. Malar J *18*, 396.

170) Sundararaman, S.A., Plenderleith, L.J., Liu, W., Loy, D.E., Learn, G.H., Li, Y., Shaw, K.S., Ayouba, A., Peeters, M., Speede, S.*, et al.* (2016). Genomes of cryptic chimpanzee Plasmodium species reveal key evolutionary events leading to human malaria. Nature communications *7*, 11078.

171) Suryavanshi, S., Choudhari, A., Raina, P., and Kaul-Ghanekar, R. (2019). A polyherbal formulation, HC9 regulated cell growth and expression of cell cycle and chromatin modulatory proteins in breast cancer cell lines. Journal of ethnopharmacology *242*, 112022.

172) Syin, C., Parzy, D., Traincard, F., Boccaccio, I., Joshi, M.B., Lin, D.T., Yang, X.M., Assemat, K., Doerig, C., and Langsley, G. (2001). The H89 cAMP-dependent protein kinase inhibitor blocks Plasmodium falciparum development in infected erythrocytes. European journal of biochemistry *268*, 4842-4849.

173) Tambo, M., Mwinga, M., and Mumbengegwi, D.R. (2018). Loop-mediated isothermal amplification (LAMP) and Polymerase Chain Reaction (PCR) as quality assurance tools for Rapid Diagnostic Test (RDT) malaria diagnosis in Northern Namibia. PloS one *13*, e0206848.

174) Tangpukdee, N., Duangdee, C., Wilairatana, P., and Krudsood, S. (2009). Malaria diagnosis: a brief review. The Korean journal of parasitology *47*, 93-102.

175) Tanner, M., Greenwood, B., Whitty, C.J., Ansah, E.K., Price, R.N., Dondorp, A.M., von Seidlein, L., Baird, J.K., Beeson, J.G., Fowkes, F.J.*, et al.* (2015). Malaria eradication and elimination: views on how to translate a vision into reality. BMC medicine *13*, 167.

176) Tarkang, P.A., Okalebo, F.A., Ayong, L.S., Agbor, G.A., and Guantai, A.N. (2014). Anti-malarial activity of a polyherbal product (Nefang) during early and established Plasmodium infection in rodent models. Malar J *13*, 456.

177) Taylor, H.M., McRobert, L., Grainger, M., Sicard, A., Dluzewski, A.R., Hopp, C.S., Holder, A.A., and Baker, D.A. (2010). The malaria parasite cyclic GMP-dependent protein kinase plays a central role in blood-stage schizogony. Eukaryotic cell *9*, 37-45.

178) Tham, W.H., Lim, N.T., Weiss, G.E., Lopaticki, S., Ansell, B.R., Bird, M., Lucet, I., Dorin-Semblat, D., Doerig, C., Gilson, P.R.*, et al.* (2015). Plasmodium falciparum Adhesins Play an Essential Role in Signalling and Activation of Invasion into Human Erythrocytes. PLoS pathogens *11*, e1005343.

179) Thomas, D.C., Ahmed, A., Gilberger, T.W., and Sharma, P. (2012). Regulation of Plasmodium falciparum glideosome associated protein 45 (PfGAP45) phosphorylation. PloS one *7*, e35855.

180) Thu, A.M., Phyo, A.P., Landier, J., Parker, D.M., and Nosten, F.H. (2017). Combating multidrug-resistant Plasmodium falciparum malaria. The FEBS journal *284*, 2569-2578.

181) Treiber, D.K., and Shah, N.P. (2013). Ins and outs of kinase DFG motifs. Chemistry & biology *20*, 745-746.

182) Tse, E.G., Korsik, M., and Todd, M.H. (2019). The past, present and future of anti-malarial medicines. Malaria journal *18*, 93.

183) Tuteja, R. (2007). Malaria - an overview. The FEBS journal *274*, 4670-4679.

184) Vaid, A., Ranjan, R., Smythe, W.A., Hoppe, H.C., and Sharma, P. (2010). PfPI3K, a phosphatidylinositol-3 kinase from Plasmodium falciparum, is exported to the host erythrocyte and is involved in hemoglobin trafficking. Blood *115*, 2500-2507.

185) Vaid, A., Thomas, D.C., and Sharma, P. (2008). Role of Ca2+/calmodulin-PfPKB signaling pathway in erythrocyte invasion by Plasmodium falciparum. The Journal of biological chemistry *283*, 5589-5597.

186) Valsaraj, R., Pushpangadan, P., Smitt, U.W., Adsersen, A., Christensen, S.B., Sittie, A., Nyman, U., Nielsen, C., and Olsen, C.E. (1997). New anti-HIV-1, antimalarial, and antifungal compounds from Terminalia bellerica. Journal of natural products *60*, 739-742.

187) van Dooren, G.G., Reiff, S.B., Tomova, C., Meissner, M., Humbel, B.M., and Striepen, B. (2009). A novel dynamin-related protein has been recruited for apicoplast fission in Toxoplasma gondii. Current biology : CB *19*, 267-276.

188) Venugopal, K., Hentzschel, F., Valkiūnas, G., and Marti, M. (2020). Plasmodium asexual growth and sexual development in the haematopoietic niche of the host. Nature reviews Microbiology *18*, 177-189.

189) Viebig, N.K., Wulbrand, U., Förster, R., Andrews, K.T., Lanzer, M., and Knolle, P.A. (2005). Direct activation of human endothelial cells by Plasmodium falciparum-infected erythrocytes. Infection and immunity *73*, 3271-3277.

190) Vijayan, R.S., He, P., Modi, V., Duong-Ly, K.C., Ma, H., Peterson, J.R., Dunbrack, R.L., Jr., and Levy, R.M. (2015). Conformational analysis of the DFG-out kinase motif and biochemical profiling of structurally validated type II inhibitors. Journal of medicinal chemistry *58*, 466-479.

191) Vimee, R., Kumar, A., Subhashis, J., Subhendu Sekhar, B., and Vishal, T. (2019). Virtual Screening, Molecular Modelling and Biochemical Studies to Exploit PF14_0660 as a Target to Identify Novel Anti-malarials. Letters in Drug Design & Discovery *16*, 417-426.

192) Volz, J.C., Yap, A., Sisquella, X., Thompson, J.K., Lim, N.T., Whitehead, L.W., Chen, L., Lampe, M., Tham, W.H., Wilson, D.*, et al.* (2016). Essential Role of the PfRh5/PfRipr/CyRPA Complex during Plasmodium falciparum Invasion of Erythrocytes. Cell host & microbe *20*, 60-71.

193) Vonlaufen, N., Kanzok, S.M., Wek, R.C., and Sullivan, W.J., Jr. (2008). Stress response pathways in protozoan parasites. Cellular microbiology *10*, 2387-2399.

194) Wang, S., and Jacobs-Lorena, M. (2013). Genetic approaches to interfere with malaria transmission by vector mosquitoes. Trends in biotechnology *31*, 185-193.

195) Wang, Z., and Cole, P.A. (2014). Catalytic mechanisms and regulation of protein kinases. Methods in enzymology *548*, 1-21.

196) Ward, P., Equinet, L., Packer, J., and Doerig, C. (2004). Protein kinases of the human malaria parasite Plasmodium falciparum: the kinome of a divergent eukaryote. BMC Genomics *5*, 79.

197) Wat'senga, F., Agossa, F., Manzambi, E.Z., Illombe, G., Mapangulu, T., Muyembe, T., Clark, T., Niang, M., Ntoya, F., Sadou, A., *et al.* (2020). Intensity of pyrethroid resistance in Anopheles gambiae before and after a mass distribution of insecticide-treated nets in Kinshasa and in 11 provinces of the Democratic Republic of Congo. Malaria journal *19*, 169.

198) Wataya, Y., Arai, M., Kubochi, F., Mizukoshi, C., Kakutani, T., Ohta, N., and Ishii, A. (1993). DNA diagnosis of falciparum malaria using a double PCR technique: a field trial in the Solomon Islands. Molecular and biochemical parasitology *58*, 165-167.

199) Weiss, G.E., Gilson, P.R., Taechalertpaisarn, T., Tham, W.H., de Jong, N.W., Harvey, K.L., Fowkes, F.J., Barlow, P.N., Rayner, J.C., Wright, G.J., *et al.* (2015). Revealing the sequence and resulting cellular morphology of receptor-ligand interactions during Plasmodium falciparum invasion of erythrocytes. PLoS pathogens *11*, e1004670.

200) White, N.J. (2004). Antimalarial drug resistance. The Journal of clinical investigation *113*, 1084-1092.

201) Wicht, K.J., Mok, S., and Fidock, D.A. (2020). Molecular Mechanisms of Drug Resistance in Plasmodium falciparum Malaria. Annual review of microbiology *74*, 431-454.

202) Wilson, M.L. (2012). Malaria rapid diagnostic tests. Clinical infectious diseases : an official publication of the Infectious Diseases Society of America *54*, 1637-1641.

203) Wu, Y., Nelson, M.M., Quaile, A., Xia, D., Wastling, J.M., and Craig, A. (2009). Identification of phosphorylated proteins in erythrocytes infected by the human malaria parasite Plasmodium falciparum. Malaria journal *8*, 105.

204) Yang, A.S., and Boddey, J.A. (2017). Molecular mechanisms of host cell traversal by malaria sporozoites. Int J Parasitol *47*, 129-136.

205) Yeh, E., and DeRisi, J.L. (2011). Chemical rescue of malaria parasites lacking an apicoplast defines organelle function in blood-stage Plasmodium falciparum. PLoS Biol *9*, e1001138.

206) Zimmerman, P.A., and Howes, R.E. (2015). Malaria diagnosis for malaria elimination. Current opinion in infectious diseases *28*, 446-454.

207) Zuber, J.A., and Takala-Harrison, S. (2018). Multidrug-resistant malaria and the impact of mass drug administration. Infection and drug resistance *11*, 299-306.

List of Publications

1) **Anil Kumar D**, Shrivastava D, Sahasrabuddhe AA, Habib S, Trivedi V. Plasmodium falciparum FIKK9.1 is a monomeric serine-threonine protein kinase with features to exploit as a drug target. **Chem Biol Drug Des. 2021** Apr;97(4):962-977. doi: 10.1111/cbdd.13821.

2) **Anil Kumar D**, Pallab Karjee, Punniyamurthy T, Trivedi V. Plasmodium falciparum FIKK 9.1 kinase modeling to screen and identify potent antimalarial agents from chemical library. (communicated).

3) **Anil Kumar D** and Vishal Trivedi. Triphala causes ROS mediated mitochondria membrane potential to induce programmed cell death in malaria parasite. (Manuscript in preparation).

List of Conference Presentations

1) Presented poster entitles "Cloning, over-expression and preliminary biochemical study of FIKK9.1 kinase from *Plasmodium falciparum* 3D7" in INSCR International conference 2018 on Trends in biotechnology for innovations in **Health and Environment**, held during 26th -27th September 2018, organized by KIIT, Odisha.

2) Participated in the workshop, conference, and presented a poster in the International conference on **Drug Design**, held during 7-9 April 2017, organized by Schrodinger, JNU, New Delhi.

3) Presented a poster entitles "Potentials of *Plasmodium Falciparum* FIKK kinases in drug discovery and diagnostics" in National seminar on **Science and Technology** for national development held at Dr. Harisingh Gour University 23rd–24th September 2016, Sagar, Madhya Pradesh.